Thesis Title: The role of Synaptic Genes *NRXN1* and *SHANK3* in Autism: an induced pluripotent stem cell study

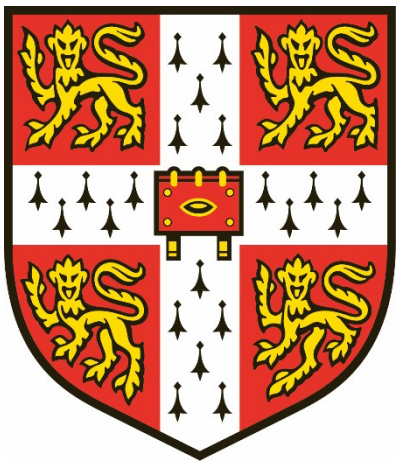

ARKOPROVO PAUL
Department of Psychiatry
University of Cambridge

This dissertation is submitted for the degree of
Doctor of Philosophy

St John's College September 2020

Thesis Title: **The role of Synaptic Genes NRXN1 and SHANK3 in Autism: an induced pluripotent stem cell study**

Arkoprovo Paul

Abstract:

Autism is a complex neurodevelopmental condition with hundreds of genes associated with its pathophysiology. A number of autism related genes have been reported to be strongly associated with the structural or functional aspects of neuronal connections or synapses. However, it is poorly understood how the loss of function of these synaptic genes contribute to the neuronal morphology, network physiology and atypical communication between brain cells.

This thesis aims to first establish and characterise an induced pluripotent cell (iPSC) derived neuronal model suitable for studying autism related synaptic genes. Secondly, it aims to study the effect of pre-synaptic *NRXN1* and post-synaptic *SHANK3* deletions on neuronal morphology and synaptic network activity.

The first hypothesis of this thesis is that iNeurons derived by *NGN2* forward programming approach would express autism related genes, post synaptic density molecules, synaptic receptors and demonstrate mature electrophysiological activity relevant for studying autism related functional phenotypes, within four weeks of neuronal induction. The second hypothesis is that iNeurons with deletions in *NRXN1* or *SHANK3* derived from individuals with autism would show altered morphological and electrophysiological cellular phenotypes.

This study proposes a novel *in vitro* model for generating more homogenous and functional neurons compared to the existing methods adopted in the field of autism research. It has been exemplified that the effect mutations in synaptic genes such as *NRXN1* and *SHANK3* on mature cellular phenotypes can be studied using iNeurons. Further research is needed for technological fine-tuning to establish a robust scalable cell-based platform that would potentially be useful to investigate cellular phenotypes caused by anomalies in any autism risk gene and better understand the pathophysiology of neurodevelopmental conditions.

Declaration

This dissertation is the result of my own work and includes nothing which is the outcome of work done in collaboration except as declared in the Acknowledgements and specified in the text. It is not substantially the same as any that I have submitted, or is being concurrently submitted for a degree or diploma or other qualification at the University of Cambridge or any other university or similar institution. This dissertation does not exceed the prescribed word limit of 60,000 words set by the Degree Committee for Clinical Medicine and Clinical Veterinary Medicine.

Arkoprovo Paul

September 2020

Acknowledgements

I would like to thank my supervisor Prof Simon Baron Cohen for accepting me as his PhD student at University of Cambridge and being a source of continuous support and encouragement. I am very grateful to my co-supervisor Dr Mark Kotter for providing me with all the lab resources and being supportive of my scientific endeavours throughout my PhD. I would like to also thank my advisor Dr Deepak Srivastava at King's College London for continuous scientific guidance and kind advice during my PhD. My gratitude to my collaborator Dr John O'Neil at MRC Laboratory of Molecular Biology for giving me kind access to lab facilities.

I thank Commonwealth Scholarship Commission, UK, and Autism Research Trust for giving me this wonderful opportunity to undertake my PhD at Autism Research Centre, University of Cambridge. I am also grateful to St John's College for support beyond work environment.

I am deeply grateful to all my colleagues and friends at Cambridge for helping me understand several scientific ideas and making my PhD a wonderful experience. I thank my lab mate Kaiser Karim for helping me understand bioinformatical data analysis. A very special thanks goes to Aicha Massrali for her kind support at work and being a wonderful friend. I would like to also thank postdoctoral fellows in my lab, Dr Dwaipayan Adhya and Dr Koby Baranes for their support and advice at different stages of my PhD. Last but not the least, I would like to thank my mother Dr Atreyi Paul for being a constant source of encouragement and love.

1 Table of Contents

LIST OF FIGURES

LIST OF TABLES

1 Chapter 1: Introduction

1.1 Autism

Autism Spectrum Conditions (henceforth "autism") are a set of neurodevelopmental conditions involving impairments in social communication and unusually restricted interests and repetitive behaviour that manifest within the first three years of life (Lai, Lombardo and Baron-Cohen, 2014). The clinical diagnosis of autism is usually based on interviews and behavioural assessments of language and social behaviour skills (Baird et al, 2003). In 1943, the term "autism" was first introduced by Leo Kanner (Kanner, 1943), an Austrian-American psychiatrist, as a diagnostic label to define a specific condition observed in young children manifested by impairments in social and emotional relationships. Autism is now recognized as Autism Spectrum Disorder (ASD), as defined in DSM-5 (Diagnostic and Statistical Manual of Mental Disorders, 5th Edition) by the American Psychiatric Association (DSM-5, American Psychiatric APA 2013) and the ICD-10 (International Classification of Diseases, 10th Revision) by the World Health Organization (International Statistical Classification of Diseases and Related Health Problems: Tenth Revision, World Health Organization, 2004). The prevalence rate of autism has risen increasingly over the years since the first epidemiological study in 1966 estimating 4.5 per 10,000 individuals (Lotter, 1966). Recent data on prevalence of autism in the United States until 2016 as reported by CDC (Centre for Disease Control and Prevention) shows 18.5 per 1,000 (1 in 54) children aged 8 years are affected by autism (Maenner et al, 2020). A recent report reveals a sharp increase in the prevalence rates of autism in UK schools between 2010 and 2019 (McConkey R, 2020). Autism affects 1-2% of the population in the UK i.e. 1 per 100 children and 2 per 100 adults (NHS Digital, 2020). It has been reported by the NHS that there are approximately 100,000 children and 1,000,000 adults with autism in the UK.

Several factors such as changes in diagnostic criteria of the years, increase in risk factors and increased awareness have collectively contributed to an increase in the prevalence rate of autism (Elsabbagh et al, 2012). The biology of autism is complex and cannot be used as a diagnostic measure like most other psychiatric conditions and therefore, the diagnostic criteria of autism solely rely upon behavioural symptoms. The term "Autism Spectrum Disorder" (ASD) is more frequently used to describe autism, however, Autism Spectrum Condition (ASC) is also used to refer to the neurodevelopmental condition without the negative connotation of the term "disorder" which implies something is "broken" (Lai, Lombardo, Chakrabarti, & Baron-Cohen, 2013). The characteristic behavioural symptoms of Autism comprise of impairments in social communication and atypical repetitive interests with an early onset prior to the age of three years. The diagnostic scales for autism, as recommended by the American Academy of Pediatrics (Hyman et al, 2020), are Autism Diagnostic Interview-Revised (ADI-R) and the Autism Diagnostic Observation Schedule, Second Edition (ADOS-2) which should be administered by trained professionals along with evaluation of the child's clinical history and symptom presentation (Lord et al, 2012; Rutter et al, 2003).

Autism affects 1-2% of children in the United States with increasing genetic risk factors with aetiological heterogeneity and can be considered as a behavioural syndrome rather than a specific categorical mental disorder (Tordjman et al, 2018). The spectrum of autism encompasses "syndromic autism" (autism associated with symptoms directing towards specific genetic disorders) and "non-syndromic autism" (idiopathic autism with no apparent manifestation of symptoms). Multiplex autism refers to those with a family history of affected individuals and alludes to the genetic complexity and heterogeneity of the condition (Miles et al, 2005; Cohen et al, 2005). Although the behavioural phenotype of autism comprises of impairments in socio-cognitive domains, a subset of individuals with autism may also possess abilities to process information differently which may be an example of "neurodiversity" and

may lead to talent (Baron-Cohen and Lombardo, 2017). The theory of "hypersystemising" in autism, which was first proposed in 2003 (Baron-Cohen et al, 2003) explains the potential link between restricted interests and superiority in specific abilities in individuals with autism compared to typically developing individuals. Moreover, enhanced attention to detail and sensory-perceptual processing could result in exceptional abilities in such group of autistic individuals (Baron-Cohen et al. 2009; Mottron et al. 2013).

1.2 Genetics and Epigenetics

1.2.1 Autism Genetics

Autism is aetiologically heterogeneous and not fully understood though heritability estimates for autism, as determined from twin and family studies, are 70- 90% in monozygotic twins and up to 20% in dizygotic twins, (Bailey et al, 1995; Abrahams et al, 2008; Hallmayer et al, 2011; Schaefer et al 2013). Moreover, a linkage scan from an international collaborative study has mapped putative risk loci in families with at least two affected individuals (Szatmari et al, 2007). Recent data has shown that up to 20% autism patients have an underlying genetic aberration (Betancur, 2011). In a multiplex family, the recurrence rate of autism might be 25-30% if a second child is also diagnosed with autism. Chromosomal microarray analysis probes for copy number variants and comparative genomic hybridization data show that de novo germline mutations pose more significant genetic risk for autism (Sebat et al, 2007). In this study, CNVs were present in 10% of the individuals with autism from simplex families, whereas only 3% of individuals from multiplex families with more than one family member affected showed CNVs compared with 1% observed in typically developing children. Syndromic autism, caused by single gene conditions, contributes to approximately 10-20% individuals with autism whereas epigenetics influenced by environmental risk factors could alter gene transcription through methylation without changing the gene sequence (Shen et al,

2010; Schaefer et al, 2010; Wenger et al, 2016). Autism manifests with a recognized genetic cause in ~10% of cases, most commonly with Fragile X syndrome, Tuberous sclerosis, Rett syndrome, Angelman syndrome, Timothy syndrome and cytogenetically detectable chromosome abnormalities (Xu et al, 2004, Veenstra-Vanderweele wt al, 2004, Kleijer et al 2014). The most frequent cytogenetic anomaly is maternally derived duplication of chromosome 15q11-q13 (1%–3%); however, numerous other chromosomal regions have been reported, with a higher frequency of events observed in syndromic forms of autism (Jacquemont et al,, 2006, Vostman et al, 2006)). Based on twin and familial studies, the genetic contribution towards autism is approximately 61.9%, whereas environmental causes are about 38.9% (Hueget et al, 2016) as shown in Fig 1.1. According to multiple sources of evidence, approximately 40-50% of variance in autism liability is conferred by environmental factors (Gaugler et al, 2014; Hallmayer et al, 2011; Edelson et al, 2009; Hoekstra et al, 2007; Stilip et al, 2010; Deng et al, 2015). Several environmental risk factors for autism such as parental age, pregnancy related conditions, medication used during pregnancy, lifestyle choices, nutritional factors, exposure to toxins, air pollution, heavy metals, vaccination, inflammation and oxidative stress, neurotransmitter alterations and endocrine disruptions have been investigated in systemic reviews and meta-analyses (Cheroni et al, 2020; Modabbernia et al, 2017).

Genome-wide linkage and association studies (GWAS) have identified more than 1000 autism risk gene loci in all human chromosomes. Rare genetic variants, both inherited and *de novo*, are estimated to contribute to 10-13% individuals with autism (Buxbaum et al 2009, Ronemus et al 2014, Sanders et al 2016). According to the Human Gene Module of Simons Foundation Autism Research Initiative (SFARI), one of the largest online databases of annotated list of genes studied in the context of autism research, currently 1171 genes have been linked with autism (till April 2020). SFARI Gene platform classifies and scores autism related genes into several categories such as S (syndromic), high-confidence (category 1), strong-confidence

(category 2) and suggestive evidence (category 3), based on available scientific data. The 192 high-confidence (category 1) autism genes in this list are the ones that meet the most rigorous threshold of genome-wide significance (at least false discovery rate < 0.1) and are all found on SPARK gene list or recently reported by Satterstrom et al., 2020. Each of these genes has been clearly implicated in autism—typically by the presence of at least three de novo likely-gene-disrupting mutations being reported in the literature. In the later sections of this introduction, we have further described the roles of two such high-confidence genes: *NRXN1* and *SHANK3*.

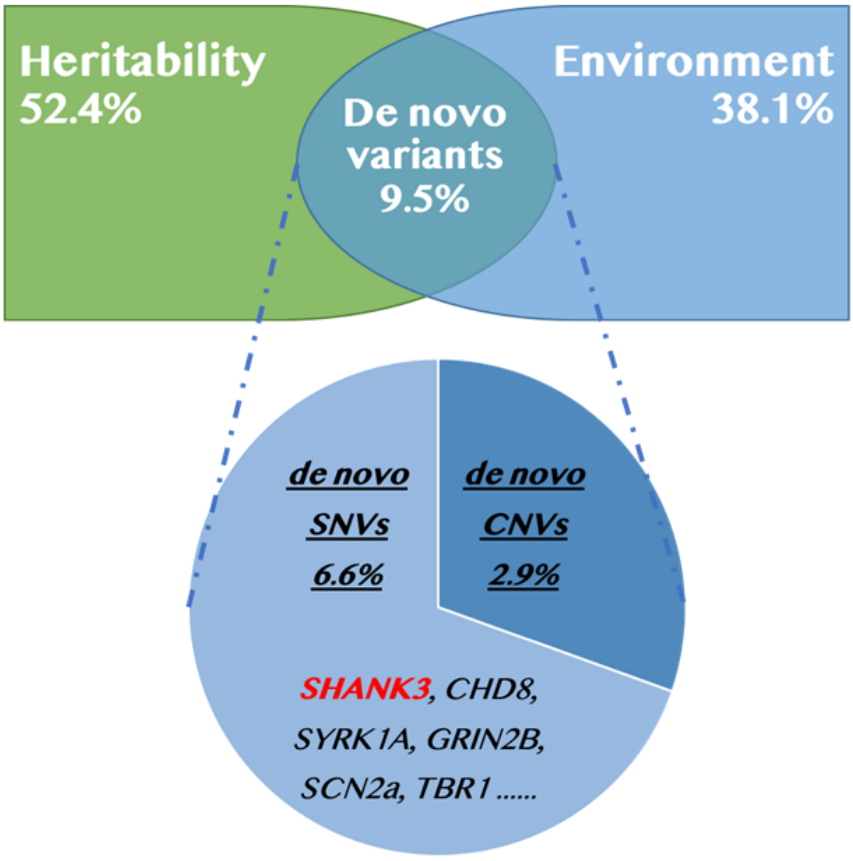

Figure 1-1 Genetic and Environment risk in Autism

The heritable contribution of autism risk genes mostly comprises of common variants, with a small contribution from rare genetic variants (Adapted from Huguet and Bourgeron 2016).

1.2.2 Autism Epigenetics

Epigenetic mechanisms modulate chromatin structure and gene expression without altering the gene sequence (Adalsteinsson et al, 2014; Schiele et al, 2018). Multiple reports reveal that the expression levels of epigenetic-related genes were significantly altered in individuals with autism compared to neurotypicals suggesting that epigenetic regulations play an important role in autism pathophysiology (Ben-David et al, 2013; Anney et al, 2017; Waye et al, 2018). There are mainly three mechanisms involved in epigenetic gene expression: DNA methylation, histone modifications and noncoding RNAs which regulate fine-tuning of brain development (Yoon et al, 2020). Most studies have investigated DNA methylation as a putative epigenetic mechanism and how it links genes with environmental factors in aetiology of autism (James et al, 2004; Dolinoy et al, 2007; Jirtle et al, 2007; Rusiecki et al, 2008; LaSalle et al, 2013; Jang et al, 2017). The first known epigenetic analyses in autism discordant monozygotic twins reported altered DNA methylation patterns and identified methylated CpG regions (Wong et al, 2014). Methyl-CpG binding protein 2 (*MeCP2*) is one of the most extensively studied epigenetic factors in autism research. MeCP2 protein plays dual role of activation and suppression of transcription and its altered expression caused due to duplication or mutation in *MeCP2* leads to Rett Syndrome, characterized by social behavioural symptoms similar to autism (Peters et al, 2013). Abnormal methylation of *MeCP2* promoter regions has been identified as one of the key mechanisms underlying autism-like phenotypes (Nagarajan et al, 2006; Lu et al, 2020). Histone modifications and chromatin remodelling is another important mechanism investigated in the context of autism pathophysiology; for example, H3K4me3, the fourth lysine residue trimethylation of histone protein H3, recruits chromatin remodellers to transcription start site and is involved in the regulation of hippocampal synaptic plasticity (Shilatifard et al, 2008; Gupta et al, 2010). Altered expression profiles of H3K4me3 found in postmortem tissue of prefrontal cortex were related to autism (Shulha et al, 2012).

Chromodomain helicase DNA-binding protein encoding gene *CHD8* is one of the most widely studied autism-related genes identified using whole exome sequencing in autism subjects (Sanders et al, 2015). ATP-dependent helicase CHD8 is reported to inhibit the target genes of Wnt/β-catenin and pathogenic mutations in *CHD8* have been related to autistic phenotypes (Cotney et al, 2015; Bernier et al, 2014). MicroRNAs (miRNAs) are noncoding short RNA molecules, ranging from 15 to 22 nucleotides, that regulate expression of 50% of human genes by mRNA degradation or inhibiting protein synthesis and control pathways involved in cellular differentiation, development and apoptosis (Fregeac et al, 2016; Bernstein et al, 2003). Correlation between upregulated miRNA profile with genome-wide DNA methylation data has revealed that miRNAs significantly expressed in autistic brains were related to synaptic pathways (Mor et al, 2015). In a post-mortem brain study, 28 out of 466 miRNAs studied were found to be differentially expressed between autism and controls (Abu-Elneel et al, 2008) which was further supported by evidence from whole blood and lymphoblastoid cell analysis (Seno et al, 2011; Papov et al, 2012).

Differential gene expression in lymphoblastoid cell lines (LCLs) from males with autism and their unaffected brothers showed significant enrichment of genes involved in steroid and androgen biosynthesis pathways (Hu et al, 2009). However, sex-differential biology in autism, has thus far been preliminarily studied in the context of epigenetic mechanisms underlying autistic phenotype (Werling DM, 2016). A follow-up study on differential methylation patterns in LCLs and post-mortem brain tissue identified an autism candidate gene retinoic acid-related orphan receptor alpha (*RORA*), a transcription factor involved in sex steroid regulatory pathway, with increased methylation and decreased expression in frontal cortex and cerebellum in autistic samples (Nguyen et al, 2010). *RORA* binding sites have been identified upstream from *CYP19A1* (aromatase), an enzyme that converts testosterone to estradiol, and both *CYP19A1* and *RORA* expression were downregulated in post-mortem brain

tissue from autism cohort. In an SH-SY5Y cell culture study, *RORA* expression was increased on treatment with estradiol and decreased in response to testosterone, and *RORA*'s transcriptional start site was found to be downstream from estrogen and adrogen receptor binding sites (Sarachana et al, 2011). The correlation between *RORA* and its target expression was also found to be stronger in males, thereby indicating *RORA*'s role in sex-differential biology (Hu et al, 2015). The effect of elevated foetal testosterone on brain development and epigenetic programming has been reported as a risk factor in autism pathophysiology (Baron-Cohen et al, 2014). This study compared foetal steroid hormone levels of boys who were later diagnosed with autism or Asperger's syndrome to typically developing controls and individuals with autism showed higher amniotic levels progesterone, testosterone and cortisol.

1.3 Synaptic Development

Autism is often considered as a disorder caused by aberrant synaptogenesis due to various mutations of synaptic genes such as *NRXN*, *NLGN*, *SHANK3*, *CNTNAP2* implicated in this condition (Walsch et al, 2011). The exome-sequencing analysis of 3871 autism cases implicated many genes that encode proteins for voltage-gates ion channels or proteins that are involved in synapse formation, synaptic scaffolding, and synaptic cell adhesion proteins (Rubeis SD et al., 2014; Bourgeon 2009; Zoghbi 2003). This data strongly indicates that synaptic dysfunction contributes to the cellular cause of autism. Several synaptic cell adhesion molecules have been linked to autism. These include Neurexins (*NRXN*s) and Neuroligins (*NGLN*s), *NRXN*s and *NGLN*s play an important role in the formation, maturation and maintenance of synapses (Kleijer et al., 2014) by acting as the glue between scaffolding protein and synaptic receptors. As mentioned above, multiple studies have identified deleterious *SHANK3* mutations in patients with ASD (Moessner et al., 2007; Hamdan et al., 2011; Denayer et al., 2012).

During human brain cortex formation, neurons make trillions of connections (Azevedo et al., 2009). After being formed at the ventricular zone (VZ), about 90% of human neurons migrate radially into the developing neocortex using glial-guided migration directed by a number of guidance molecules (Letinic et al., 2002) and form a 6-layered organized cortical structure (Marín and Rubenstein, 2001; Huang, 2009; Valiente and Marin, 2010). After neuronal migration, during prenatal and early postnatal stages, neurons undergo extensive morphological changes and lay the foundations of neuronal circuitry across brain regions. The axons extend and connect with target neurons, whereas dendrites grow and branch to establish dendritic fields. Finally, neurons form synaptic connections through activity-dependent structural modelling and refinement of neural circuitry to establish functional neural networks. Co-expression network analyses of autism risk genes show overlapping pathways of neurogenesis and synaptogenesis are impaired in early developmental stages in autism (Parikshak et al, 2013). Genetic aberrations or environmental insults disrupting any of these developmental processes ranging from neurogenesis to neuronal migration, axon-guidance, neurite outgrowth, synaptogenesis and neural circuit formation may lead to neurodevelopmental conditions including autism (Gilbert and Man, 2017).

1.3.1 Neurogenesis and neuron migration

Several reports have indicated that a subset of individuals with autism demonstrate atypical brain growth patterns (Wegiel et al., 2010; Courchesne et al., 2011). The size of the cerebral cortex may be normal at birth in individuals with autism, but subsequently display increased overgrowth followed by a decline compared to typically developing individuals. Aberrant laminar positioning of projection neurons was identified by Weigel et al, 2010, in children diagnosed with autism. Moreover, Courchesne et al, 2011, reported that excess neurogenesis in the prefrontal cortex may be an underlying pathophysiology of autism. Comparison of

neuron numbers in prefrontal postmortem tissue indicated the presence of 67% more neurons in individuals with autism compared to age matched controls. This evidence supports the theory of aberrant neurogenesis, which mostly occurs in 7-20 weeks of gestation and coincides with the end of the embryonic period and early foetal stage. Since cortical projection neurons comprise approximately 80% of cortical neurons, the development of lamination and number of projection neurons along with their dendritic arbors, axonal processes, myelin sheath and synapses could contribute to grey and white matter volume in affected individuals. Large scale anatomical abnormalities in brain sizes are often linked to autism as both macrocephaly and microcephaly have been identified in adolescents with autism with 15% and 20% of occurrence respectively (Lainhart et al., 1997; Fombonne et al., 1999; Cody et al., 2002; Pardo and Eberhart, 2007). A shift in the balance between neuron generation and elimination could be the reason of such brain growth aberrations since cell formation can outnumber cell elimination by 100-fold in the developing cortex in absence of optimal programmed cell death or pruning (Rakic and Zecevic, 2000; De Zio et al., 2005; Yamaguchi and Miura, 2015). Newly born projection neurons subsequently migrate from subventricular zone (SVZ) to different cortical layers in an "inside-out" fashion to form the 6-layered neocortex (Gupta et al., 2002; Nadarajah and Parnavelas, 2002; Kriegstein and Noctor, 2004). Thus, changes in neurogenesis and/or neuronal migration may contribute to impairments in lamination of neocortex, as identified in seven out of eight autism cases probed by brain imaging and postmortem histology by Hutsler et al., 2007. Another study identified disorganized cortical lamination in ten out of eleven autism cases (Stoner et al, 2014) which further indicates that enhanced neurogenesis, upregulation of neuronal proliferation and differentiation, and changes in neuronal migration may play a major role in autism pathophysiology.

1.3.2 Neurite outgrowth and spine formation

Neurons are highly specialized cell types with distinct morphological characteristics and comprise of mainly three sections: 1) soma, containing the nucleus and cellular organelles, 2) axonal process for transmitting information and 3) dendritic arbor for receiving information from adjacent neurons. The dendrites are extensively branched structures and occupy large volume within brain tissue (Tahirovic and Bradke, 2009). The establishment of dendritic field follows several discreet stages (Gilbert and Man, 2017). After birth from neural progenitors as a simple soma, neurons first undergo polarisation. The multipolar morphology with several minor neurites is established first. The migration of such neurons takes place by reorganisation of microtubules in response to extracellular cues and intracellular polarity signalling molecules. Thereafter, stabilisation of a single neurite resulting into a leading process occurs, which eventually develops into axon. This step is critical for the neurons to exit the multipolar state and enter the cortical plate (Shim et al., 2008; Witte and Bradke, 2008). The dendritic branching and establishment of dendritic field further takes place according to neuronal subtype when the neurons have reached their destined cortical layers (Tahirovic and Bradke, 2009; Jan and Jan, 2010). The development of dendrites begins during early prenatal period; however, dendritic spine morphogenesis and turnover and extensive dendritic branching extends until adulthood (Forrest et al, 2018). Aberrations in dendritic growth and/or morphological anomalies can have severe consequences on neural network formation and circuit assembly. Disruptions in neuronal network connections between higher order brain regions have been identified as one of the major defects in autism (Geschwind and Levitt, 2007). Brain imaging studies have reported both large and small changes in connectivity of neuronal networks in autism; however, the cellular and neurobiological basis of such dysconnectivity still remains poorly understood (Casanova and Casanova, 2014; Maximo et al., 2014). Besides dendritic development, a large number of studies have also investigated and linked atypical spine morphology and atypical

dendritic structural plasticity with autism pathophysiology (Persico and Bourgeron, 2006; Kelleher and Bear, 2008; Bourgeron, 2009). Dendritic spines are defined as small, microscopic protrusions on dendritic branches that are sites of majority of excitatory synapses in the brain (Forrest et al, 2018). Dendrites from each neuron can have more than a thousand spines, and each spine can potentially form an excitatory synaptic connection upon maturation. Although spines and synapses are produced in excess during neuronal development, later synaptic numbers undergo activity dependent pruning or stabilisation during postnatal period until adolescence and adulthood, which is critical in majority of neuropsychiatric conditions including autism (Bourgeron, 2009; Penzes et al 2011; Forrest et al, 2018). Dendritic spines are highly dynamic structures which undergo turnover and structural plasticity depending on developmental age and activity. Post-mortem analysis of cortical neurons using Golgi staining has shown increased spine density in brain tissues of individuals with autism compared to controls (Hutsler and Zhang, 2010). Several studies have further validated this theory that formation and maintenance of dendritic spines are key cellular processes in autism (Kelleher and Bear, 2008; Bourgeron, 2009; Phillips and Pozzo-Miller, 2015).

1.3.3 Neuronal activity and Synaptic plasticity

Synapses are highly specialized structures in the mammalian brain and functional sites of neuronal connections for facilitating information processing across brain regions. A synapse is comprised of the presynaptic compartment, the synaptic cleft that acts as a bridge and the postsynaptic compartment. The presynaptic region is filled with neurotransmitter containing vesicles which are fused with the plasma membrane and released into the synaptic cleft; and tightly coupled spatio-temporarily with the arrival of action potentials and calcium influx. The neurotransmitters, thus released into the synaptic cleft thereafter bind to the cluster of receptors

in a region called the postsynaptic density (PSD) on the postsynaptic compartment, thereby propagating the chemical messengers across the synapse (Gilbert and Man, 2017).

Emergence of neuronal activity in the mammalian cortex is key in regulation of activity dependent transcription of gene involved in many aspects neuronal circuit development, including dendritic branching, synapse maturation, and synapse elimination (Flavell and Greenberg, 2008). Human cortical development begins at around gestational week 5 and continues for approximately 100 days, completing by week 28 (Meyer et al., 2000; Rabinowicz et al., 1996). Development of spontaneous synaptic activity coincides with embryonic synapse formation (Katz and Shatz, 1996; Zhang and Poo, 2001). Synaptogenesis in human cortex is reported to initiate during week 9 to week 10 period of foetal development (de Graaf-Peters and Hadders-Algra, 2006). Thereafter, oscillations and synchronised bursts emerge in developing human cortex which is dependent on glutamatergic synaptic activity in excitatory networks of functional neurons and also inputs from inhibitory neurons (Robinson et al., 1993; Buzsaki G, 2006). Bursting activity or oscillations are a critical mechanism for fine tuning of neural circuits and establishment of neuronal connectivity (Katz, 1993; Wong, 1993; Wong et al., 1995).

Synaptic plasticity is a phenomenon where synapses undergo modifications or turnover, e.g. strengthening or weakening over time as a function of neuronal inputs and activity. These dynamic changes in synaptic strength depends on synapses being active or inactive and activity dependent structural plasticity due to gene transcription or protein translation (Bailey, Kandel, and Harris 2015). Several animal model studies have investigated the link between autism and synaptic plasticity, both in terms of synaptic strength and synaptic inputs (Sidorov, Auerbach, and Bear 2013, Sudhof 2008). Many autism related loss or gain of function gene mutations lead to altered gene transcription or protein translation of synapse related transcripts, thereby

altering synaptic function and plasticity (Kelleher and Bear, 2008; Akins et al., 2009; Darnell et al., 2011; Qiu et al., 2012; Gilbert and Man, 2014; Ung et al. 2017). Some studies have classified autism risk genes and proteins based on their impacts on synaptic structure and functions (Banerjee, Riordan, and Bhat 2014, Bourgeron 2015, Ebrahimi-Fakhari and Sahin 2015, Liu et al. 2017).

Historically, Hebb (1949) proposed the theory that neuronal circuit connectivity would be dictated by neuronal activity through a mechanism of synapse consolidation and elimination. This later on led to the idea that neuronal activity drives the formation and refinement of neuronal circuitry during typical brain development or disease states based on Hubel and Wiesel's pioneering experiments on monocular deprivation and activity manipulations in cat visual cortex (Hubel and Wiesel, 1959; 1962, 1970; Wiesel and Hubel, 1963). The highly dynamic synaptic connections in human brain also show similar activity (or experience dependent) dependent synaptic development during establishment of neuronal circuitry (Doll and Broadie, 2014). In human cerebral cortex, the first synapses emerge approximately at around 40^{th} day of conception and subsequently, the rate of synapse formation and elimination exhibit distinct phases (Bourgeron, 2009). However, the most dramatic changes in this process of synaptic contact formation and stabilisation take place during the perinatal period, which coincides with first three years of life i.e. the time window for emergence of autistic features (Bourgeron, 2009; Penzes et al, 2011; Doll and Broadie, 2014). In this context, the "critical period" theory has emerged to explain the changes in synaptic dynamics as a mechanistic foundation towards understanding autism pathophysiology. A critical period refers to a temporary developmental window of increased sensory sensitivity, which drives neuronal connectivity changes (Holmaat and Svoboda, 2009). Although synaptic modifications continue throughout life (Holtmaat et al, 2005; Grillo et al, 2013), the peak of synaptogenesis occurs only during the early postnatal life (Pan and Gan, 2008). Activity-

dependent synaptic remodelling during the critical period is a key phenomenon for formation and proper functioning of neuronal circuits which are often found to be disrupted or altered in autism, critically reviewed by Vasa et al, 2017. Bourgeron, 2009, had hypothesised that synaptic NRXN-NLGN-SHANK pathway (shown in Fig 1.2) is required during the stabilization period of a synapse in response to neuronal activity. In the subsequent sections of this chapter, we have focused mainly on *NRXN* and *SHANK* family in the context of autism and synaptic function.

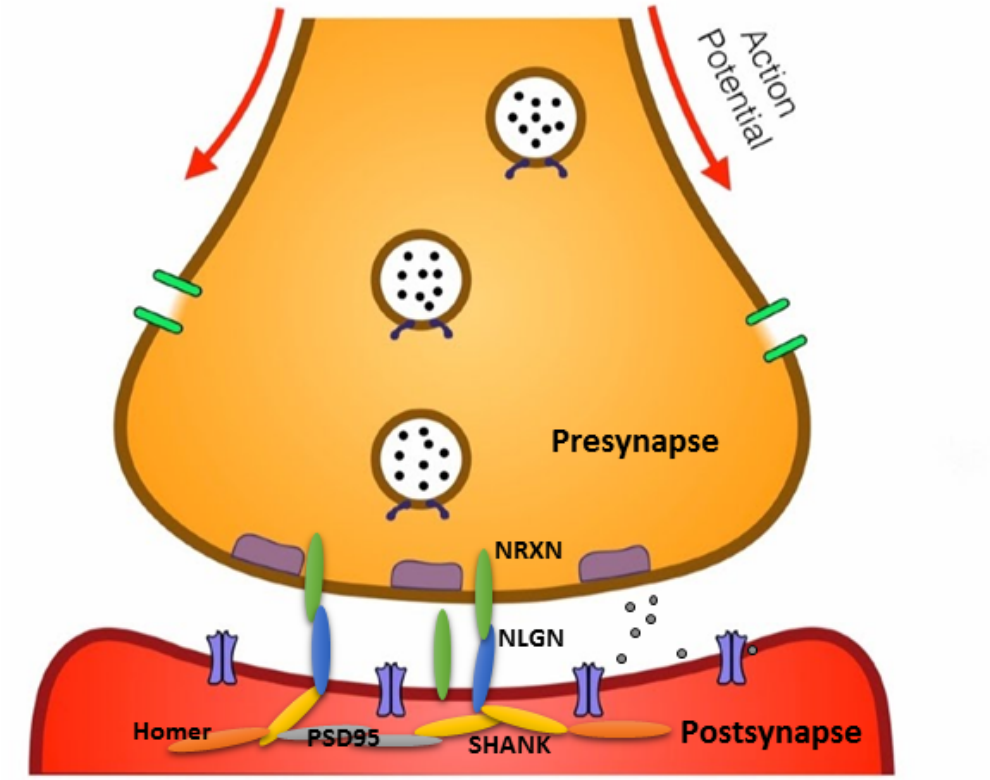

Figure 1-2 NRXN-NLGN-SHANK complex at the Synapse

A schematic representation of presynaptic cell adhesion molecule NRXN1 binding to its postsynaptic binding partner NLGN which interacts with SHANK, PSD95, HOMER and other postsynaptic density proteins to form a trans-synaptic complex at the synapse (Based on Monteiro and Feng, 2017).

1.3.4 Synaptic genes

Autism is detected at an early stage of life, usually within three years of age, when key synaptic connections are formed (Huttenlocher and Dabholkar, 1997). Multiple studies have reported that mutations in genes like *TSC1/2*, *FMR1*, *UBE3A*, *MECP2 NRXN*, *NLGN* and *SHANK* converge at cellular and molecular pathways related to the synapse (Stessman et al., 2017; Wang T. et al., 2016). These genes mostly encode proteins involved in synaptic transcription and translation, cell adhesion molecules, scaffold proteins. *TSC1* and *TSC2* genes encode protein products hamartin (TSC1) and tuberin (TSC2) respectively which bind together and inhibit the activity of mTOR complex. Mutations in *TSC1/2* genes results in disinhibition of mTOR resulting in tuberous sclerosis complex (TSC) which is characterised by formation of hamartomas in multiple organs, epilepsy, intellectual disability and autism. 40% patients with TSC are estimated to be affected by autism (Richards et al., 2015). *FMR1* gene encodes Fragile Mental Retardation Protein (FMRP), an mRNA binding translational inhibitor and is involved in modulating synaptic plasticity (Davis and Broadie, 2017). Fragile X Syndrome is a syndromic and monogenic form of autism and the most common cause of intellectual disability caused by loss of FMRP. 16–45% of female and 60–74% of male Fragile X Syndrome patients meet the diagnostic criteria of autism (Klusek et al., 2014). *UBE3A* gene which is located in an imprinted region on chromosome 15q11-q13 encodes Ubiquitin-protein ligase E3A (UBE3A) protein involved in proteasomal degradation. Mutations in of maternally expressed *UBE3A* gene leads to Angelman Syndrome characterised by intellectual disability, microcephaly, speech impairment and autism. Loss of function of UBE3A results increase in synaptic turnover and dysregulation of synaptic development and function. 1-3% of autism cases worldwide have been estimated to be caused by duplication or triplication of maternally inherited 15q11-q13 (Hogart et al., 2010; LaSalle et al., 2015). Mutations in genes encoding

cell adhesion complex NRXN1/NLGN and scaffold protein SHANK3 are also key players in autism pathophysiology and are discussed in subsequent sections 1.4 and 1.5 respectively.

1.4 *NRXN1*

1.4.1 *NRXN1* structure and function

The gene *NRXN1* encodes a member of the neurexin family of proteins which is well known for its function in vertebrate nervous system ranging from synapse formation, development and synaptic signalling (Reissner et al, 2013). *NRXN1* spans 1.12 Mb on the mammalian genome i.e. ~ 0.1% of the entire human genome and is one of the largest genes with 23 exons (Rowen et al, 2002.). *NRXN1* encodes the protein Neurexin1 which is translated from three major isoforms *NRXN1α*, *NRXN1β* and *NRXN1γ*. These isoforms of *NRXN1* are transcribed under the control of independent promoters (Ulrich et al, 1995). *NRXN1α* isoform is transcribed from a promoter at the 5' end of the gene, whereas the promoter for the *NRXN1β* isoform is located downstream of exon 17. Genetic variations and microdeletions relating to psychiatric conditions are interestingly found to affect the *NRXN1α* promoter more frequently rather than the *NRXN1β* promoter (Tabuchi et al, 2002; Missler et al, 2003; Jenkins et al, 2014).

Historically, the discovery of neurexins occurred more than a decade ago when these proteins were identified to be located at the synapse and as receptors for α-latrotoxin, a neurotoxin that induces vesicular release of neurotransmitters (Ushkaryov YA et al, 1992). Neurexin1 was found to be enriched at the presynaptic terminal such as the growth cone (Dean et al, 2003). Further studies reported that *NRXN1* mRNA was widely expressed in pre- and postnatal brains, and *NRXN1β* is particularly enriched in cognition related brain areas such as cortical plate, thalamus and hippocampus (Harkin et al, 2017; Puschel et al, 1995). These findings confirm the pivotal roles of *NRXN1* in mammalian neurophysiological processes. The studies on the distinct protein structures of neurexin1 isoforms helped us further understand its

biological function. Neurexin1α isoform has three epidermal growth factor (EGF)-like domains, six extracellular Laminin G domains, binding domains for laminin, neurexins and sex hormones referred to as LNS and PDZ binding domain in its cytoplasmic tail, as shown in Fig 1.3. On the other hand, the extracellular LNS domain and the carboxy terminal domain are present in neurexin1β isoform. The neurexin1γ is the shortest of the three isoforms and lacks all EGF-like and LNS domains and it has only the transmembrane region and cytoplasmic tail (Yan et al, 2008). Additionally, neurexin1α and neurexin1β both have extracellular glycosylated regions, which bind to heparan sulfate to form proteoglycans which contribute to the synaptic development (Zhang P et al, 2018). A range of ligands such as neuroligin, leucine-rich repeat transmembrane neuronal protein (LRRTM), neuroxophilin, dystroglycan, latrophilin, and cerebellin bind to the extracellular LNS domain of neurexin1α and neurexin1β. Therefore, neurexin1 can mediate critical synaptic functions by forming trans-synaptic complex by binding to its postsynaptic binding partners. The PDZ-binding domain of neurexin1 is also crucial for binding and recruitment of presynaptic scaffolding proteins such as spinophilin, Syd-1 and Cbln1 at the synaptic density (Zhang B et al, 2017; Muhammad K et al, 2015). Genetic mutations and deletions in *NRXN1* have been frequently linked to the impairment of such synaptic structure and functions and reported to play pathophysiological roles in a diverse range of psychiatric conditions and neurological disabilities, such as schizophrenia, epilepsy and Alzheimer's disease (Rujescu et al, 2009; Dabell et al, 2013; Moller et al, 2013; Swaminathan et al, 2012; Duong et al, 2012; Bena et al, 2013; Kirov et al, 2009; Ikeda et al, 2010).

1.4.2 *NRXN1* and risk of autism

Multiple cohort studies have reported loss of function variants of *NRXN1* in individuals affected by autism (Marshall et al., 2008; Morrow et al., 2008; Glessner et al., 2009). A wide array of

neurodevelopmental disorders including intellectual disability without autism (Camacho-Garcia et al., 2012; Yangngam et al., 2014), language impairments, dysmorphic features and dystonia (Ching et al., 2010) and neuropsychiatric conditions like Schizophrenia (Rujescu et al, 2009; Kirov et al, 2008; Walsh et al 2008) have been identified in individuals with mutations or deletions in *NRXN1*. However, variants of other members of *NRXN* family, *NRXN2* and *NRXN3* are much rarer but several studies have found evidence of association of these two genes with autism and other neurodevelopmental and neuropsychiatric conditions (Gauthier et al., 2011; Vaags et al., 2012; Yuan et al., 2018). In a candidate gene study, two missense mutations linking *NRXN1* with autism was identified disrupting known neuronal functions of β-neurexins (Feng et al, 2006). The involvement of *NRXN1* in autism was confirmed when Autism Genome Consortium screened 1181 families with at least two individuals diagnosed with autism and discovered a hemizygous deletion disrupting the coding regions of the gene (Autism Genome Project C, 2007). Subsequently, independent studies reported disruption of *NRXN1* exon (Kim et al, 2008) and ultra-rare structural variants of *NRXN1* (Yan et al, 2008) associated with autistic individuals. Around the same time, several common variants in *NRXN1* was also identified to be associated with autism. Single nucleotide polymorphisms (SNPs) were indicated to be linked with autism pathogenesis in a large GWAS study (Wang et al, 2009). In a Chinese cohort, *NRXN1* variants were screened and a synonymous mutation rs2303298 was found to be significantly associated with autism (Liu et al, 2012). However, further investigations are needed to decipher the involvement of common variants of *NRXN1* in autism. Larger studies have generated accumulating evidence of linking *NRXN1* deletions and copy number variants (CNVs) with autism risk and pathophysiology (Glessner et al, 2009; Marshall et al, 2008; Ching et al, 2010; Pinto et al, 2010; Wisniowiecka-Kowalnik et al, 2010; Camacho-Garcia et al, 2012; Iossifov et al, 2012; Prasad et al, 2012; Girirajan et al, 2913; Walker et al, 2013; De Rubeis et al, 2014). Additionally, impairments in *NRXN1* in smaller family studies

with autistic probands have further confirmed its involvement in autism (Duong et al, 2012; Wisniowiecka-Kowalnik et al, 2010; Kong et al 2012; Jiang et al, 2013; Imitola et al, 2014); especially in affected individuals with more severe clinical symptoms (Dabell et al, 2013; Bena et al, 2013; Schaaf et al, 2012; Koshimozu et al, 2013; Vinas-Jormet et al, 2014). More recently, a number of investigations have reported consistent evidence of different types of genetic disruptions in *NRXN1* contributing to autism pathophysiology (Li et al, 2016; Williams et al, 2018).

Presynaptic Nrxn binds to its postsynaptic interacting partner Nlgn to form neurexin-neuroligin complex, which is critical for synaptogenesis and synaptic signalling (Craig and Kang, 2007). Neuroligins (Nlgns) are a family of cell adhesion molecules on postsynaptic membrane encoded by four genes (*NLGN1*, *NLGN2, NLGN3* and *NLGN4*) in human genome. Nlgn binds to Nrxn1 through laminin/neurexin/sex hormone (LNS) binding domain and the Nrxn-Nlgn complex recruits synaptic receptors and scaffolding proteins to facilitate synaptic assembly and maturation (Krueger et al., 2012; Reissner et al., 2013; Sudhof, 2017). Nlgn1 is expressed exclusively in excitatory glutamatergic synapses and preferentially binds to PSD-95, whereas Nlgn2 is present in inhibitory synapses and interacts with Gephyrin (Song et al., 1999; Varoqueaux et al., 2004). Nlgn3 and Nlgn4 are reported to be expressed in both types of synapses (Budreck and Scheiffele, 2007). NRXN or NLGN overexpression can increase synapse number leading to alteration of excitation-inhibition (E/I) ratio (Chih et al., 2004; Chubykin et al., 2007; Dahlhaus et al., 2010). Balance of excitation and inhibition, E/I ratio, is known to be a key regulator of neural circuit development and synaptic plasticity, and its alterations may cause disruptions in information transfer and social functioning leading to a number of neurodevelopmental conditions including autism (Gatto and Broadie, 2010; Nelson and Valakh, 2015).

1.4.3 Synaptic role of *NRXN1*

Impairment of synaptic function and disruption of structural plasticity have been implicated as recurrent pathophysiology in many neuropsychiatric conditions (Penzes et al, 2011; Forrest et al, 2018). Cell adhesion molecule Nrxn1 has two distinct roles at the synapses: 1) formation and organisation of synapse and 2) synaptic signalling and plasticity. Presynaptic Nrxn1 has been reported as a key protein responsible for organising synaptic architecture by binding to presynaptic and postsynaptic ligands to form trans-synaptic signalling complex. The first characterised postsynaptic interacting partners of Neurexin1 are neuroligins (Ichtchenko et al, 1995; Sudhof, 2008). As briefly mentioned in the previous section, presynaptic Nrxn1 binds to Nlgns to form heterophilic Ca^{2+}-dependent trans-synaptic complex across the synaptic cleft to mediate synaptic signalling (Arac et al. 2007; Chen et al, 2008; Comoletti et al, 2007; Fabrichny et al, 2007; Miller et al, 2011). The LNS domain of Nrxn1 plays key role in such complex formation between Nrxns and Nlgns (Graf et al, 2004; Reissner et al, 2008), which leads to pre- and postsynaptic specialisation and promotes both GABAergic and glutamatergic synaptogenesis (Graf et al, 2004; Nam et al, 2005).

Nrxn1 also plays an important role in synaptic signalling by modulating the presynaptic release of vesicles. Nrxn1α deficient neurons demonstrate a reduction in excitatory synaptic strength and neurotransmitter release probability, thereby altering the E/I balance (Etherton et al., 2009; Pak et al., 2015). Nrxn1α acts as a positive modulator of Ca^{2+} influx through CaV2.1 pore-forming subunits in the process of synaptic vesicle release from the presynaptic terminal (Brockhaus et al., 2018) and this mechanism is mediated specifically by N- and P/Q type Ca^{2+} channels (Tong et al, 2017; Zhang et al, 2005; Brockhaus et al, 2018). Nrxn1α-deficient human neurons also show increased CASK, a binding partner of Nrxn and scaffolding protein which is implicated in several brain abnormalities, mental retardation and autism (Najm et al., 2008; Hackett et al., 2010). Moreover, Nrxns trigger the recruitment and stabilisation of several

receptors such as AMPAR, NMDAR and $GABA_AR$, thereby playing a critical role in synaptic transmission and plasticity (Sudhof 2008; Tong et al, 2015; Mondin et al, 2011; Barrow et al, 2009). Mouse studies show that deletion of *NRXN1α*, or triple knockout of all three Nrxn1βs cause a reduction in miniature excitatory spontaneous current (mEPSC) frequency, without altering the miniature inhibitory spontaneous current (mIPSC) (Etherton et al, 2009; Anderson et al, 2015). Moreover, triple knockout of all three *NRXNα*s in neocortical slice cultures lead to decrease in AMPA-mediated mEPSC and $GABA_A$-mediated mIPSC (Missler et al, 2003). Consistently, such reduction in mEPSC is also observed in human embryonic stem cell derived induced neurons bearing *NRXN1* heterozygous conditional mutations (Pak et al, 2015).

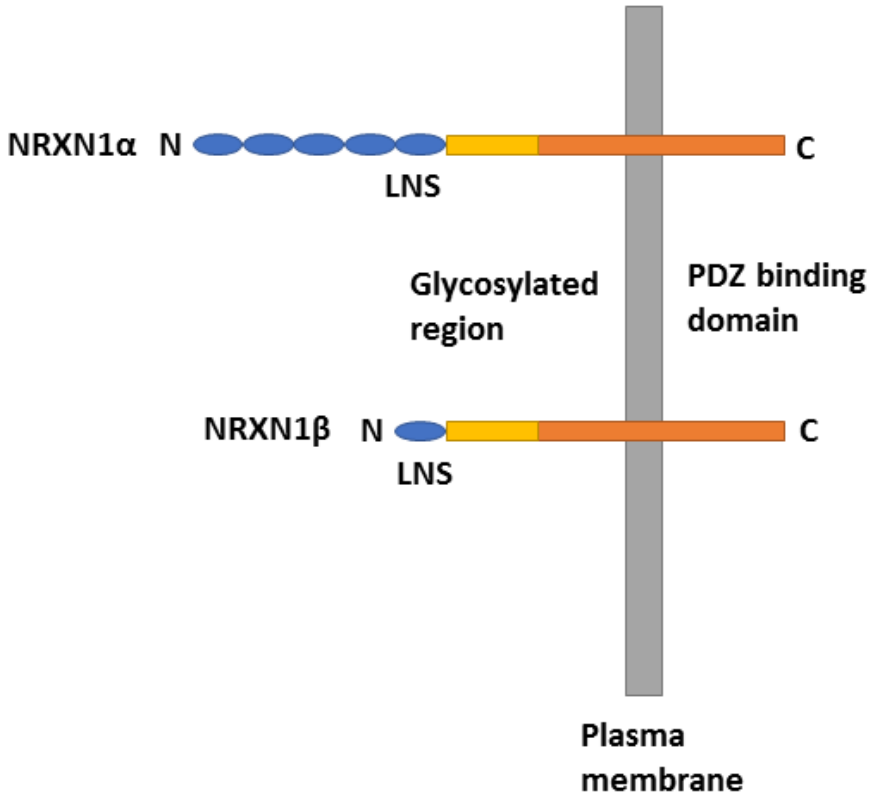

Figure 1-3 NRXN1 protein structure on presynaptic membrane

NRXN1 has two major isoforms: NRXN1α and NRXN1β. NRXN1α has several LNS (protein-binding domains for laminin, neurexins, and sex hormones) domains, a highly glycosylated region, and a PDZ domain-binding motif wheras Neurexin 1-β has one single LNS domain and identical sequence as neurexin 1-α at their C terminus (Adapted from Hu et al, 2019).

1.5 *SHANK3*

1.5.1 *SHANK3* structure and function

The *SHANK3* gene consists of 22 exons and encodes a multidomain protein that contains ankyrin repeats (ANK), an Src homology 3 (SH3) domain, a postsynaptic density 95/discs large/zone occludens-1 (PDZ) domain, a proline-rich region, a homer-binding region, a cortactin-binding region and a sterile alpha motif (SAM) (Urchino et al, 2013; Naisbitt et al, 1999). *SHANK3* is abundantly expressed in the heart and moderately expressed in the brain and spleen (Lim et al, 1999). In the brain, *SHANK3* is mainly expressed in neurons, especially in their synapses, and acts as a scaffolding protein in its interactions with various synaptic molecules, including with the N-methyl-D-aspartate receptor (NMDA-R) via the post-synaptic density-95 (PSD-95)/guanylate kinase-associated protein (GKAP) complex, the metabotropic glutamate receptor (mGluR) via Homer, and the GluR1 a-amino-3-hydroxy-5-methyl-4-isoxazole propionic acid receptor (AMPA-R) (Sheng et al, 2000; Bockers et al, 2004; Uchino et al, 2006).

Various transcriptional studies have deduced the gene structure of *SHANK3*, for both mouse and human (Bonaglia MC et al., 2006; Wang et al., 2011; Boeckers TM et al., 1999). mRNA studies (Durand et al., 2007; Wang et al., 2011; Maunakea et al., 2010) have reported the existence of six isoforms, as shown in Fig 1.4 in both human and mouse. An interesting phenomenon is that different autistic individuals have different mutations in *SHANK3* gene, these could be isoform specific. For instance, a splicing mutation in intron 5 encoding the N terminal ANK repeats would only affect *SHANK3* isoforms a and b. Other deletions, in exons1-9, will affect different isoforms of *SHANK3*. Thus, we could propose that isoform specific disruption of *SHANK3* could lead to different phenotypic effects. This could also explain clinical heterogeneity seen in autistic individuals with *SHANK3* deletions.

In adult neurons, actin participates in the formation and dynamics of pre- and postsynaptic structural integrity (Cingolani et al, 2008). Therefore, it is not a surprise that, in many neurodevelopmental and neurodegenerative disorders, actin structure and dynamics are altered. For example, in case of autism, a dysregulation of scaffolding proteins as well as receptors, signaling molecules, small GTPases, and actin dynamics in the postsynaptic density (PSD) is observed (Bourgeron, 2009). Shank (SH3 domain and ankyrin repeat containing protein) proteins (alternatively known as ProSAP, proline-rich synapse associated protein), a family comprised of 3 members, are major scaffolding proteins found in PSDs of many excitatory (mainly vGluT1 positive) synapses (Heise et al, 2016) and have been associated with autism (Guilmatre et al, 2014). Mutation or deletion of Shank proteins leads to alteration in NMDA and AMPA receptor trafficking, actin remodeling, and/or alteration in synaptic signaling, in particular mGluR5 signaling, in several *in vitro* and mouse models (Jiangand et al, 2013). There is a dynamic interplay between SHANK3 and actin via proteins that attach directly or indirectly to actin. For instance, Densin -180 binds to the SH3 domain and N terminal ANK domain of SHANK3 protein antagonizes dendritic branching. SHANK3 binds to C terminus of Densin-180 making the PDZ domain of Densin-180 inaccessible to δcatenin, which binds with Densin-180 and is required for the formation of new branches (Quitsch et al., 2005). Thus, suggesting that SHANK3 plays a role in maintenance of dendritic morphology. Alpha fodrin interacts with the ANK domain of SHANK3 and helps regulate F actin elements in the spines (Bocker et al., 2001). There is also evidence to suggest that actin cytoskeleton is remodeled upon synaptic activity though a number of small signaling molecules such as Rho GTPases (Sarowar et al, 2016). A recent study (Kathuria et al, 2018) has shown significant decrease in both F and G actin in hypothalamic neurons derived from iPSCs of shank3 patients compared to healthy. This suggests that Shank3 patient neurons have a deficit in both the amount of G and F actin which might account for the reduction in synaptic puncta density.

1.5.2 Rodent models of *SHANK3*

Most of the known function of *SHANK3* has come from studying mice engineered to comprehend the role of *SHANK3* in autism. Five lines of *SHANK3* mutant mice carrying different deletions in the *SHANK3* gene have been generated (Wang et al., 2011; Yang et al., 2012; Bozdagi et al., 2010; Peca et al., 2011; Schmeisser et al., 2012). Three of these carry deletions in the N terminal ankyrin domain (ANK); the homozygous deletion of exon4-9$^{-/-}$ (Wang et al (2011); the heterozygous deletion of exon4-9$^{+/-}$ (Bozdagi et al., 2010) and a homozygous deletion in exon4-7$^{-/-}$ (Peca et al 2011). Peca et al (2011) also made a *SHANK3* mutant line with homozygous deletion in exon13-16$^{-/-}$, which encodes for PDZ domain, while Schmeisser et al (2012) made mutant mice with a homozygous deletion in exon11$^{-/-}$ that encodes for SH3 domain. Since, *SHANK3* plays a major role in cytoskeleton modeling of the neuron, the neuronal structure was examined in these *SHANK3* mutant mice models. The neuronal structure of medium spiny neurons in the striatum brain slices was analyzed in exon13-16$^{-/-}$ mice and an increase in dendritic length and arborization was reported (Peca et al., 2011). Furthermore, they examined PSD thickness and length, which were both decreased, suggesting that *SHANK3* helps in the development of the PSD. Spine length was increased and spine density was decreased in the hippocampus of exon4-9$^{-/-}$ mice (Wang et al., 2011) and similar observations were observed in exon13-16$^{-/-}$ mice, where spine density was decreased in the striatum (Peca et al., 2011). Neuron morphology has not been examined in any of the other mutant mice (Jiang et al., 2013). From the above studies we can reflect that *SHANK3* through its various cytoskeleton binding partners regulates neuronal and spine morphology. Another example of morphological changes to neurons was reported by Durand et al (2012), where they introduced two inherited deletion variants of *SHANK3* and two de novo mutations

of *SHANK3* were transfected into rat hippocampal neurons. The inherited mutations (R12C and R300C) caused a decrease in spine density, while the two de novo mutations (truncating mutation STOP and ankyrin domain mutation Q321) decreased the development of dendritic spines and inhibited growth cone motility. They proposed that the mechanism by which *SHANK3* regulated spine formation was through F actin polymerization, as discussed above. They overexpressed wild type *SHANK3* in rat hippocampal neurons and this led to an increase in spine density and the same spines showed co-localization of SHANK3 with F actin. Hence, suggesting that SHANK3 binds to F actin to regulate spine formation. Thus, the morphological analysis of SHANK3 in mutant mice revealed that *SHANK3* plays a complex role in synapse development particularly, its shape, size and structure.

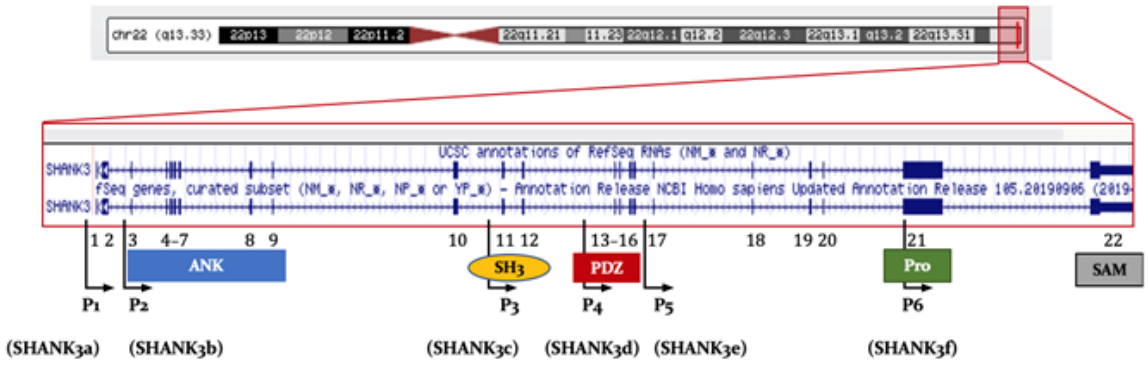

Figure 1-4 Isoforms of mouse *SHANK3*
The mouse SHANK3 has 22 exons (conserved in humans) which encode six SHANK3 isoforms. The arrows show transcription start sites from a number of promoters. Different regions of the gene encode for different binding domains such as Ankyrin, SH3, PDZ, Proline-rich and SAM. (Adapted from Jiang and Ehlers, 2013)

1.5.3 Human models of *SHANK3*

Haploinsufficiency, or loss of one copy of *SHANK3*, in humans is known to cause a rare neurodevelopmental condition characterized by global developmental delay, speech delay, intellectual disability, poor motor coordination and autism, also known as Phelan McDermid Syndrome (PMDS) or 22q13 deletion syndrome (Phelan and McDermid, 2011; Bonaglia et al, 2001; Wilson et al, 2003, Sarsua et al, 2014; Costales Jesse et al., 2015). Although the overall prevalence of PMDS is estimated as 1% of autism cases, there have been over 2000 cases identified worldwide until December 2018, according to the Phelan–McDermid Syndrome Foundation. PMDS is now considered to be a relatively common cause of autism and intellectual disability, accounting for between 0.5 % and 2.0 % of cases. The cause of PMDS has been isolated to loss of function of one copy of *SHANK3*, which codes for a master scaffolding protein found in the postsynaptic density of excitatory synapses. One of the few penetrant genes reported to be implicated in autism is *SHANK3* (Betancur et al., 2013). Several studies have claimed that *SHANK3* has the highest penetrance rate in monogenic cause of autism (Kolevzon A et al., 2011; Nemirovsky et al., 2015; Bentancur et al., 2013). Mutations in *SHANK3* gene are highly penetrant and the vast majority of individuals carrying a mutation in this gene develop severe cognitive deficits. Several studies have been published to document small deletions and mutations that affect only *SHANK3* on chromosome 22, and result in a similar phenotype, including autism and intellectual disability (Soorya et al, 2013; Durand et al, 2007; Moessner et al, 2007; Gauthier et al 2009; Boccuto et al, 2013). Several different mutations and deletions have been reported in autism cases. For example, Moessner et al (2007) a missense mutation in exon 8 while Bonaglia et al (2001) describes a mutation that disrupts exon 21 of the *SHANK3* gene. The first subject in Moessner's study has a verbal repetitive behaviour, understands complex instruction and has no motor disorder while in Bonaglia's study the affected individual has severe language delay, mental retardation and hypotonia.

Although the individuals with autism have deletion in the same gene, the clinical symptoms are highly heterogeneous. This could be due to the different *SHANK3* isoforms that are disrupted by each mutation.

A burning issue is to understand the common pathophysiology that underlies autism, as this will help us develop better diagnostic tools and drugs to treat or prevent the disease. Studies on *SHANK3* mutant mice have provided somewhat overlapping but not identical phenotypes indicating, cellular disruption which leads synaptic dysfunction. However, this is still not robust enough because of the variability between mice models probably reflecting the heterogeneity of mutations studied. Thus, there is a need to study specific *SHANK3* mutations that correspond to the mutations that occur in humans and are known to cause autism. One way of doing this would be to study these *SHANK3* mutations in human cellular models. These studies could help us understand the cellular pathway that forms the basis of autism. Among the various synaptic genes deleted in autism, *SHANK3* is considered the most likely candidate for causing the neurological abnormalities observed in affected individuals (Scheglovitov et al., 2013). This study found that iPSC-derived PMDS neurons have a reduced expression of SHANK3 and impaired excitatory synaptic transmission. Both amplitude and frequency of mEPSCs were significantly reduced and synaptic puncta staining revealed a decrease in both pre- and post-synaptic puncta, suggesting that there were fewer synapses in these neurons. Interestingly, these phenotypes could be rescued by treating the neurons with *SHANK3* overexpression.

1.6 Cellular Model

1.6.1 hiPSC model

Most of our knowledge on synaptic pathologies in brain disorders are either based on evidence from studies on post-mortem samples or from animal models. The scarcity of brain tissue sample and the fact that it precludes the analysis of dynamics of synaptic events makes it

unsuitable for most studies. On the other hand, animal models present with another set of major drawbacks. With the first establishment of human induced pluripotent stem cell (iPSC) technology (Takahashi et al, 2007) opened new avenues towards generation of human cellular models to study neuropsychiatric conditions. iPSCs could be generated by reprogramming human fibroblasts with a combination of transcription factors such as *Oct3/4, Sox2, Klf4,* and *c-Myc* (Park et al., 2008; Takahashi et al., 2007) or Oct4, Sox2, Nanog, and Lin28 (Yu et al., 2007). There are several advantages of using iPSC model and neurons derived from iPSCs over rodent models, especially in the context of understanding neurodevelopmental conditions (Shen et al, 2019). First of all, the use of rodent system is limited to the interpretation of human neuropsychiatric conditions involving genotype-phenotype relationships because of the fundamental differences in developmental patterning and neuronal characteristics between human and rodent neurons. Besides, the composition of synapses and post synaptic density proteins are also significantly different between human and rodent brains as elucidated by mass spectrometry (Bayés et al., 2012). Human iPSCs is provides an unprecedented opportunity to study patient specific mutations or deletions with specific genetic background which is not possible to explore in mouse models with genetic manipulations. iPSC derived neurons are mostly advantageous in studying complex neuropsychiatric conditions such as autism and schizophrenia, which may not have a clear genetic or epigenetic factor identified (Maki et al., 2005; Chaste and Leboyer, 2012; Karimi et al., 2017; Chen et al., 2018) and also for patient-specific drug screening and human clinical trials due to low effectiveness and toxicity in animal models (Tall et al., 2007; Kira, 2017).

1.6.2 Neuronal differentiation

Several neuronal differentiation protocols for generating neurons from human iPSCs help scientists to study specific neuronal subtypes in health and disease states (Cho et al., 2008; Fasano et al., 2010; Kriks et al., 2011; Shi et al., 2012; Chambers et al., 2012; Ma et al., 2012).

Shi et al 2012, reported a differentiation method that could generate all three classes of excitatory projection neurons that form glutamatergic synapse. The iPSC derived excitatory neurons showed first spontaneous activity at post induction day 28 and synchronous activity starting from day 58 in culture (Kirwan et al., 2015). Several other studies have also established three dimensional (3D) neuronal cultures from NPC or rosette aggregates to mimic the brain environment (Mariani et al., 2012; Hogberg et al., 2013; Gouder et al., 2015; Hookway et al., 2016; Chandrasekaran et al., 2017).

1.6.3 Transcription factor reprogramming

There were two major limitations of neuronal differentiation approach of generating neurons from iPSCs. First, differences among particular pluripotent cell lines; therefore, neurons derived using the same protocol from multiple lines showed distinct characteristics (Wu et al., 2007; Hu et al., 2010). Secondly, it was cumbersome, time consuming to generate mature functional neurons which rendered large scale studies extremely difficult (Johnson et al., 2007). To overcome these major drawbacks of neuronal differentiation protocol, Zhang et al., 2013, established a lentiviral overexpression system of transcription factor *NGN2* which was sufficient to drive pluripotent cells to excitatory functional neurons within 2-3 weeks' time. This protocol was further refined by using stable gene targeting of *rtTA* and *NGN2* in genomic safe harbour (GSH) sites of a Tet-ON system by Pawloski et al, 2017. This inducible overexpression system of *NGN2* transcription factor forward programming of pluripotent stem cells, also referred to as OPTI-Ox, set up a robust platform for rapid generation of homogenous populations of excitatory neurons displaying neuronal morphology and expressing pan-neuronal markers βIII-Tubulin and MAP2 after week 1 (Pawloski et al, 2017). However, the functional electrophysiological properties of this system were not investigated which has been carried out for the first time in this thesis work.

1.7 Aims and Hypotheses

Human iPSC technology has paved the way for studying cortical development and its dysfunctions in neurodevelopmental conditions including autism (Vitrac and Cloëz-Tayarani, 2018). With the advent of rapid neuronal induction protocols using overexpression of single transcription factor *NGN2* it is now possible to characterise cellular phenotypes in a relatively shorter time frame of few weeks (Zhang et al, 2013, Pawlowski et al, 2017). Our first aim was to study and characterise iNeurons derived by *NGN2* overexpression for autism related gene expression and relevant electrophysiological parameters. Secondly, this thesis is aimed at understanding the disruptions in autism related key synaptic genes *NRXN1* and *SHANK3* by utilising the advantages of such technological advancement.

1.7.1 Hypothesis 1 (Chapter 3)

The first hypothesis of this thesis was that iNeurons would express autism related genes, post synaptic density molecules and synaptic receptors during neuronal induction until day 21. The rationale behind choosing a 3-week time course is that the first report using *NGN2* overexpression system (Zhang et al, 2013) showed that within 2-3 weeks iNeurons mature and can be used for synaptic assays. A combination of gene expression and imaging methods were used to characterise iNeurons in this section.

1.7.2 Hypothesis 2 (Chapter 4)

The second hypothesis of this thesis was that iNeurons derived by *NGN2* OPTi-OX forward programming approach would show mature electrophysiological activity relevant for studying autism related functional phenotypes. The aim was to study the electrophysiological properties of iNeurons using multi-electrode arrays since spiking and bursting properties are hallmark of a developing cortex and disruptions may lead to several neuropsychiatric conditions including autism (Kirwan et al, 2015).

1.7.3 Hypothesis 3 (Chapter 5)

The third hypothesis was that transient knockdown of *NRXN1* or *SHANK3* would alter the electrophysiological properties of control iNeurons. A siRNA mediated knockdown approach was adopted for understanding whether presynaptic *NRXN1* or postsynaptic *SHANK3* molecules may alter the functional properties in this cellular model.

1.7.4 Hypothesis 4 (Chapter 6)

The fourth hypothesis was that iNeurons with deletions in *NRXN1* or *SHANK3* derived from individuals with autism would show altered morphological and electrophysiological cellular phenotypes. A combination of imaging analyses and multi-electrode array experiments were conducted to characterise autism iPSC derived iNeurons to address this hypothesis.

1.7.5 Thesis Structure

The empirical chapters (Chapter 3 to Chapter 6) in this thesis are arranged in the same order as the hypotheses (1 to 4) outlined above. Chapter 3 and Chapter 4 can be seen as thematically complementary as they are aimed at understanding autism related gene expression patterns and relevant functional electrophysiological properties of iNeurons as a cellular model. Subsequently, in Chapter 5 the functional phenotype of *NRXN1* and *SHANK3* are reported by manipulation by siRNA mediated knockdown in control iNeurons. Chapter 6 is focussed on understanding morphological and electrophysiological properties in iNeurons derived from iPSCs generated from autistic individuals with deletions in *NRXN1* or *SHANK3*. In Chapters 3 to 5, iNeurons have been derived using the *NGN2* OPTi-OX forward programming (Pawlowski et al, 2017) approach, whereas the lentiviral *NGN2* overexpression (Zhang et al, 2013) method is used in Chapter 6 for inducing iNeurons from multiple iPSC lines with individuals with autism. The switching of the protocol has been done under the assumption that overexpression of transcription factor *NGN2* will yield iNeurons with similar functional properties. Hopefully the results from these chapters will expand our current understanding of autism related cellular phenotypes due to disruptions in *NRXN1* and *SHANK3* genes and pave the way for future

investigations using iNeurons as an *in vitro* model system for characterising cellular phenotypes in neurotypical and neurodevelopmental conditions.

2 Chapter 2: Materials and methods

2.1 hiPSC culture

2.1.1 hiPSC cell lines

Human induced pluripotent stem cell (hiPSC) lines from healthy controls and individuals clinically diagnosed with autism bearing mutation or deletion in autism related synaptic scaffold genes *NRXN1* and *SHANK3* were used in this study. **Table 2.1** lists the control and autism hiPSC lines. Genetic information and clinical description of *NRXN1* and *SHANK3* autism subjects and iPSC lines are described in Chapter 4 and Chapter 5 respectively. The autism lines were generated and characterised for quality control at our collaborators, Prof Jack Price and Dr Deepak Srivastava's labs at King's College London (Cocks et al., 2014; Kathuria et al., 2018; Adhya et al., 2020).

Table 2.1 hiPSC lines used in this study

Groups	Name used	iPSC line name	Condition
1. Control lines	C1	Bob	Healthy control
	C2	Kolf	Healthy control
2. Neurexin1 lines	NXM	109NXM	~60 kb deletion (male)
	NXF	092NXF	~200 kb deletion (female)
3. Shank3 lines	S3M	114SM	SHANK3 deletion (male)
	S3F	S3F107	SHANK3 deletion (female)

2.1.2 hiPSC maintenance

HiPSCs were grown feeder-free in commercial E8 media or StemFlex E8, containing Penicillin-Streptomycin (100x). Cells were kept in a humidified incubator at 37°C and 5% CO2. The medium was changed every day for E8 and every other day for StemFlex E8 and cells were passaged every 4-6 days depending on confluency. For passaging, the medium was removed, washed once with Dulbecco's PBS (dPBS) and cells were incubated in dPBS-EDTA

for 2-4 minutes, depending on the cell line. Subsequently, the solution was aspirated, and cells were detached by forcefully releasing 1 ml of plain DMEM with a p1000. This was repeated until most of the cells were detached. With a 5ml stripette, cells were transferred to a 15 ml tube (Falcon) containing 5mls of DMEM. Cell clumps were allowed to settle for about 5 minutes and the supernatant was aspirated. The cell pellet was then re-suspended in fresh E8 medium and pipetted up and down twice with a p1000. Cells were then plated onto tissue-culture treated plates (Corning) that were coated with vitronectin (10 µg/ml) (StemCell Tech) at room temperature for 1 hour. The splitting ratio was usually between 1:10 and 1:20.

2.2 iNeuron culture

2.2.1 Ngn2 overexpression: gene targeting

The hROSA26 locus was targeted using a CRISPR/Cas9 gene editing system while the AAVS1 with a zinc finger gene editing system. For both loci, gene targeting was accomplished by nucleofection. At least 7 hours prior to nucleofection, cells were fed with maintenance media supplemented with Rock-inhibitor (10µm). On the day of nucleofection, cells were dissociated into single cells with StemPro Accutase for five minutes. Two million cells were used in a 100µl total volume and 12µg of DNA (two plasmids, each carrying guides or zinc fingers for the 5' or 3' end of the locus and the donor plasmid; 4µg of each plasmid). Nucleofections were performed using the Lonza P3 Primary Cell 4D-Nucleofector X Kit and the cycle CA-137 on a Lonza 4D-Nucleofector System, according to manufacturer's instructions. Subsequently, the cells were seeded onto 2 vitronectin-coated 10cm plates at a density of 1 million cells per plate, in cloning medium that consisted of P/S-free E8 media and CloneR (StemCell Technologies). Cells were left in cloning medium for 48 hours, before a full medium change with cloning medium (E8 supplemented with P/S was used here onwards). The following day, the medium was exchanged cloning medium with 25% of the initial concentration of CloneR. The day after,

use of CloneR in the medium was ceased and antibiotic selection was initiated using, either 100 µg/ml of G418 (Thermo Scientific) for hROSA26 targeting or 1µg/ml of puromycin for AAVS1 targeting. G418 selection proceeded for at least 5 days and puromycin selection was carried out for at least two days. Colonies were picked and expanded after around 10-14 days of culture. Clones were then screened for correct targeting by PCR. Genomic DNA was isolated using the Wizard Genomic DNA Isolation Kit (Promega) according to manufacturer's instructions. The PCR was performed with LongAmp Polymerase (NEB) according to the following protocol:

PCR grade H2O	4.1 µl
100% DMSO	0.2 µl
10 mM dNTPs	0.3 µl
5x buffer	2.0 µl
Primer F (10 µM)	0.5 µl
Primer R (10 µM)	0.5 µl
DNA (50 ng/µl)	2.0 µl
LongAmp Polymerase	0.4 µl

Through gel agarose electrophoresis, PCR products were then analysed for size against a 1 kb Hyperladder (BioLine). The genotyping strategy carried using a list of primers described in Table2.2.

Table 2.2 List of primers for genomic PCR

Locus	PCR type	Primer	Primer location	Primer sequence	Amplicon ctr	Amplicon target	Amplicon plasmid
AAVS1	WT (locus)	FW	Genomic; 5' to 5' HAR	CTGTTTCCCCTTCCCAGGCAG	1692 bp	Variable; missing if using CAG promoter (GC-rich)	no band
		REV	Genomic; 3' to 3' HAR	TGCAGGGGAACGGGGGCTCA			
AAVS1	5'INT	FW	Genomic; 5' to 5' HAR	CTGTTTCCCCTTCCCAGGCAG	no band	1103bp	no band
		REV	Puromycin	TCGTCGCGGGTGGCGAGGCGCACCG			
AAVS1	3'INT	FW	NGN2 cds 3'end	AGCTGCACTTTATCGCCCG	no band	1282 bp	no band
		REV	Genomic; 3' to 3' HAR	TGCAGGGGAACGGGGGCTCA			
AAVS1	5' BB	FW	Backbone; 5' to HAR	ATGCTTCCGGCTCGTATGTT	no band	no band	1227 bp
		REV	Puromycin	TGAGGAAGAGTCTTGCAGCTC			
AAVS1	3' BB	FW	NGN2 cds 3'end	AGCTGCACTTTATCGCCCG	no band	no band	2036 bp
		REV	Backbone; 3' to 3' HAR	ATGCACCACCGGGTAAAGTT			
ROSA	WT (locus)	FW	Genomic; 5' to 5' HAR	GAGAAGAGGCTGTGCTTCGG	2186 bp	Variable; missing if using CAG promoter (GC-rich)	no band
		REV	Genomic; 3' to 3' HAR	ACAGTACAAGCCAGTAATGGAG			
ROSA	5'INT	FW	Genomic; 5' to 5' HAR	GAGAAGAGGCTGTGCTTCGG	no band	1264 bp	no band
		REV	Splice acceptor	AAGACCGCGAAGAGTTTGTCC			
ROSA	3'INT	FW	rTTA	GAAACTCGCTCAAAAGCTGGG	no band	1807 bp	no band
		REV	Genomic; 3' to 3' HAR	ACAGTACAAGCCAGTAATGGAG			
ROSA	5' BB	FW	Backbone; 5' to HAR	CGTTGTAAAACGACGGCCAG	no band	no band	1148 bp
		REV	Neomycin	GTGCCCAGTCATAGCCGAAT			
ROSA	3' BB	FW	rTTA	CTGGCACGTGAAGAACAAGC	no band	no band	1752 bp
		REV	Backbone; 3' to 3' HAR	TGACCATGATTACGCCAAGC			

Ngn2 hiPSCs were grown in colonies as described in 2.1.2. Then, they were dissociated into single cells using StemPro Accutase for 4 minutes and seeded (100 000 cells per well of a 12 well plate) onto Geltrex-coated plates. Cells were seeded in E8 media supplemented with 10 μM of ROCK-Inhibitor. Differentiation was initiated 24 hours after seeding. For the first two days of differentiation, cells were switched to **iN Induction media** consisting of: DMEM F12 (Gibco). N2 supplement (100x, Gibco), Glutamax (100x, Gibco), Non-essential amino acids (100x, Gibco), 2-Mercaptoethanol (50 μm, Gibco), Penicillin-Streptomycin (100x).Media was supplemented with dox (1 μg/ml) and changed daily. For subsequent differentiation and maintenance of neurons, cells were switched to **iN Maintenance media** consisting of: Neurobasal (Gibco), B27 supplement (100x, Gibco), Glutamax (100x, Gibco), 2-Mercaptoethanol (50 μm, Gibco), Penicillin-Streptomycin (100x). Media was supplemented with dox (1 μg/ml), NT3 (10 ng/ml) and BDNF (5 ng/ml) and changed daily. Full media changes were performed until day 3 post-induction. There onwards, half-media changes were performed every other day. Dox was withdrawn from day 7 onwards.

2.2.2. *NGN2* overexpression: lentiviral method

All lentiviral cell culture procedures were conducted at biosafety level-2 (BSL-2) cell culture facility following standard safety guidelines. For lentiviral particle production, HEK293T cells were first seeded in T175 flasks in normal growth medium (DMEM high glucose, sodium pyruvate, 10% FBS, 1% Pen/Strep) and incubated overnight at 37 °C with 5% CO2. The following day when cell confluency reached 85-95% transfection with CaCl2 precipitation method was performed. Dharmacon Trans-Lentiviral packaging kit containing packaging plasmids were used with CaCl2 and 2xHBSS following the manufacturer's protocol. FUdeltaGW-rtTA (Addgene plasmid 19780) and plV-TetO-hNgn2-eGFP-puro (addgene plasmid 79823) were used as lentiviral transfer vectors separately for packaging (kind gift from

Sudhof and Wernig lab). The mixture of plasmids and reagents were added dropwise on confluent layer of HEK293T cells and incubated at 37 °C with 5% CO2 for 10-16 hours. After >16 hours the medium was replaced with reduced serum medium (High Glucose DMEM, 5% Fetal Bovine Serum, 2 mM L-glutamine, 1% Pen/Strep) and incubated for an additional 48 hours. Thereafter, the media containing lentiviral particles was harvested by several rounds of centrifugation at 4 °C. Non-adherent cells and debris were pelleted down by centrifugation at 1600 × g at 4 °C for 10 minutes. The supernatant containing virus was aspired and passed through a sterile, 0.22-0.45 μM low protein binding filter by centrifugation at 4000 rpm at 4 °C for an hour. The highly concentrated viral particles were then tittered, aliquoted and stored at -80 °C.

hiPSCs were dissociated on Day (-2) and plated as single cells with ROCK-inhibitor on matrigel coated plates at a density such that the confluency reaches 80-90% on the following day. On Day (-1) the lentivirus particles (rtTA and hNgn2-eGFP-puro) were used to transduce the iPSC cells. After 16-18 hours, on Day0 the induction was initiated by removing the virus-containing media and adding N2 media with Doxycycline, BDNF, NT-3, and laminin (Pak et al. 2018). On Day 1-2, the media was supplemented with puromycin for 24-48 hours for selection of transduced cells. At this stage the GFP expression could be visualised to assess transduction and antibiotic selection efficiency. Rat astrocytes were added on Day3 and the cells from this stage onwards could be maintained with neuronal maintenance media consisting of Neurobasal (Gibco), B27 supplement (100x, Gibco), Glutamax (100x, Gibco), 2-Mercaptoethanol (50 μm, Gibco), Penicillin-Streptomycin (100x). Media was supplemented with dox (1 μg/ml), NT3 (10 ng/ml) and BDNF (5 ng/ml). Dox was withdrawn from day 7 onwards. All assays on i-Neurons thus generated were performed from this stage following the timepoints Day7, Day14, Day21, Day28 and Day35 for different assays and experiments.

2.2.3. Primary rat astrocyte culture

Primary mixed glial cultures were derived from P0-P2 neonatal Sprague Dawley rats and were generated along the previous guidelines (McCarthy & de Vellis, 1980), with minor modifications. The pups were euthanized following Schedule 1 rules and regulations from the Home Office Animal Procedures Committee UK (APC). To maintain aseptic conditions, all procedures were performed in a laminar flow hood. A horizontal flow hood was used to perform dissections and a vertical flow hood for tissue culture. In brief, the meninges, midbrain and olfactory bulbs were removed, and dissociated rat neonatal cortices cut thoroughly and incubated at 37°C for 30 min in Minimum Essential Medium Eagle (MEM) containing 4% Papain, 1% of 4 mg/mL DNase I Type IV and 1% of 24 mg/mL L-cysteine (Figure 1). After the digestion step the dissociated cells were plated into poly-D-lysine (PDL) coated cell culture flasks at a density of 2 brains/T75 flask. These mixed glia cultures were cultured for 10 days in Dulbecco's Modified Eagle's Medium (DMEM) supplemented with 10% FBS (Fetal Bovine Serum) and 1%Pen/Strep and kept under a humidified atmosphere at 37°C and 7% CO2. Rat astrocytes, suspended in iN Maintenance media supplemented with dox, were added to iNeuron cultures on day 3, at a 1:1 ratio. On day 5, medium was supplemented with 2 μM of Ara-C, to inhibit astrocyte proliferation**.** Cultures were maintained in iNeuron maintenance media and Dox was withdrawn from day 7 onwards.

2.2.4 iNeuron culture on MEAs

For cultures on MEA, the MEA plates were coated with 100ug/ml of poly-D-lysine (PDL) for 1 hour at 37°C. After 3 washes with sterile water, they were air-dried in a Class II safety hood and sterilised under a UV light for 30 minutes. Then, a 20μl drop of laminin (20 μg/ml; Sigma) was placed in the centre of the plate, so that it only covered the electrode surface. It was then left to incubate at 37°C for 30 minutes. Then, Day 3 iNeurons were dissociated and mixed with

rat astrocytes at a ratio of 1:1 for a final total concentration of 4000 cells/µl. For seeding, cells were maintained in iN Maintenance media supplemented with 10 µM Rock-I and dox. The drop of laminin was then aspirated and replaced with 15 µl of the cell mixture. Cells were allowed to attach for one hour in an incubator at 37°C and 5% CO2, before topping up with iN maintenance medium supplemented with dox. Half-media changes were performed from day 5 onwards, with 2 µM Ara-C being added to the medium on Day 5 to inhibit astrocyte proliferation. Dox was withdrawn from Day 7 onwards.

2.3 Molecular Biology

2.3.1. Real time quantitative PCR

To determine gene expression, RNA was isolated from cultured cells using the GeneElute Mammalian total RNA kit (Sigma-Aldrich) and additional on-column DNAse digestion (Sigma-Aldrich) was performed to avoid contamination of genomic DNA. The concentration and quality of the isolated DNA was evaluated by NanoDrop (Thermo Fisher). 500 ng of RNA was then

used to generate cDNA with Maxima First Strand Synthesis Kit (Thermo Fisher, K1672). The resulting cDNA solution was then diluted 1:15 in DEPC treated water. Real-time qPCR reactions were composed of 3 µl of diluted cDNA, 2.5 µl of fast reagent mix (Applied Biosystems 4385614), 4.1 µl water (DEPC treated) and 0,2 µl of each, forward and reverse primers. Samples were run on the Applied Biosystems 7500 fast PCR machine. All samples were analysed in technical duplicates and normalized to the house-keeping gene Porphobilinogen Deaminase 1 (PBGD1). Primers were designed to have an annealing temperature close to 60ºC, generate amplicons between 70bp and 200bp in size and were blasted against the human genome to exclude amplification of genomic DNA and were ordered from Sigma.

2.3.2 Western blotting

Further analysis of protein expression was performed by western blot. CellLytic M(Sigma-Aldrich) with addition of complete Protease Inhibitor (Roche) was used to prepare the protein lysates. After quantification (Protein Quantification Kit- Rapid, Sigma-Aldrich), electrophoresis was run on 4-12% NuPAGE Bis-Tris Precast Gels (Invitrogen) and NuPAGE LDS Sample Buffer (Invitrogen). The proteins were transferred on PVDF with the NuPAGE Transfer Buffer (Invitrogen). 4% milk in PBS 0.05% Tween (PBST2) was used to block the membrane for 1 hour at room temperature. Primary antibodies were incubated overnight in PBST2 and 4%milk. Subsequently, the membranes were washed thrice with PBST2 and incubated with the horseradish peroxidase (HRP)-conjugated secondary antibody (Sigma-Aldrich) again in 4% milk PBST2. After another three washes in PBST2, the membranes were incubated in Pierce ECL2 Western Blotting Substrate (Thermo) and visualised on X-Ray Super RX Films (Fujifilm).

2.3.3 siRNA knockdown

ThermoFisher predesigned siRNA were used for knockdown experiment using Lipofectamine RNAiMAX as transfection reagent following the manufacturer's protocol. iNeurons at day 27 were incubated with siRNAs in the following three conditions: scrambled negative control siRNA (siRNA ID 4390843), *NRXN1* siRNA (siRNA ID s17948) and *SHANK3* siRNA (siRNA ID s533055). The incubation time was 72 hours following which multi-electrode array recordings were carried out on transfected cells.

2.4 Imaging

2.4.1 Live cell imaging

Time lapse imaging of i-neurons over 15 days were carried out using an automatic robotic cell chamber and bright field microscope in Nikon Biostation. Cells were fed with neuronal maintenance media on every alternative day and images were acquired from the same fields of view as coordinates set initially over the entire time course at an interval of every hour. The images were used to make time lapse video with ImageJ software for visualisation.

2.4.2 Immunocytochemistry

Prior to immunocytochemistry, cells were washed in PBS to remove debris and medium and fixed in 4 % paraformaldehyde (in PBS) for 20 minutes at room temperature and subsequently washed again in PBS. Then, the cells were blocked and permeabilised in 0.02 % saponin with 10 % normal goat serum (in PBS) for 30 minutes. After that, the cells were incubated with the primary antibodies in 2% goat serum for 2-3 hours at room temperature or at 4°C overnight. After three 5-minute washes with PBS, fluorescent-labelled secondary antibodies in 2% goat serum were added and allowed to incubate at room temperature for 1 hour. Then, cells were given two 5-minute washes with PBS, followed by a 10-minute incubation in 4',6-diamidino-2-phenylindole (DAPI). Lastly, they were washed once with PBS and kept in PBS for imaging. hiPSCs, i-neurons and co-cultures were imaged with EVOS fluorescence microscope and Zeiss LSM700 confocal microscope. All morphological analyses were performed with several plugins such as Simple Neurite Tracer and NeuronJ with the ImageJ software package. All relevant statistical analyses were carried out using GraphPad Prism software.

2.4.3 Morphological analysis

Morphological metrics such as cell soma size and neurite outgrowth were analysed at day 14 iNeurons using ImageJ software, NeuronJ and Simple Neurite Tracer (SNT) plugin (Longair et al, 2011). iNeurons induced from control (Kolf) and four autism iPSC lines with *NRXN1* (NX1M, NX1F) and *SHANK3* (SH3M, SH3F) by transducing with rtTA and NGN2-eGFP

lentiviral particles were analysed on day 14 from at least 45 neurons in each group from three biological replicates. Image to be analysed was opened with SNT plugin and the GFP stained neuron was identified to be traced. To trace each neuronal process, the starting point was selected as the cell body and the furthest point by clicking twice. The software allowed automatic tracing of the length of the neurite and each process were colour coded and measured. The longest process was defined as "primary neurite" or axon and all other processes as "secondary neurites" or dendrites. Number of neurite branches emanating from the cell body were also quantified for each neuron and defined as "branching point". The "total neurite length" was calculated as sum of primary (axonal) and all secondary (dendritic) processes for each individual neuron. Cell soma size was calculated by drawing an ROI along the circumference of each cell body and measuring the selected area by "analyze particles" command. All measurements were exported to a spreadsheet table for further analyses in Prism.

2.5 RNA-seq analysis

Bulk and single cell RNA sequencing data collection was performed by Kaiser Karim, at Dr Mark Kotter's lab and sequenced at Cambridge Stem Cell Institute. Data analysis was performed with in house codes in R statistical package.

2.5.1 Bulk RNA seq

For neurons co-cultured with or without glia, total RNA was isolated in triplicates for each timepoint. For cell lysis and RNA extraction, cells were firstly treated with 5 minutes of StemPro Accutase to detach cells from culture surface and washed once to remove the accutase. Cell pellets were either flash frozen and stored at -80C, or immediately processed for RNA extraction using the Direct-zol RNA Miniprep kit (Zymo Research, R2071). Transcriptome libraries were generated at the Wellcome Sanger Institute with the Illumina TruSeq stranded RNAseq kit. All samples were sequenced using Illumina HiSeq with 40 million mapped reads

on average for each sample. Adapters and basic read quality filter was done using utilities the from the biobambam2 package (Tischler & Leonard, 2014). Reads were aligned using the STAR aligner v 2.5.3a using the GRCh38 genome assembly (Dobin et al., 2013). Reads without a unique mapping location or non-canonical splicing were excluded from the analysis. To generate the gene expression vectors, featureCounts was used from the package, Subread-1.6.3, with the default parameters and the GRCh38.91 gene annotation file. Pre-processing involved removal of non- and low-expressed genes (retained only genes with at least 1 count per million aligned reads in at least 3 of the samples), followed by removal of outlier samples. Additionally, the data was normalized by variance stabilising transformation, using the R package DESeq2 (Love et al., 2014). DESeq2 was also used to perform differential expression (DE) analysis with a minimum |log2 (fold change)| > 2 and false discover rate (FDR) < 0.05. Enrichment analysis of significantly DE genes was carried out using gene ontology collections from the Gene Ontology Consortium (Ashburner et al., 2000; The Gene Ontology Consortium, 2019), where, as background only 17844 protein-coding genes with valid Entrez ID were used. Mixed-species RNA-seq reads from different timepoints (4, 14, and 21 days) were separated to species of origin with the Sargasso pipeline version 2.0.1 (Qiu et al. 2018). Sargasso was run with the "--conservative" option designed by the program authors. Clustered heatmaps were generated using this data set to investigate the relative expression of genes of interest.

2.5.2 Single cell RNA seq

Each sample/timepoint was harvested from one well of a 6-well plate, except for Day 0, 12 hours and 1, which were harvested from 2 wells of 6 well plate. First, media was aspirated from each well and given a gentle one-time wash with dPBS (calcium and magnesium free). For Day 0 (iPSCs that have been seeded and kept in ROCK-I for 24 hours), 12 hours, Day 1, Day 2, Day 3 and Day 4 with and without rat glia co-culture, samples were treated with 1ml/well of plain Accutase for 6 minutes at 37°C. For Days 14 and 21 (with and without glia), samples

were treated with 1ml/well of dissociation solution made up of papain (Worthington) resuspended in Accutase, for a final concentration of 20 U/ml. These late time points were then left in the incubator for 30 minutes at 37°C. A plain rat glia sample that had been cultured with the same culture protocol for iNeurons for up to 21 days, were also treated with this dissociation solution for 30 minutes at 37°C. At the end of their incubation period, 1 ml of dissociation buffer, made up of DMEM/F-12, ROCK-I (10μm) and DNAse 1 (33μg/ml), was added to each well. Then, the cells were dissociated into a single-cell suspension by pipetting up and down with a p1000, at least 5 times, against the culture surface. Cell suspensions were then transferred into a 15 ml falcon tube capped with a 40μm mini-cell strainer (Pluriselect), containing 1 ml of dissociation buffer (2ml for pooled samples). Wells were further washed with 1ml of dissociation buffer and transferred to the falcon tube. Samples were centrifuged at 300g for 3 mins at room temperature. Pellets were then resuspended in 2 ml of resuspension buffer made up of DMEM/F-12, 0.04% BSA and 10μM ROCK-I. Repeat centrifuge at 300g for 3 mins at RT. Finally, pellets were resuspended in 1ml of resuspension buffer and transferred to a 1.5ml Eppendorf tube capped with a 40μm mini-cell strainer, keeping the cells on ice for the rest of the protocol. Cell viability was determined using a Countess II (Thermofisher Scientific), with 4 counts obtained for each sample. The average viability and cell number was determined and recorded for each sample. From this main cell suspension, a 500 cells/ul cell suspension was prepared for each sample and kept on ice for further processing with the Chromium™ Single Cell 3' Reagent Kit (v2) by 10x Genomics.

The Bulk and single RNA sequencing data acquisition was done by my colleague Kaiser Karim at Dr Mark Kotter's lab. I took bioinformatics training at the Downing site, Cambridge to do the analysis. The data analysis was carried out by me with assistance from Kaiser. This particular data set is currently being used by other members of the lab as well to understand iNeurons in various projects.

2.6 Electrophysiology

2.6.1. Calcium imaging

Non-ratiometriic dye Fluo-4 AM was used as calcium indicators in this study to check spontaneous activity in i-neurons at Day 21. i-neurons were grown on PDL/laminin coated coverslips for the calcium imaging assay. The media was washed 3 times with PBS and dye loading solution (Thermofisher live cell imaging solution supplemented with 10 mM d-glucose and 5 µm Fluo-4 AM + 0.02 % Pluranic F-127 vortexed) was added and the cells were kept in dark coldroom for 30-45 mins for optimal loading. Thereafter, the dye loading solution was aspirated and washed with fresh live cell imaging solution and incubated at 37 °C with 5% CO2 for another 15 minutes. The cells were then time-lapse recorded with confocal microscope at 1Hz frequency of acquisition and excitation/emission at 490nm/520nm settings.

The relative fold change in intensity was calculated offline by extracting time series of fluorescence intensity from regions of interest drawn on individual cell bodies in ImageJ software. Spontaneous calcium transients were measured as df/f0 plotted over time and measured by the following formula: df/f0= (F-f0)/f0 where F is the instantaneous fluorescence intensity and f0= min basal intensity. The analysis was done using GraphPad Prism software.

2.6.2 Multi-electrode array (MEA) recordings

The extracellular electrical activity of cultured iNs was recorded using an MEA2100-System (Multichannel Systems, Reutlingen, Germany) with an integrated amplifier. Each 6-well MEA dish (60-6wellMEA200/30iR-Ti, Multichannel Systems) contained 54 electrodes (TiN, 30 µm diameter), with each of the 6 wells containing a grid of 9 electrodes. Recordings started 10min after the MEA plates were placed on the head stage, which was set to 37 °C in a humidified chamber. All MEA recordings were performed in culture medium and each recording lasted

10 minutes. The electric signals were collected at 10 kHz using MCRack (Version 4.4.2; Multichannel Systems) and analysed offline. Spontaneous activity was recorded from Day14 up to Day 35 post-induction. Pharmacological treatment with AMPA antagonist NBQX (2,3-Dioxo-6-nitro-1,2,3,4-tetrahydrobenzo[*f*]quinoxaline-7-sulfonamide, Tocris) and sodium channel blocker TTX (tetrodotoxin, Sigma) were performed on Day30 i-neurons. NBQX and TTX were used at final concentrations of 10 µm and 1 µm respectively. Each individual recording session was of 10 minutes duration followed by washout with medium without drug for another 10 minutes. The software MCRack was used for spike detection. Raw MEA data were first high-pass filtered at 200 Hz to remove low-frequency local field potentials. Spikes were detected using a threshold-based detector set to a downward excursion beyond 3.0 or 4.0 × the standard deviation (calculated from 500 ms of filtered data that did not contain spike activity) above the peak-peak noise level. The filtered data was then analysed using plugins within Neuroexplorer software for further analyses. Spike parameters were used to calculate spike rate or mean firing rate (Hz), mean peak frequency, mean interspike interval (ISI). Bursts of neuronal activity were detected at minimum 3.5 standard deviations threshold and with minimum 3 distinct spiking events. Burst parameters were calculated as burst duration, burst frequency, mean interburst interval and burst surprise. Spike characteristics within burst were described as mean frequency in burst, mean peak frequency in burst, mean ISI in burst and mean spikes in burst. All data analyses were carried out within Neuroexplorer platform and then plotted using GrpahPad Prism software.

2.7 Statistical analyses

The sample size and description of replicates are described in the experimental design section of each Chapter or in the figure legend. Normal distribution of MEA data set was checked using Kolmogorov-Smirnov's test. For all graphs, bars represent the mean average and error bars are presented as standard error of the mean (SEM), unless otherwise mentioned. A one-

way ANOVA was used for comparisons between multiple conditions and Bonferroni's post-hoc test was performed to correct for multiple comparisons of parametric data. The Kruskal Wallis test by ranks with Dunn's multiple comparisons test was performed on non-parametric data. All statistical analyses were done with Graphpad Prism 8.4.3.

3 Chapter 3: Gene expression in iNeurons

3.1 Introduction

The advent of human induced pluripotent stem cells (hiPSCs) (Takahashi et al, 2007) followed by forward cellular programming to forebrain neurons (Habela et al, 2016) have paved the way towards modelling of complex diseases of the nervous system and neuropsychiatric conditions. Rapid generation of neurons and other cell types through forced expression of transcription factors has emerged as a new frontier in the field of disease modelling with hiPSCs. Development of an inducible overexpression system of transcription factor Neurogenin-2 (*NGN2*) to differentiate neurons from hiPSCs is an attempt to overcome some of the challenges such as immaturity of neurons and heterogeneity of cellular populations (Zhang et al, 2013). However, the cellular identity, regional specification, gene expression patterns of induced neurons remain somewhat inconsistent across different neural reprogramming protocols.

Autism is a complex neurodevelopmental condition with several hundreds of genes implicated posing a greater challenge towards cellular modelling due to genetic variability and genes not being fully penetrant for the pathophysiology. A number of synaptic genes such as *NRXN1*, *SHANK3*, *CNTNAP2*, *NLGN3* and *NLGN4* are considered among the top high-confidence genes (SFARI) with gene score 1 (https://gene.sfari.org/autdb/GS_Home.do). Physiological expression of synaptic scaffold and receptor genes are key aspects of typical cortical development especially with respect to early neurodevelopmental conditions. Therefore, robust transcriptomic profiling of induced neurons is of prime importance for reliable *in vitro* modelling of complex brain conditions such as autism.

This chapter reports a characterisation study of gene expression patterns of i-neurons generated through an inducible overexpression system of Ngn2, focussing on key synaptic scaffold and receptor genes that are relevant to cortical development, neurotransmission and synaptic connectivity in autism.

3.2 Aims

1. To characterise gene expression patterns of iNeurons during time course of neuronal induction until day 21

2. To conduct quantitative and unbiased characterisation of cellular heterogeneity in iNeurons

3. To examine whether i-neurons express autism related genes and thus potentially serve as a cellular model to study autism related phenotypes

4. To characterise the gene expression patterns related to several synaptic markers, postsynaptic density molecules and synaptic receptors

3.3 Design

Control bob-Ngn2 hiPSC cells were induced into i-neurons following the neural induction protocol as described in Chapter 2 and gene expression characterised by qPCR, bulk RNA-sequencing and single cell RNA-sequencing data analyses. (**Figure 3.1**). Timepoints for characterisation of transcription were chosen as day 7, day 14 and day 21 based on previous iNeuron study using lentiviral method which showed iNeurons mature within 2-3 weeks' time (Zhang et al, 2013). Live imaging weas performed on iNeurons until day 15. The timepoints for bulk RNA seq data was day 4, day 14 and day 21. The single cell RNA seq data had the following timepoints: 12 hours, 1 day, 2 day, 3 day, 4 day, 14 day and 21 day. All methods and analyses were carried out as described in Chapter 2.

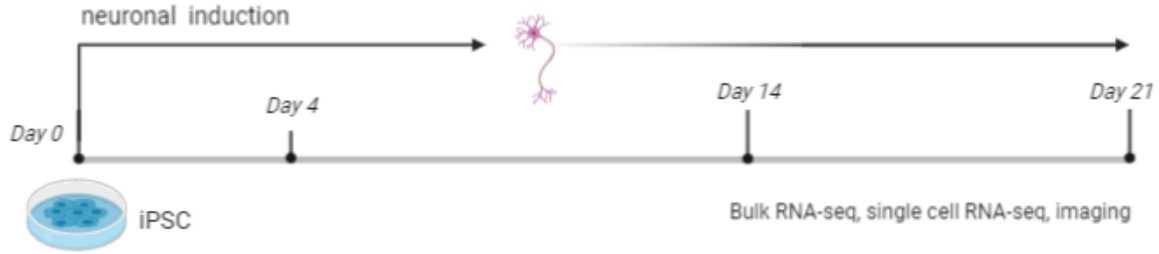

Figure 3-1 Experimental timeline of iNeuron characterisation

3.4 Results

3.4.1 Cellular reprogramming of hiPSCs to hiNeurons

Forward programming (Moreau et al, 2016) is method of combining the principles of hiPSC differentiation and direct cellular reprogramming by overexpressing master transcription factors, for generating human cell types; for example, overexpression of NGN2 transcription factor leads to rapid generation of excitatory cortical neurons (Zhang et al, Pawlowski et al). "OPTi-OX" (optimised inducible overexpression) is such a platform of controllable expression of inducible transgenes using the Tet-ON system (Pawlowski et al). As described in Fig3.2 the Tet-ON system in OPTi-OX strategy consists of two components: 1) a constitutively expressed transcriptional activator, responsive to doxycycline (dox) [reverse tetracycline transactivator (rtTA)];, and 2) an inducible promoter regulated by rtTA [Tet-responsive element (TRE)] that drives the transcription of transgene, such as *NGN2*. The activator rtTA and the responder TRE elements were designed to be targeted sequentially into two distinct gene safe harbour (GSH) sites such as ROSA26 and AAVS1 respectively. Dual GSH targeting has a number of advantages: promoter interference between the two transgenes would not affect inducible overexpression is dual GSH targeting strategy. Secondly, homozygous targeting of transgenes would ensure the maximum number of transgene copies in each safe harbour site. Finally, this strategy allows a larger cargo capacity of each transgene to be inserted thereby making it a flexible and efficient design for large reprogramming cassettes. Thus, OPTi-Ox was devised as an optimised inducible overexpression platform of Tet-ON-controlled transgenes targeted at dual GSHs to develop rapid and deterministic forward programming of mature human cell types from hiPSCs.

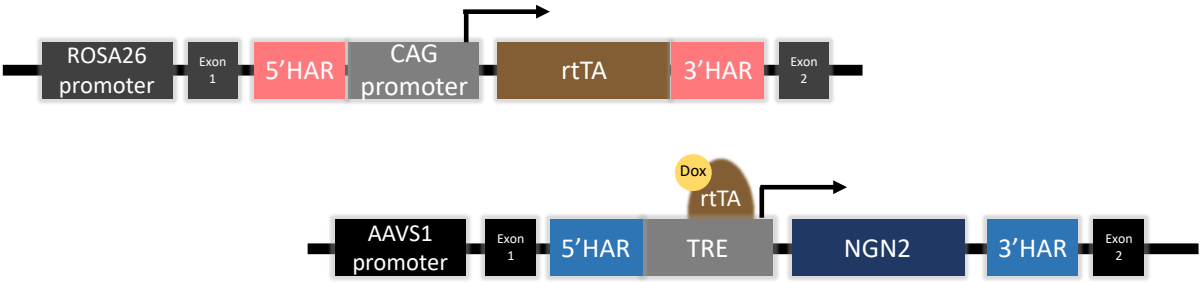

Figure 3-2 A schematic of OPTi-Ox system

A schematic of OPTi-Ox system for inducible overexpression of NGN2 transcription factor for generation of iNeurons from iPSCs

iPSCs with integrated OPTi-Ox NGN2 system were initially examined for pluripotency using the markers OCT4 and TRA-160 prior to neuronal induction [Fig 3.3 (A)]. At day 15 post induction stage, the neurons were seen to be expressing neuronal marker β3-tubulin and synaptic marker Synapsin1 [Fig 3.3 (B)]. To test the efficiency OPTi-Ox NGN2 system we used time-lapse imaging for more than 2 weeks post-induction. Images from the same field of view were taken every hour for the entire duration in a humidified chamber using a Nikon Biostation. The bright field time-lapse images showed that starting from day 1 of induction the *NGN2* i-neurons gradually grow in size, extend their branches and form network like structures by day 12 [Fig 3.3 (C)]. We observed that the neuronal cell bodies tend to clump at around two week time, therefore optimisation of coating substrate such as geltrex, matrigel, PDL-laminin was necessary in an assay dependent manner and primary astrocytes were added to inhibit clumping and to facilitate formation of a single layer of mature iNeurons.

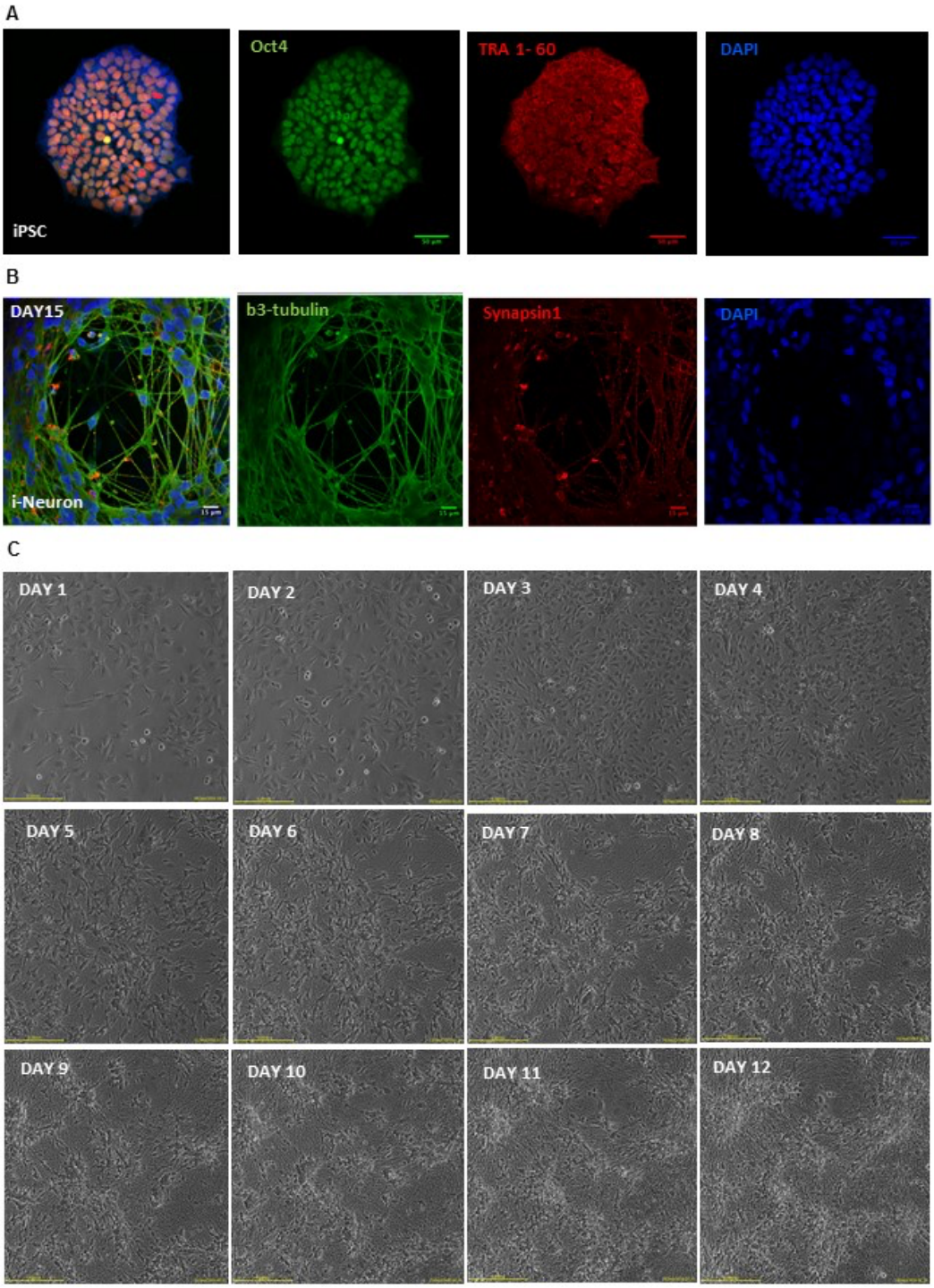

Figure 3-3 Imaging of hiPSC and hiNeurons.

(A) hiPSC colony stained with pluripotency markers. (B) iNeurons stained with neuronal markers at Day15. (C) Time lapse phase contrast images of iNeurons (Day1-Day12).

3.4.2 Cellular identity and heterogeneity of hiNeurons

Single cell gene expression analysis of control *NGN2* i-neurons was conducted at the following stages of induction: early time points (12 hours, 1 day, 2 day, 3 day, 4 day), two week (14 day) and three week (21 day). The clustering of gene expression at different timepoints are colour coded for reference [upper left inset, Fig 3.4 (C)]. To validate the inducible over-expression of Neurogenin-2 we first checked its levels at those timepoints. Figure 3A shows that *NGN2* or NEUROG2 expression increases only after addition of Dox at 12 hours and remains high and stable till day 14 following a decline when the cells are already at a more mature state. A group a Neuronal Progenitor Cell (NPC) markers such as *NES, VIM, MEF2C, PAX6, FABP7, ROR2, SOX2* were found to be mostly expressed at early timepoints 12 hours to day 4 which suggests that the cells were at an NPC state at this period of induction [Fig 3.4 (B)]. Figure 3C shows expression of several developmental stage and brain region markers in NGN2 i-neurons. We observe that pluripotency marker Nanog to be present only at iPSC stage whereas *POU5F1* or *OCT4* until day 3 but absent on the following stages of induction. Neural Stem Cell (NSC) and radial glia markers *SOX2* and *PAX6* were expressed until day 4 and NPC marker Nestin (*NES*) was prevalent only at early timepoints, however Vimentin (*VIM*) was found to be expressed until day 21. The upper layer (layer 2/3) cortical marker *SATB2* expression was totally absent throughout the time course. Surprisingly, deep layer cortical marker *FOXP2* showed up on day 4 and *BCL11B* or *CTIP2* mildly on day 21 in presence of glia which makes it difficult to interpret the cortical regional specificity of *NGN2* i-neurons. Presence of supporting matrix of glia could be crucial in attaining deep layer cortical characteristics. *STMN2* expression, which correlates to neurite outgrowth and length in cortical neurons through stabilisation of microtubule dynamics, was seen to increase steadily until day 21 as the cells matured. A similar pattern of expression was also observed for neuronal growth cone associated *GAP43* which suggests that actin filaments were actively stabilised and neuronal growth enhanced.

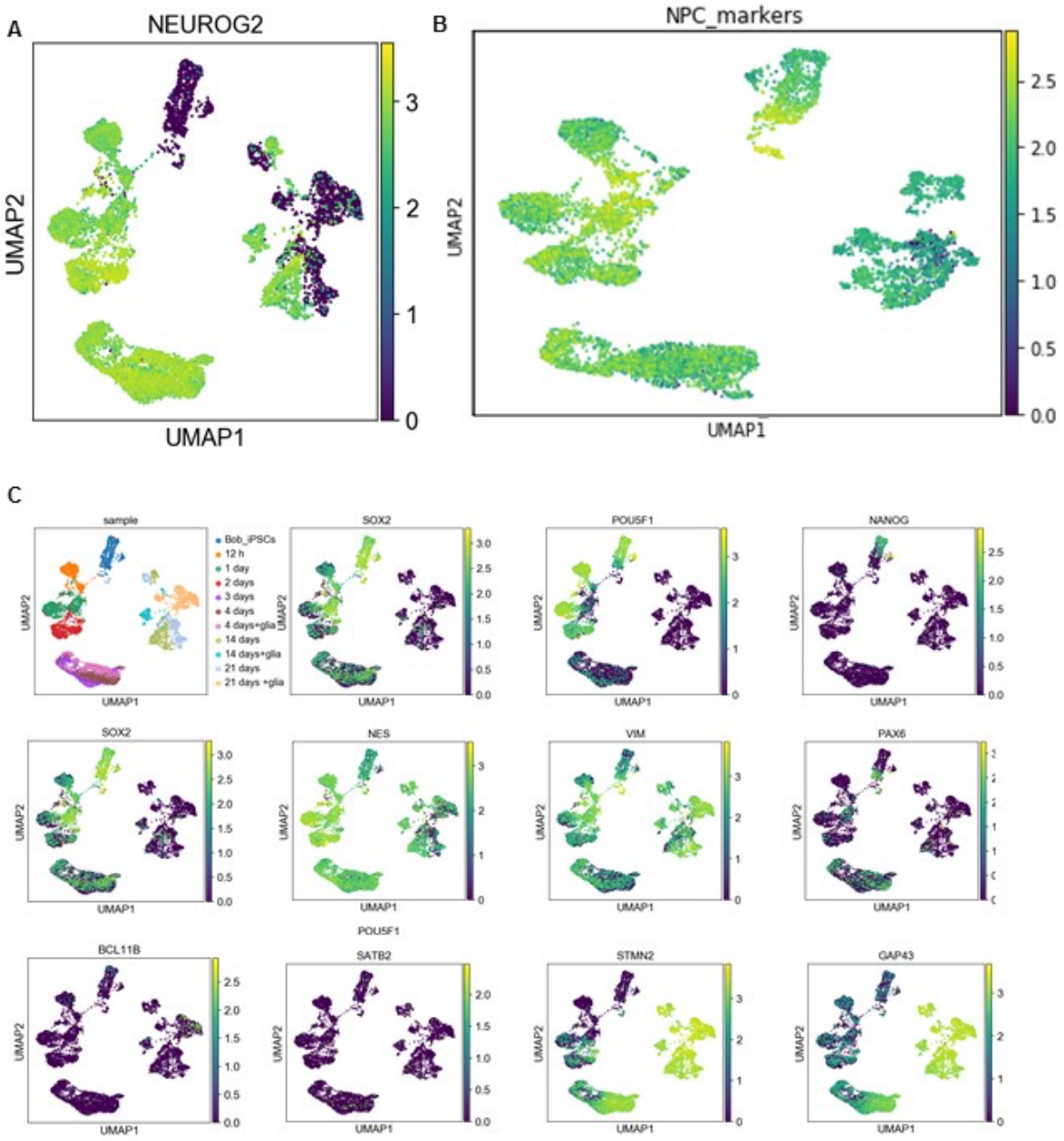

Figure 3-4. Heterogeneity of i-neurons

UMAP profiles from single cell RNA sequencing data showing time-course of expression of (A) Neurogenin2 (NEUROG2) transcription factor (B) Neural progenitor cell (NPC) markers and (C) markers of various cortical layers and developmental stages in neuronal differentiation. Top upper left panel in (C) depict the colour coded timepoints: iPSCs, 12-hour, 1 day, 2 days, 3 days, 4 days, 14 days, 14 days + glia, 21 days, 21 days + glia.

3.4.3 High confidence autism related gene expression pattern

Autism is a complex neurodevelopmental condition with more than 1000 genes implicated in its pathophysiology (Abrahams et al., 2013; Banerjee-Basu et al., 2009). Rare genetic variants, both inherited and *de novo*, are estimated to contribute to 10-13% individuals with autism (Buxbaum et al 2009, Ronemus et al 2014, Sanders et al 2016). According to the Human Gene Module of Simons Foundation Autism Research Initiative (SFARI, https://gene.sfari.org/autdb/GS_Home.do), one of the largest online databases of annotated list of genes studied in the context of autism research, currently 1171 genes have been linked with autism (till April 2020). SFARI Gene platform classifies and scores autism related genes into several categories such as S (syndromic), high-confidence (category 1), strong-confidence (category 2) and suggestive evidence (category 3), based on available scientific data. The 192 high-confidence (category 1) autism genes in this list are the ones that meet the most rigorous threshold of genome-wide significance (at least false discovery rate < 0.1) and are all found on SPARK gene list or recently reported by Satterstrom et al., 2020. Each of these genes has been clearly implicated in ASD—typically by the presence of at least three de novo likely-gene-disrupting mutations being reported in the literature.

Bulk RNA sequencing of control NGN2 i-neurons was conducted in triplicate (A, B, C) at timepoints day 4, day 14 and day 21 with or without glia (Fig 3.5) and heatmap of 192 high-confidence (category 1) autism gene expression was plotted for visualisation of expression patterns. A cluster of genes consisting of *DPYSL2*, *ANK2, DYNC1H1, CTNNB1, ELAVL3, STXBP1, MAP1A, EBF3, HDLBP, SON, KDM5B, DDX3X* was found to be most highly expressed across all three timepoints whereas a cluster of genes such as *ARX, TEK, TBR1, MKX, GFAP, FOXG1* showed the lowest expression. The highly expressed autism-risk genes can be broadly classified into two distinct subgroups based on cellular functions on encoded protein: 1) cell growth and adhesion molecules and 2) transcription and RNA binding

factors. The genes regulating cell growth and adhesion molecules include *DPYSL2* which facilitates neuron guidance, growth and polarity, *ANK2* links actin cytoskeletal molecules, *DYNC1H1* regulates microtuble-associated ATPases, *STXBP1* promotes trafficking of neurotransmitter release, *CTNNB1* mediates cell growth and adhesion and *MAP1A* is involved in microtubule assembly and neurogenesis. The genes encoding transcription factors comprise of *ELAVL3* which regulates neural-specific RNA binding proteins, *EBF3* encodes DNA binding transcription factors, *HDLBP* induce heterochromatin formation, *SON* and *DDX3X* are involved in pre-mRNA splicing and transport and *KDM5B* encodes a histone demethylase. Among the autism risk genes with lowest expression *ARX* and *TBR1* are implicated in normal brain development, *FOXG1* establishes regional subdivision in developing brain, *MKX* plays a role in cell adhesion, *TEK* mediates signalling in vascular development and *GFAP* is an astrocytic marker.

The group of genes with second lowest expression profile consisted of *GABRB2, NR4A2, RORB, GRIN2B, SLC6A1 and KATNAL2*; mostly neuronal receptors which are previously reported to be absent in *NGN2* iNeurons. *GABRB2* and *SLC6A1* are both involved in GABA (gamma-aminobutyric acid) signalling, *GRIN2B* encodes a NMDA receptor subunit, *NR4A2* and *RORB* give rise to are nuclear hormone receptors. *KATNAL2* regulates microtubule reorganisation. Interestingly, a cluster of genes consisting of *NRXN1, RAI1, NLGN2, CIC, ASXL3, NRXN2, ANK3* showed a marked increase in expression on day 14 until day 21. This particular temporal expression pattern of cell adhesion transcripts of *NRXN1, NLGN2, NRXN2* and *ANK3* suggests that these high-confidence autism-risk genes are suitable candidates for modelling autism using NGN2 i-neurons. Another group of genes (*NRXN3, LRRC4C, IQSEC2, PTCHD1, NEXMIF, BCL11A, SCN1A, TSHZ3, DSCAM*) followed the similar profile in increase of expression after day 4, however, not as much as the previously mentioned cluster.

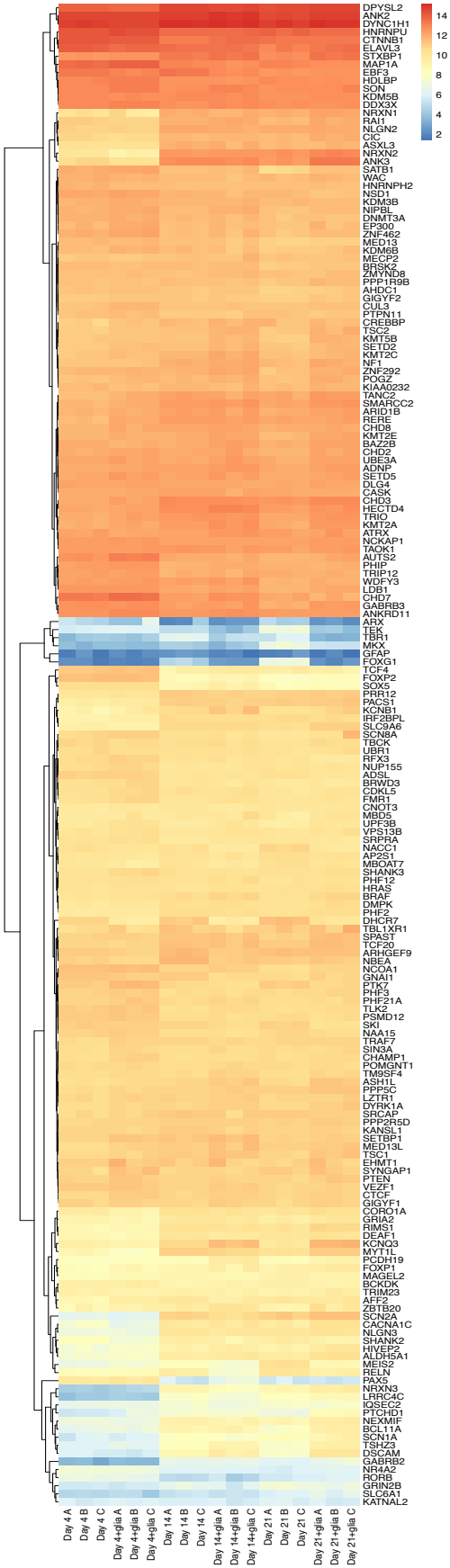
14
12
10
8
6
4
2
DPYSL2
ANK2
DYNC1H1
HNRNPU
CTNNB1
ELAVL3
STXBP1
MAP1A
EBF3
HDLBP
SON
KDM5B
DDX3X
NRXN1
RAI1
NLGN2
CIC
ASXL3
NRXN2
ANK3
SATB1
WAC
HNRNPH2
NSD1
KDM3B
NIPBL
DNMT3A
EP300
ZNF462
MED13
KDM6B
MECP2
BRSK2
ZMYND8
PPP1R9B
AHDC1
GIGYF2
CUL3
PTPN11
CREBBP
TSC2
KMT5B
SETD2
KMT2C
NF1
ZNF292
POGZ
KIAA0232
TANC2
SMARCC2
ARID1B
RERE
CHD8
KMT2E
BAZ2B
CHD2
UBE3A
ADNP
SETD5
DLG4
CASK
CHD3
HECTD4
TRIO
KMT2A
ATRX
NCKAP1
TAOK1
AUTS2
PHIP
TRIP12
WDFY3
LDB1
CHD7
GABRB3
ANKRD11
ARX
TEK
TBR1
MKX
GFAP
FOXG1
TCF4
FOXP2
SOX5
PRR12
PACS1
KCNB1
IRF2BPL
SLC9A6
SCN8A
TBCK
UBR1
REX3
NUP155
ADSL
BRWD3
CDKL5
FMR1
CNOT3
MBD5
UPF3B
VPS13B
SRPRA
NACC1
AP2S1
MBOAT7
SHANK3
PHF12
HRAS
BRAF
DMPK
PHF2
DHCR7
TBL1XR1
SPAST
TCF20
ARHGEF9
NBEA
NCOA1
GNAI1
PTK7
PHF3
PHF21A
TLK2
PSMD12
SKI
NAA15
TRAF7
SIN3A
CHAMP1
POMGNT1
TM9SF4
ASH1L
PPP5C
LZTR1
DYRK1A
SRCAP
PPP2R5D
KANSL1
SETBP1
MED13L
TSC1
EHMT1
SYNGAP1
PTEN
VEZF1
CTCF
GIGYF1
CORO1A
GRIA2
RIMS1
DEAF1
KCNQ3
MYT1L
PCDH19
FOXP1
MAGEL2
BCKDK
TRIM23
AFF2
ZBTB20
SCN2A
CACNA1C
NLGN3
SHANK2
HIVEP2
ALDH5A1
MEIS2
RELN
PAX5
NRXN3
LRRC4C
IQSEC2
PTCHD1
NEXMIF
BCL11A
SCN1A
TSHZ3
DSCAM
GABRB2
NR4A2
RORB
GRIN2B
SLC6A1
KATNAL2
Day 4 A
Day 4 B
Day 4 C
Day 4+glia A
Day 4+glia B
Day 4+glia C
Day 14 A
Day 14 B
Day 14 C
Day 14+glia A
Day 14+glia B
Day 14+glia C
Day 21 A
Day 21 B
Day 21 C
Day 21+glia A
Day 21+glia B
Day 21+glia C

Figure 3-5 Expression pattern of high-confidence autism risk genes

Hierarchical clustering analysis and heatmap visualisation of expression profiles of high confidence autism risk genes in bulk RNA sequencing data at day 4, day 14 and day 21 in triplicates (A, B, C) for each time point. The colour scale represents the scaled abundance of each gene, with red indicating high abundance and blue indicating low abundance.

3.4.4 Synaptic gene expression in iNeurons

Genes conferring risk for autism are often classified as either involved in cortical developmental or synaptic homeostasis (Heavner and Smith, 2020). Multiple studies have revealed that mutations or deletions in genes such as *NRXN, NLGN, SHANK, TSC1/2, FMR1*, and *MECP2* converge on common cellular and molecular pathways that contribute to synaptic development, maturation or maintenance (Guang et al, 2018). Therefore, in order to establish i-neurons as a cellular *in vitro* model for studying autism, we must investigate the key synaptic gene expression in this system. We observed that *NGN2* iNeurons express neuronal marker *MAP2* and synaptic marker Synapsin1 on day 21 through immunocytochemistry [Fig. 3.6(A)]. Next, we investigated the expression profiles of synaptic markers in our single cell gene expression dataset [Fig. 3.6(B)]. Synapsin1, encoded by *SYN1* gene, is a key endogenous substrate for cyclic AMP-dependent and calcium-dependent protein kinases in the presynaptic vesicle that regulates neurotransmitter release (Leenders and Sheng, 2005)]; i-neurons showed an enhanced expression on day 14 onwards, peaking at day 21 which indicates synaptic maturation. Synaptophysin (*SYP*) is the most abundant synaptic vesicle membrane glycoprotein of neuroendocrine secretory granules and its expression was observed to emerge from early timepoints and steadily increasing till day 21. Doublecortin (*DCX*) is a microtubule associated protein expressed by immature developing young neurons during neurogenesis and it showed a similar pattern of gradual increase in expression with highest levels at day 21. However, doublecortin is also suspected to label some mature neurons that require reorganizing their dendritic arbor through microtubule dynamics and thus in adult neurogenesis (Balthazart et al, 2014).

The release of neurotransmitters through docking and fusion of presynaptic vesicles and exocytosis at the synaptic cleft is mediated by SNARE (soluble N-ethylmaleimide-sensitive factor-attachment protein receptors) complexes consisting of key proteins encoded by VAMP2, *STX1A* and *SNAP-25*. *VAMP2* (Vesicle Associated Membrane Protein 2) is a member of synaptobrevin family which is essential for vesicular exocytosis and activity-dependent neurotransmitter release. Together with its interacting partners syntaxin-1A (*STX1A*) and synaptosomal-associated protein 25 (*SNAP25*), *VAMP2* mediates calcium triggered fusion of synaptic vesicles to release neurotransmitters. We observed that *VAMP2* is highly enriched on day 14 and day 21 in the single cell RNA sequencing data set on i-neurons [Fig. 3.6(B)]. *SNAP-25* showed a similar expression pattern though much lower and *STX1A* expression only emerged as late as on day 21. This could possibly mean that fully functional SNARE assembly can form at a later stage of i-neuron induction (day 21) when its key components are expressed. In a physiological context this implies that synaptic neurotransmitter release and neuronal network activity is likely to be established at a mature stage of neuronal development. The violin plot of *VAMP2, STX1A* and *VAMP2* expression from the same data set demonstrate that within the culture there are two distinct populations of neurons expressing these genes and their relative abundance alter in the course of induction [Fig. 3.6(C)]. For example, some neurons at earlier timepoints (until day4) show low levels of *VAMP2* expression but as the neurons mature, increasingly more cells tend to be expressing the *VAMP2* at a higher level thereby altering its relative abundance in the population of cells. *STX1A* and *SNAP25* both show similar expression profiles though unlike *VAMP2* two distinct populations always coexist until day 21.

As presynaptic vesicle release is an essential biological mechanism for synaptic homeostasis in mammalian brain, so is the formation and maintenance of postsynaptic density across the synaptic cleft. The postsynaptic density (PSD) is a large protein complex composed

of more than 1,000 proteins including scaffold proteins, membrane receptors, signalling molecules and cytoskeletal components. In the human cortex, most excitatory glutamatergic synapses are located on small protrusions along dendrites, called dendritic spines and Homer is one of the most abundant scaffold proteins in the PSD which regulates the maturation of dendritic spines along with its interacting partners thereby facilitating synaptic plasticity.

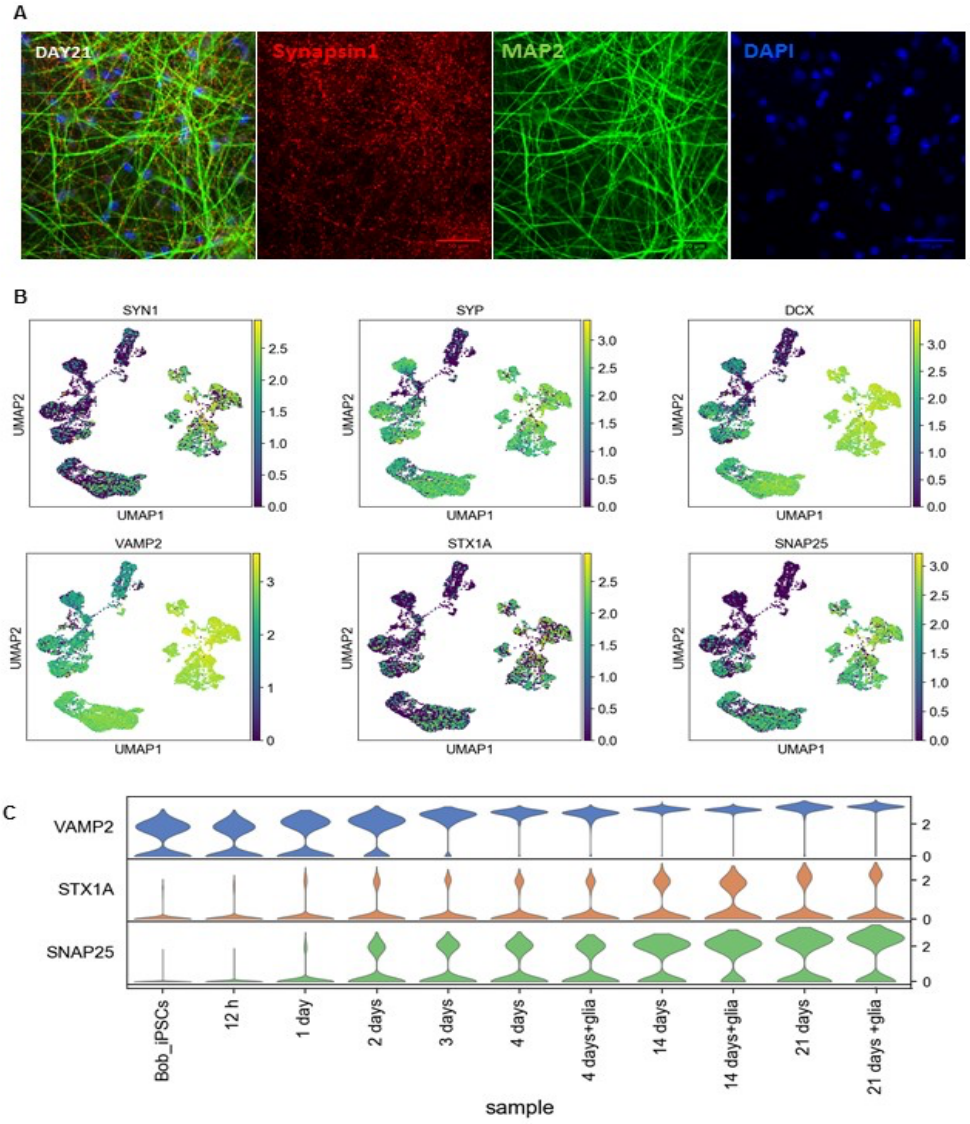

Figure 3-6. Expression of synaptic markers in iNeurons.

(A) Confocal images of Day 21 i-neurons expressing Synapsin1 and MAP2. (B) UMAP profiles of single cell RNA sequencing analysis of several synaptic markers (C) Violin plots of key regulators of SNARE complex at iPSC stage, induction of 12-hour, 1 day, 2 day, 3 day, 4 day 14 day, 14 day+glia, 21 day, 21 day+glia.

In order understand the development of PSD in i-neurons, we chose Homer1 as a reference gene and investigated the expression of its key interacting partners in the PSD complex. The comparing the different clusters of gene expression at different timepoints in the single cell RNA sequencing data set [Fig. 3.7(A)], we found that Homer1 is most abundant at day 21 [Fig. 3.7(B)]. Interestingly, Homer1 was found be present on day 21 only when i-neurons were cultured in presence of glia which underlines the importance of non-neuronal supporting cells in culture for proper maturation of PSD proteins. This was validated through imaging protein expression of Homer1 on day 21 i-neurons [Fig. 3.7(E)]. Next, we looked at the physiologically interacting partners of Homer1 using a widely used online database STRING (https://string-db.org/) for functional protein association network [Fig. 3.7(C)]. The top 20 interacting partners of Homer1 were found to be *GRM5, GRM1, HOMER2, SHANK1, HOMER3, DLGAP1, DLG4, SHANK2, DLG2, DLGAP3, DLG3, DLGAP2, NLGN1, DLGAP4, NLGN3, NLGN2, NLGN4X, NRXN1, NRXN3* and *NRXN2* in decreasing order of predicted functional association score [Fig. 3.7(D)]. At the PSD, Homer binds to Shank scaffold proteins and actin cytoskeletal elements and interact with metabotropic glutamate receptors working synergistically for formation of dendritic spines (Sala et al., 2001). Surprisingly, *SHANK s*caffold proteins (*SHANK1, SHANK2, SHANK3*) and metabotropic glutamate receptors (*GRM1, GRM5*) were observed to be lowly expressed in the i-neurons though isoforms of Homer1 (Homer2, Homer3) were abundantly present [figure citation?]. Members of disk large homolog family such as *DLG2, DLG3* and *DLG4*, which are mainly associated with NMDA receptor mediated signalling and synaptic plasticity were also showed low expression profile except for *DLG4*. This might be due to the reason that i-neurons do not express NMDA receptors and mediate neuronal signalling mainly via AMPA receptors. Most of the disk large associated proteins (*DLGAP1, DLGAP2, DLGAP3*) which mediate organisation of synaptic

architecture and neuronal signalling were found to be poorly expressed in i-neurons though *DLGAP4* was abundant across timepoints. However, neurexin family of cell adhesion molecules (*NRXN1, NRXN2, NRXN3*) were abundantly expressed day 14 onwards. The neuroligins, interacting partners of neurexins, such as *NLGN1, NLGN2, NLGN3* and *NLGN4X* mostly followed the same pattern of same expression which indicates that neurexin-neuroligin complex formation and signalling is most likely to occur in i-neurons after 2 weeks of induction.

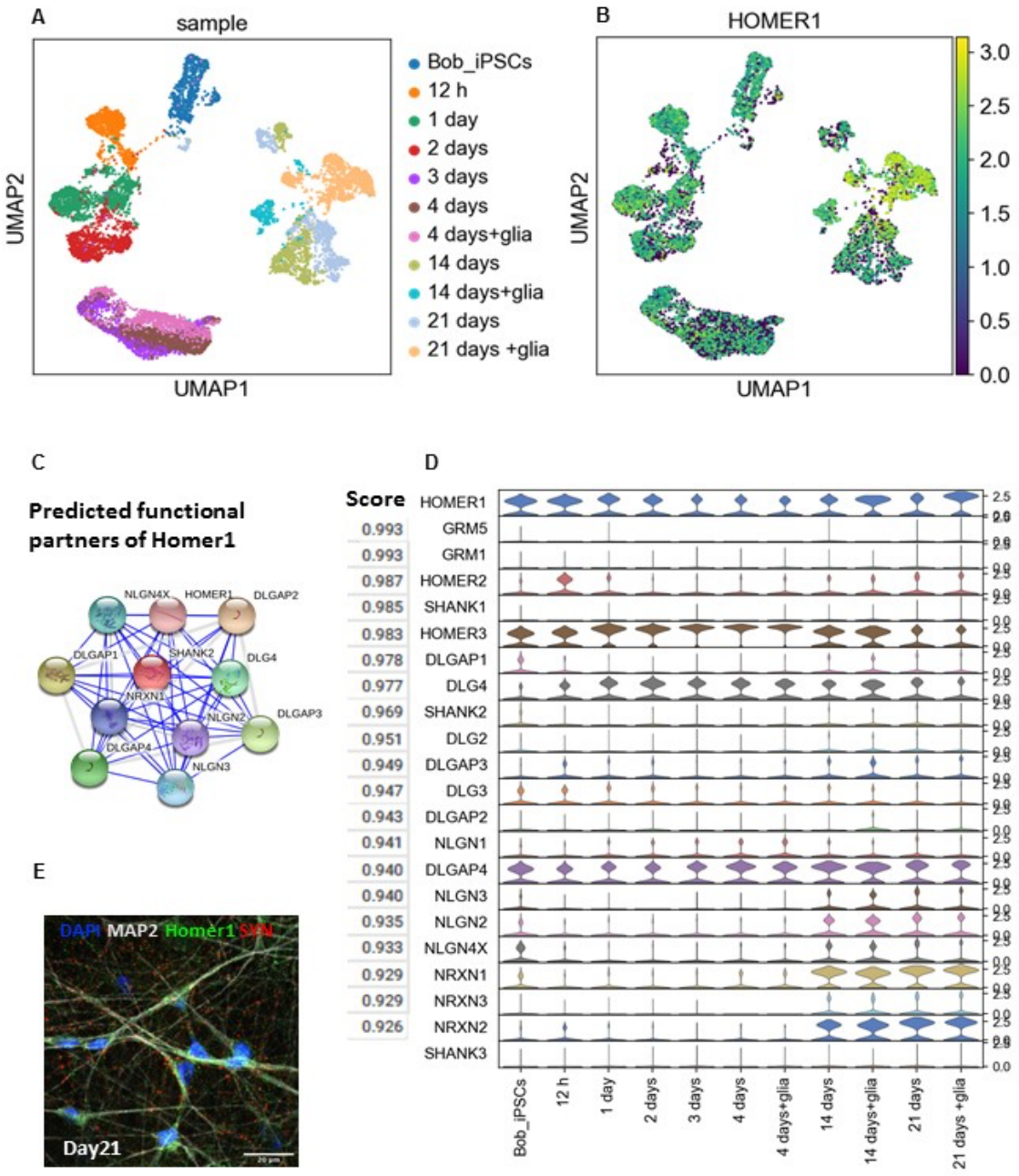

Figure 3-7 Expression of synaptic density protein Homer1 and its functionally interacting partners

(A) UMAP clustering of distinct subpopulations of i-neurons based on expression profiles as analysed from single cell RNA sequencing. (B) Expression of Homer1 over 21 days of induction. (C) STRING analyses of predicted functional interacting partners of Homer1 with interaction score (D) Gene expression pattern of top 20 interacting partners of Homer1 at postsynaptic density at iPSC stage, induction of 12-hour, 1 day, 2 day, 3 day, 4 day 14 day, 14 day+glia, 21 day, 21 day+glia. (E) Image of Day21 i-neuron expressing Homer1, Synapsin and MAP2.

3.4.5 Synaptic receptor gene expression in iNeurons

Synaptic plasticity is regulated both at the presynaptic compartment by altering neurotransmitter release and at the postsynaptic site by modulation of number or properties of different kinds of neurotransmitter receptor molecules. The most prevalent neurotransmitter receptor in *NGN2* iNeurons was reported as AMPA (α-amino-3-hydroxy-5-methyl-4-isoxazolepropionic acid) - type receptors responsible for fast neurotransmission (Zhnag et al, 2013). Therefore, we investigated the presence of AMPA receptor in OPTi-OX *NGN2* i-neurons by surface labelling the i-neurons at day 21 with AMPA receptor specific antibody [Fig. 3.8(A)]. The schematic shows that AMPA receptor membrane localisation and trafficking at the postsynaptic membrane works synergistically with neurotransmitter release from the presynaptic terminal of a glutamatergic excitatory synapse [Fig. 3.8(B)]. The violin plots of single cell RNA sequencing data demonstrated that *AMPA* receptor subunits, especially *GRIA2* and *GRIA4* were highly expressed day 14 onwards and may contribute to spiking activity at this stage. *GRIA2* subunit is often considered the most important component of AMPA receptor as its sole presence determines calcium permeability of the receptor. However, the NMDA receptor subunits (*GRIN1, GRIN2A, GRIN2B, GRIN2C, GRIN2D*) were all almost very low expression. NMDA (N-methyl-D-aspartate) - type receptors trigger long-term changes in synaptic transmission: long-term potentiation (LTP) and long-term depression (LTD); and are important for learning and memory formation.

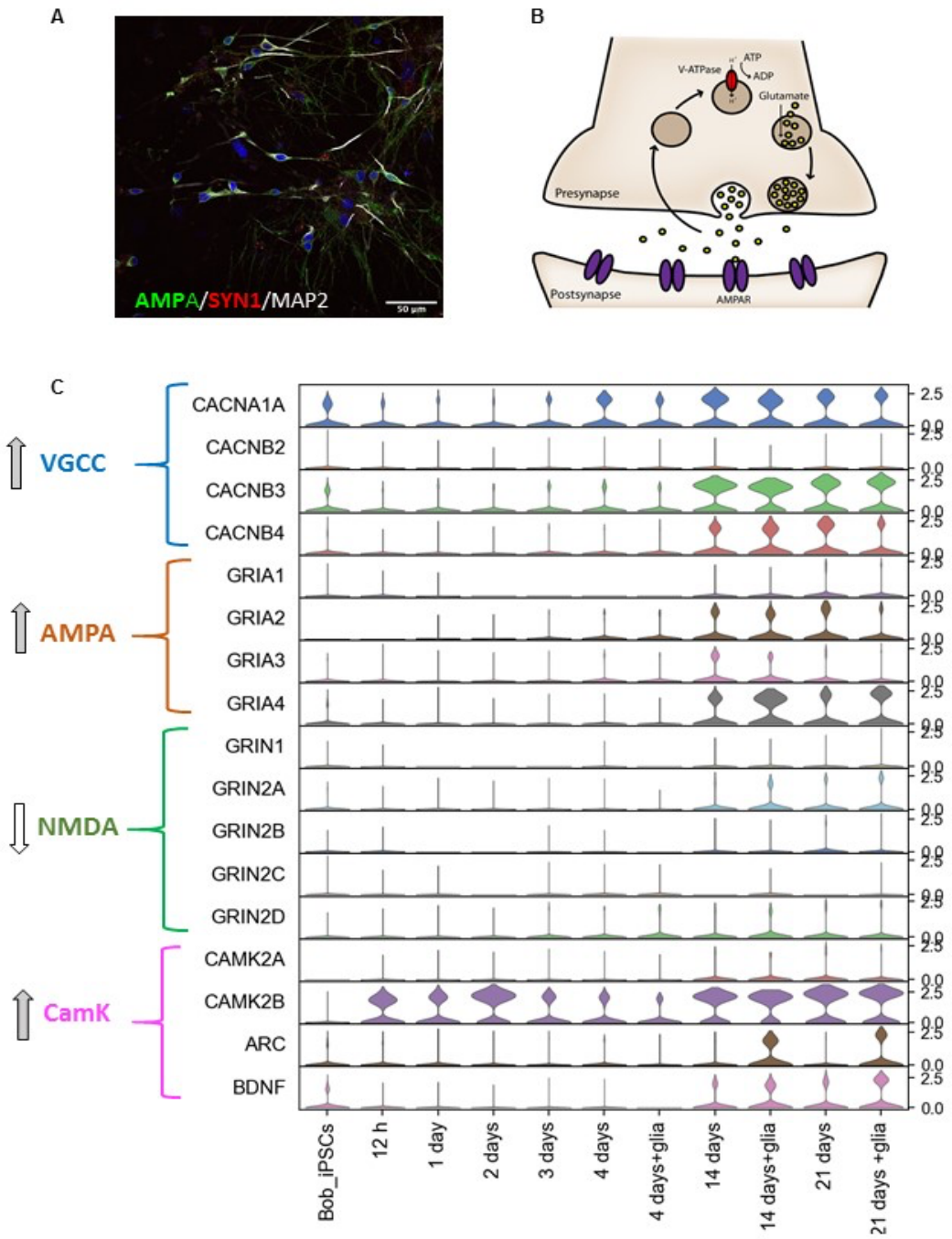

Figure 3-8 Synaptic receptor gene expression in iNeurons.

(A) Surface labelling of AMPA receptors on Day21 hiNeurons (B) schematic of AMPA receptor and V-ATPase mediated synaptic vesicle recycling at synaptic density (C) Violin plots of expression profiles of families of channel receptors at excitatory synapse from single cell RNA sequencing dataset at iPSC stage, induction of 12-hour, 1 day, 2 day, 3 day, 4 day 14 day, 14 day+glia, 21 day, 21 day+glia.

Our findings on AMPA receptor expression but not NMDA in OPTi-OX *NGN2* iNeurons corroborates with previous studies on *NGN2* iNeurons using lentiviral method (Zhang et al, 2013). Voltage-gated calcium channels (VGCCs) such as *CACNA1A, CACNB3, CACNB4* were found to be highly expressed on day 14 and later in i-neurons. VGCCs are transmembrane channels that are activated in response to cell membrane depolarisation and facilitate the import calcium ions (Ca2+) in neurons and this could be another mechanism of synaptic transmission in our model. Calcium-calmodulin dependent kinase (CamK) complex is also critical for various forms of synaptic plasticity that underlie learning and memory (Zalcman et al., 2018) and we observe that *CAMK2B* subunit to be highly enriched on day 14 and day 21 in i-neurons. *CamK2B* mediates plasticity by affecting downstream ARC (encodes Arc: activity-regulated cytoskeleton-associated protein) for reorganisation of synaptic structure and transcriptional activity of *BDNF* (Brain derived neurotrophic factor) which promotes neuronal survival and growth. Interestingly, we found that both *ARC* and *BDNF* were expressed at a higher level in i-neurons when the cells were co-cultured with primary glial cells. This again highlights the importance of presence of astrocytes in synaptic maturation and plasticity for *NGN2* iNeurons.

3.5 Discussion

In this chapter, we have presented results on gene expression profiles of autism related and synaptic genes in order to critically examine the suitability of OPTi-OX *NGN2* as a model system to study autism related cellular and synaptic phenotypes. As depicted in the time-lapse video *NGN2* iNeurons rapidly grow to form neuronal network and mature quickly in presence of primary astrocytes. *NGN2* iNeurons express NPC markers until day 4 and mature synaptic markers day 14 onwards. We observed that the markers for neurogenesis such as *STMN2* and *GAP43* increase until day 21 which is indicates that the cells were still maturing at 3 weeks post-induction. Among 192 high-confidence autism risk genes, a number of genes such as

NRXN1, NRXN2, NLGN2 and ANK3 showed increased expression day 14 onwards till day 21 which could be a suitable time window to use this model for gene specific cellular phenotyping. The key genes involved in presynaptic neurotransmitter release such as *VAMP2, STX1A* and *SNAP25* show expression on day 21 indicating that the i-neurons at this stage are potentially capable of neurotransmission and plasticity through vesicle docking, fusion and release. At the postsynaptic density Homer1 expression and its interacting partners especially Neurexins (*NRXN1, NRXN2* and *NRXN3*) demonstrate promising gene expression profile with respect post synaptic density organisation and transsynaptic signalling in i-neurons on day 14 onwards. Among synaptic receptor genes AMPA, VGCC and CamK genes were abundantly expressed in i-neurons; however, NMDA receptor genes were found to be absent in this model suggesting functional properties of these cells must be interpreted in the light of synaptic receptor composition.

One of the main challenges of using the OPTi-OX system to model patient iPSC lines with mutation or deletion is that the targeting of rtTA and NGN2 into genomic safe harbour sites could be technically challenging. Integration of rtTA and NGN2 involves independent nucleofection, clonal selection and sequencing steps which could be time consuming when multiple patient lines are involved compared to the classical lentiviral transduction approach of NGN2 i-neurons (Zhang et al, 2013). Secondly, as shown in the results in this chapter, not all high confidence autism-risk genes are abundantly expressed in NGN2 i-neurons. Therefore, this model may not be suitable for certain autism related gene mutations. Thirdly, the regional specificity of *NGN2* iNeurons still remains unclear since as we observed that only deep layer cortical marker *CTIP2* showed up on day 21 when cultured in presence of glial cells. Finally, certain synaptic receptors such as *NMDA* receptors are found to be absent in this model and could be circumvented by combining *NGN2* overexpression with developmental patterning (Nehme et al, 2018). A recent study (Rosa et al, 2020) compared the "fast" *NGN2* protocol

with a more “native” embryoid body protocol and elucidated that *NGN2* neurons reach the cellular signatures of that of second trimester of human gestation when cultured with astrocytes; whereas the embryoid body protocol is capable of modelling third trimester with more complex neuronal network activity. Nevertheless, *NGN2* iNeuron model has less cellular heterogeneity compared to most other existing models of neuronal differentiation and its main advantages are rapidity and scalability to form relatively mature neurons in less time. In order to fully understand the functional properties of these cells and how the synaptic gene expression contribute towards firing activity in terms of electrophysiological parameters, further in-depth phenotyping is required which is to be discussed in the next chapter (Chapter 4).

4 Chapter 4: Electrophysiology of iNeurons

4.1 Introduction

Autism is a complex neuropsychiatric condition and presents a unique challenge to cellular modelling of its pathophysiological phenotype. Human induced pluripotent stem cell (hiPSC) derived neuronal cultures offer a possibility to produce mature neurons with high scalability to investigate patient specific cellular phenotype. However, most of the existing developmental neural differentiation protocols generate heterogenous population of excitatory neurons and other cell types and often with limited functional maturity. Since generation *NGN2* iNeurons with forward programming allows us to overcome some of these challenges of immaturity, heterogeneity and scalability as discussed in Chapter 3, we have further looked at the functional electrophysiological properties.

There are several existing methods of functional characterisation of neurons in vitro. Most of the studies in the past have relied on single cell intracellular patch-clamp recordings. The advent of multi electrode array (MEA) technology allows for repeated measurements of extracellular electrophysiological activity of functional neuronal networks of a population of cells over an extended period of time. Over the last decade of neuroscience research, this is becoming an increasingly popular method of functional characterisation of neurons among researchers due to manifold technical advantages of data acquisition and importance of information regarding the electrophysiological state and behaviour of cells under control or treatment conditions (Spira et al, 2013).

Developmental pattern of neuronal firing in human cortex follows several distinct stages such as asynchronous spontaneous firing, synchronous bursting activity or oscillations and complex network activity (Kirwan et al, 2015). Synaptic activity and neurotransmission deficits have been identified as core pathophysiology of neuropsychiatric disorders. In this

chapter, we have therefore made an attempt to conduct an in-depth functional characterisation of iNeurons over a time course of 5 weeks to test whether this model is suitable for investigating several spiking and bursting properties of functionally mature excitatory neurons.

4.2 Aims

1. To examine whether i-neurons spontaneously fire under basal condition and respond to ionomycin
2. To characterise the development of spontaneous activity of i-neurons during time course of neuronal induction at day 21
3. To measure and characterise the development of network burst properties of i-neurons
4. To examine whether network burst properties are altered in response to AMPA channel blocker NBQX

4.3 Design

Control bob-Ngn2 hiPSC cells were induced to i-neurons following the neural induction protocol as described in Chapter 2 for characterising functional and electrophysiological properties from extracellular recordings (Figure 4.1). Calcium imaging with non-ratiometric dye Fluo-4 AM was performed on Day 21. Multi-electrode array analyses for measuring spiking and burst properties were carried out on day 14, day 21, day 28 and day 35. The pharmacological experiment top test response to AMPA channel blocker NBQX was carried out on day30. All methods and analyses have been followed as described in Chapter 2.

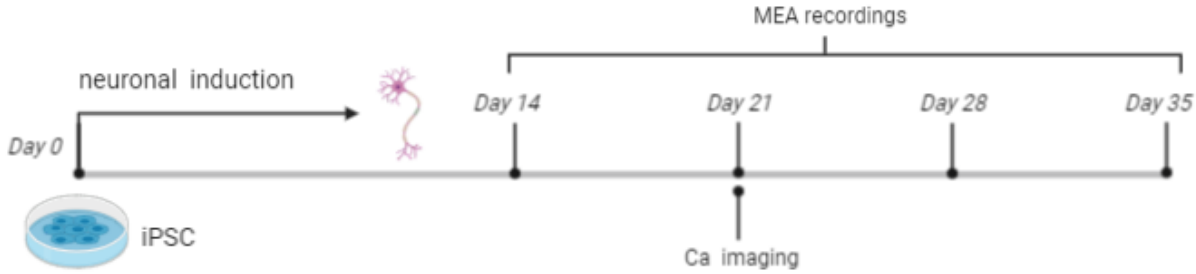

Figure 4-1 Timeline of electrophysiological experiment

4.4 Results

4.4.1 iNeurons exhibit spontaneous activity

It is evident that iNeurons express a wide range of synaptic scaffold proteins as shown in the imaging and transcriptimic profiling data in Chapter 3. Therefore, we aimed to examine whether these neurons demonstrate physiological neuronal activity with calcium imaging. Fluo-4 AM, a well known non-ratiometric fluorescence indicator with peak excitation and emission at 340 nm and 520 nm wavelengths respectively, was used to investigate transient calcium transients in Day 21 i-neurons [Fig4.2(A)], induced from iPSCs following the protocol as outlined in Chapter 2. Ionomycin, a calcium ionophore which increases intracellular Ca^{2+}-concentration by faciltating Ca^{2+}-ionic influx across plasma membrane and releasing intracellular Ca^{2+} stores in subcellular compartments, was used as a loading control dye to visualise maximum fluorescence intensity in regions of interest [Fig4.2(B)]. Fig4.2(C) shows the fold change of fluorescence intensity of randomly selected regions of interest (ROIs) on neuronal cell bodies, before and after addition of ionomycin over a span of 3 minutes. The first 1 min duration of basal activity before stimulation demonstrates spontaneous Ca^{2+}-influx [Fig4.2(D)]. In order to quantitatively characterise the spontaneous spiking properties of i-neurons, we further investigated the electrophysiological development of i-neurons using extracellular recordings with multi-electrode arrays (MEA) (Fig4.3).

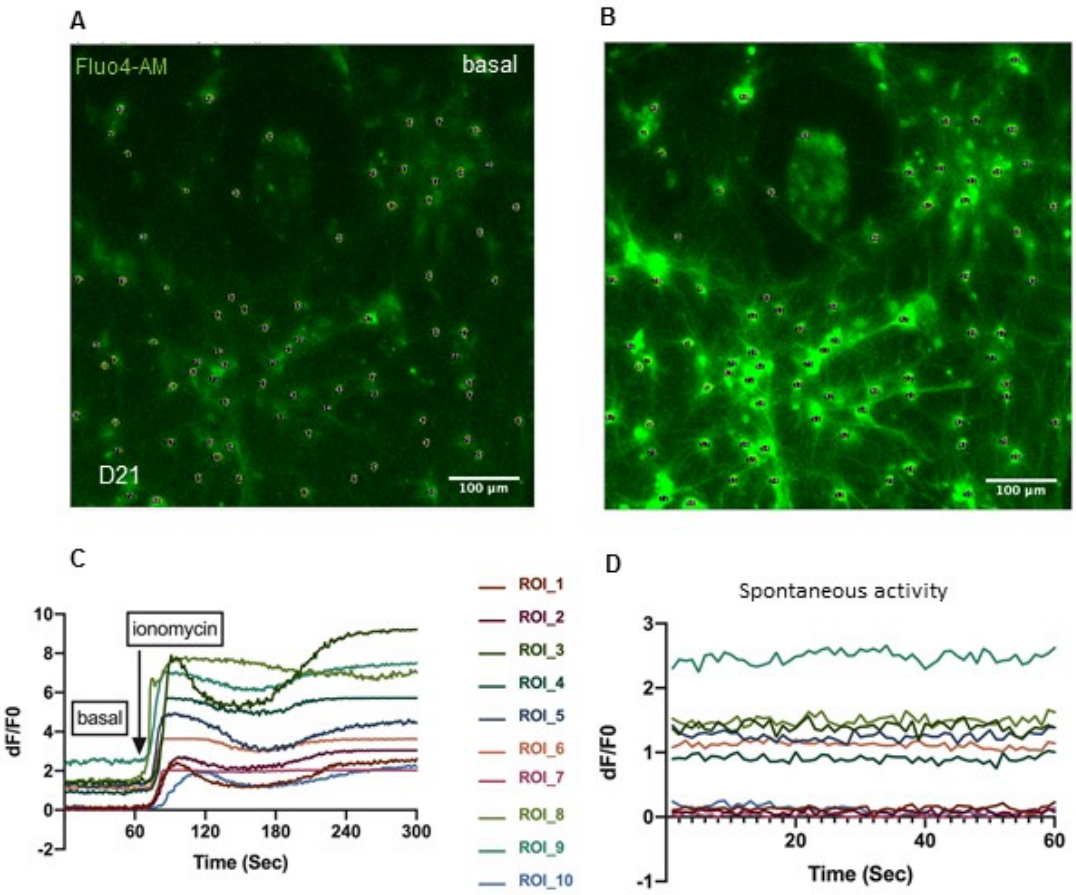

Figure 4-2 Calcium imaging of day21 iNeurons.

(A) i-neurons loaded with Fluo-4 AM at basal condition (B) i-neurons after addition of ionomycin (C) Fold change of fluorescence intensity over time as recorded from several cell bodies before and after addition of ionomycin (D) First 1 min of basal spontaneous activity vs time curve of i-neurons.

4.4.2 Development of spontaneous firing activity in iNeurons

Ngn2 i-neurons were induced from iPSCs and plated with rat astrocytes on Multichannel Systems 6-well electrodes [Fig4.3(B)] as described in Chapter 2 and cultured until day 35 to study the development of spontaneous activity over timepoints day 14, day 21, day 28 and day 35 (Figure 4.1). Fig4.3(C) shows the brightfield image of a representative well with i-neurons and 9 recording electrodes for recording extracellular activity.

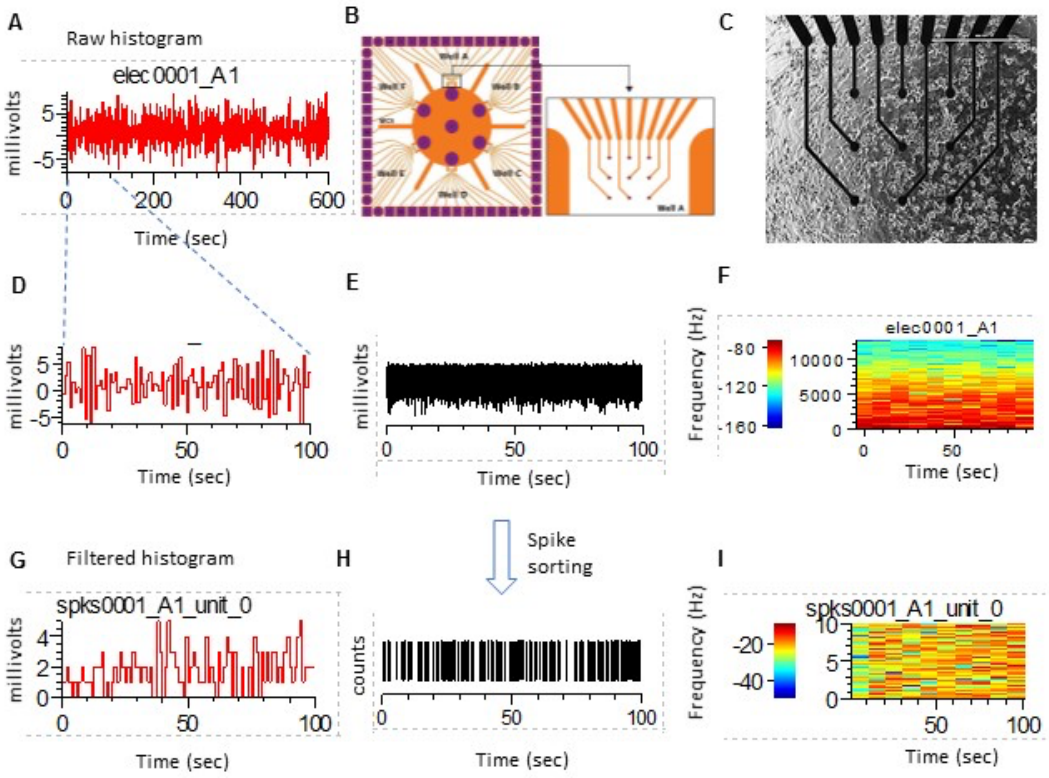

Figure 4-3 Multi-Electrode Array (MEA) analysis pipeline.

(A) Raw traces of spontaneous activity of day14 i-neurons recorded from electrode A1 (B) Schematic of 6-well MEA with 9 electrodes in each well (C) 3D histogram of raw traces of all electrodes. (D) Histogram of first 100 seconds of raw traces of A1 electrode, (E) raster plot and (F) frequency spectrogram. (G) Histogram (H) raster plot and (I) frequency spectrogram of the same recording shown after spike sorting.

The raw recording was acquired and sorted for spikes using MC_Rack and analysed on Neuroexplorer platform for spike and burst parameters. Fig4.3(A) shows a representative histogram of a 10 minute long raw extracllular recording of an electrode A1 from the well A of day14 iNeurons. [Fig4.3(D), (E) and (F)] demonstrate the frequency histogram, rastor plot and spectrogram of the first 100 seconds of the same raw recording from A1. After spike sorting of the raw data following 6 SD threshold, the "filtered" data was used for comparison of spiking and burst parameters across all timepoints. A visual representation of the frequency histogram,

rastor, and spectrogram of the same recording from A1 is shown in [Fig4.3(G), (H) and (I)] respectively demonstrate the changes in frequency distrubution over time after spike sorting.

3D histograms of frequency distribution of the earliest timepoint i.e. day 14 [Fig4.4(A)] and the latest timepoint i.e. day 35 [Fig4.4(B)] over 100 milliseconds across all electrodes shown significant differences in spiking activity. The peak and the dynamic range of spiking activity are higher and wider respectively on day 35 compared to day 14. This suggests that a significant proportion of the i-neurons on day 35 spike at a much higher frequency although some neurons are still at the basal level. 3D histograms of waveform comparison of i-neurons on day 14 [Fig4.5(A)] and day 35 [Fig4.5(B)] over 3 milliseconds reveal that the shape of the waveform changed significantly as the neurons mature and the amplitude of waveform sharply increases on day 35.

To characterise the temporal development of spike properties of Ngn2-iNeurons, the filtered data was plotted as a function of time for each timepoint; an example the frequency and inter-spike interval (ISI) vs time distribution from a representative electrode B4 of Day 21 i-neurons are shown in [Fig4.6(A) and (B)] respectively. The spike parameters for all the electrodes across 6 wells were pooled for each timepoint to compare across the neural induction on day 14, day 21, day 28 and day 35.

The mean firing rate (MFR) was observed to significantly increase and peak at week 4 i.e. day 28 followed by a decrease on day 35 [Fig4.6(C)]. At Day 14, the lowest MFR was observed and the ISI was found to be very high [Fig4.6(C) and (D)] compared to all other time points. This suggests that the rate of spiking was very low and the spikes were sparely distributed across the recorded interval. This explains the electrophysiological immaturity of iNeurons at this early timepoint of day 14.

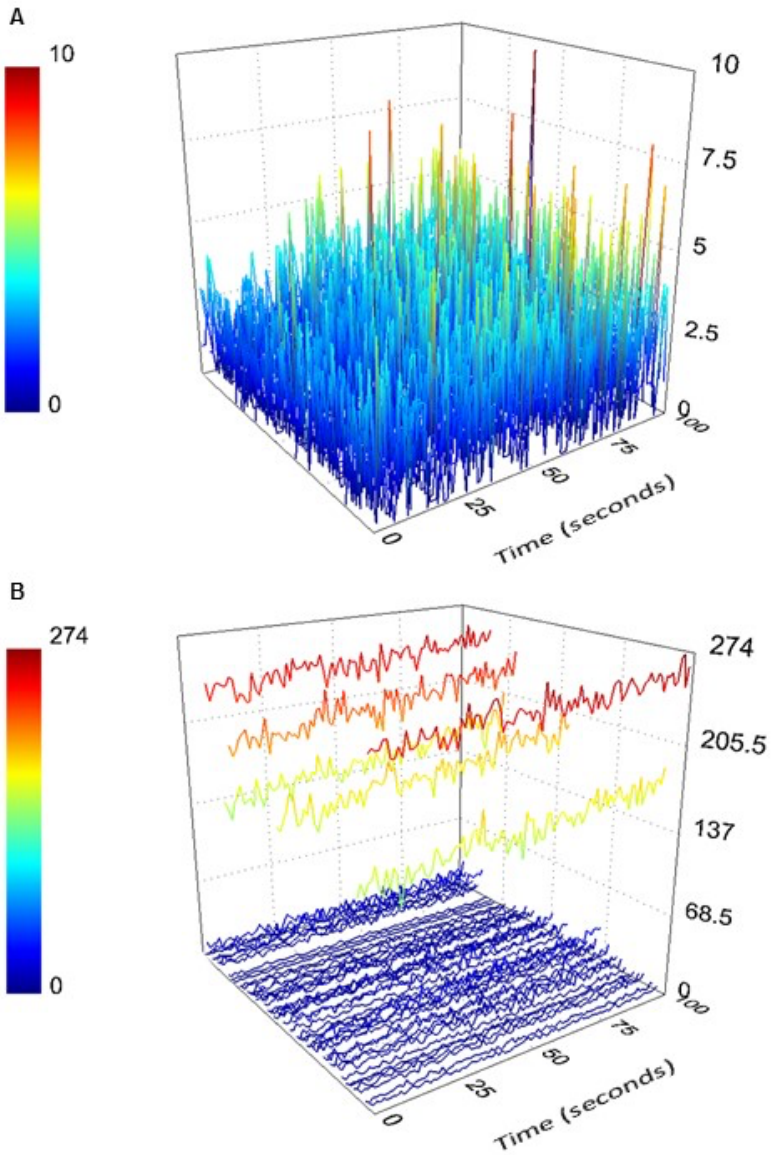

Figure 4-4 3D Histograms of frequency distribution of spikes

3D Histograms of frequency distribution of spikes (A) day14 vs (B) day35 i-neurons. Colour bar indicates frequency range of the spike trains. Spikes from 45 electrodes were plotted.

However, the ISI dipped significantly after day 14, being lowest at day 21 and then gradually showed an increase till day 35. The mean spikes followed the same trend as that of MFR quite evidently since the mean number of spikes is directly proportional to the firing rate [Fig4.6(E)]. The mean peak frequency also exhibited the same pattern over all four timepoints [Fig4.6(F)].

The spike analysis suggests that the i-neurons progressively mature and show highest spiking activity around a month post-induction.

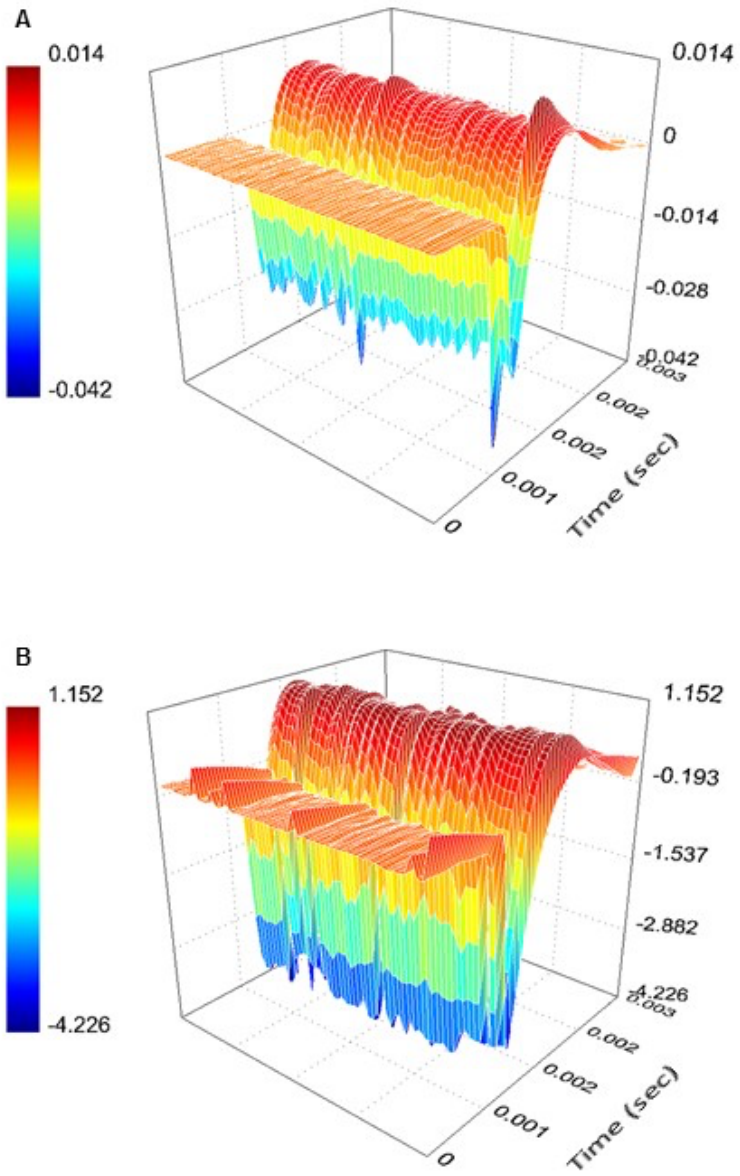

Figure 4-5 3D Histogram of waveform comparison of spikes

3D Histogram of waveform comparison of spikes from (A) day14 vs (B) day35 i-neurons. Colour bar indicates amplitude range of the waveforms. Waveforms from 45 electrodes were plotted.

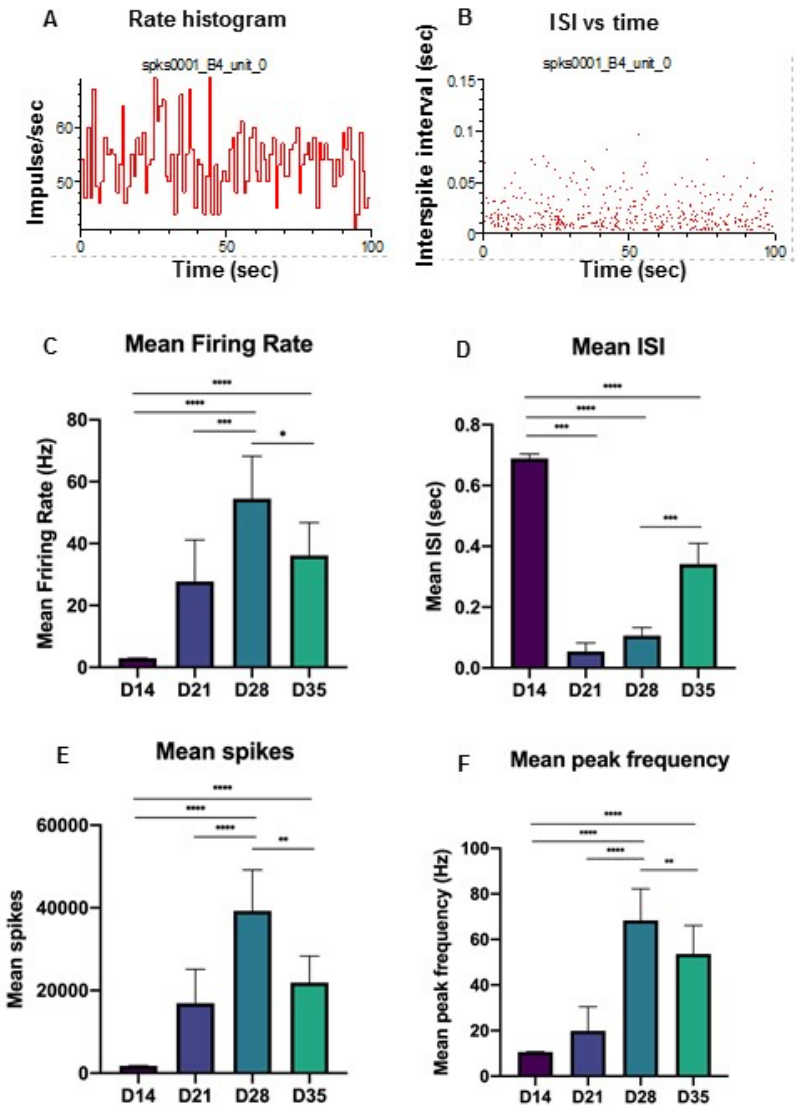

Figure 4-6 Spike analysis of iNeurons.

Representative (A) rate histogram of an electrode from D14 i-neuron recording. Characterisation of spike properties such as (B) ISI vs time (C) mean firing rate (D) mean ISI (E) mean spikes and (F) mean peak frequency of recordings from i-neurons at Day 14, Day 21, Day 28 and Day 35. (3 biological replicates, 54 electrodes for each timepoint, Kruskal-Wallis statistical test for multiple comparisons).

4.4.3 iNeurons display distinct network burst properties

Bursting behaviour is a hallmark of developing cortical neuronal network (Kirwan et al. 2015). In mammalian cortex bursting properties typically emerge after the development of asynchronous spontaneous activity as a characteristic of mature neurons. We therefore

excluded the earliest timepoint of day 14 from our analysis of bursting parameters, since Ngn2-iNeurons display very low level of firing (shown in Fig4.6) due to immaturity at this stage. Bursts were detected as minimum of 3 spikes and 3.5 standard deviations (Chapter 2) for all the recordings over timepoints day 21, day 28 and day 35. [Fig4.7(A) and (B)] show an example of burst duration and mean ISI in burst within first 100 seconds recorded from electrode A1 of day 28 i-neurons. During the time course of maturation, the i-neurons exhibited a significant increase in mean burst duration and burst frequncy peaking at day 35 [Fig4.7(C) and (E)]. This could mean that the neurons continue maturing and increasingly exhibit more synchronous activity beyond week 4 or day28, despite their MFR decreasing signficantly at day35 [Fig4.6(A)]. However, the "mean ISI in burst" followed the same trend as previously observed in mean ISI [Fig4.6(D)]. Interestingly, the mean inter-burst interval peaked at day 28 and significantly dipped at day 35 suggesting that the bursting activity becomes denser at this later stage of induction [Fig4.7(F)].

We further characterised the spikes within bursts and their properties to better understand the local effect of spike trains of action potentials on global bursting behaviour. [Fig4.8(A), (B)] show the number of spikes in burst and the peak frequncy in burst from the same recording as in [Fig4.7(A), (B)]. We observe that all three parameters, such as the mean spikes in burst, mean peak frequency in burst and mean frequency in burst [Fig4.8(C), (D), (E)] follow the same trend as that of [Fig4.6(E), (F), (C)] respectively from day 21 to day 35.

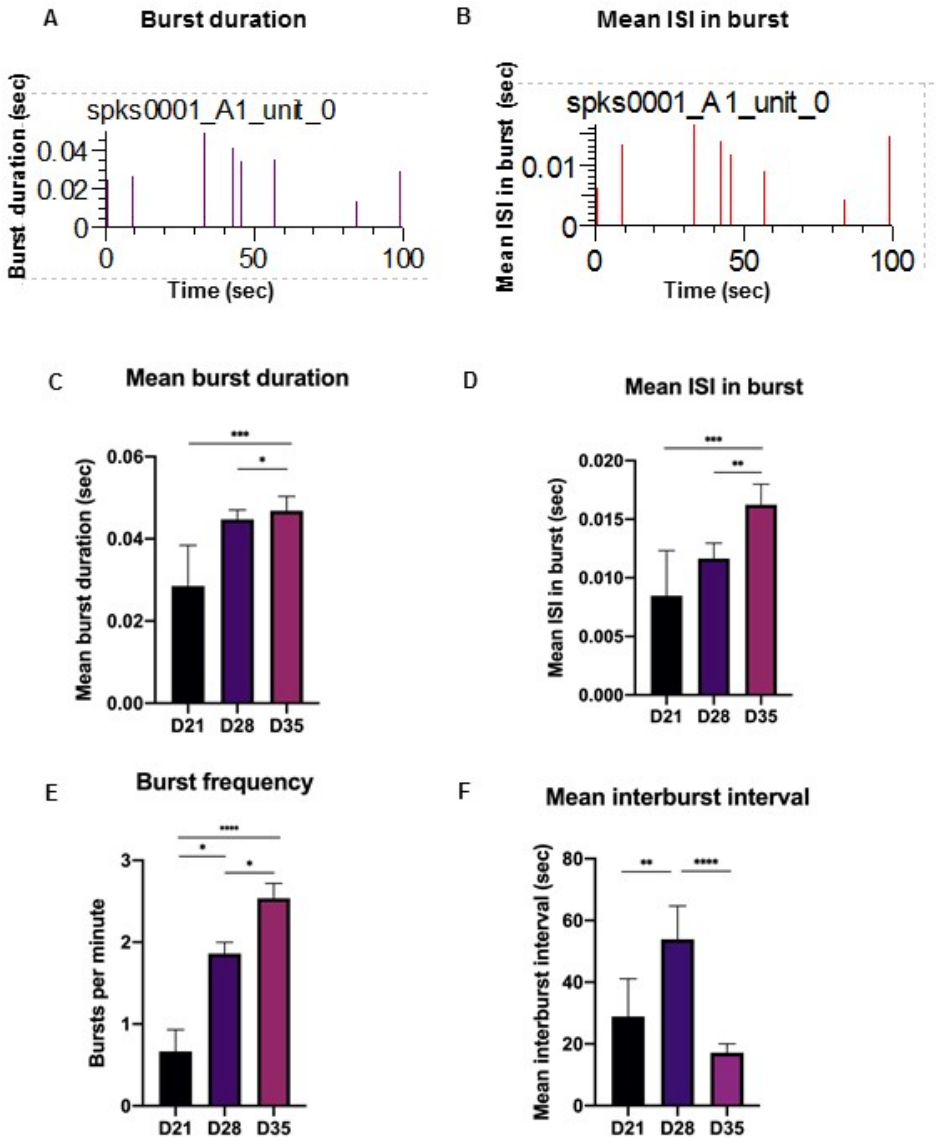

Figure 4-7 Burst analysis of iNeurons.

Representative diagrams of (A) burst duration and (B) mean ISI in burst from an electrode showing bursts of Day28 i-neurons. Bursting properties are characterized as (C) mean burst duration (D) mean ISI in burst (E) burst frequency and (F) mean interburst interval for Day21, Day28 and Day35 i-neurons (3 biological replicates, 54 electrodes for each timepoint, Kruskal-Wallis statistical test multiple comparisons).

We also examined a metric called “mean burst surprise” based on the probability of bursting which shows that the i-neurons are more likely to exhibit bursting phenomena as they mature from day21 to day35 [Fig4.8(F)]. We observe emergence of synchronous activity as a global bursting phenomena over from day21 to day35 of temporal development of Ngn2-iNeurons.

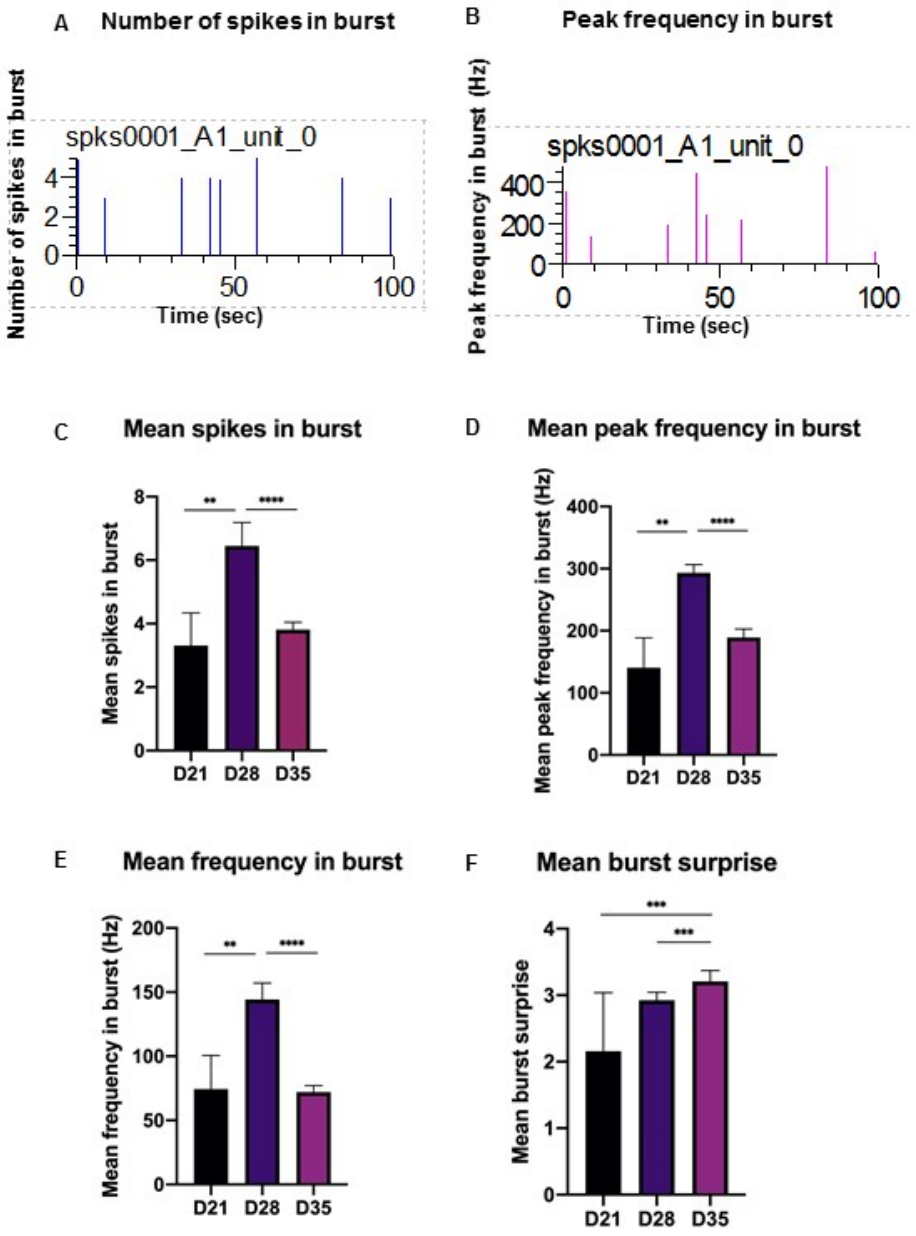

Figure 4-8 Spiking characteristics within bursts.

Representative diagrams of (A) number of spikes in burst and (B) peak frequency in burst from an electrode showing bursts of Day28 i-neurons. Spiking properties within burst activity are characterised as (C) mean spikes in burst (D) mean peak frequency in burst (E) mean frequency in burst and (F) mean burst surprise for Day21, Day28 and Day35 i-neurons (3 biological replicates, 54 electrodes for each timepoint, Kruskal-Wallis statistical test multiple comparisons)

4.4.4 Network bursting frequency is reduced on AMPA antagonist NBQX treatment

We have previously demonstrated that Ngn2-iNeurons exhibit AMPA receptor expression but do not express NMDA receptor in our transcriptomic study in Chapter3. In order to examine how spiking and bursting properties of i-neurons might behave in response to pharmacological agents, we therefore used AMPA receptor antagonist NBQX which blocks excitatory transmission and firing activity by binding to the receptors at the synapse. By visual inspection of waveform analysis of day30 i-neurons under baseline, NBQX treatment and washout conditions, we observe that the amplitude of some neurons remains relatively unaffected [e.g. A1 electrode: Fig4.9(A)] across conditions; whereas some show significant change in waveform shape on treatment [e.g. F9 electrode: Fig4.9(B)]. However, the cumulative waveform analysis of all electrodes reveals that the range of amplitude is decreased on treatment with NBQX (-0.055 to 0.013 mV) compared to baseline (-0.069 to 0.017 mV) or washout conditions (-0.071 to 0.017) [Fig4.9(C)].

To further characterise the spiking patterns on treatment with NBQX we looked at the mean firing rate and inter-spike interval under the above-mentioned conditions. Recordings from a representative elecetrode A1 and show the frequency [Fig4.10(A)] increases and the inter-spike intervals [Fig4.10(B)] decrease from baseline to NBQX and washout conditions.

It was surprising to find that the mean firing rate significantly increases on treatment with NBQX and further on washout across all electrodes [Fig4.10(C)]. The inter-spike interval quite evidently follows the opposite trend as the spiking becomes denser across the same conditions [Fig4.10(D)]. Although the mean firing rate increased on treatment with NBQX (Fig4.10), the bursting parameters such as mean burst duration, mean ISI in burst and burst frequency were found to be significantly decreased which suggests that NBQX blocks the network oscillations or synchronous activity in i-neurons [Fig4.11(A), (B) and (C)]. However, the washout

condition could not restore the bursting frequency or mean ISI in burst, only mean burst duration was observed to come up although the variability was quite high.

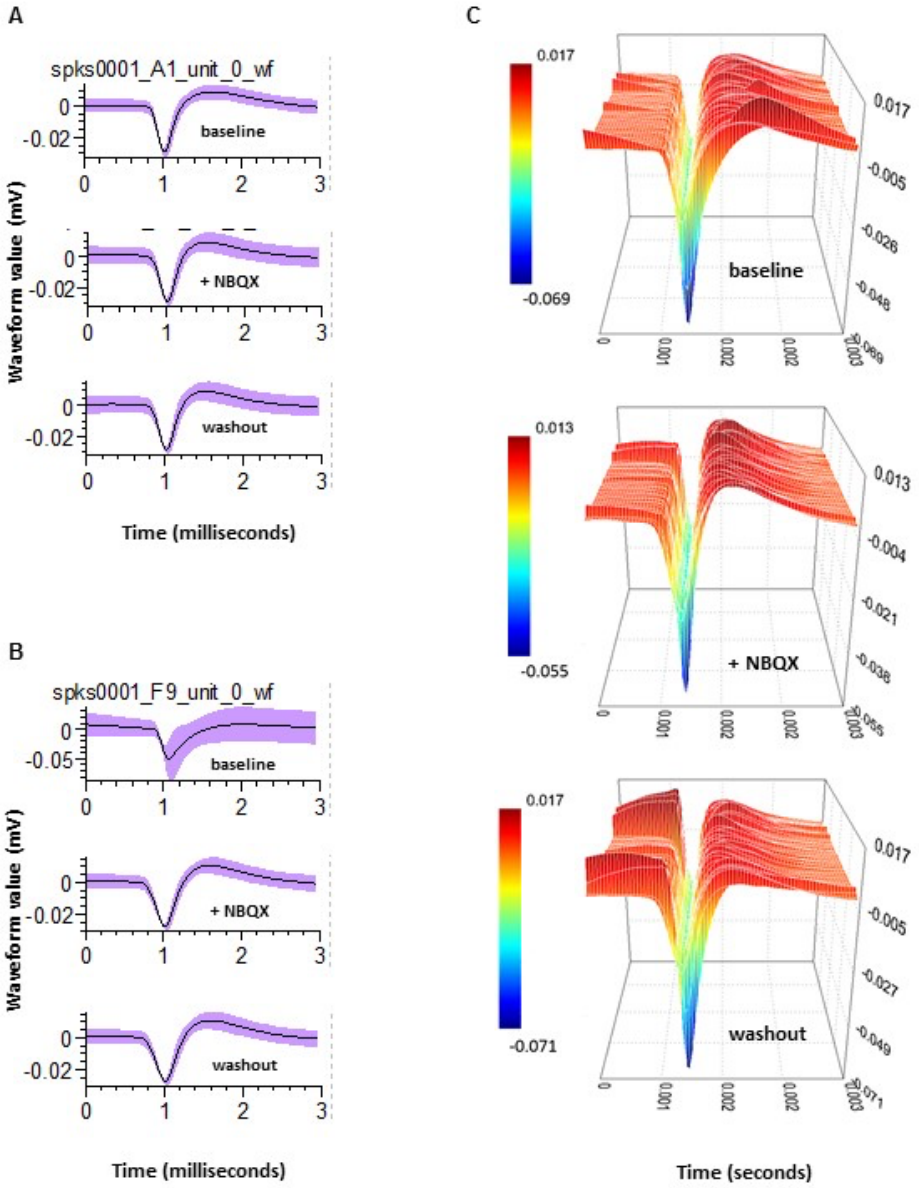

Figure 4-9 Waveform analysis on pharmacological treatment

Waveform comparisons of (A) A1 electrode and (B) F9 electrode under baseline, NBQX treatment and washout conditions. Standard deviations are shown in lavender colour. (C) 3D histograms of waveforms of all 54 electrodes from 3 replicates under baseline, NBQX treatment and washout conditions. Colour bar indicates amplitude range of the waveforms.

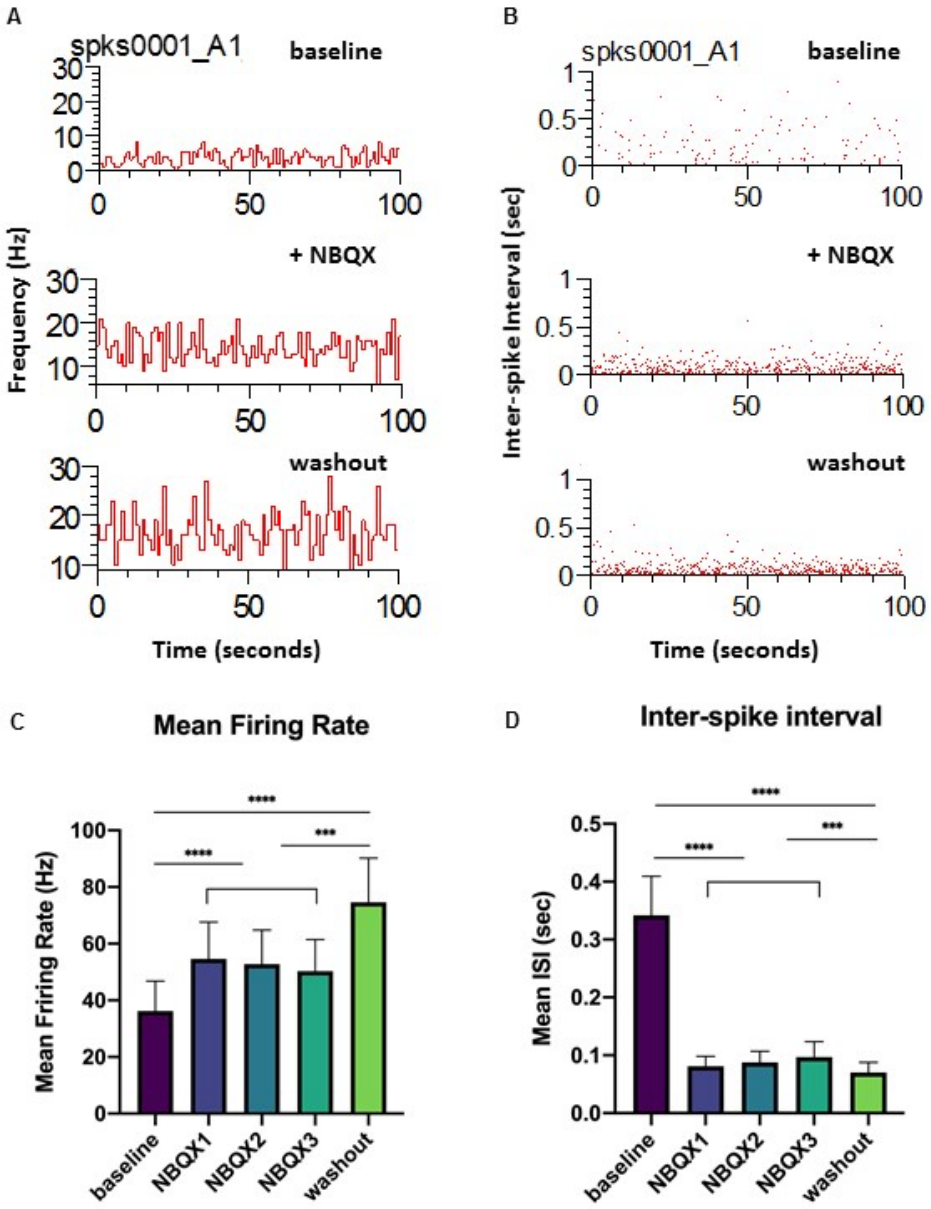

Figure 4-10 Spike analysis of Day 30 i-Neurons on pharmacological treatment.

(A) Rate histogram of spikes from a representative electrode A1 under baseline, NBQX treatment and washout conditions. (B) Inter-spike interval (ISI) vs time for electrode A1 under same conditions. (C) Mean firing rate comparison across baseline, NBQX treatment and washout conditions for Day30 i-neurons. (D) Mean ISI comparison across same conditions for Day30 i-neurons (54 electrodes from 3 replicates for each timepoint, Friedman test for repeated measures).

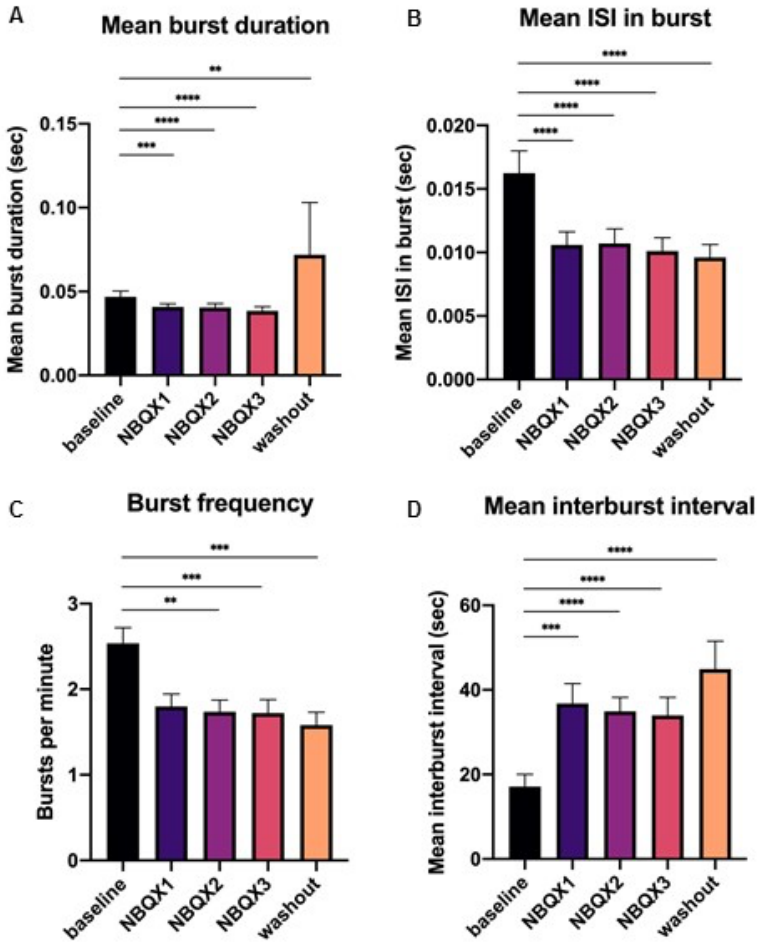

Figure 4-11 Burst analysis of Day30 i-neurons on pharmacological treatment.

Bursting properties characterized as (A) mean burst duration (B) mean ISI in burst (C) burst frequency and (D) mean interburst interval for baseline, NBQX treatment (three successive recordings: NBQX1, NBQX2, NBQX3) and washout conditions (54 electrodes from 3 replicates for each timepoint, Friedman statistical test for repeated measures).

Moreover, the mean interburst interval [Fig4.11(D)] gradually increased following the same trend as mean firing rate [Fig4.10(C)] which means that the bursts became increasingly sparse. The spiking parameters within bursts such as mean spikes in burst, mean peak frequency in burst and mean frequency in burst were all also observed to increase like mean firing rate

discussed earlier [Fig4.12(A), (B) and (C)]. Although the washout condition was not similar to the baseline in terms of any burst parameter, the variability and the probability of bursting was higher on the washout condition [Fig4.12(D)].

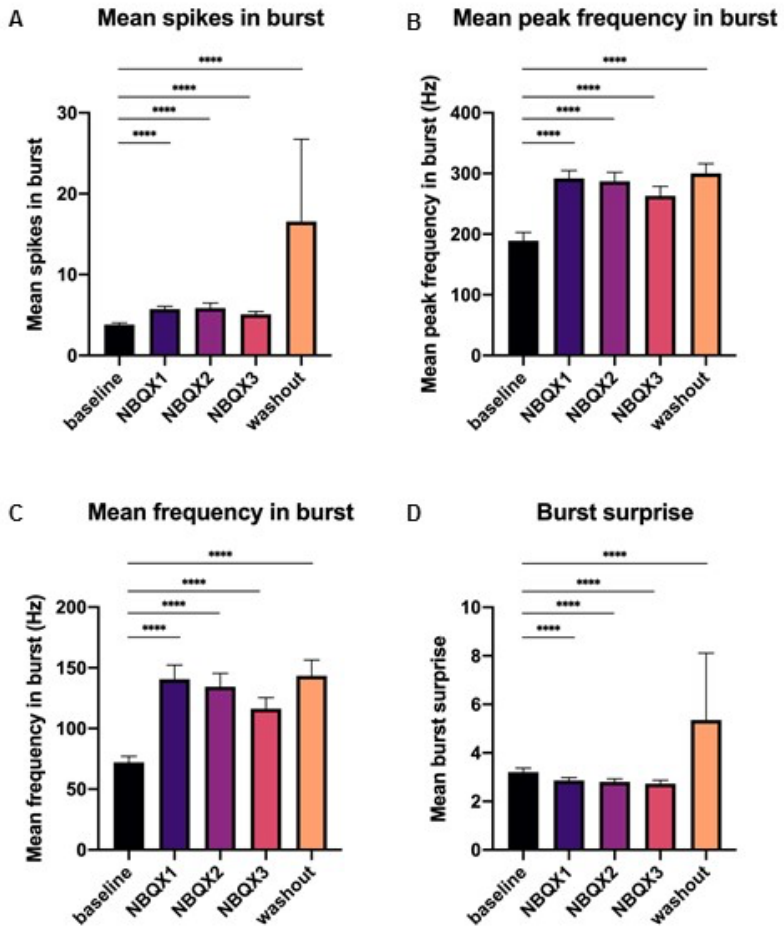

Figure 4-12 Spiking characteristics within bursts on pharmacological treatment.

Spiking properties characterised as (A) mean spikes in burst (B) mean peak frequency in burst (C) mean frequency in burst and (D) mean burst surprise for baseline, NBQX treatment (three successive recordings: NBQX1, NBQX2, NBQX3) and washout conditions (54 electrodes from 3 replicates for each timepoint, Friedman statistical test for repeated measures).

4.5 Discussion

This is the first report of in-depth functional characterisation of OPTi-OX *NGN2* iNeurons using extracellular recordings with multi-electrode arrays (MEA). The only previous study using this model had reported emergence of excitatory synchronous activity in the context of oxidative metabolism and synaptic vesicle recycling (Tourigny et al, 2019). We for the first time looked at spontaneous spiking activity with calcium imaging and MEA and extended our analysis to waveform and several bursting parameters to understand the electrophysiological characteristics of NGN2-i-neurons. We observed that the mean firing rate peaks at week 4 whereas the bursting activity peak later at week 5 which suggests that spontaneous activity and synchronous activity may emerge at different timepoints of neuronal induction. Bursting activity is a hallmark of developing cortex and is reported to emerge at a much later timepoint in other methods of neuralisation from iPSCs (Kirwan et al, 2015). We also found that the AMPA receptor antagonist NBQX blocks the bursting activity globally but surprisingly increases the local spiking activity. In summary, the findings reported here imply that forward programming of i-neurons from iPSCs is a robust and rapid method of generating functionally active neurons, with distinct time course of spiking and bursting properties, which can potentially respond to pharmacological agents.

However, there are several limitations of this study. First of all, the time course of our experiment was till day35 i.e. week 5 and we observed the bursting activity to peak at week 5. Previously *NGN2* iNeurons (lentiviral method) have been reported to demonstrate highest mean firing rate at week 5 depending on the cell line used but bursting parameters were not reported (Deneault et al, 2019). It is not possible to conclude from experiments how the spiking and bursting activity may be affected beyond the timepoint of week 5. Hence, we are planning to conduct experiments with longer span of time post induction. Secondly, there was a quite some variability in the data we collected. Although we have

used 3 biological replicates and 2 wells of each and the data shown is the pooled data from all 54 electrodes, after thresholding some recordings had to be rejected following our stringent criteria. Moreover, it is also worth mentioning that the criteria, threshold and method of analysis (Chapter2) are to be kept in consideration while interpreting the results. For example, the results shown in spiking parameters and spikes within burst may appear as counter-intuitive. From the standpoint of analyses, the spike readouts, thresholded for spike detection using 6 standard deviations from the raw data, are binned into clusters based of bursting criteria of 3.5 standard deviations. Therefore the metrics under consideration, such as MFR, mean spikes, mean peak frequency and mean ISI are most likely to follow the same trend as in bursting.

The advantages of forward programming are rapid maturation, scalability and relatively homogenous population of functionally active excitatory neurons and could be effectively used to model neuropsychiatric conditions such as autism. There are only a few studies until date which have used NGN2-i-neurons for functional characterisation of atypical cellular phenotypes. Moreover, previously weighted mean firing rate (wMFR) has been used as the principle readout of neuronal activity using extracellular MEA recordings in the context of cellular pathophysiology of autism (Deneault et al, 2018). Array-wide spike detection (ASDR) is another parameter used for functional characterisation. Feng et al, 2016 used ASDR to characterise Shank3 deficient cultured cortical neuronal network. Deneault et al, 2019 had extensively looked at several autism related mutations in Ngn2-i-neurons using the lentiviral method (Zhang et al, 2013). The primary readout in this MEA study was the mean firing rate (MFR) recorded from every active electrode. However, we observe that the global bursting properties may differ independently of local environment of spiking neurons. Therefore, we extended our analyses and propose that the bursting parameters along with spiking properties such as MFR, ISI would potentially provide a

more thorough and robust understanding of the electrophysiological behaviour of developing neurons in an *in vitro* model. Finally, i-neurons can be potentially used for drug screening and characterising the effect and dose response of pharmacological agents on excitatory neuronal network at different stages of maturation.

5 Chapter 5: Knockdown of *NRXN1* and *SHANK3* in iNeurons

5.1 Introduction

Autism is a complex neuropsychiatric condition with multiple autism risk genes implicated in synaptic pathways and plasticity. A number of genetic studies have revealed that mutations, deletions or haploinsufficiency of genes such as *NRXN, NLGN, SHANK, FMR1, TSC1/2* and *MECP2 c*ontribute to cellular pathways that converge at synapses (Guang et al, 2018; Stessman et al, 2017; Wang et al, 2016). These risk genes linked to autism are reported to encode synaptic cell adhesion molecules, scaffolding proteins, or proteins that are key regulators of synaptic transcription, chromatin remodelling, protein turnover or cytoskeletal dynamics. Alteration of expression of these developmentally important genes can potentially affect synaptic strength and number of connections and neurotransmission, and ultimately, brain plasticity and connectivity, which are often considered as underlying cellular pathophysiology in autism and related neurodevelopmental conditions.

Among the autism related high-confidence synaptic genes, *NRXN1* and *SHANK3* encodes two key synaptic scaffolding proteins at the presynaptic and postsynaptic compartments respectively. NRXN1 is a presynaptic cell adhesion membrane protein that interacts with postsynaptic neuroligins (NLGNs), SHANKs and other postsynaptic density proteins and is a key regulator of synaptic transmission (Südhof TC, 2017). SHANK3, on the other hand, is a postsynaptic scaffolding protein with multiple domains such as ankyrin repeat, PDZ motif, proline-rich and Homer binding site through it extensively interacts with several molecules to form postsynaptic signalling complex (Monteiro and Feng, 2017). Several components of presynaptic-postsynaptic protein complex have been previously reported to be associated with autism and neurodevelopmental disorders since early 2000s (Südhof TC, 2008; Dean C et al, 2006; Moessner R et al 2007; Jamain S et al 2003; Laumonnier F et al 2004;

Tabuchi K et al 2007). However, the effect of loss of function of *NRXN1* and *SHANK3* on neuronal phenotypes has never been tested in human iPSC derived OPTi-OX *NGN2* iNeurons. Therefore, in this chapter, we have investigated the effect of transient knockdown of *NRXN1* and *SHANK3* in OPTi-OX *NGN2* iNeurons. *NRXN1* and *SHANK3* are both synaptic cell adhesion molecules that may affect functional electrophysiological properties as well as structural actin cytoskeleton dynamics. Besides, we have also optimised the classical lentiviral NGN2 method (Zhang et al, 2013; Pak et al, 2018) to generate excitatory neurons for future experiments on multiple iPSC lines from individuals with autism.

5.2 Aims

1. To characterise the expression of *NRXN1* and *SHANK3* in *NGN2* iNeurons
2. To examine the effect of transient knockdown of *NRXN1* and *SHANK3* on iNeuron electrophysiology
3. To optimise lentiviral iNeuron generation method to for future studies on multiple autism iPSC lines

5.3 Design

Control bob-NGN2 iPSCs were induced to generate i-neurons and expression of *NRXN1* and *SHANK3* were tested using qPCR, imaging or immunoblotting. siRNA mediated knockdown on *NGN2* iNeurons were carried out following the methods outlined in Chapter 2. Electrophysiological experiments to investigate the amplitude and frequency and firing properties were conducted under non-specific control siRNA, *NRXN1* siRNA and *SHANK3* siRNA conditions on day 30 i-neurons. The timeline of these experiments is outlined in Fig5.1. Finally, lentiviral NGN2 method was optimised, following the methodology in Chapter 2, as an alternative approach to rapidly generate *NGN2* iNeurons from hiPSCs. Characterisation of

NGN2-GFP transduced control iNeurons was conducted using calcium imaging, time-lapse imaging and morphological analyses.

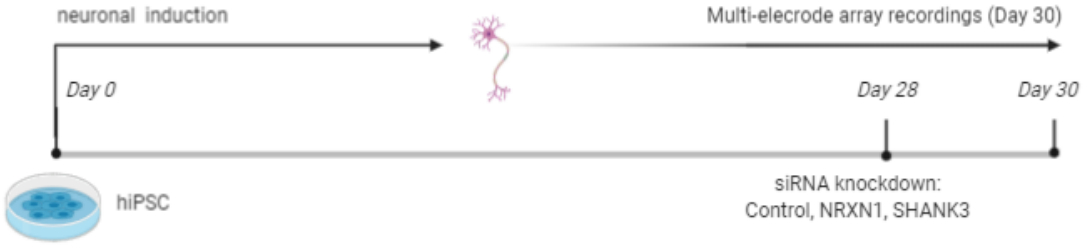

Figure 5-1 Schematic of experimental timeline

5.4 Results

5.4.1 *NRXN1* and *SHANK3* expression in iNeurons

Prior to conducting a loss of function knockdown experiment, we checked the level of expression of *NRXN1* and *SHANK3* to select a suitable timepoint. Due to unavailability of a good antibody specific against NRXN1 protein we based our experiment on RNA expression. The left panel in Fig5.4(A) shows the distinct subpopulations of RNA transcripts colour coded according to early time points: iPSCs/day 0, 12 hour, day 1, day 2, day 3, day 4 and later timepoints: day 14 and day 21 with or without glial cells in the single cell RNA expression data on control bob *NGN2* iNeurons. The right panel displays that *NRXN1* RNA transcripts show up at very low level as early as day 4 and gradually increases on day 14 and peaks on day 21. However, the PCR results on mRNA expression of pan-NRXN1 did not show any significant change over timepoints till day 21 [Fig5.4(B)]. This could be due to differential expression of different isoforms of *NRXN1*. Therefore, we compared the time course of expression of two main isoforms of NRXN1: NRXN1α and NRXN1β in bob *NGN2* iNeurons [Fig5.4(C)]. NRXN1α showed a significant increase on day 14 (*$p < 0.05$) and day 21 (***$p < 0.001$) compared to iPSCs. However, the NRXN1β did not show any significant change which might have affected the pan-NRXN1 expression since NRXN1β expression was significantly higher (**$p < 0.01$) than NRXN1α expression.

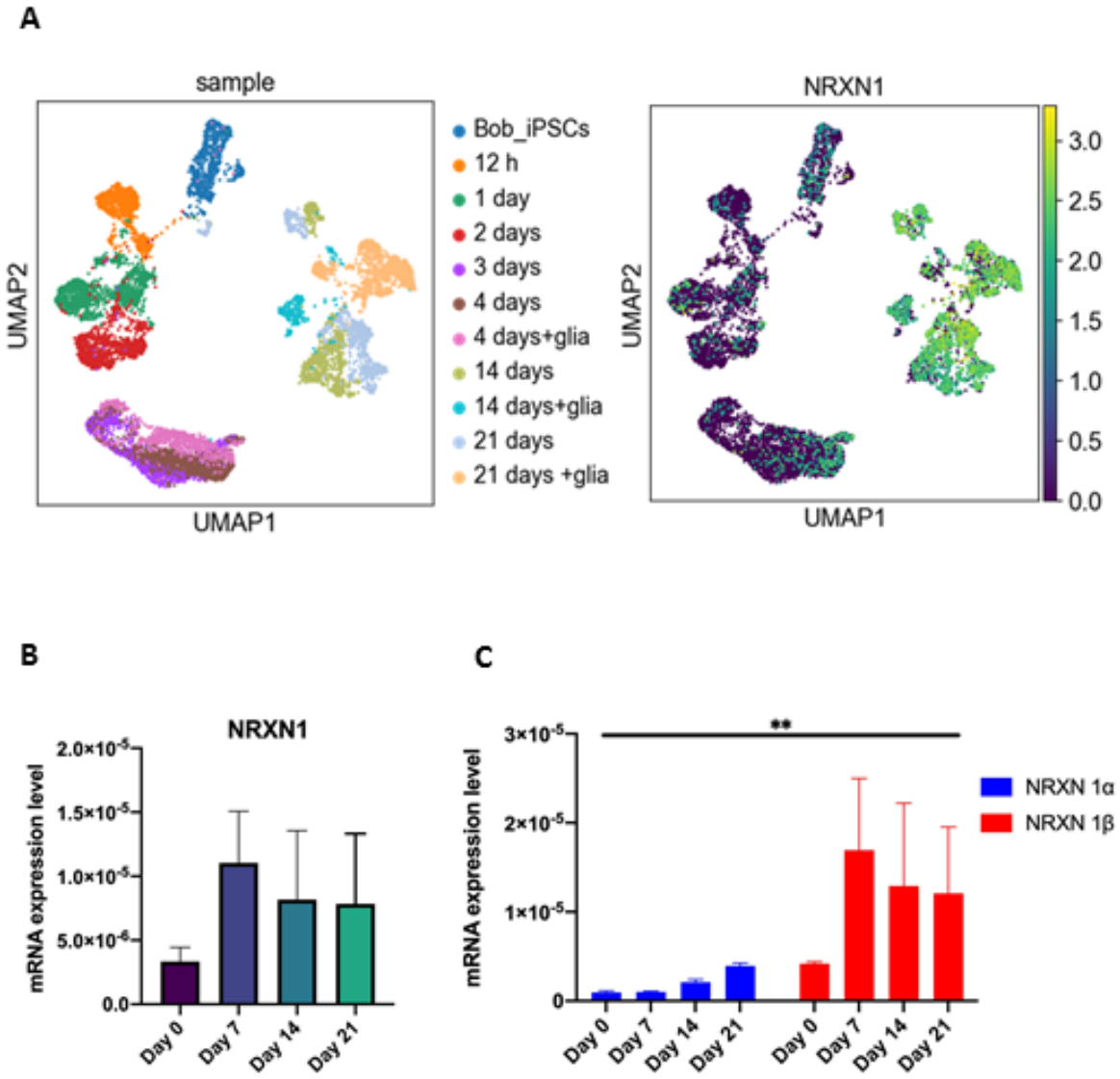

Figure 5-2 NRXN1 expression in NGN2 i-neurons

(A) UMAP projection of single cell RNA sequencing data showing NRXN1 expression across timepoints from iPSC stage to day 21 (B) Time course of mRNA expression of pan-NRXN1 in NGN2 i-neurons (C) Comparison of mRNA expression of NRXN1 isoforms: NRXN1α and NRXN1β (data from three experiments).

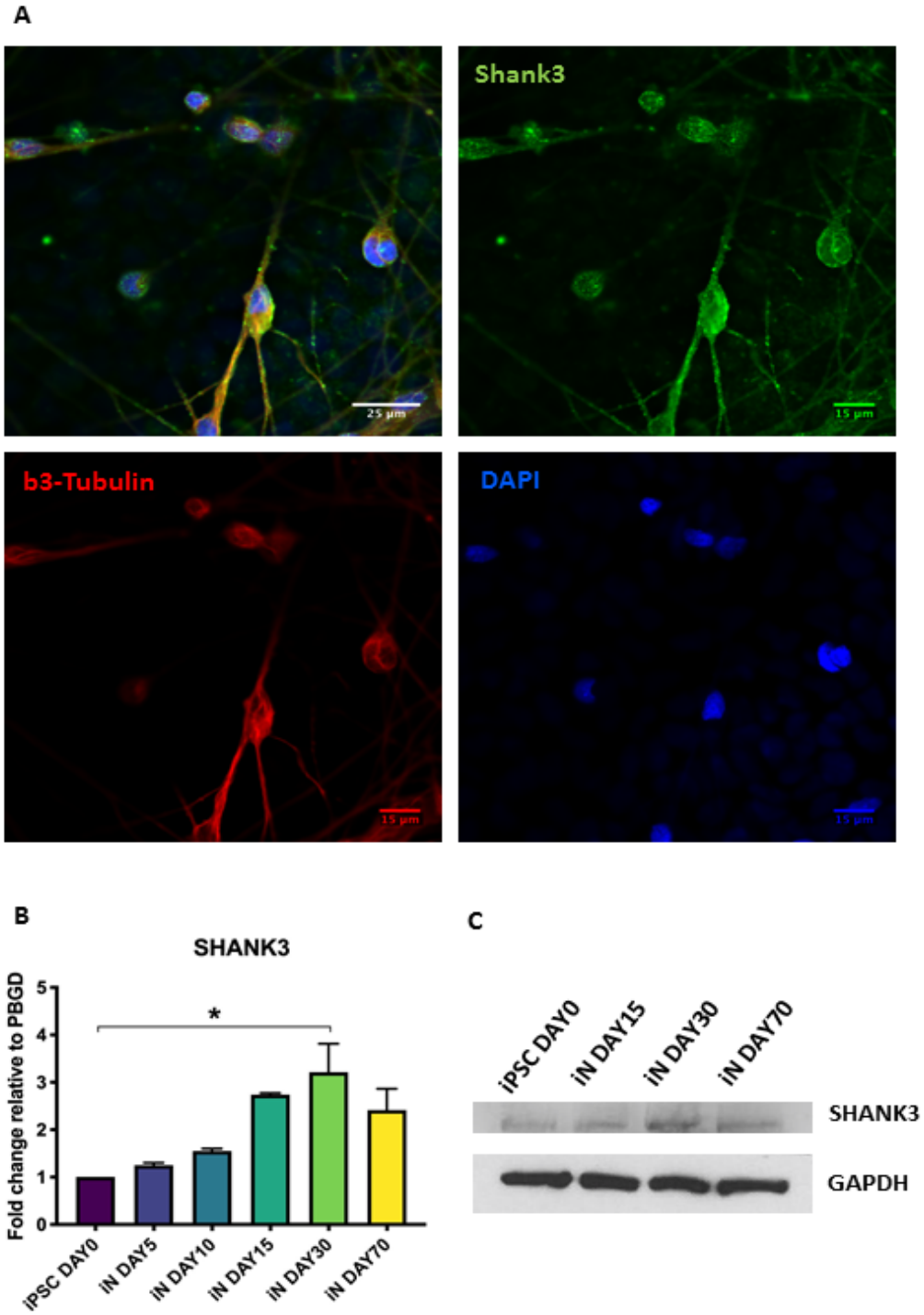

Figure 5-3 SHANK3 expression in NGN2 iNeurons

(A) Immunocytochemistry images of iNeurons at day 21 expressing SHANK3 (B) mRNA expression of SHANK3 in i-neurons across timepoints till day 70 (C) Protein expression of SHANK3 in i-neurons across timepoints till day 70.

Next, we checked whether and when *SHANK3* is enriched in control bob i-neurons. To capture a snapshot of *SHANK3* expression we first imaged i-neurons on day 21 and found the cells to be expressing SHANK3 protein [Fig5.3(A)]. The PCR data on mRNA expression of *SHANK3* showed a significant increase only on day 30 (*$p < 0.05$) [Fig5.3(B)]. The immunoblot also confirmed that the SHANK3 protein level was highest at day 30 timepoint [Fig5.3(C)]. Therefore, we chose day 30 as a suitable timepoint for knocking down *NRXN1* and *SHANK3* and to explore and compare the loss of function in terms of electrophysiological properties.

5.4.2 *NRXN1* and *SHANK3* knockdown in i-Neurons: functional characterisation

To characterise the effect of *NRXN1* and *SHANK3* knockdown on control *NGN2* induced neurons, multi-electrode array extracellular recordings were conducted on day 30 of induction (Fig 5.4). [Fig5.4(A)] displays an overview of mean firing rate of induced neurons transfected with non-specific negative control siRNA (CTRL), siRNA targeting NRXN1 (NX1 KD) and siRNA targeting SHANK3 (SH3 KD). The experimental conditions were baseline, AMPA receptor antagonist NBQX treatment (three successive treatments: NBQX1, NBQX2 and NBQX3) and washout. Under the negative control siRNA condition, mean firing rate increased significantly on addition of NBQX but no further change was observed on washout. Induced neurons on *NRXN1* knockdown showed a similar pattern of increase in mean firing rate on NBQX treatment. *SHANK3* knockdown also showed a similar effect on NBQX treatment, however, the firing rate significantly declined following the removal of the drug. There was no noticeable change on mean firing rate on addition of successive NBQX treatment under any transfection condition. [Fig 5.4(B)] shows the frequency time histogram of first 100 seconds duration of three representative electrodes from control siRNA (CTRL), NRXN1 siRNA (NX1 KD) and SHANK3 siRNA (SH3 KD) transfected i-neurons. Recordings from all three groups showed surprisingly low level of firing activity under baseline condition.

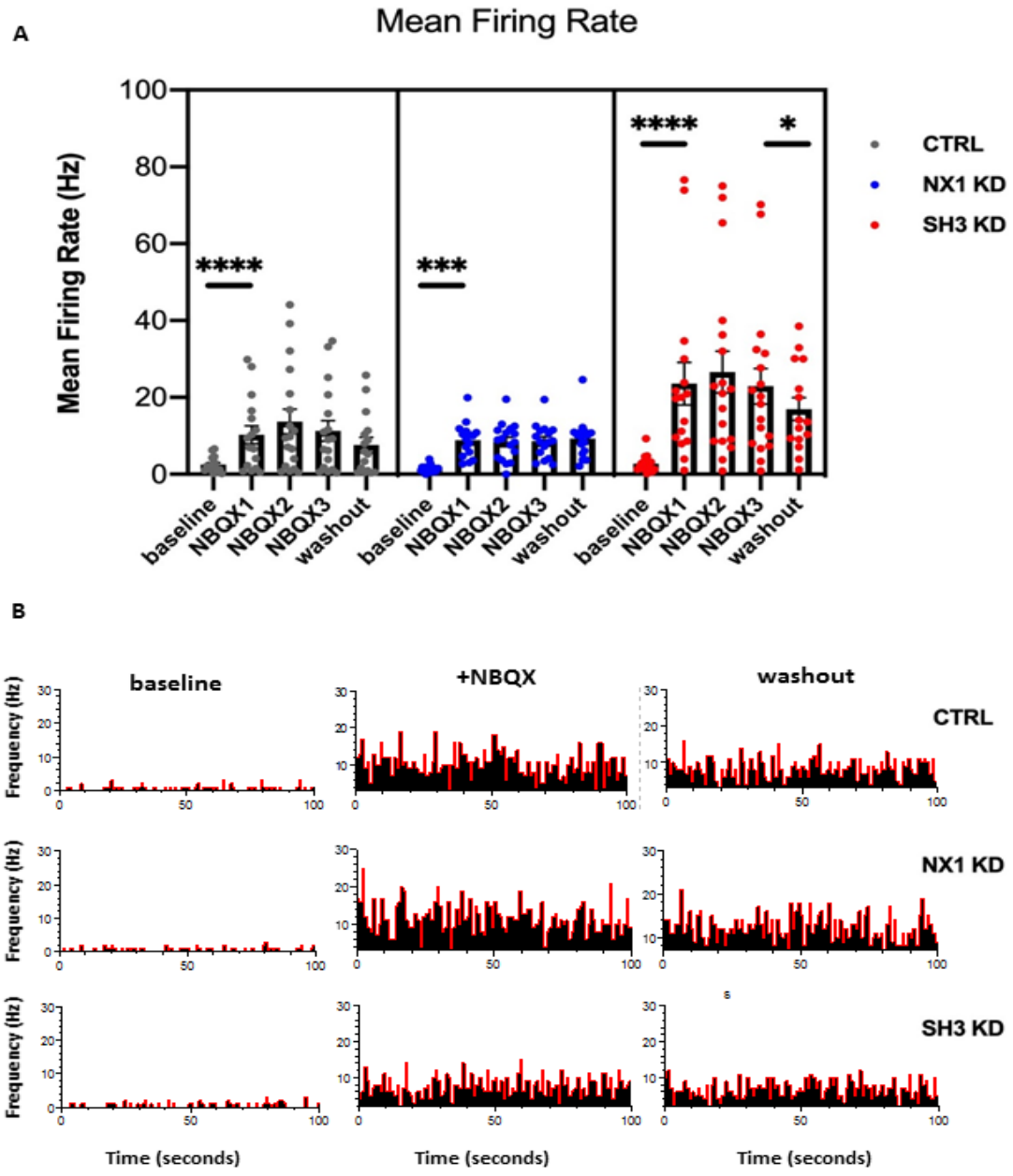

Figure 5-4 MEA spike analysis on *NRXN1* or *SHANK3* knockdown of control i-neurons at day 30.

(A) Mean firing rate of CTRL, NX1 and SH3 knockdown conditions at baseline, NBQX treatment and washout (18 electrodes in each group, 2 biological replicates, Friedman test with multiple comparisons). (B) Representative frequency histograms from single electrode from each CTRL, NX1 KD and SH3 KD groups at baseline, treatment and washout.

A common attribute of i-neurons observed is that the addition of NBQX elicits increase in mean firing activity, as earlier reported in Chapter 4. This intrinsic functional characteristic was unaffected by different transfection conditions. However, except for the *SHANK3* knockdown, the other two conditions did not exhibit any significant change in mean firing rate on washing out the exogenous drug from the recording media which could be due to presence of traces of residual NBQX. The spike analysis in conjunction with burst analysis would give a clearer picture of the effect of transient knockdown of *NRXN1* and *SHANK3* on *NGN2* iNeurons.

Fig5.5 displays the 3D histograms of amplitude waveforms of induced neurons at day 30 transfected with A) non-specific control siRNA (CTRL), B) siRNA targeting NRXN1 (NX1 KD) and C) siRNA targeting SHANK3 (SH3 KD). The y axis of the histograms represents waveform amplitude value in millivolt (mV) and the x axis is a 3 milli-second time window for action potentials. Each panel (A, B or C) shows the maximum voltage (peak) and minimum voltage (valley) values of waveforms for i-neurons in control, *NRXN1* knockdown or *SHANK3* knockdown conditions respectively, from which we can estimate the waveform amplitude (peak-valley range) for each condition. The i-neurons in negative control siRNA condition showed an amplitude of 53 µV (-41 µV valley to 12 µV peak) in baseline, 57 µV (-44 µV valley to 13 µV peak) on NBQX treatment and 45 µV (-32 µV valley to 13 µV peak) on washout condition [Fig 5.6(A)]. On NBQX treatment the amplitude increased from 53 µV to 57 µV and decreased again to 45 µV on removal of NBQX in washout condition. On NRXN1 knockdown condition, the i-neurons demonstrated amplitudes of 61 µV (-42 µV valley to 19 µV peak) in baseline, 40 µV (-29 µV valley to 11 µV peak) on NBQX treatment and 40 µV (-29 µV valley to 11 µV peak) on washout condition [Fig 5.6(B)]. It is interesting to find that on NBQX treatment the amplitude decreased from 61 µV to 40 µV and did not further change on washout.

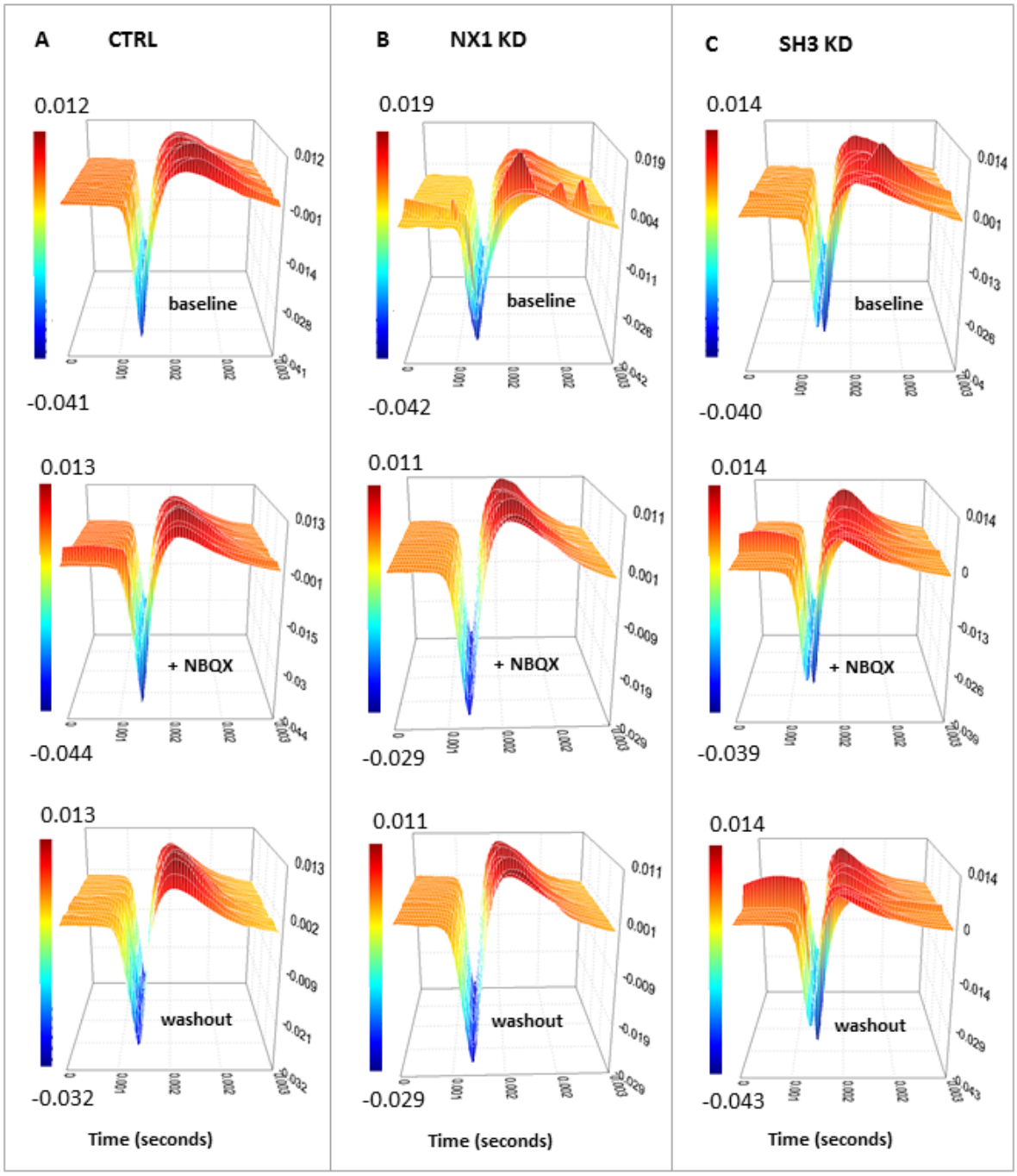

Figure 5-5 MEA waveform histogram comparison of i-neurons at day 30 on knockdown of *NRXN1* and *SHANK3*

Waveform amplitude (millivolt) in y-axis plotted against 3 millisecond duration of action potentials in x-axis for (A) Control non-specific siRNA transfected cells at baseline, NBQX treatment and washout conditions (B) NRXN1 specific siRNA transfected cells at baseline, NBQX treatment and washout and (C) SHANK3 specific siRNA transfected cells at baseline, NBQX treatment and washout. Colour bar indicates range of amplitude.

Similarly, in SHANK3 knockdown condition the i-neurons showed amplitudes of 54 μV (-40 μV valley to 14 μV peak) in baseline, 53 μV (-39 μV valley to 14 μV peak) on NBQX treatment and 57 μV (-43 μV valley to 14 μV peak) on washout condition [Fig 5.6(C)]. In SHANK3 condition there was no drastic change in waveform amplitude across baseline (54 μV), NBQX treatment (53 μV) or washout conditions (57 μV). The pattern of waveform amplitude, a frequency independent phenomenon, was observed to be different from MFR shown earlier.

We further analysed the effect of *NRXN1* and *SHANK3* knockdown on the burst properties of i-neurons. The mean burst duration in the control siRNA group remains unaffected by NBQX treatment [Fig 5.6(A)]. However, neurons with *NRXN1* and *SHANK3* knockdown show significant decrease in the duration of burst, but only after the second treatment. The mean inter-spike interval (ISI) in burst remains unaffected in control siRNA transfected neurons until the third treatment with NBQX [Fig 5.6(B)]. Neurons in *NRXN1* knockdown group exhibit a significant decrease in ISI in burst on second treatment and *SHANK3* knockdown group even sooner, on the first treatment of NBQX. This suggests that knockdown of *NRXN1* and *SHANK3* may alter the susceptibility of neurons to AMPA antagonist NBQX to different degrees thereby affecting the ISI in burst. However, the burst frequency and inter-burst interval across all conditions remained unaffected [Fig 5.6(C), (D)].

The mean spikes in burst showed a significant increase on addition on NBQX and plateaued on successive NBQX treatments [Fig 5.7(A)]. Thea mean peak frequency in burst and mean frequency in burst followed a similar trend across control and knockdown conditions with positive increase on NBQX treatment and no significant change on washout [Fig 5.7(B), (C)]. The burst surprise parameter exhibited an opposite pattern i.e. significant decrease on AMPA receptor blocking by NBQX. These electrophysiological properties were observed

across all transfection conditions. which indicates that transient knockdown did not alter these burst parameters.

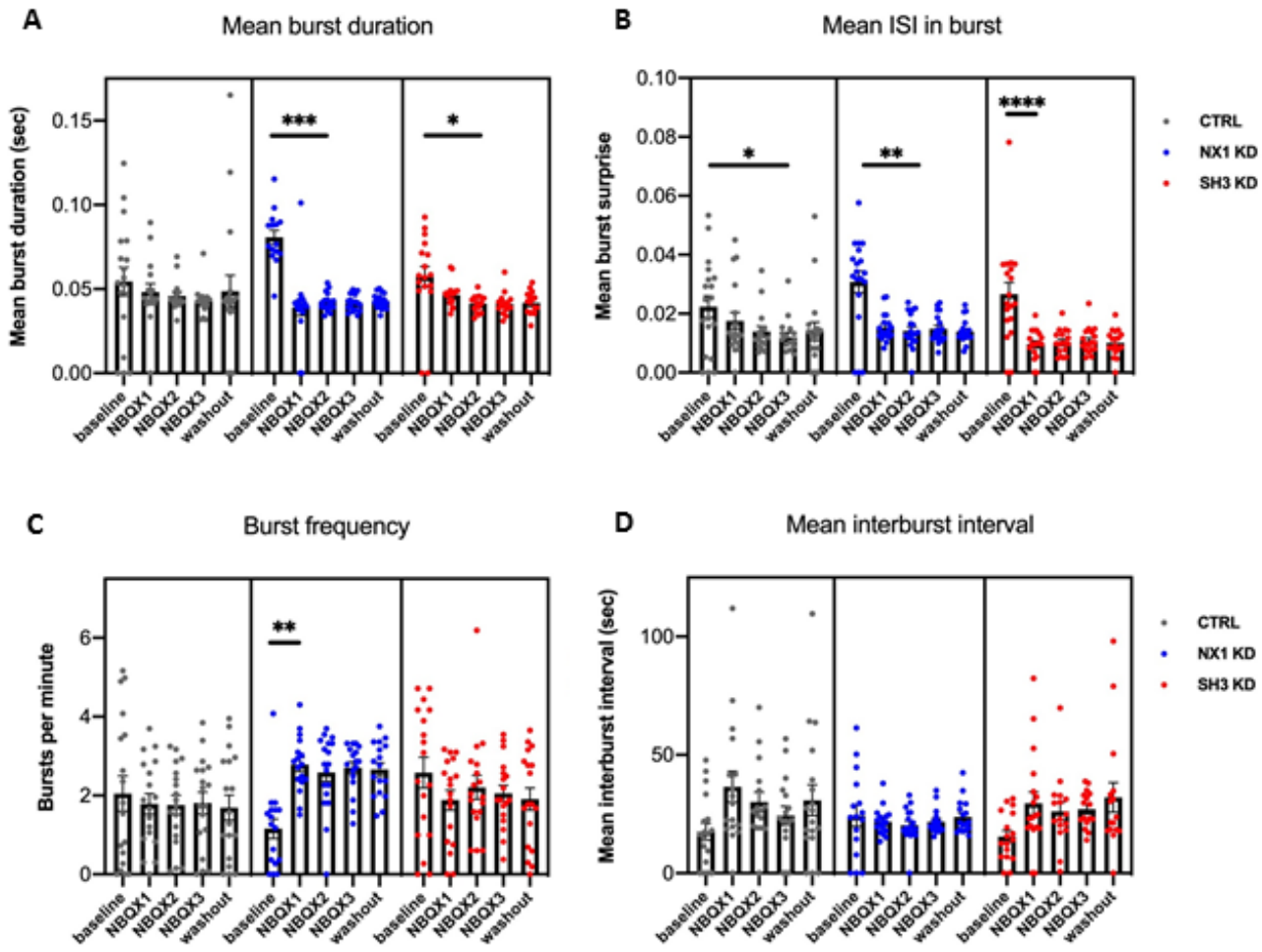

Figure 5-6 MEA burst analysis of day 30 i-neurons on knockdown conditions and pharmacological treatment

Bursting properties characterized as (A) mean burst duration (B) mean ISI in burst (C) burst frequency and (D) mean interburst interval for baseline, NBQX treatment (three successive recordings: NBQX1, NBQX2, NBQX3) and washout conditions, recorded from 18 electrodes for each condition, 2 biological replicates (Friedman statistical test for repeated measures).

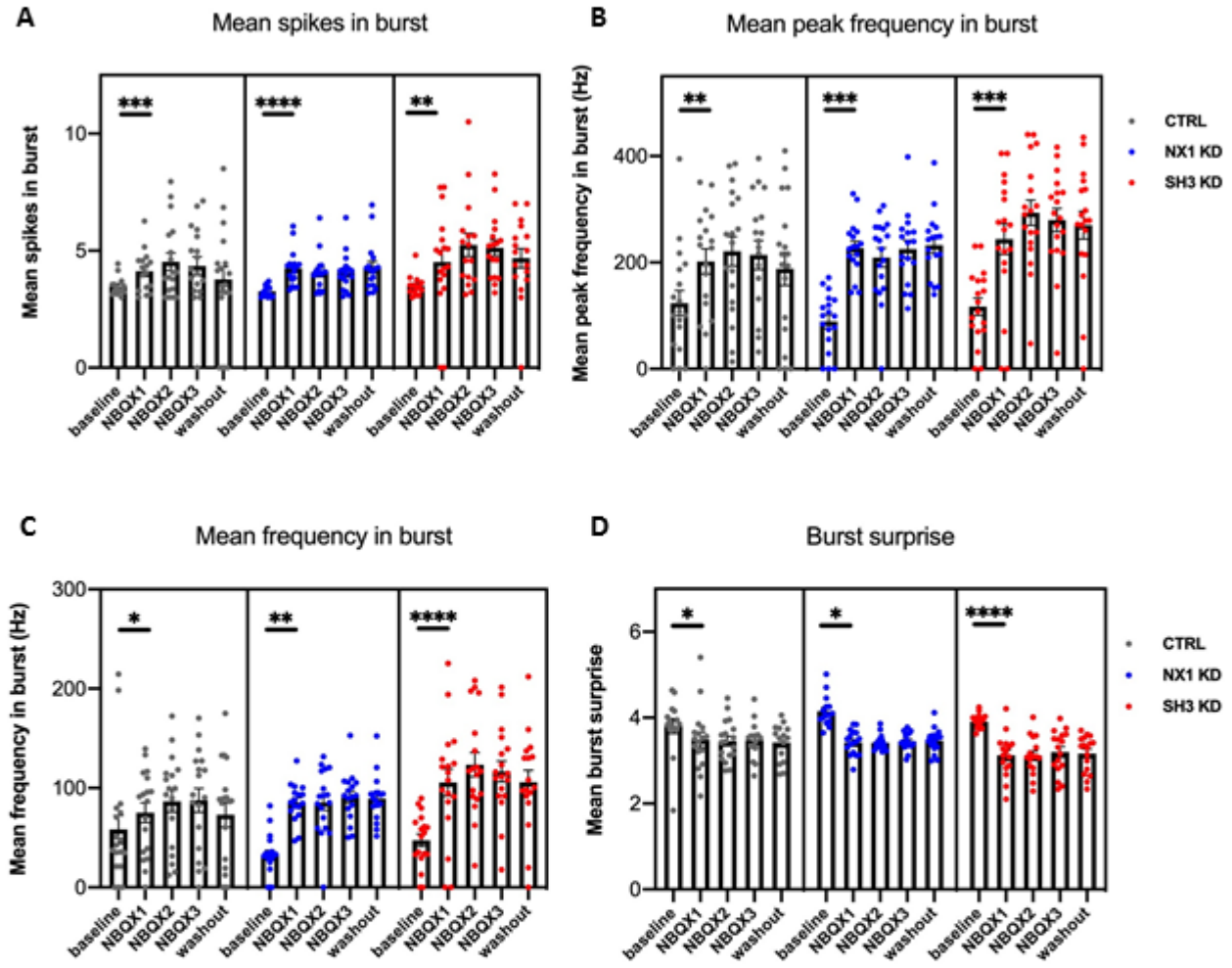

Figure 5-7 Spiking characteristics within bursts on knockdown conditions and pharmacological treatment.

Spiking properties characterised as (A) mean spikes in burst (B) mean peak frequency in burst (C) mean frequency in burst and (D) mean burst surprise for baseline, NBQX treatment (three successive recordings: NBQX1, NBQX2, NBQX3) and washout conditions (recorded from 18 electrodes for each condition, 2 biological replicates (Friedman statistical test for repeated measures).

We observed significant increase in mean firing rate in induced neurons on treatment with AMPA antagonist NBQX which was surprising. This could be due to changes in the binding properties of AMPA receptors or altered expression on the membrane. To further understand whether this could occur due to change in surface expression of AMPA receptors we imaged the i-neurons under untreated control, stimulant KCl and antagonist NBQX treatment conditions following methods described in Chapter 2. [Fig 5.8(A)] displays that bob NGN2 i-neurons express surface AMPA receptor subunit GluA2 when imaged under non-permeabilised conditions along with MAP2 and SYN1. Comparison of mean intensity of surface expression of GluA2 under stimulating condition of KCl treatment or AMPA antagonist NBQX treatment did not show any significant change [Fig 5.8(B)]. This indicates that NBQX does not alter AMPA receptor expression on the membrane surface of i-neurons, at least at the concentration of 5 μM and 24-hour treatment duration, which was followed in this experiment.

5.4.3 Lentiviral *NGN2*-overexpression

Opti-Ox NGN2 system is an efficient system for generation i-neurons rapidly in a very short span of time as discussed earlier. However, the main challenge of using this system is that each iPSC line needs to be targeted twice, with rtTA and NGN2, which requires nucleofection, clonal selection, clonal expansion and sequencing. This could be time consuming and also patient lines with mutations or deletions are often vulnerable to harsh treatment such as nucleofection as observed in our experience. Therefore, we further optimised the classical NGN2 lentiviral transduction protocol (Zhang et al, 2013; Pak et al, 2018) to generate neurons from multiple autism iPSC lines with deletions in *NRXN1* and *SHANK3*. [Fig 5.9(A)] shows the timeline of lentiviral NGN2 transduction protocol adapted from Zhang et al, 2013 and described in Chapter 2.

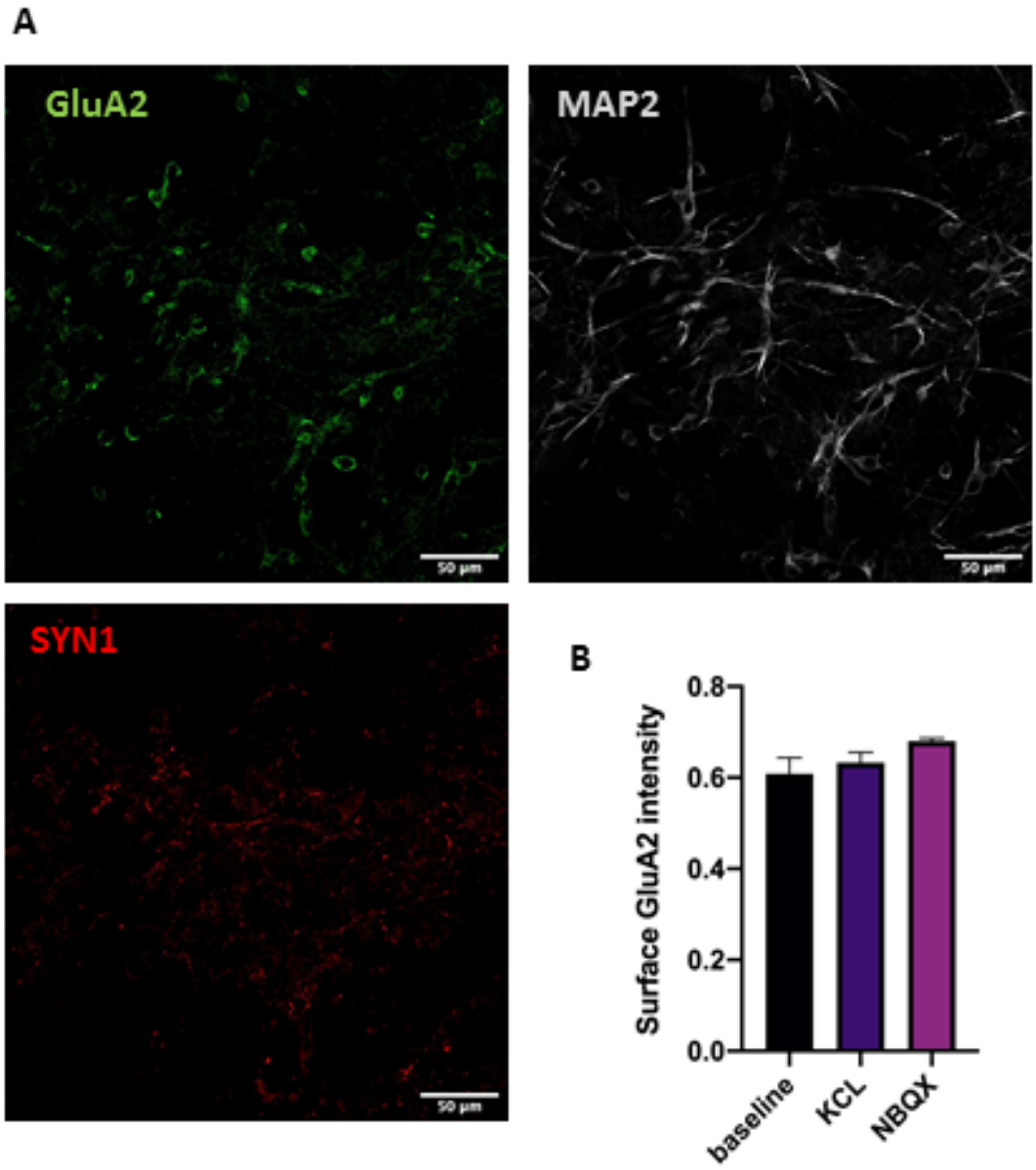

Figure 5-8 AMPA receptor GluA2 surface expression in *NGN2* iNeurons on day 30

(A) Confocal images of bob i-neurons expressing surface GluA2 AMPA receptor. (B) Comparison of surface GluA2 expression intensity on baseline/untreated, KCl treatment and NBQX treatment conditions (at least 45 images from 2 biological replicates per condition).

[Fig 5.9 (B)] demonstrates a confocal image of i-neurons expressing eGFP tagged human NGN2 on day 11, generated by lentiviral transduction method. We have used two vectors in this method: 1) FUdeltaGW-rtTA (a gift from Konrad Hochedlinger, addgene plasmid# 19780)

[Fig 5.9 (C)] and 2) pLV-TetO-hNGN2-eGFP-Puro (a gift from Kristen Brennand, addgene plasmid# 79823) [Fig 5.9 (D)]. The rtTA plasmid contained a reverse tetracycline transactivator gene insert under CMV promoter in a lentiviral FUdeltaGW backbone (Maherali et al, 2016). The NGN2 plasmid contained human Neurogenin-2 (hNGN2), eGFP tag and puromycin resistance gene (Puro) under control of TetON promoter. This third-generation lentiviral vector was previously reported to generate NGN2-iNs from hiPSCs and hiPSC-NPCs (Ho et al, 2016). Both these plasmids were packaged using HEK 293T cells into lentiviral particles as described in Chapter 2. Thereafter, the viral particles were used to transduce iPSCs on day (-1) and the TetOn inducible overexpression system was switched on day 0 by adding doxycycline (Dox). The following day i.e. on day 1, puromycin (Puro) antibiotic selection was carried out to get rid of the cells that were not transduced.

To check if there is any leaky GFP expression, confocal images were taken in presence or in absence of Dox and Puro till day 7 of induction protocol (Fig 5.10). At day 0, both Dox treated conditions showed eGFP expression, though more untransduced cells survived in without Puro antibiotic selection condition (Dox+/Puro-) on day 1. In absence of Dox (Dox-/Puro-), there was no eGFP expression at all, from day 0 till day 7, which confirms absence of any leaky GFP expression. We noticed that without Puro selection a significant proportion of Dox treated cells demonstrated atypical morphology. The Dox and Puro treated cells (Dox+/Puro+) showed immature neuron-like neuronal morphology at day 7 and therefore this condition was adopted further for generation and phenotyping of *NGN2* iNeurons from one control and four autism iPSC lines, as described in Chapter 6.

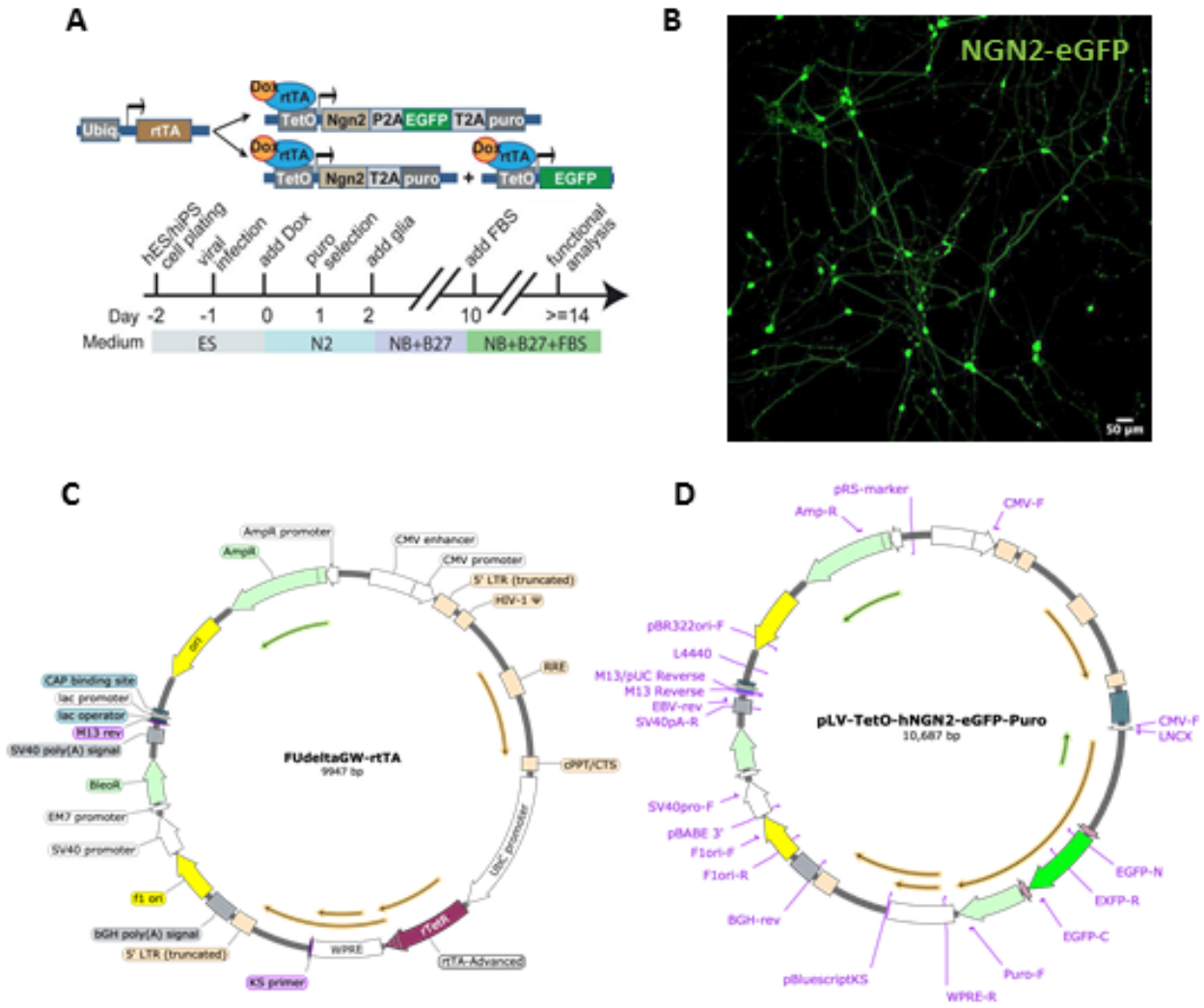

Figure 5-9 Lentiviral NGN2 method for generation of i-neurons

(A) Schematic of lentiviral NGN2 transduction protocol to generate i-neurons (adapted from Zhang et, 2013)
(B) A control iPSC Kolf line expressing eGFP tagged NGN2 on day 11 post transduction
(C) The vector map of rtTA (addgene plasmid# 19780)
(D) The vector map hNGN2-eGFP-Puro (addgene plasmid# 79823)

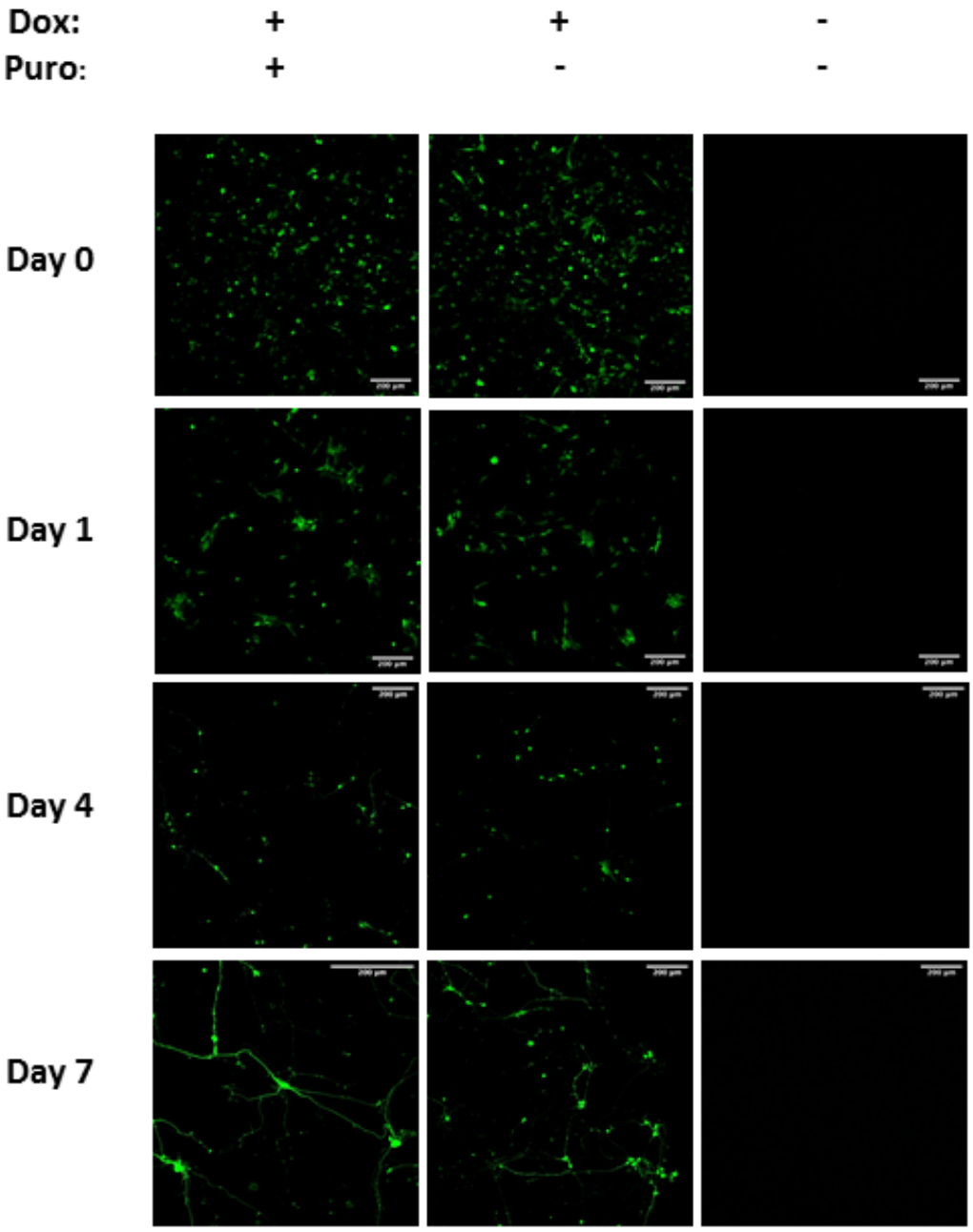

Figure 5-10 Lentiviral *NGN2* method optimisation

Confocal images of control Kolf iPSC lines post induction with rtTA and hNGN2-eGFP-Puro at time points: day 0 (within 24 hour of induction), day 1, day 4 and day 7. The different conditions shown are with both Dox and puro treatment (+/+), only dox but no puro (+/-) and without dox and puro (-/-).

5.5 Discussion

It has been reported recently that *NGN2* iNeurons reach second trimester of foetal cortical development within 2 to 3 weeks in culture (Rossa et al, 2020). It is also known that *NRXN1* isoform expression increase during foetal brain development, reaching its peak at week 39 gestation during second trimester (16-39 weeks) (Jenkins et al, 2016). In our data, we observed that NRXN1α expression corroborated with previous findings with a significant increase at the same developmental stage (day14 - day 21) in control i-neurons. However, the more abundantly expressed isoform NRXN1β did not display such expression profile. *SHANK3*, on the other hand, was found be significantly enriched in i-neurons on day 30 or week 4. The primer used to detect SHANK3 was against exons 8-9 region (encoding ankyrin domain) which is present in two major isoforms of SHANK3 i.e. SHANK3a and SHANK3b (Wang et al, 2014). Therefore, expression profile of NRXN1α and SHANK3 in iNeurons indicated that week 4 is a suitable time point for siRNA mediated loss of function experiment.

The multi-electrode array data suggests that there was no significant difference in firing rate (MFR) in NRXN1 or SHANK3 knockdown conditions from the negative control. Moreover, the NBQX treatment elicited similar pattern of firing response in i-neurons across all transfection conditions. It was surprising to find that treatment with NBQX increased MFR in i-neurons in control, NRXN1 and SHANK3 knockdown conditions. NBQX treatment also significantly increased the burst parameters such as mean spikes, mean frequency and mean peak frequency; whereas burst duration and mean ISI was found to decrease. The imaging results of surface expression of AMPA receptor subunit GluA2 on treatment with 5 μM NBQX for 24-hour revealed that there was no significant change of AMPA expression. The working concentration of exogeneous AMPA antagonist NBQX could be a reason for this. A titration with different concentrations of NBQX and time intervals should be carried out to investigate this further. Moreover, NBQX blocks only AMPA receptor mediated fast excitatory

postsynaptic current, whereas Tetrodotoxin (TTX) blocks all excitatory and inhibitory inputs, therefore it would be interesting to the effect of TTX on MFR of i-neurons. Lentiviral shRNA mediated knockdown of NRXN1α in neurons derived from hiPSC has previously shown perturb cell adhesion pathway (20 genes, P=2.8×10−6) and neuron differentiation pathway (13 genes, P=2.1×10−4) (Zeng et al, 2013), though it is not known whether alteration of gene expression could affect electrophysiological behaviour. Knockdown of SHANK3 in hiPSC derived neurons by lentiviral shRNA have been found to reduce the frequency of excitatory post synaptic current (sEPSC) relative to control neurons in 3.5 and 5.5 weeks along with transcriptional perturbation of gene related to neurogenesis and synapse development (Huang et al, 2019).

Some of the challenges of using Opti-Ox system for generation of *NGN2* iNeurons are that it is time consuming to target iPSCs with rtTA and NGN2 and conduct clonal selection, expansion and sequencing and patient iPSC lines with mutations or deletions are often vulnerable to nucleofection procedure. For phenotyping experiments on multiple iPSC lines derived from individuals with autism, we have optimised the lentiviral NGN2 method (Zhang et al, 2013, Pak et al, 2018). The method established in this chapter will be used in future to generate and subsequently phenotype morphological and functional properties of *NGN2* iNeurons from control and four autism iPSC lines with *NRXN1* or *SHANK3* deletions.

6 Chapter 6: iNeurons with *NRXN1* or *SHANK3* deletions

6.1 Introduction

Human induced pluripotent stem cells (iPSC) technology has been a key tool to model autism in a dish and study different cellular phenotypes arising due to specific loss of function mutations/deletions (Russo FB et al, 2019). Taking advantage of the transcription factor-based reprogramming approach, iPSCs can be efficiently programmed into different types of brain cells by forced inducible expression of a combination of transcription factors important for neuronal cell fate determination. Neurogenin-2 (*NGN2*) was identified as a single transcription factor sufficient to generate functional and homogeneous population of excitatory cortical layer 2/3 neurons only in 3 weeks *in vitro* (Zhang et al, 2013; Pak et al, 2018). This technological advancement has enabled researchers to perform structural and functional characterisation of genes and conduct disease modelling studies in a relatively shorter time frame (Pak et al, 2015; Yi et al, 2016). Very recently, NGN2 induced neurons have been reported to recapitulate the second trimester of human gestation when cultured with astrocytes (Rosa et al, 2020).

In this chapter, we have investigated one control and four iPSC lines derived from individuals diagnosed with autism bearing deletions in *NRXN1* (n=2, 1 male, 1 female) and *SHANK3* (n=2, 1 male, 1 female). The lentiviral NGN2 method optimised in the previous chapter (Chapter 5) was used to generate excitatory neurons from these autism iPSC lines. Autism risk genes *NRXN1* and *SHANK3* both encode cell adhesion molecules in presynaptic and postsynaptic terminals and are reported to affect actin dynamics (Südhof, 2018; Kathuria et al, 2018; Nia et al, 2018). Therefore, we looked into the morphological characteristics such as soma size, neurite length and branching points in the neurons induced from the autism lines with deletions in *NRXN1* and *SHANK3*. These synaptic genes also affect neurotransmission and firing properties of excitatory neurons (Pak et al, 2015; Yi et al, 2016). Previously most studies have used intracellular patch clamp recordings to characterise the effect of genetic

mutations on synaptic transmission. We have looked at extracellular functional phenotypes such as amplitude and frequency patterns using multi-electrode arrays from populations of neurons induced from autism iPSC lines.

6.2 Aims

1. To investigate morphological phenotypes in autism hiPSC lines with deletions in *NRXN1* or *SHANK3*
2. To characterise the electrophysiological properties of i-neurons induced from hiPSC lines with deletions in *NRXN1* or *SHANK3*

6.3 Design

Packaging of lentiviral particles was carried out using HEK 293T cells and Dharmacon trans-lentiviral packaging kit. Lentiviral transductions with rtTA and hNGN2-eGFP-puro transfer vectors were performed on one control and four autism iPSC lines with *NRXN1* (n=2, 1 male, 1 female) and *SHANK3* (n=2, 1 male, 1 female) deletions. GFP-tagged neurons were grown in presence of rat astrocytes following the neuronal induction protocol outlined in Chapter 2. The neurons were imaged using fluorescence microscope and morphological parameters measured using imageJ software. Spontaneous activity was checked using ratio-metric calcium indicator Fura red on autism neurons. Thereafter, functional characterisation such as waveforms, firing activity and bursting parameters were measured using multi-electrode arrays, MC_Rack and Neuroexplorer softwares. All statistical analyses were carried out using Prism. The experimental timeline is depicted in Fig6.1 and the details of experimental methodologies described in Chapter2.

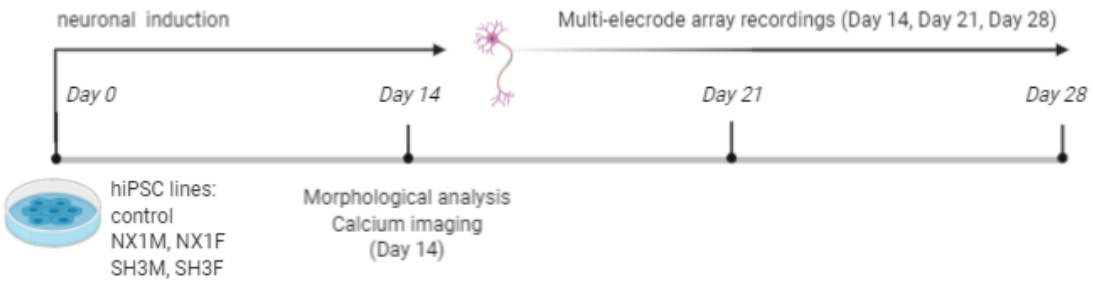

Figure 6-1 Schematic of autism lines experiment

6.4 Results

6.4.1 Autism iPSC lines with NRXN1 or SHANK3 deletions

NRXN1 is a 1,114,057 bp gene located on chromosome 2 (chr2: 49,918,505 - 51,032,561) and is reported as a high confidence autism related gene (https://gene.sfari.org/database/human-gene/NRXN1) according to SFARI gene consortium (https://gene.sfari.org/autdb/GS_Home.do; Banerjee-Basu et al., 2009; Abrahams et al., 2013) [Fig6.2(A)]. In this study we have used two hiPSC lines with deletions in *NRXN1* such as 109_NXM and 092_NXF. 109_NXM is a male iPSC line with maternally inherited deletion ~60kb in short arm of chromosome 2 – 2p16.3 (50,888,852 – 50,947,729) with no other additional abnormalities as depicted from whole exome sequencing. The 092_NXF is a female line with a *de novo* deletion of ~200kb in short arm of chromosome 2 – 2p16.3 (50,806,991 – 51,013,685). Both these lines were generated and characterised at Prof Jack Price and Dr Deepak Srivastava's labs in King's College London and kindly provided for our study. 109_NXM and 092_NXF have been referred to as male and female *NRXN1* lines i.e. NX1M and NX1F respectively throughout this study. Clinical symptoms associated with NX1M line are autism, developmental delay and microcephaly. However, both parents were neurotypicals and with normal head circumference. Array CGH results did not detect any CNV in father, although mother had the chromosome 2 deletion – _2p16.3 (50,888,852 – _50,947,729). The clinical symptoms of NX1F were reported as autism, socio-communicative difficulties and developmental delays. Family medical history suggests that both parents were neurotypicals

with no CNV in mother, but father carried a chromosome 1 duplication 1q21.1 (144,679,874 – _145,747,269) which is likely to be benign. This paternally inherited duplication was an additional CNV besides *de novo* deletion of ~200kb in short arm of chromosome 2 – _2p16.3 (50,806,991 – _51,013,685) in NX1F.

On the other hand, *SHANK3* is a relatively smaller gene of 78,884 bp on chromosome 22 (chr22: 50,666,969 - 50,745,852) and is also considered as a high confidence autism risk gene [(Fig6.2(B)] (https://gene.sfari.org/database/human-gene/SHANK3). The two autism lines with *SHANK3* deletions used in this study are 114_S3M and 107_S3F. 114_S3M is from a male diagnosed with autism with a deletion from *SHANK3* exon 4 to the next gene ACR and 107_S3F from a female diagnosed with autism with a deletion extending from *SHANK3* exon4 to the next two genes ACR and RABL2. Both these lines were previously characterised in Jack Price lab (KCL) and used to study morphological phenotypes in hypothalamic neurons (Kathuria et al, 2018). We have referred to 114_S3M and 107_S3F lines as SH3M and SH3F respectively in our study. The SH3M patient was a four-year-old male diagnosed with autism, regression of motor skills, language and speech delay, with a deletion in SHANK3 exon4 to the next gene ACR (Acrosin). The SH3F patient line is from a five-year-old female diagnosed with autism, social communication disorder and speech delay. The patient has a deletion extending from SHANK3 exon4 to the next two genes ACR and RABL2 (Ras oncogene family like 2).

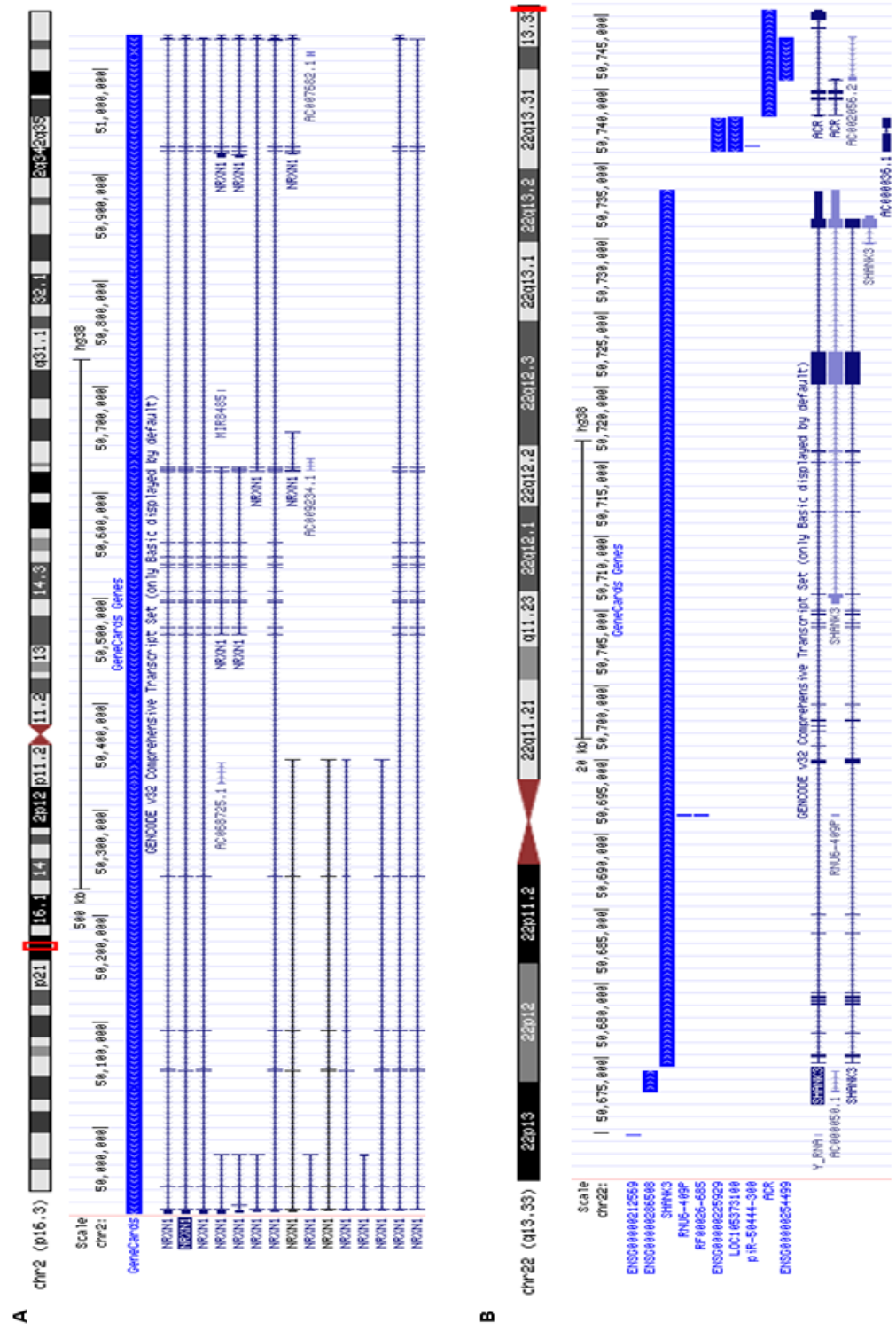

Figure 6-2 Genomic map of NRXN1 and SHANK3

Genomic maps of A) *NRXN1* on Chromosome 2. B) *SHANK3* on Chromosome 22.

6.4.2 Morphological characterisation

To study the effect of *NRXN1* and *SHANK3* deletions on neuronal morphology, we characterised the morphological metrics such as cell soma size and neurite outgrowth at day 14. Control (Kolf) and four autism iPSC lines with *NRXN1* (NX1M, NX1F) and *SHANK3* (SH3M, SH3F) deletions were transduced with rtTA and NGN2-eGFP lentiviral particles and analysed on day 14 from at least 45 neurons in each group from three biological replicates. [Fig6.3(A)] shows representative images from NX1M, NX1F, SH3M and SH3F i-neurons expressing GFP. We did not observe any significant differences in neuronal soma size across the control and autism, except for the SH3F neurons, with smaller cell size (adjusted p 0.0347) compared to controls [Fig6.3(B)]. Primary neurites (axons, as defined in the methods section in Chapter 2) were shorter in SH3F neurons (adjusted p 0.0120) compared to controls, though no other autism line showed any significant difference [Fig6.4(A)]. However, the total neurite length (sum of primary and secondary processes) was found to be significantly decreased in NX1M, SH3M and SH3F i-neurons [Fig6.4(C)]. This was due to the presence of shorter secondary neurites in NX1M, SH3M and SH3F i-neurons which indicates decreased length of dendritic processes in these cell types [Fig6.4(B)]. Branching points, number of processes emanating from cell soma (both axonal and dendritic), were also observed to be significantly lower in the autism lines [Fig6.4(D)]. A number of autism neurons (NX1M=6.67%, NX1F=2.2%, SH3M= 13.33% and SH3F=42.22%) showed branching point=1 i.e. a single primary neurite emanating from the cell body without any secondary or dendritic branching. The data on morphological measurements suggests that at day 14 most of the autism i-neurons were relatively immature and possibly at stage 3 of neuronal development in culture, identified by the presence of a long axon and short emerging dendrites (Dotti et al, 1988). Establishment of dendritic field was found to be absent at this stage of day 14.

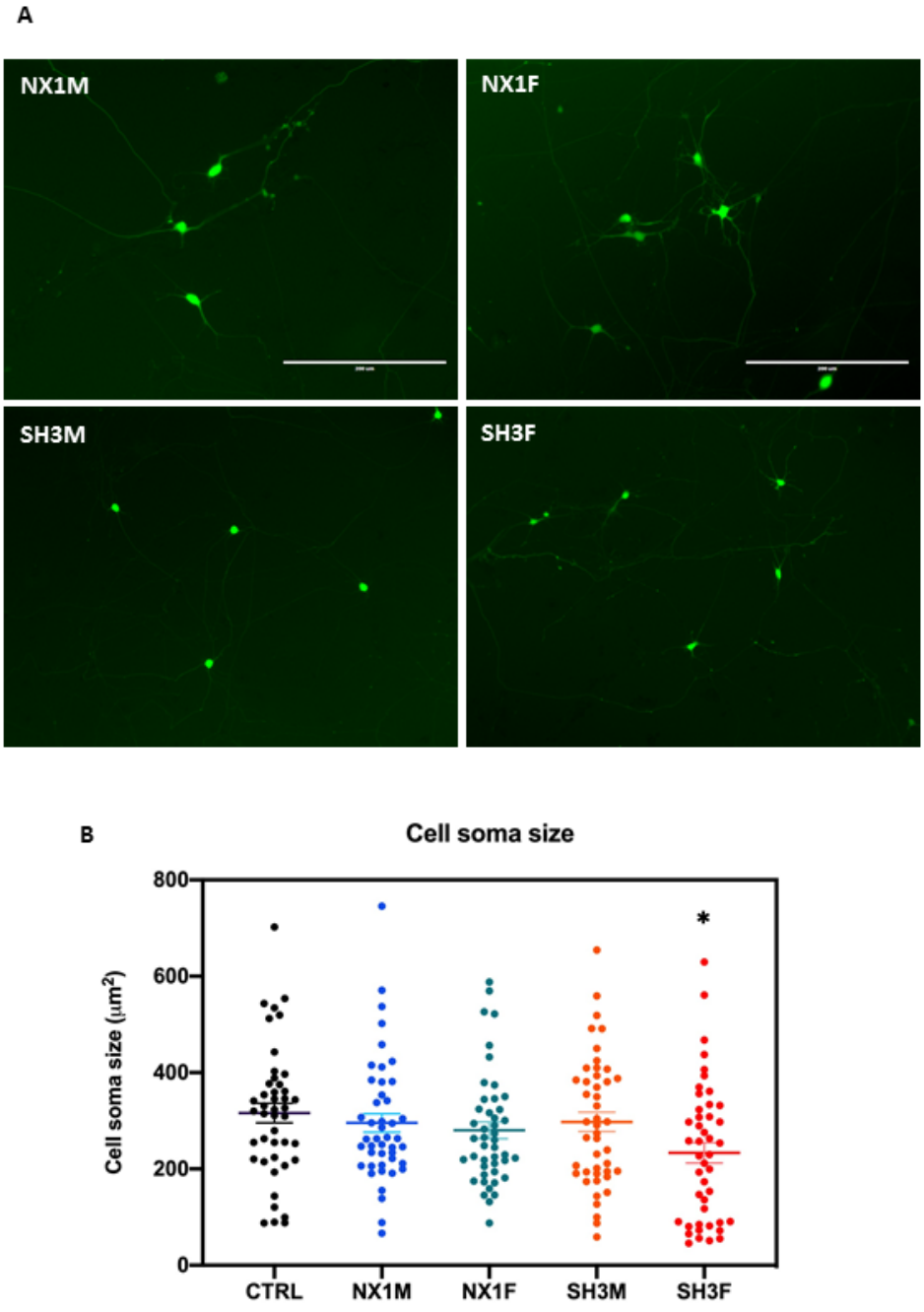

Figure 6-3 Morphology of i-neurons with *NRXN1* or *SHANK3* deletions

(A) Representative images of GFP expressing i-neurons with NRXN1 (NX1M, NX1F) or SHANK3 (SH3M, SH3F) deletions at day 14 (B) Comparison of cell soma size of CTRL, NX1M, NX1F, SH3M, SH3F i-neurons (at least 45 neurons from 3 biological replicates analysed per group, one-way ANOVA with Holm-Sidak test for multiple comparisons).

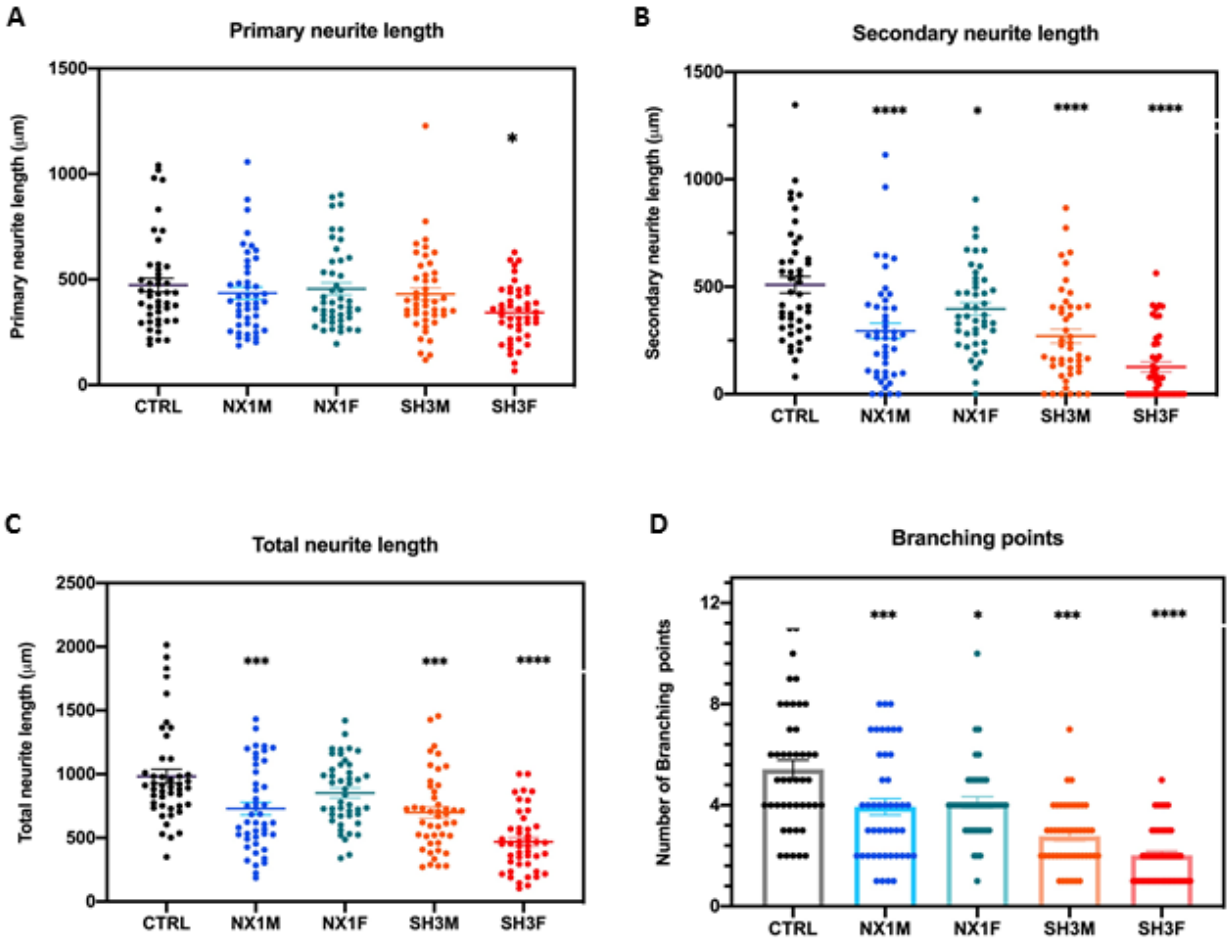

Figure 6-4 Neurite characterisation of i-neurons with *NRXN1* or *SHANK3* deletions

CTRL, NX1M, NX1F, SH3M, SH3F i-neurons at D14 compared for (A) Primary neurite length (B) Secondary neurite length, (C) Total neurite length and (D) Branching points (at least 45 neurons from 3 biological replicates analysed per group, one-way ANOVA with Holm-Sidak test for multiple comparisons).

6.4.3 Functional characterisation

To investigate whether the i-neurons generated from autism iPSC lines (NX1M, NX1F, SH3M and SH3F) are functionally viable with spontaneous electrophysiological activity, we first

checked the calcium transients in these neurons. Since lentiviral NGN2 i-neurons were eGFP-tagged we chose a red shifted calcium indicator Fura red so that GFP and the change in fluorescence intensity of Fura dye could be simultaneously measured using a single excitation wavelength of 488 nm (Schauer et al, 2012). The interesting property of Fura red is that its fluorescence intensity at 650 nm diminishes when the chelator binds to calcium ions. Therefore, resting neurons with low Ca^{2+} concentration show relatively high fluorescence intensity. [Fig6.5(A)] shows an example of NX1M NGN2-eGFP expressing i-neurons at day 14 loaded with Fura red dye. GFP marker was conveniently used to identify and select regions of interest (ROIs) on cell soma of *NGN2* expressing i-neurons from the background astrocytes which were also loaded with Fura red. The Fura red ratio (ratio of fluorescence emission intensity at 525 nm and 650 nm) demonstrate the intracellular calcium transients of each individual neurons [Fig6.5(B)]. Similarly, ROIs were drawn on eGFP expressing individual neurons and Fura red ratio of NX1F, SH3M and SH3F i-neurons on day 14 were plotted [Fig6.5(C), (D), (E)]. At least 60% of neurons from all recordings demonstrated greater than 1.5-fold change in fluorescence intensity across all four autism NGN2 i-neurons (NX1M, NX1F, SH3M and SH3F). This indicates that at day 14, these lentiviral transduced *NGN2* expressing i-neurons show spontaneous change in intracellular calcium flux in the autism lines. However, this was carried out at only one timepoint as a preliminary experiment to get a first-hand idea whether the cells are functional. Thereafter, a more detailed quantitative analysis of firing patterns of these neurons till day 21, when the cells reach a more physiologically mature state was carried out using extracellular multi-electrode array recordings.

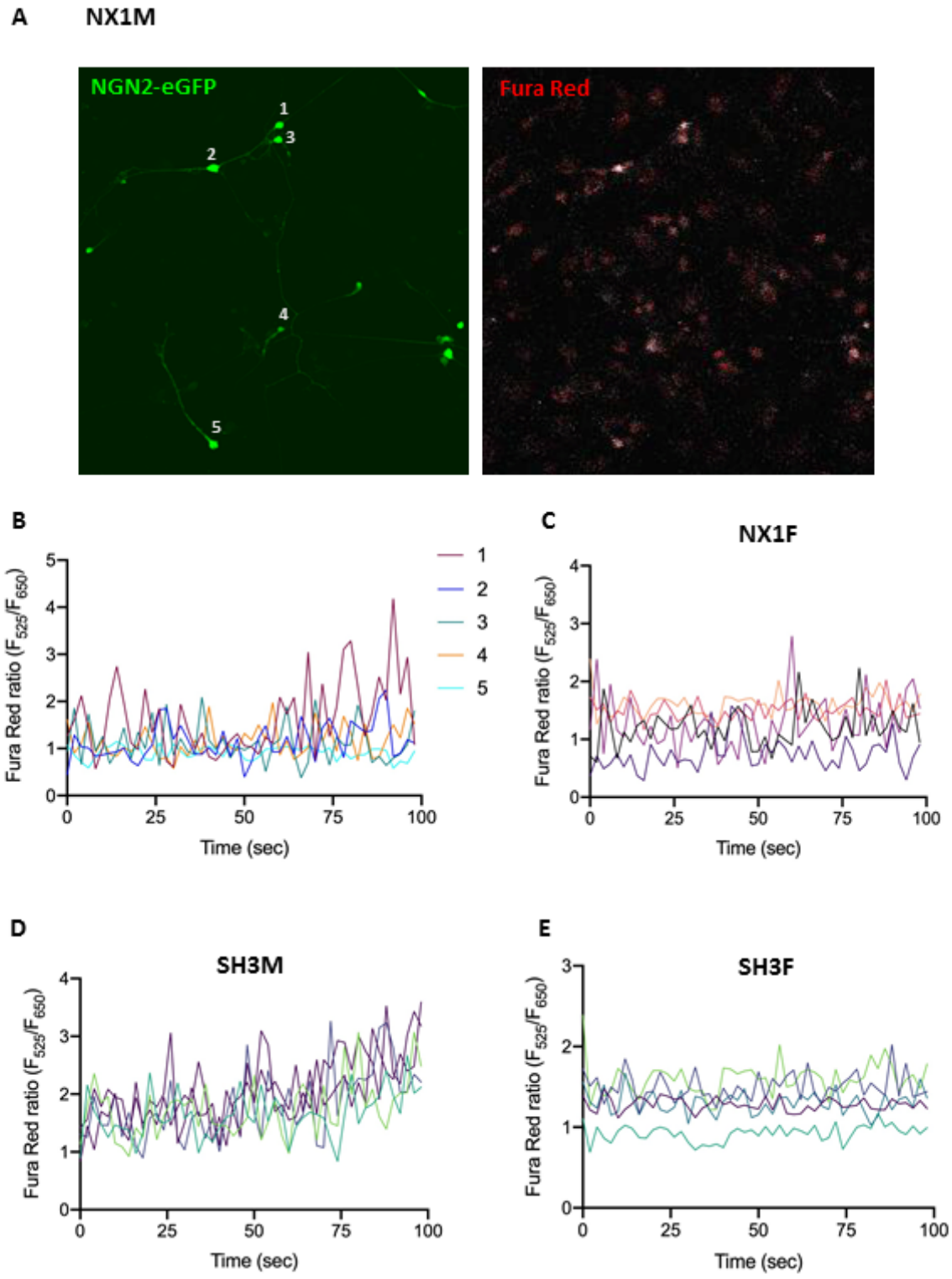

Figure 6-5 Calcium imaging of induced neurons generated from autism lines

A: Confocal image of NGN2-eGFP expressing NX1M day 14 i-neurons loaded with Fura Red B: Spontaneous calcium traces from selected ROIs over 100 second interval. C, D, E: Calcium traces from day 14 i-neurons generated from NX1F, SH3M, SH3F respectively.

To characterise the emergence of firing activity and the temporal pattern of spiking properties in neurons induced from autism iPSC lines, we performed multi-electrode array recordings at timepoints day 14, day 21 and day 28 post lentiviral transduction [Fig6.6(A)]. The control i-neurons showed a significant increase in mean firing rate (MFR) on day 21 and no further change till day 28. NX1M and NX1F both i-neurons exhibited a similar pattern of significant rise in MFR on day 21 and also on day 28. Among SH3M and SH3F, only the female line showed a rise on day 21. However, both demonstrated a significant increase in MFR on day 28 when all the autism i-neurons peaked. [Fig6.6(A)] displays an overview of frequency-time histograms of one representative electrode from NX1M, NX1F, SH3M and SH3F longitudinally from day 14, day 21 and day 28 to visualise the emergence of spikes. All i-neurons showed firing activity close to baseline on day 14 and firing activity gradually increased till day 28. It is interesting to note that both NRXNI lines (NX1M and NX1F) showed much higher firing activity on day 28 than the control or SHANK3 lines. However, some electrodes at later time points such as day 21 and day 28 still showed very low activity which have not been excluded from the data.

The spiking patterns of neurons induced from the autism lines at the latest timepoint i.e. day 28 can be better visualised in the 3-dimensional frequency histogram (Fig6.7). Both NX1M and NX1F showed very high firing rates, maximum frequencies being 369 Hz and 388 Hz respectively [Fig6.7 (A), (B)]. The lowest frequencies at this time point for NX1M and NX1F were 24 Hz and 45 Hz respectively, still higher than baseline. On the other hand, *SHANK3 l*ines showed a lower firing rate compared to the *NRXN1* lines [Fig6.7 (C), (D)].

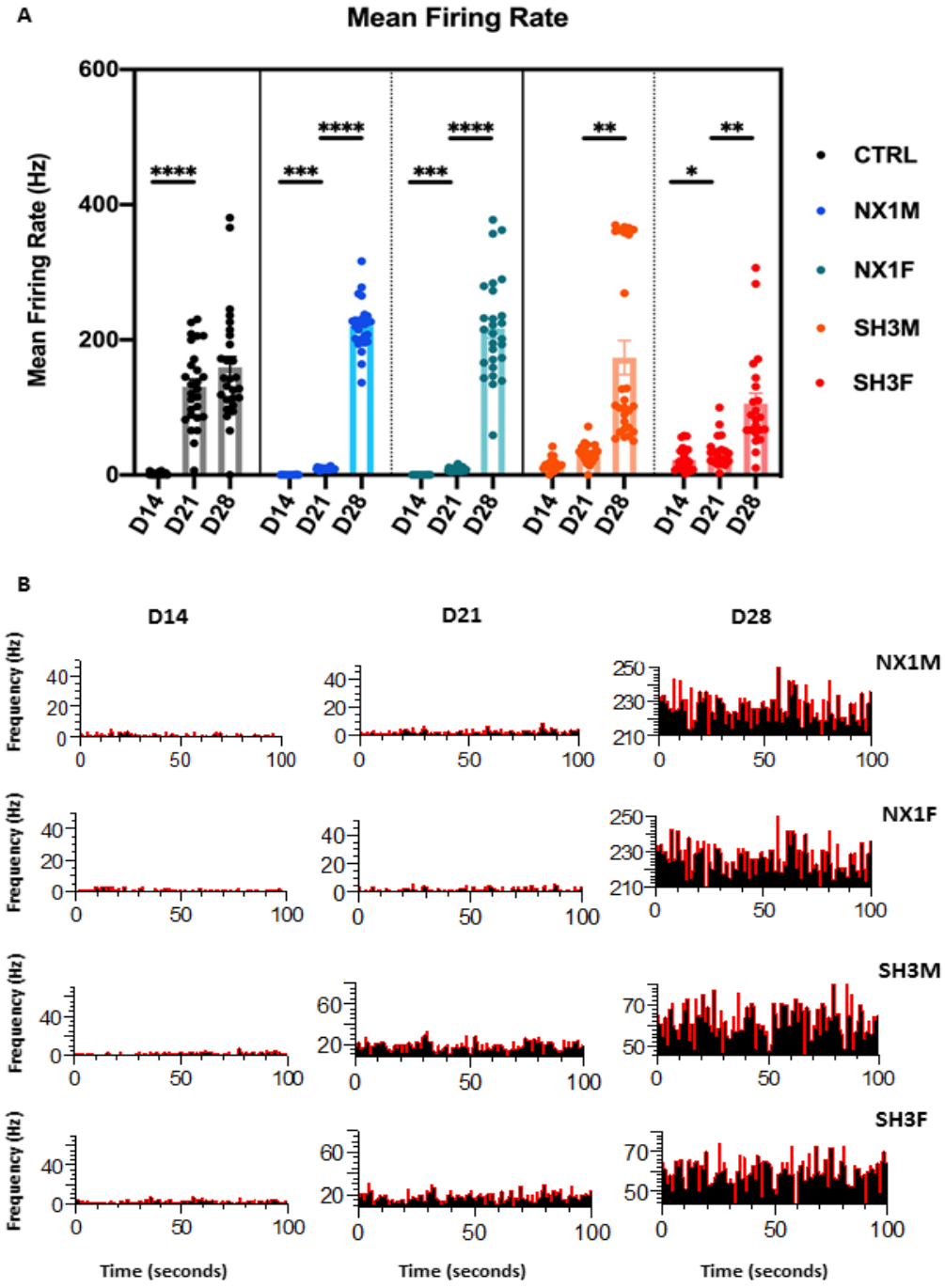

Figure 6-6 MEA spike analysis of i-neurons with *NRXN1* or *SHANK3* deletions

(A) Mean firing rate (MFR) comparison of CTRL, NX1M, NX1F, SH3M, SH3F i-neurons at timepoints day 14, day 21 and day 28 (24-28 electrodes per timepoint, 3 biological replicates, Kruskal-Wallis statistical test for multiple comparisons). (B) Representative frequency histogram of a single electrode each from NX1M, NX1F, SH3M, SH3F across timepoints.

The range of frequencies exhibited by SH3M (maximum frequency= 327 Hz, minimum frequency= 0) and SH3F (maximum frequency= 316 Hz, minimum frequency=0) at day 28 demonstrate that a number a electrodes recorded baseline recording which could be due several reasons such as intrinsic cell-autonomous trait (delayed firing) or heterogeneity of cell population, cell density and extrinsic technical issues of cell to electrode contact.

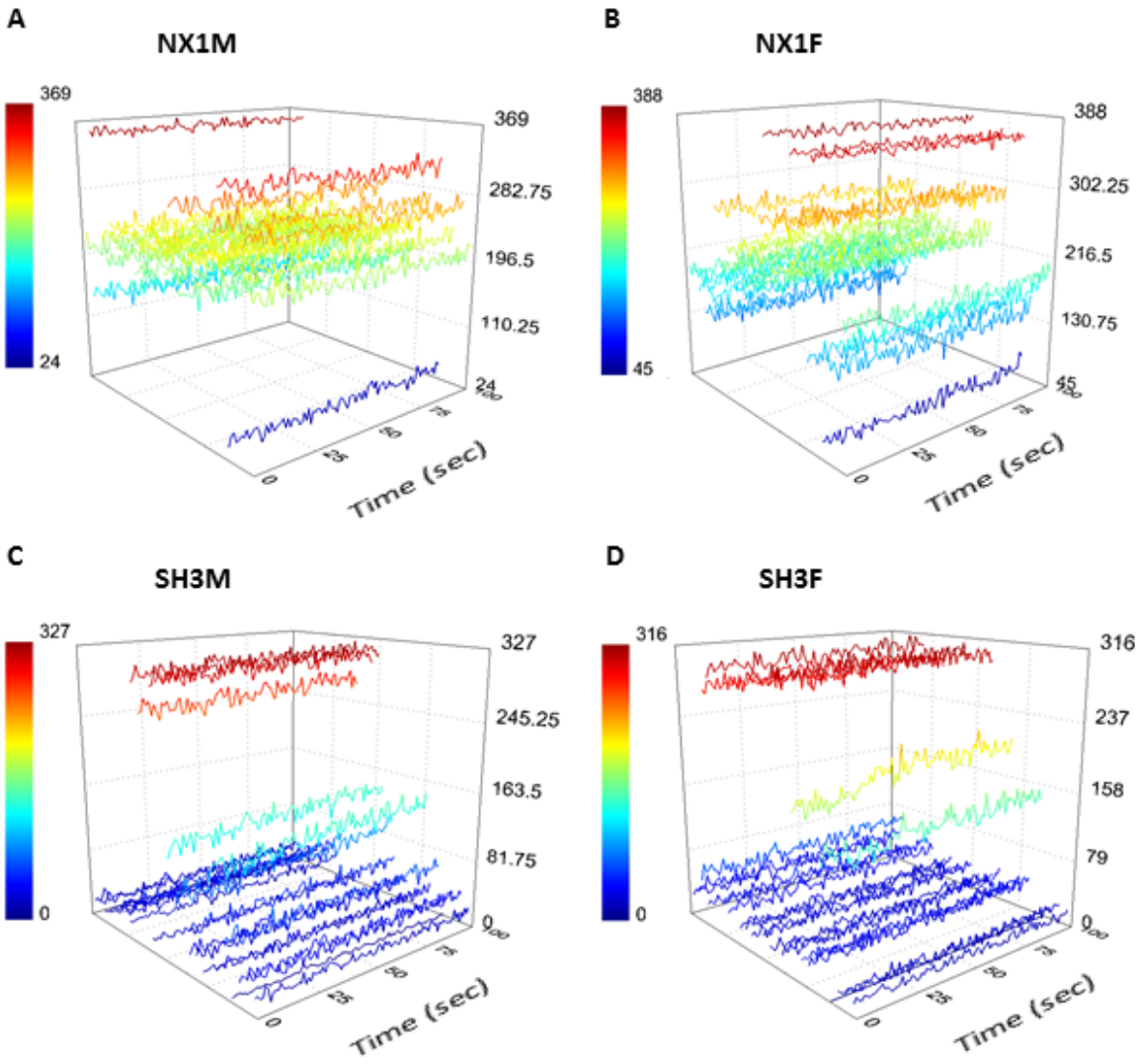

Figure 6-7 MEA frequency histograms of iNeurons with NRXN1 or SHANK3 deletion

3D histograms of 100 seconds of firing of i-neurons at day 28 from (A) NX1M, (B) NX1F, (C) SH3M and (D) SH3F groups. Colour bar indicates frequency range of the spike trains. Spikes from 25 electrodes were plotted.

The amplitude waveform 3-dimensional histogram comparison further displays the amplitude maxima and minima in voltage (millivolts) over a time window of 3 milliseconds action potential, which are independent of frequency distribution and spike trains of autism i-neurons (Fig6.8). The NX1M i-neurons showed amplitudes of 62 µV (-42 µV valley to 20 µV peak) on day 14, 58 µV (-45 µV valley to 13 µV peak) on day 21 and 56 µV (-42 µV valley to 14 µV peak) on day 28. The NX1F i-neurons demonstrated amplitudes of 54 µV (-35 µV valley to 19 µV peak) on day 14, 57 µV (-44 µV valley to 13 µV peak) on day 21 and 65 µV (-52 µV valley to 13 µV peak) on day 28. The amplitudes for SH3M i-neurons were 60 µV (-46 µV valley to 14 µV peak) on day 14, 66 µV (-51 µV valley to 15 µV peak) on day 21 and 77 µV (-65 µV valley to 12 µV peak) on day 28. Similarly, the same for SH3F i-neurons were 59 µV (-46 µV valley to 13 µV peak) on day 14, 73 µV (-61 µV valley to 12 µV peak) on day 21 and 79 µV (-62 µV valley to 17 µV peak) on day 28. Waveform amplitude is related to membrane conductance and the cylindrical neuronal morphology is known to affect the waveform amplitude (Pettersen and Einevoll, 2008). Therefore, it was interesting to find that at day 14 NX1M, SH3M and SH3F showed similar amplitudes (62 µV, 60 µV and 59 µV respectively) which could be due to the atypical neurite length of dendritic branching of these neurons at the same induction stage as shown in Fig 6.4. We also observed that on day 28 both SH3M and SH3F displayed the highest amplitudes: 77 µV and 79 µV respectively.

To further characterise the bursting properties of autism lines bursting parameters were plotted for three different timepoints: day 14, day 21 and day 28. [Fig6.9 (A)] displays the mean burst duration of control and autism lines (NX1M, NX1F, SH3M, SH3F). The control neurons showed a decline in burst duration from day 14 to day 21. Both *NRXN1* lines (NX1M and NX1F) showed similar decrease on day 21, however, followed by a surprising increase in burst duration again on day 28. Both *SHANK3* lines (SH3M and SH3F) exhibited a significant decrease on day 21 similar to controls but remained unaltered afterwards.

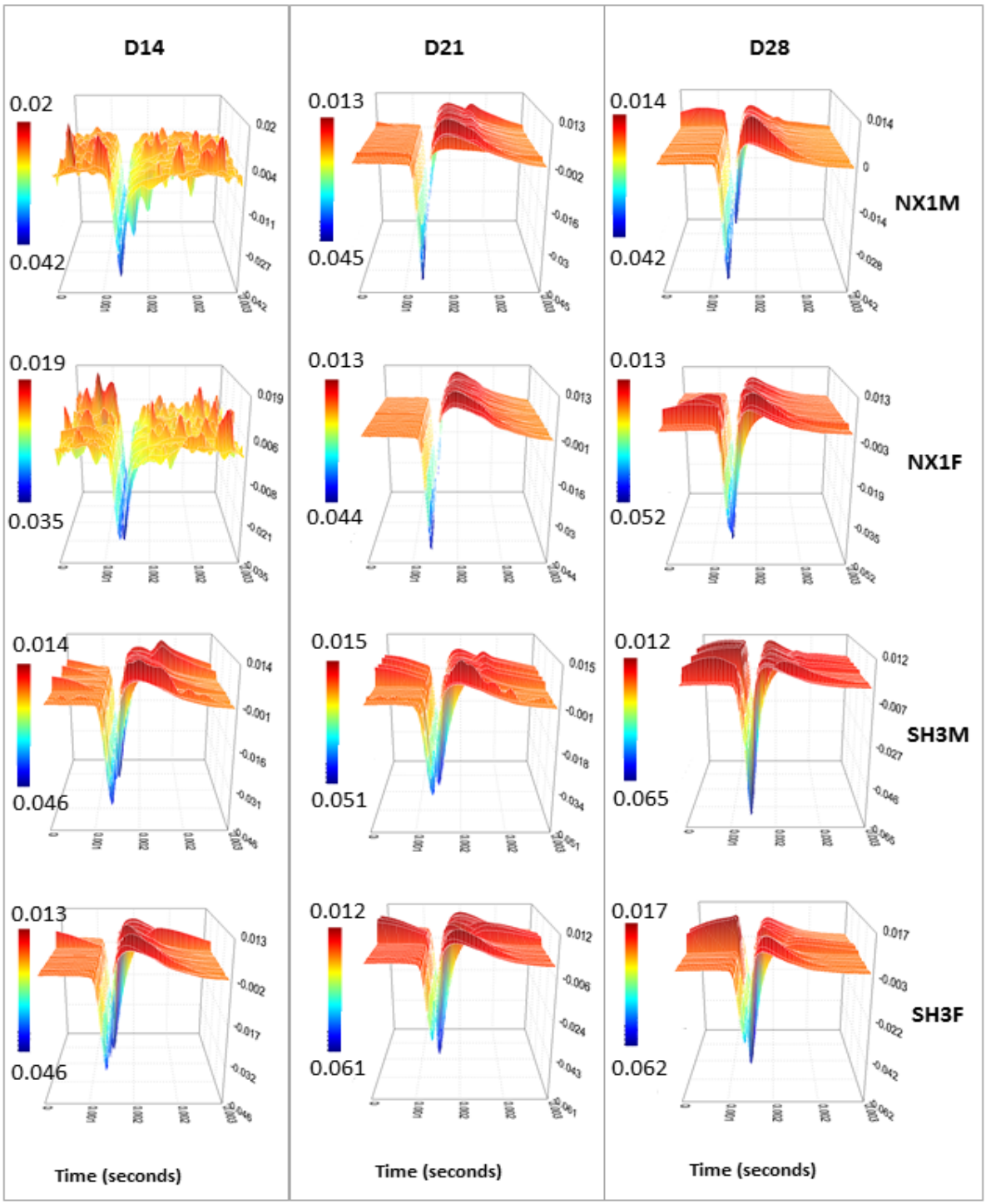

Figure 6-8 MEA waveform histograms of i-neurons with *NRXN1* or *SHANK3* deletions

3D histograms of amplitude waveforms of i-neurons from NX1M, NX1F, SH3M and SH3F at day 14, day 21 and day 28. Y-axis denotes voltage (millivolt) and x- axis: 3 millisecond time window of action potential. Colour bar indicates amplitude range of the waveforms. Waveforms from 25 electrodes were plotted.

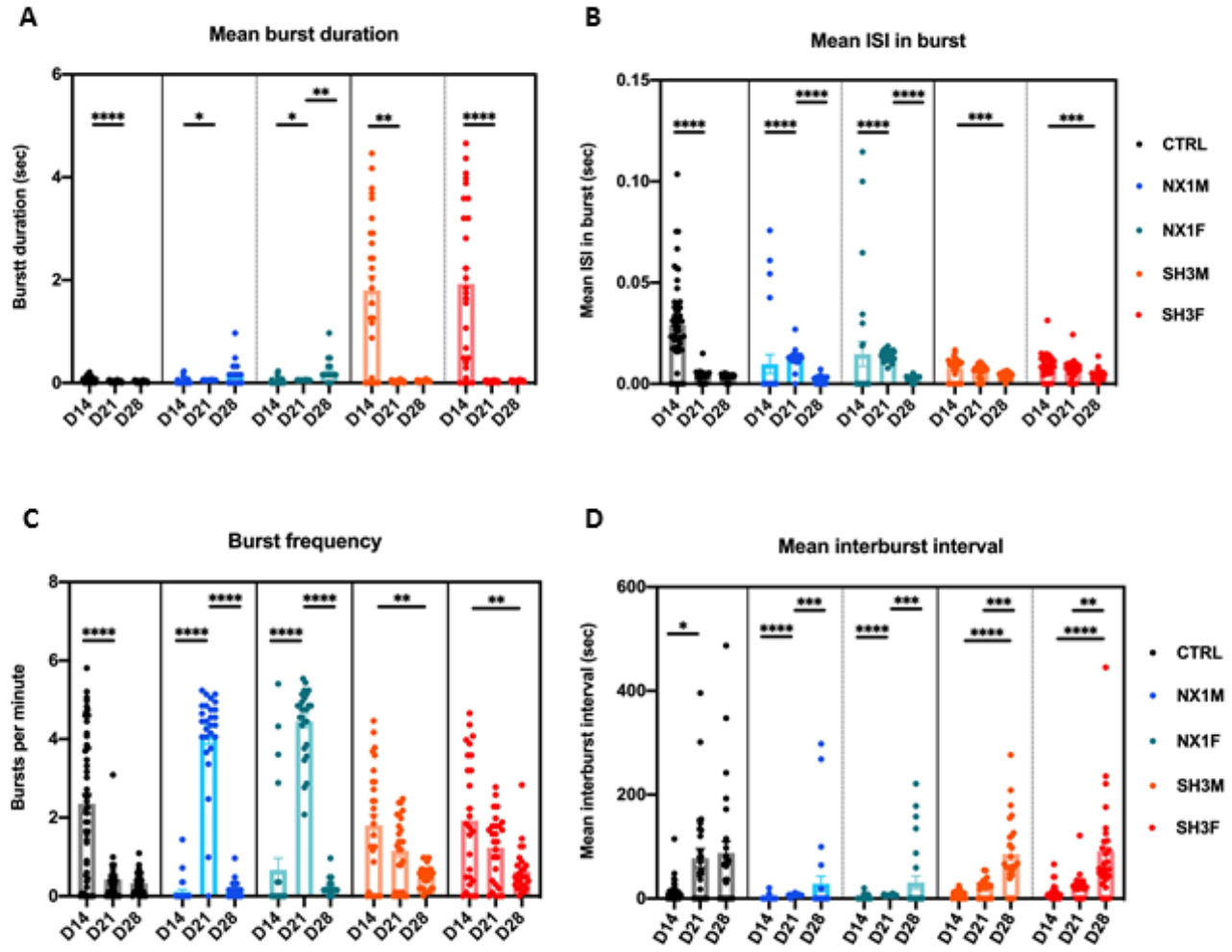

Figure 6-9 Time course comparison of MEA burst analysis of i-neurons with *NRXN1* or *SHANK3* deletions

Bursting properties characterized as (A) mean burst duration (B) mean ISI in burst (C) burst frequency and (D) mean interburst interval for CTRL, NX1M, NX1F, SH3M and SH3F i-neurons at day 14, day 21 and day 28. Data analysed from 26-28 electrodes, 3 biological replicates, for each timepoint per cell line (Kruskal-Wallis statistical test with Dunn's post-hoc multiple comparisons test).

The mean inter-spike interval (ISI) in burst in control neurons decreased from day 14 to day 21 [Fig6.9 (B)]. The same pattern was observed in both SH3M and SH3F, however, the decrease in mean ISI was only significant between day 14 and day28. Interestingly, Both NRXN1 lines, NX1M and NX1F, demonstrated an increase in mean ISI on day 21 followed

by a decline on day 28. The pattern for burst frequency was similar as that of mean ISI in burst across all cell lines [Fig6.9 (C)]. The burst frequency drastically decreased for control neurons on day 21 onwards. Whereas, SH3M and SH3F showed more gradual decline in burst frequency from day 14 to day 28. For NX1M and NX1F the burst frequency increased from day 14, peaked on day 21 and then declined again on day 28, a trend that was unique to NRXN1 lines. The mean interburst interval showed an increase for all control and autism neurons [Fig6.9 (D)]. For the control lines, interburst interval plateaued at day 21 but for all four autism lines the increase was prolonged till day 28.

The mean spikes in burst was found to increase in control neurons till day 21 and unaltered thereafter [Fig6.10 (A)]. The NRXN1 lines showed a similar increase on day 21, however, only NX1F was found increase beyond day 21. For both SHANK3 lines, SH3M and SH3F, the mean spikes remained at similar levels till day 21 followed by a significant increase on day 28. The mean peak frequency in burst [Fig6.10 (B)] and mean frequency in burst [Fig6.10 (C)], which are related parameters, consequently showed the same trend as that of the mean spikes in burst. Comparing with the mean firing rate (Fig 6.6), we observe that autism lines show similar pattern of firing behaviour within bursts. The burst surprise parameter [Fig6.10 (D)] showed similar trend as that of burst frequency and mean ISI in burst. The control showed a decrease in burst surprise on day 21. The decline was more gradual till day 28 for both SHANK3 lines, SH3M and SH3F. However, the NRXN1 lines, NX1M and NX1F exhibited an increase on day 21 and then declined significantly on day 28. It is noteworthy that in our findings across electrophysiological parameters with multi-electrode recordings the two *SHANK3* lines and the two *NRXN1* lines show distinct temporal development and functional phenotypes.

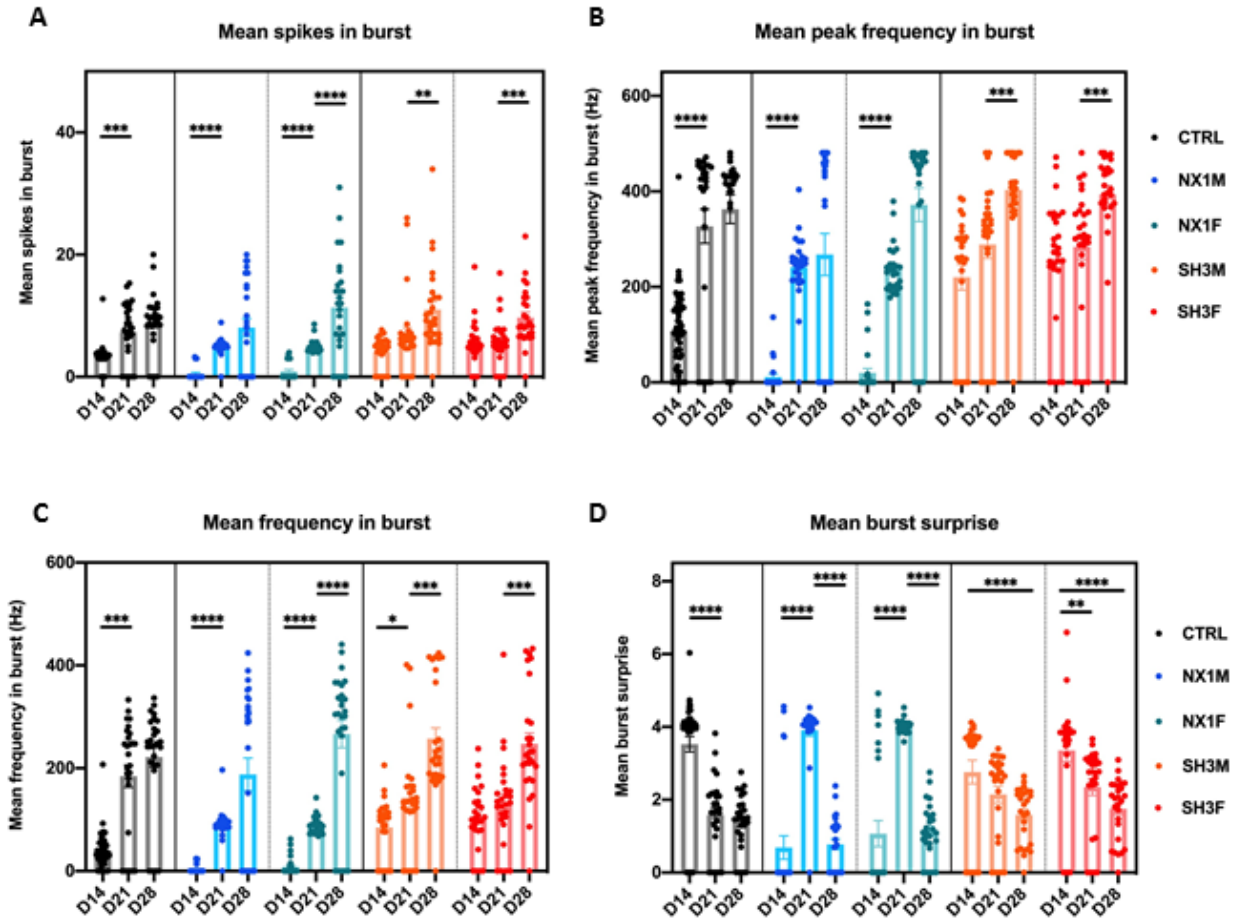

Figure 6-10 Time course analysis of spiking characteristics within bursts in neurons with *NRXN1* or *SHANK3* deletions.

Spiking properties characterised as (A) mean spikes in burst (B) mean peak frequency in burst (C) mean frequency in burst and (D) mean burst surprise for CTRL, NX1M, NX1F, SH3M and SH3F i-neurons at day 14, day 21 and day 28. Data analysed from 26-28 electrodes from 3 biological replicates, for each timepoint per cell line (Kruskal-Wallis statistical test with Dunn's post-hoc multiple comparisons test).

6.5 Discussion

In this chapter, we have characterised the morphology and electrophysiological phenotypes of NGN2 i-neurons derived from one control and four autism lines with deletions in *NRXN1* (NX1M, NXM1F) and *SHANK3* (SH3M, SH3F). The morphological results show that NX1M, SH3M and SHF i-neurons have reduced total neurite length and all four autism i-

neurons demonstrate decreased secondary neurite length and branching from the soma. In our multi-electrode array recordings, we found that the mean firing rate (MFR) increased gradually from day 14 to day 28 in i-neurons derived from control and all autism lines (NX1M, NX1F, SH3M, SH3F). In bursting properties of autism i-neurons, such as burst frequency, burst duration and mean inter-burst interval, we found that *NRXN1* and *SHANK3* groups show distinct electrophysiological pattern. The spiking characteristics within bursts, such as mean frequency, mean peak frequency, mean spikes and burst surprise in *NRXN1* and *SHANK3* mutant i-neurons followed the same trend as that of the control i-neurons.

Mutations or knockdown of *NRXN1* in iPSCs have been earlier studied to yield no significant differences in neuronal morphology (Pak et al, 2015; Zeng et al, 2013). NX1F i-neurons in our data did not show aberrant primary neurite length or total neurite length from the controls, however, the secondary neurite length, total neurite length and branching points were significantly reduced in NX1M i-neurons. It was interesting to find in our multi-electrode array results that both NX1M and NX1F i-neurons demonstrated significantly higher firing rates on day 28 compared all other cell types. A recent study has reported that cortical excitatory neurons differentiated from NRXN1α+/− iPSC lines display significantly increased frequency, duration and amplitude of spontaneous calcium transients (Avazzadeh et al, 2019) which could be a similar functional phenotype that we observe in our *NRXN1* mutant neurons. However, it has been previously reported that heterozygous *NRXN1* mutations human i-neurons significantly decrease frequency of spontaneous excitatory postsynaptic currents (mEPSCs) in whole cell patch clamp recordings (Pak et al, 2015).

We did not observe any significant difference in cell soma size in the autism lines, except for SH3F which showed smaller neuronal soma compared to controls (adjusted p=0.0347). Cortical neurons derived from iPSC with *SHANK3* deletions have been previously reported to exhibit morphogenetic deficits, smaller soma and shorter neurites (Kathuria et al,

2018; Yi et al, 2016). Knockdown of *SHANK3* in iPSC derived neurons also affects early stage of neuronal developmental function, as demonstrated by a reduction in neuronal soma size, growth cone area, neurite length and branch numbers (Huang et al, 2019). The i-neurons generated from both *SHANK3* autism lines, SH3M and SH3F, in our study show similar phenotypes of reduced total neurite length, secondary neurite length and branching points emanating from the soma. In multi-electrode array recordings both SH3M and SHF showed increase in firing rates from day 21 to day 28, but bursting frequency was reduced. Multi-electrode array study of cultured neurons from SHANK3 knockout mice earlier reported reduction in firing rates, burst frequency, burst duration and number of spikes in burst at DIV 21 (Lu et al, 2016). Moreover, conditional heterozygous and homozygous deletions of *SHANK3* in hESC derived neurons showed reduction in synaptic transmission due to a specific impairment of HCN channels (Yi et al, 2016).

The main limitation of this study is the use of unrelated control iPSC line with different genetic background. The ideal design to model autism using iPSC derived neurons would be to use isogenic knockout for comparing morphology and electrophysiological phenotypes (Merkle and Eggan, 2013). Secondly, it was beyond the scope of these experiments to investigate the effect of different isoforms of *NRXN1* and *SHANK3* on neuronal characteristics. *NRXN1* is known to undergo extensive alternative splicing and the functional phenotype could be isoform specific (Dai et al, 2019; Flaherty et al, 2019). Studies on mouse models of *SHANK3* have reported isoform specific neuronal phenotypes (Yoo et al, 2019; Wang et al, 2014; Kouser et al, 2013; Wang et al, 2011) however, it is poorly understood in human neurons. In future, we would like to conduct RNA sequencing on the *NRXN1* and *SHANK3* autism lines to explore how gene expression is correlated with functional phenotypes. Thirdly, the number of data points used in this study was not sufficient to perform finer analysis of network behaviour to better understand the frequency and amplitude properties of subpopulations of autism i-

neurons. For example, clustering of waveform shapes and firing properties can be conducted in future with more data points (Negri et al, 2020). It must be mentioned that the MEA data was noisy and did not follow normal distribution as reported in many studies (Nehme et al, 2018; Alshawaf et al, 2018). Therefore, we have used non-parametric statistical tests for multi-electrode array data sets. Moreover, we have used calcium imaging only to check the emergence of spontaneous activity. There is a scope of extending our calcium imaging experiment to quantitatively assess the firing rate and amplitudes of calcium transients and correlate with multi-electrode array data. In future we aim to replicate and extend our functional characterisation to network analysis in autism i-neurons with a larger data set and at timepoints beyond day 28 to understand cellular behaviour on synaptic maturation. An RNA sequencing experiment will be performed on two controls (Bob and Kolf) and four autism lines with *NRXN1* deletions (NX1M, NX1F) and *SHANK3* deletions (SH3M and SH3F) to establish the transcriptomic basis of functional phenotypes. We also aim to extend our characterisation of autism hiPSC lines to non-neuronal brain cells such as astrocytes and microglia to understand the mechanism of immune regulation and contribution to autism pathophysiology.

7 Chapter 7: Discussion

7.1.1 Thesis summary

Autism Spectrum Conditions (ASC) consist of a of range of complex heterogeneous conditions characterised by impaired social interactions, restrictive interests and repetitive behaviour that manifest within first three years of age (Landa et al, 2008; Lai, Lombardo and Baron-Cohen, 2014). It is estimated that genetics and environmental factors equally (1:1) contribute to the risk of autism, with most of the genetic component comprising of common variants present in general population, and a small contribution of rare variants (Huguet et al., 2016). Multiple studies have so far highlighted the involvement of mutations in genes like *NRXN, NLGN, SHANK, TSC1/2, FMR1*, and *MECP2* converge on common cellular pathways that intersect at synapse and cause disruptions in neurogenesis, neurite outgrowth, synaptogenesis and synaptic plasticity (Guang et al., 2018; Gilbert and Man, 2017). However, the scarcity of human brain tissue sample, its poor quality and that it precludes the assessment of dynamics of synaptic changes makes it unsuitable for most studies related to cortical development. On the other hand, animal models cannot reliably recapitulate human behavioural phenotypes for studying human neurodevelopmental conditions such as autism (Shen et al, 2018). Human iPSC technology involves reprogramming of somatic cells with a combination of transcription factors and presents new avenues towards generating cellular models to study human brain conditions (Park et al., 2008; Takahashi et al., 2007; Yu et al., 2007). iPSC technology, in combination with overexpression platform of single transcription factor *NGN2* thus provides scientists with a rapidly scalable source of generating functional neurons in a few weeks' time to efficiently study complex brain mechanisms in health and disease (Zhang et al, 2013, Pawlowski et al, 2017).

The first aim of this thesis was to study and characterise iNeurons derived by *NGN2* overexpression system as a model for studying autism related cellular phenotypes. The second

aim was to study the loss of function and disruptions in autism related synaptic genes *NRXN1* and *SHANK3* using this *in vitro* model of iPSC derived neurons. In Chapter 3, characterisation of iNeurons was carried out to understand synaptic gene expression relevant to autism. Subsequently, Chapter 4 was aimed at elucidating the electrophysiological behaviour of iNeurons using extracellular recordings with multi-electrode arrays. In Chapter 5, the effect of siRNA mediated knockdown of *NRXN1* or *SHANK3* on control iNeurons in terms of functional properties was studied. Finally, Chapter 6 comprises of morphological and electrophysiological analyses of iNeurons derived from iPSCs generated from autistic individuals with deletions in *NRXN1* or *SHANK3*. Some of the key findings of the above-mentioned studies and limitations of this thesis are discussed in the following sections.

7.2 iNeurons: Cellular Model of Autism

7.2.1 Gene expression

We have presented results on expression profiles of autism related and synaptic genes in order to characterise the suitability of OPTi-OX NGN2 as a model system to study autism related cellular and functional phenotypes. Transcriptomic analyses of autism risk genes have suggested that overlapping pathways of neuronal development and synaptic function are impaired during critical period of developmental stages in autism (Voineagu et al., 2011; Parikshak et al., 2013). In our study we have identified key neurogenesis markers such as *STMN2* and *GAP43* progressively increase until day 21 which clearly indicates maturation of iNeurons at this stage as earlier reported (Zhang et al, 2013; Pak et al, 2018). Among 192 high-confidence autism risk genes, a subset of genes such as *NRXN1, NRXN2, NLGN2 and ANK3* showed increased expression from day 14 onwards until day 21 which could be a suitable time window to use this model for cellular phenotyping of autism risk genes implicated in early cortical development.

Presynaptic vesicle release mechanism and organisation of postsynaptic density are essential for synaptogenesis and synaptic function (Südhof T., 2018). We have shown that critical genes involved in presynaptic neurotransmitter release such as *VAMP2, STX1A* and *SNAP25* show expression on day 21 indicating that the i-neurons at this stage are potentially capable of vesicle docking, fusion and release, which are mechanisms of neurotransmission and plasticity through (Antonucci et al., 2016). Activity dependent plasticity is a key mechanism in synaptogenesis and circuit development and often impaired in neurodevelopmental conditions (Vasa et al., 2016). At the postsynaptic density we have found the expression of key scaffold molecule *Homer1* and its interacting partners, which indicates organisation of synaptic architecture and activity dependent synaptic plasticity (Clifton et al., 2019) in iNeurons on day 14 onwards. Moreover, synaptic receptors such as *AMPA*, *VGCC* and *CamK* genes were abundantly expressed in i-neurons which further suggests that ion channel mediated information transfer and synaptic plasticity is likely to occur in these neurons (Heyes et al., 2015; Mattenson and Tomita, 2015; Voglis and Tavernarakis, 2006).

7.2.2 Functional characteristics

Neuronal activity is key in regulation of activity dependent transcription of gene involved in many aspects neuronal circuit development, including dendritic branching, synapse maturation, and synapse elimination (Flavell and Greenberg, 2008). Human iPSC-derived cortical neurons provide a platform for studying synaptogenesis as well as development of human cortical circuits (Weick et al., 2011). In order to understand whether iNeurons can recapitulate the functional properties of developing neurons *in vitro,* electrophysiological characterisation of OPTi-OX NGN2 iNeurons has been carried out in this thesis, using extracellular recordings with multi-electrode arrays (MEA). The MEA technology provides us the tool to study the neuronal network activity of populations of neurons. The only report that

has used this model has reported emergence of excitatory synchronous activity in the context of oxidative metabolism and synaptic vesicle recycling (Tourigny et al, 2019). We for the first time looked at spontaneous spiking activity and have extended our analysis to waveform and several bursting parameters to understand the electrophysiological characteristics of iNeurons. We observed that the mean firing rate (MFR) peaks at week 4 whereas the bursting activity peak later at week 5 which suggests that spontaneous activity and synchronous activity may emerge at different timepoints of neuronal induction. Bursting activity is a hallmark of developing cortex and is reported to emerge at a much later timepoint in other methods of neuralisation from iPSCs (Kirwan et al, 2015).

Human cortical development begins at around gestational week 5 and continues for approximately 100 days, completing by week 28 (Meyer et al., 2000; Rabinowicz et al., 1996). Synaptogenesis in human cortex is reported to initiate during week 9 to week 10 period of foetal development (de Graaf-Peters and Hadders-Algra, 2006). iNeurons in our study display a gradual increase in bursting frequency and burst duration from day 21 to day 35 which recapitulates the emergence of oscillations and synchronised bursts in developing human cortex which is dependent on glutamatergic synaptic activity in excitatory networks of functional neurons (Robinson et al., 1993). We observe that at synaptic gene expression and bursting activity in iNeurons both show a steady increasing trend until week 3 which is promising since embryonic synapse formation coincides with the development of spontaneous synaptic activity (Katz and Shatz, 1996; Zhang and Poo, 2001). This also suggests that this time window might be suitable to study impairments of neuronal connections in autism and other neurodevelopmental conditions, since bursting activity or oscillations are a critical mechanism for fine tuning of neural circuits and establishment of neuronal connectivity (Katz, 1993; Wong, 1993; Wong et al., 1995).

7.3 The role of *NRXN1* and *SHANK3*

7.3.1 *NRXN1* phenotype

NRXN1 as a gene encoding presynaptic cell adhesion molecule is a key regulator of neuronal development, synaptogenesis and synaptic function ( ). In Chapter 6, we have characterised the morphological phenotypes of iNeurons derived from two autism iPSC lines with *NRXN1* deletions (NX1M, NXM1F). We found that both NX1M and NX1F showed reduced secondary neurite length and branching from the soma compared to control. However, the total neurite length with only decreased in the NX1M iNeurons. Knockdown of *NRXN1* in iPSCs have been earlier studied to yield no significant differences in neuronal morphology (Zeng et al, 2013). Pak et al., 2015, had used an isogenic ESC model with two conditional mutations in *NRXN1* (a conditional knockout and another truncating mutation) and found that iNeurons derived from any of these knockout lines did not show any difference in total neurite length or soma size. However, Flaherty et al., 2019, reported decreased neurite number and length in iPSC derived $NRXN1^{+/-}$ neurons with heterozygous intragenic deletions. This variability of such morphological phenotypes is most likely to occur in a genotype specific manner due to shift in isoforms as earlier established by Flaherty et al, 2019.

In multi-electrode array recordings of iNeurons with deletions in *NRXN1*, we found that the mean firing rate (MFR) increased gradually from day 14 to day 28 in both autism lines (NX1M, NXM1F). The neuronal bursting properties, such as burst frequency, burst duration and inter-burst interval of both *NRXN1* deficient lines demonstrated similar trend which was distinct from the control iNeurons and iNeurons with disruptions in *SHANK3*. This could be due to loss of synaptic function as reported earlier (Pak et al, 2015). However, the spiking characteristics within bursts, such as mean frequency, mean peak frequency, mean spikes and burst surprise followed the same pattern as that of the control iNeurons. It was interesting to find in our multi-electrode array results that both NX1M and NX1F iNeurons demonstrated

significantly higher firing rates on day 28 compared to iNeurons derived from all other cell lines which is a similar functional phenotype reported by a recent of calcium imaging study (Avazzadeh et al, 2019). This study compared neurons derived by dual smad inhibition neuronal differentiation protocol (Chambers et al., 2009; Shi et al., 2012) from six *NRXN1α*+/− iPSC lines from three autism cases and six controls from five healthy individuals and found that neurons with heterozygous deletions in *NRXN1α* demonstrate significantly increased frequency, duration and amplitude of spontaneous calcium transients. In contrast, Pak et al, 2015 had earlier reported that *NGN2* iNeurons derived from heterozygous conditional isogenic knockouts show decreased frequency of spontaneous excitatory postsynaptic currents (mEPSCs) in whole cell patch clamp recordings.

In contrast, the multi-electrode array data in siRNA mediated *NRXN1* knockdown condition suggests that there was no significant difference in firing rate (MFR) from the control, as reported in Chapter 5. Lentiviral shRNA mediated knockdown of *NRXN1α* in neurons derived from hiPSC has previously shown perturb cell adhesion pathway (20 genes, P=2.8×10−6) and neuron differentiation pathway (13 genes, P=2.1×10−4) (Zeng et al, 2013), though it is not clear whether perturbation of gene expression profiles could affect functional properties and electrophysiological behaviour. Nevertheless, siRNA-mediated knockdown can efficiently shift the expression profile of specific isoforms (Lee et al., 2008; Gaur, 2018). As we have reported in OPTi-OX iNeurons express both two major isoforms of *NRXN1, NRXN1α* and *NRXN1β. NRXN1α* expression showed a significant increase at the (day14 - day 21) in control i-neurons, whereas more abundantly expressed isoform *NRXN1β* did not display such profile, which corroborated with previous findings by Jenkins et al, 2016 on expression profiles of *NRXN1* isoforms from prenatal gestational weeks to adulthood. Jenkins et al, 2016 reported for the first time that *NRXN1* isoform expression increase during foetal brain development, reaching its peak at week 39 gestation during second trimester (16-39 weeks). The comparison

of developmental timeline between *NGN2* iNeurons and human gestational age could be made in the light of a recent study by Rosa et al., 2020, which estimated that *NGN2* iNeurons closely mimic the transcriptomic and electrophysiological profile of second trimester of foetal cortical development.

7.3.2 *SHANK3* phenotype

SHANK3 encodes a postsynaptic scaffold protein disruption of which is implicated in a several kinds of neuronal impairments also known as shankopathies (Carbonetto, 2014). In our morphological analyses we did not observe any significant difference in cell soma size in iNeurons from individuals with autism bearing deletions in *SHANK3*, except for SH3F which showed smaller neuronal soma compared to controls (adjusted p=0.0347). Several morphological anomalies, such as smaller soma, shorter neurites and morphogenetic deficits have been reported previously in human pluripotent stem cell derived cortical neurons with deletions in *SHANK3* (Kathuria et al, 2018; Yi et al, 2016). Knockdown of *SHANK3* also perturbs early cortical development and function, as displayed by a decrease in neuronal soma size, growth cone area, neurite length and branch numbers (Huang et al, 2019). In our study, i-neurons generated from both *SHANK3* deficient autism lines, SH3M and SH3F exhibited similar morphological phenotypes of reduced total neurite length, secondary neurite length and branching points emanating from the soma.

In our multi-electrode array recordings, SH3M and SH3F showed similar trend of gradual increase in mean firing rate (MFR) from day 14 to day 28 as that of the control as well as the *NRXN1* deficient neurons. Bursting properties also followed the similar pattern of emergence like all other iPSC lines during the time course of neuronal induction. Surprisingly, increase in MFR from day 21 to day 28 was coupled with reduction in bursting frequency. The interesting phenotype was that both SH3M and SH3F derived iNeurons displayed distinct pattern in all spiking and bursting parameters which could be due to disruptions in *SHANK3*.

The first report of *SHANK3* phenotype in iPSC-derived neurons from control and autistic individuals with Phelan McDermid Syndrome had shown that reduced SHANK3 expression leads to major disruptions in excitatory synaptic transmission (Shcheglovitov et al., 2013). Previous multi-electrode array study from *SHANK3* rodent model has reported that cultured neurons at DIV 21 with lack of *SHANK3* exhibited decrease in firing activity, duration of burst and number of spikes in a burst (Lu et al, 2016). Moreover, conditional heterozygous and homozygous deletions of SHANK3 in hESC derived *NGN2* iNeurons showed reduction in synaptic transmission due to a specific impairment of HCN channels (Yi et al, 2016). We characterised the expression of *SHANK3* in iNeurons using primers against exons 8-9 region (encoding ankyrin domain) which is present in two major isoforms of *SHANK3, SHANK3a* and *SHANK3b* (Wang et al, 2014). *SHANK3* was found to be significantly elevated in iNeurons on day 30 or week 4 of neuronal induction. However, the siRNA mediated knockdown of *SHANK3* did not show any significant changes from control in extracellular recordings. Previously reported lentiviral shRNA mediated *SHANK3* knockdown in hiPSC derived neurons has shown reduction in frequency of excitatory post synaptic current (sEPSC) relative to control neurons in 3.5 and 5.5 weeks along with alteration of transcriptional profile related to cortical development and synaptogenesis (Huang et al, 2019). Very recently, a study on *SHANK3* knockout mice showed that *SHANK3* is essential for homeostatic plasticity in mice visual cortex (Tatavarty et al, 2020) which could be an exciting avenue to explore using iNeuron as a model system.

7.4 Limitations

iPSC lines generated using transcription factor reprogramming can be highly variable. Keratinocytes with ectodermal lineage from hair follicles were used to generate the autism lines, which can be a source of variability due to residual epigenetic signatures (Hormanseder

et al. 2017). One of the main limitations of this thesis is the use of unrelated control iPSC line with different genetic background. The ideal design to model autism using iPSC derived neurons would be to generate isogenic knockout lines or comparing morphology and electrophysiological phenotypes (Merkle and Eggan, 2013). One of the main challenges of using the OPTi-OX system to model patient iPSC lines with mutation or deletion is that the targeting of rtTA and NGN2 into genomic safe harbour sites could be technically challenging. Integration of rtTA and NGN2 involves independent nucleofection, clonal selection and sequencing steps which could be time consuming when multiple patient lines are involved. Also, patient iPSC lines with mutations or deletions are often vulnerable to nucleofection procedure. As observed in Chapter 3, not all high confidence autism-risk genes are abundantly expressed in iNeurons. This should be taken into consideration while for studying specific gene related mutations using iNeurons. Moreover, NMDA receptors are key synaptic molecules for synaptic plasticity and absence of which renders iNeurons unsuitable for plasticity studies. However, this could be overcome by combining differentiation method with *NGN2* overexpression (Nehme et al., 2018).

It was beyond the scope of these experiments to investigate the effect of different isoforms of NRXN1 and SHANK3 on neuronal characteristics. NRXN1 is known to undergo extensive alternative splicing and the functional phenotype could be isoform specific (Dai et al, 2019; Flaherty et al, 2019). Studies on mouse models of SHANK3 have reported isoform specific neuronal phenotypes (Yoo et al, 2019; Wang et al, 2014; Kouser et al, 2013; Wang et al, 2011) however, it is poorly understood in human neurons. We have used predesigned validated siRNAs for human *NRXN1* and *SHANK3* following the manufacturer's protocol; however, the efficiency of knockdown on different isoforms of *NRXN1* and *SHANK3* was not studied. Further validation experiments would be necessary to ensure the knockdown was effective.

Another limitation of this study is that there was a quite some variability in the data was collected and the number of data points used in this study was not sufficient to perform more sophisticated analysis of network behaviour to better understand the frequency and amplitude characteristics of i-neurons. For example, clustering of waveform shapes and firing properties can be conducted in future with more data points (Negri et al, 2020). Another caveat of this thesis is that the timeline for multi-electrode array experiment was until day 35 i.e. week 5 and we observed the bursting activity to peak at week 5. Previously Ngn2-i-neurons (lentiviral method) have been reported to demonstrate highest mean firing rate at week 5 depending on the cell line used, although bursting parameters were not reported (Deneault et al, 2019). It is not possible to conclude from these experiments how the spiking and bursting activity may be affected beyond the timepoint of week 5. Hence, we are planning to conduct experiments with longer span of time post induction. There are only a few studies so far which have used iNeurons for functional characterisation of cellular phenotypes. Moreover, use of different parameters and methodologies makes it challenging to compare results between MEA studies. For example, weighted mean firing rate (wMFR) has been used as the principal readout of neuronal activity using extracellular MEA recordings in the context of cellular pathophysiology of autism (Deneault et al, 2018). Array-wide spike detection (ASDR) is another parameter used for functional characterisation. Lu et al, 2016 used ASDR to characterise Shank3 deficient cultured cortical neuronal network. Deneault et al, 2019 had extensively looked at several autism related mutations in iNeurons using the lentiviral method (Zhang et al, 2013). The primary readout in this MEA study was the mean firing rate (MFR) recorded from every active electrode. However, we observed in our data that the global bursting properties may differ independently of local environment of spiking neurons.

It is also challenging to compare the *in vitro* cellular phenotypes studied in iNeurons with foetal developmental stage for interpretation of the results in the context of human

corticogenesis. However, a recent study (Rosa et al, 2020) compared the "fast" NGN2 protocol with a more "native" embryoid body protocol and elucidated that NGN2 neurons reach the cellular signatures of that of second trimester of human gestation when cultured with astrocytes; whereas the embryoid body protocol is capable of modelling third trimester with more complex neuronal network activity. Nevertheless, NGN2 i-neuron model has less cellular heterogeneity compared to most other existing models of neuronal differentiation and its main advantages are rapidity and scalability to form relatively mature neurons in less time.

7.5 Future directions

In future, we would like to follow up the results presented in this thesis with further gene expression studies to explore how transcriptomic profile of individual specific *NRXN1* or *SHANK3* deletions might be correlated with morphological and electrophysiological phenotypes. An RNA sequencing experiment will be performed on two controls (Bob and Kolf) and four autism lines with *NRXN1* deletions (NX1M, NX1F) and *SHANK3* deletions (SH3M and SH3F) to study if there is any common cellular pathways related to neurogenesis, neurite outgrowth, synaptogenesis and synaptic plasticity. Secondly, we would like to extrapolate this study further by correcting the deletions in *NRXN1* or *SHANK3* in respective autism iPSC lines for comparison in isogenic pairs. It would be a more robust design for comparison of cellular deletion specific cellular phenotypes.

This was a pilot study to establish the morphological and functional phenotyping platform using iNeurons as a cellular model to study two autism related synaptic genes. We are planning to increase the number of iPSC lines in autism and control groups, and also collect larger data sets beyond terminal timepoint of week 4 in our experimental design to better under cellular behaviour on synaptic maturation. Future functional studies will involve multi-electrode arrays with higher density of electrodes for understanding neuronal network connectivity between local subpopulations of neurons (Schroeter,et al., 2015), which is a

pertinent question in developmental biology, especially in the context of autism pathophysiology (Geschwind and Levitt, 2007). Finally, overexpression of transcription factors can generate different types of cells from iPSCs and we are currently optimising methods to efficiently reprogram non-neuronal cell types such as astrocytes and oligodendrocytes for future studies (Julia et al., 2017; Pawloski et al., 2017).

8 References:

Abrahams, B. S., Arking, D. E., Campbell, D. B., Mefford, H. C., Morrow, E. M., Weiss, L. A., … Packer, A. (2013). SFARI Gene 2.0: A community-driven knowledgebase for the autism spectrum disorders (ASDs). *Molecular Autism*, *4*, 36. https://doi.org/10.1186/2040-2392-4-36

Abrahams, B. S., & Geschwind, D. H. (2008). Advances in autism genetics: On the threshold of a new neurobiology. *Nature Reviews. Genetics*, *9*(5), 341–355. https://doi.org/10.1038/nrg2346

Abu-Elneel, K., Liu, T., Gazzaniga, F. S., Nishimura, Y., Wall, D. P., Geschwind, D. H., Lao, K., & Kosik, K. S. (2008). Heterogeneous dysregulation of microRNAs across the autism spectrum. *Neurogenetics*, *9*(3), 153–161. https://doi.org/10.1007/s10048-008-0133-5

Adalsteinsson, B. T., & Ferguson-Smith, A. C. (2014). Epigenetic control of the genome-lessons from genomic imprinting. *Genes*, *5*(3), 635–655. https://doi.org/10.3390/genes5030635

Adhya, D., Swarup, V., Nagy, R., Dutan, L., Shum, C., Valencia-Alarcón, E. P., … Baron-Cohen, S. (2020). Atypical Neurogenesis in Induced Pluripotent Stem Cells From Autistic Individuals. *Biological Psychiatry*, *0*(0). https://doi.org/10.1016/j.biopsych.2020.06.014

American Psychiatric Association. Diagnostic and Statistical Manual of Mental Disorders (DSM-5), 5th ed.; American Psychiatric Association: Washington, DC, USA, 2013.

Anderson, G. R., Aoto, J., Tabuchi, K., Földy, C., Covy, J., Yee, A. X., … Südhof, T. C. (2015). β-Neurexins Control Neural Circuits by Regulating Synaptic Endocannabinoid Signaling. *Cell*, *162*(3), 593–606. https://doi.org/10.1016/j.cell.2015.06.056

Anney, R. J. L., Ripke, S., Anttila, V., Grove, J., Holmans, P., Huang, H., Klei, L., Lee, P. H., Medland, S. E., Neale, B., Robinson, E., Weiss, L. A., Zwaigenbaum, L., Yu, T. W., Wittemeyer, K., Willsey, A. J., Wijsman, E. M., Werge, T., Wassink, T. H., … The Autism Spectrum Disorders Working Group of The Psychiatric Genomics Consortium. (2017). Meta-analysis of GWAS of over 16,000 individuals with autism spectrum disorder highlights a novel locus at 10q24.32 and a significant overlap with schizophrenia. *Molecular Autism*, *8*(1), 21. https://doi.org/10.1186/s13229-017-0137-9

Antonucci, F., Corradini, I., Fossati, G., Tomasoni, R., Menna, E., & Matteoli, M. (2016). SNAP-25, a Known Presynaptic Protein with Emerging Postsynaptic Functions. *Frontiers in Synaptic Neuroscience*, *8*. https://doi.org/10.3389/fnsyn.2016.00007

Araç, D., Boucard, A. A., Özkan, E., Strop, P., Newell, E., Südhof, T. C., & Brunger, A. T. (2007). Structures of Neuroligin-1 and the Neuroligin-1/Neurexin-1β Complex Reveal Specific Protein-Protein and Protein-Ca2+ Interactions. *Neuron*, *56*(6), 992–1003. https://doi.org/10.1016/j.neuron.2007.12.002

Autism Genome Project Consortium, Szatmari, P., Paterson, A. D., Zwaigenbaum, L., Roberts, W., Brian, J., … Meyer, K. J. (2007). Mapping autism risk loci using genetic linkage and chromosomal rearrangements. *Nature Genetics*, *39*(3), 319–328. https://doi.org/10.1038/ng1985

Avazzadeh, S., McDonagh, K., Reilly, J., Wang, Y., Boomkamp, S. D., McInerney, V., … Shen, S. (2019). Increased Ca2+ signaling in NRXN1α+/− neurons derived from ASD induced pluripotent stem cells. *Molecular Autism*, *10*(1), 52. https://doi.org/10.1186/s13229-019-0303-3

Bailey, A., Le Couteur, A., Gottesman, I., Bolton, P., Simonoff, E., Yuzda, E., & Rutter, M. (1995). Autism as a strongly genetic disorder: Evidence from a British twin study. *Psychological Medicine*, *25*(1), 63–77. https://doi.org/10.1017/s0033291700028099

Baird, G., Cass, H., & Slonims, V. (2003). Diagnosis of autism. *BMJ*, *327*(7413), 488–493. https://doi.org/10.1136/bmj.327.7413.488

Baron-Cohen, S., Auyeung, B., Nørgaard-Pedersen, B., Hougaard, D. M., Abdallah, M. W., Melgaard, L., Cohen, A. S., Chakrabarti, B., Ruta, L., & Lombardo, M. V. (2015). Elevated fetal steroidogenic activity in autism. *Molecular Psychiatry*, *20*(3), 369–376. https://doi.org/10.1038/mp.2014.48

Baron-Cohen, S., Ashwin, E., Ashwin, C., Tavassoli, T., & Chakrabarti, B. (2009). Talent in autism: Hyper-systemizing, hyper-attention to detail and sensory hypersensitivity. *Philosophical Transactions of the Royal Society B: Biological Sciences*, *364*(1522), 1377–1383. https://doi.org/10.1098/rstb.2008.0337

Baron-Cohen, S., & Lombardo, M. V. (2017). Autism and talent: The cognitive and neural basis of systemizing. *Dialogues in Clinical Neuroscience*, *19*(4), 345–353.

Baron-Cohen, S., Richler, J., Bisarya, D., Gurunathan, N., & Wheelwright, S. (2003). The systemizing quotient: An investigation of adults with Asperger syndrome or high-functioning autism, and normal sex differences. *Philosophical Transactions of the Royal Society B: Biological Sciences*, *358*(1430), 361. https://doi.org/10.1098/rstb.2002.1206

Barrow, S. L., Constable, J. R., Clark, E., El-Sabeawy, F., McAllister, A. K., & Washbourne, P. (2009). Neuroligin1: A cell adhesion molecule that recruits PSD-95 and NMDA receptors by distinct mechanisms during synaptogenesis. *Neural Development*, *4*(1), 17. https://doi.org/10.1186/1749-8104-4-17

Basu, S. N., Kollu, R., & Banerjee-Basu, S. (2009). AutDB: A gene reference resource for autism research. *Nucleic Acids Research*, *37*(Database issue), D832–D836. https://doi.org/10.1093/nar/gkn835

Bayés, À., Collins, M. O., Croning, M. D. R., Lagemaat, L. N. van de, Choudhary, J. S., & Grant, S. G. N. (2012). Comparative Study of Human and Mouse Postsynaptic Proteomes Finds High Compositional Conservation and Abundance Differences for Key Synaptic Proteins. *PLOS ONE*, *7*(10), e46683. https://doi.org/10.1371/journal.pone.0046683

Béna, F., Bruno, D. L., Eriksson, M., van Ravenswaaij-Arts, C., Stark, Z., Dijkhuizen, T., … Schoumans, J. (2013). Molecular and clinical characterization of 25 individuals with exonic deletions of NRXN1 and comprehensive review of the literature. *American Journal of Medical Genetics. Part B, Neuropsychiatric Genetics: The Official Publication of the International Society of Psychiatric Genetics*, *162B*(4), 388–403. https://doi.org/10.1002/ajmg.b.32148

Ben-David, E., & Shifman, S. (2013). Combined analysis of exome sequencing points toward a major role for transcription regulation during brain development in autism. *Molecular Psychiatry*, *18*(10), 1054–1056. https://doi.org/10.1038/mp.2012.148

Bernier, R., Golzio, C., Xiong, B., Stessman, H. A., Coe, B. P., Penn, O., Witherspoon, K., Gerdts, J., Baker, C., Vulto-van Silfhout, A. T., Schuurs-Hoeijmakers, J. H., Fichera, M., Bosco, P., Buono, S., Alberti, A., Failla, P., Peeters, H., Steyaert, J., Vissers, L. E. L. M., … Eichler, E. E. (2014). Disruptive CHD8 mutations define a subtype of autism early in development. *Cell*, *158*(2), 263–276. https://doi.org/10.1016/j.cell.2014.06.017

Bernstein, E., Kim, S. Y., Carmell, M. A., Murchison, E. P., Alcorn, H., Li, M. Z., Mills, A. A., Elledge, S. J., Anderson, K. V., & Hannon, G. J. (2003). Dicer is essential for mouse development. *Nature Genetics*, *35*(3), 215–217. https://doi.org/10.1038/ng1253

Betancur, C. (2011). Etiological heterogeneity in autism spectrum disorders: More than 100 genetic and genomic disorders and still counting. *Brain Research*, *1380*, 42–77. https://doi.org/10.1016/j.brainres.2010.11.078

Betancur, C., & Buxbaum, J. D. (2013). SHANK3 haploinsufficiency: A "common" but underdiagnosed highly penetrant monogenic cause of autism spectrum disorders. *Molecular Autism*, *4*(1), 17. https://doi.org/10.1186/2040-2392-4-17

Boccuto, L., Lauri, M., Sarasua, S. M., Skinner, C. D., Buccella, D., Dwivedi, A., … Schwartz, C. E. (2013). Prevalence of SHANK3 variants in patients with different subtypes of autism spectrum disorders. *European Journal of Human Genetics: EJHG*, *21*(3), 310–316. https://doi.org/10.1038/ejhg.2012.175

Bock, C., Kiskinis, E., Verstappen, G., Gu, H., Boulting, G., Smith, Z. D., … Meissner, A. (2011). Reference Maps of Human ES and iPS Cell Variation Enable High-Throughput Characterization of Pluripotent Cell Lines. *Cell*, *144*(3), 439–452. https://doi.org/10.1016/j.cell.2010.12.032

Böckers, T. M., Segger-Junius, M., Iglauer, P., Bockmann, J., Gundelfinger, E. D., Kreutz, M. R., … Kreienkamp, H.-J. (2004). Differential expression and dendritic transcript localization of Shank family members: Identification of a dendritic targeting element in the 3' untranslated region of Shank1 mRNA. *Molecular and Cellular Neurosciences*, *26*(1), 182–190. https://doi.org/10.1016/j.mcn.2004.01.009

Bonaglia, M C, Giorda, R., Mani, E., Aceti, G., Anderlid, B., Baroncini, A., … Zuffardi, O. (2006). Identification of a recurrent breakpoint within the SHANK3 gene in the 22q13.3 deletion syndrome. *Journal of Medical Genetics*, *43*(10), 822–828. https://doi.org/10.1136/jmg.2005.038604

Bonaglia, Maria Clara, Giorda, R., Borgatti, R., Felisari, G., Gagliardi, C., Selicorni, A., & Zuffardi, O. (2001). Disruption of the ProSAP2 Gene in a t(12;22)(q24.1;q13.3) Is Associated with the 22q13.3 Deletion Syndrome. *American Journal of Human Genetics*, *69*(2), 261–268.

Bourgeron, T. (2009). A synaptic trek to autism. *Current Opinion in Neurobiology*, *19*(2), 231–234. https://doi.org/10.1016/j.conb.2009.06.003

Bourgeron, T. (2015). From the genetic architecture to synaptic plasticity in autism spectrum disorder. *Nature Reviews Neuroscience*, *16*(9), 551–563. https://doi.org/10.1038/nrn3992

Bozdagi, O., Sakurai, T., Papapetrou, D., Wang, X., Dickstein, D. L., Takahashi, N., … Buxbaum, J. D. (2010). Haploinsufficiency of the autism-associated Shank3 gene leads to deficits in synaptic function, social interaction, and social communication. *Molecular Autism*, *1*(1), 15. https://doi.org/10.1186/2040-2392-1-15

Bozdagi, O., Tavassoli, T., & Buxbaum, J. D. (2013). Insulin-like growth factor-1 rescues synaptic and motor deficits in a mouse model of autism and developmental delay. *Molecular Autism*, *4*(1), 9. https://doi.org/10.1186/2040-2392-4-9

Brennand, K. J., Simone, A., Tran, N., & Gage, F. H. (2012). Modeling psychiatric disorders at the cellular and network levels. *Molecular Psychiatry*, *17*(12), 1239–1253. https://doi.org/10.1038/mp.2012.20

Brockhaus, J., Schreitmüller, M., Repetto, D., Klatt, O., Reissner, C., Elmslie, K., … Missler, M. (2018). α-Neurexins Together with α2δ-1 Auxiliary Subunits Regulate Ca2+ Influx through Cav2.1 Channels. *The Journal of Neuroscience*, *38*(38), 8277–8294. https://doi.org/10.1523/JNEUROSCI.0511-18.2018

Budreck, E. C., & Scheiffele, P. (2007). Neuroligin-3 is a neuronal adhesion protein at GABAergic and glutamatergic synapses. *The European Journal of Neuroscience*, *26*(7), 1738–1748. https://doi.org/10.1111/j.1460-9568.2007.05842.x

Buzsaki, G. (2006). *Rhythms of the Brain*. Oxford University Press.

Camacho-Garcia, R. J., Planelles, M. I., Margalef, M., Pecero, M. L., Martínez-Leal, R., Aguilera, F., … Scholl, F. G. (2012). Mutations affecting synaptic levels of neurexin-1β in autism and mental retardation. *Neurobiology of Disease*, *47*(1), 135–143. https://doi.org/10.1016/j.nbd.2012.03.031

Carbonetto, S. (2014). A blueprint for research on Shankopathies: A view from research on autism spectrum disorder. *Developmental Neurobiology*, *74*(2), 85–112. https://doi.org/10.1002/dneu.22150

Chakrabarti, S., & Fombonne, E. (2005). Pervasive developmental disorders in preschool children: Confirmation of high prevalence. *The American Journal of Psychiatry*, *162*(6), 1133–1141. https://doi.org/10.1176/appi.ajp.162.6.1133

Chambers, S. M., Qi, Y., Mica, Y., Lee, G., Zhang, X.-J., Niu, L., … Studer, L. (2012). Combined small-molecule inhibition accelerates developmental timing and converts human pluripotent stem cells into nociceptors. *Nature Biotechnology*, *30*(7), 715–720. https://doi.org/10.1038/nbt.2249

Chaste, P., & Leboyer, M. (2012). Autism risk factors: Genes, environment, and gene-environment interactions. *Dialogues in Clinical Neuroscience*, *14*(3), 281–292.

Chen, L., Selvendra, A., Stewart, A., & Castle, D. (2018). Risk factors in early and late onset schizophrenia. *Comprehensive Psychiatry*, *80*, 155–162. https://doi.org/10.1016/j.comppsych.2017.09.009

Chen, X., Liu, H., Shim, A. H. R., Focia, P. J., & He, X. (2008). Structural basis for synaptic adhesion mediated by neuroligin-neurexin interactions. *Nature Structural & Molecular Biology*, *15*(1), 50–56. https://doi.org/10.1038/nsmb1350

Chih, B., Afridi, S. K., Clark, L., & Scheiffele, P. (2004). Disorder-associated mutations lead to functional inactivation of neuroligins. *Human Molecular Genetics*, *13*(14), 1471–1477. https://doi.org/10.1093/hmg/ddh158

Ching, M. S., Shen, Y., Tan, W.-H., Jeste, S. S., Morrow, E. M., Chen, X., … Wu, B.-L. (2010). Deletions of NRXN1 (Neurexin-1) Predispose to a Wide Spectrum of Developmental Disorders. *American Journal of Medical Genetics*, *153B*(4), 937–947. https://doi.org/10.1002/ajmg.b.31063

Chubykin, A. A., Atasoy, D., Etherton, M. R., Brose, N., Kavalali, E. T., Gibson, J. R., & Südhof, T. C. (2007). Activity-Dependent Validation of Excitatory versus Inhibitory Synapses by Neuroligin-1 versus Neuroligin-2. *Neuron*, *54*(6), 919–931. https://doi.org/10.1016/j.neuron.2007.05.029

Cingolani, L. A., & Goda, Y. (2008). Actin in action: The interplay between the actin cytoskeleton and synaptic efficacy. *Nature Reviews. Neuroscience*, *9*(5), 344–356. https://doi.org/10.1038/nrn2373

Clifton, N. E., Trent, S., Thomas, K. L., & Hall, J. (2019). Regulation and Function of Activity-Dependent Homer in Synaptic Plasticity. *Complex Psychiatry*, *5*(3), 147–161. https://doi.org/10.1159/000500267

Cocks, G., Curran, S., Gami, P., Uwanogho, D., Jeffries, A. R., Kathuria, A., … Price, J. (2014). The utility of patient specific induced pluripotent stem cells for the modelling of Autistic Spectrum Disorders. *Psychopharmacology*, *231*(6), 1079–1088. https://doi.org/10.1007/s00213-013-3196-4

Cohen, D., Pichard, N., Tordjman, S., Baumann, C., Burglen, L., Excoffier, E., … Héron, D. (2005). Specific genetic disorders and autism: Clinical contribution towards their identification. *Journal of Autism and Developmental Disorders*, *35*(1), 103–116. https://doi.org/10.1007/s10803-004-1038-2

Comoletti, D., Grishaev, A., Whitten, A. E., Tsigelny, I., Taylor, P., & Trewhella, J. (2007). Synaptic Arrangement of the Neuroligin/β-Neurexin Complex Revealed by X-ray and Neutron Scattering. *Structure (London, England : 1993)*, *15*(6), 693–705. https://doi.org/10.1016/j.str.2007.04.010

Costales, J. L., & Kolevzon, A. (2015). Phelan-McDermid Syndrome and SHANK3: Implications for Treatment. *Neurotherapeutics: The Journal of the American Society for Experimental NeuroTherapeutics*, *12*(3), 620–630. https://doi.org/10.1007/s13311-015-0352-z

Cotney, J., Muhle, R. A., Sanders, S. J., Liu, L., Willsey, A. J., Niu, W., Liu, W., Klei, L., Lei, J., Yin, J., Reilly, S. K., Tebbenkamp, A. T., Bichsel, C., Pletikos, M., Sestan, N., Roeder, K., State, M. W., Devlin, B., & Noonan, J. P. (2015). The autism-associated chromatin modifier CHD8 regulates other autism risk genes during human neurodevelopment. *Nature Communications*, *6*(1), 6404. https://doi.org/10.1038/ncomms7404

Cotterill, E., Charlesworth, P., Thomas, C. W., Paulsen, O., & Eglen, S. J. (2016). A comparison of computational methods for detecting bursts in neuronal spike trains and their application to human stem cell-derived neuronal networks. *Journal of Neurophysiology*, *116*(2), 306–321. https://doi.org/10.1152/jn.00093.2016

Cotterill, E., & Eglen, S. J. (2019). Burst Detection Methods. *Advances in Neurobiology*, *22*, 185–206. https://doi.org/10.1007/978-3-030-11135-9_8

Craig, A. M., & Kang, Y. (2007). Neurexin–neuroligin signaling in synapse development. *Current Opinion in Neurobiology*, *17*(1), 43–52. https://doi.org/10.1016/j.conb.2007.01.011

Dabell, M. P., Rosenfeld, J. A., Bader, P., Escobar, L. F., El-Khechen, D., Vallee, S. E., … Shaffer, L. G. (2013). Investigation of NRXN1 deletions: Clinical and molecular characterization. *American Journal of Medical Genetics. Part A*, *161A*(4), 717–731. https://doi.org/10.1002/ajmg.a.35780

Dahlhaus, R., Hines, R. M., Eadie, B. D., Kannangara, T. S., Hines, D. J., Brown, C. E., … El-Husseini, A. (2010). Overexpression of the cell adhesion protein neuroligin-1 induces learning deficits and impairs synaptic plasticity by altering the ratio of excitation to inhibition in the hippocampus. *Hippocampus*, *20*(2), 305–322. https://doi.org/10.1002/hipo.20630

Davis, J. K., & Broadie, K. (2017). Multifarious Functions of the Fragile X Mental Retardation Protein. *Trends in Genetics: TIG*, *33*(10), 703–714. https://doi.org/10.1016/j.tig.2017.07.008

de Graaf-Peters, V. B., & Hadders-Algra, M. (2006). Ontogeny of the human central nervous system: What is happening when? *Early Human Development*, *82*(4), 257–266. https://doi.org/10.1016/j.earlhumdev.2005.10.013

De Rubeis, S., He, X., Goldberg, A. P., Poultney, C. S., Samocha, K., Ercument Cicek, A., … Buxbaum, J. D. (2014). Synaptic, transcriptional and chromatin genes disrupted in autism. *Nature*, *515*(7526), 209–215. https://doi.org/10.1038/nature13772

Dean, C., & Dresbach, T. (2006). Neuroligins and neurexins: Linking cell adhesion, synapse formation and cognitive function. *Trends in Neurosciences*, *29*(1), 21–29. https://doi.org/10.1016/j.tins.2005.11.003

Dean, C., Scholl, F. G., Choih, J., DeMaria, S., Berger, J., Isacoff, E., & Scheiffele, P. (2003). Neurexin mediates the assembly of presynaptic terminals. *Nature Neuroscience*, *6*(7), 708–716. https://doi.org/10.1038/nn1074

Deneault, E., Faheem, M., White, S. H., Rodrigues, D. C., Sun, S., Wei, W., … Scherer, S. W. (2019). CNTN5-/+or EHMT2-/+human iPSC-derived neurons from individuals with autism develop hyperactive neuronal networks. *ELife*, *8*, e40092. https://doi.org/10.7554/eLife.40092

Deneault, E., White, S. H., Rodrigues, D. C., Ross, P. J., Faheem, M., Zaslavsky, K., … Scherer, S. W. (2018). Complete Disruption of Autism-Susceptibility Genes by Gene Editing Predominantly Reduces Functional Connectivity of Isogenic Human Neurons. *Stem Cell Reports*, *11*(5), 1211–1225. https://doi.org/10.1016/j.stemcr.2018.10.003

Deng, W., Zou, X., Deng, H., Li, J., Tang, C., Wang, X., & Guo, X. (2015). The Relationship Among Genetic Heritability, Environmental Effects, and Autism Spectrum Disorders: 37 Pairs of Ascertained Twin Study. *Journal of Child Neurology*, *30*(13), 1794–1799. https://doi.org/10.1177/0883073815580645

Devanna, P., Middelbeek, J., & Vernes, S. C. (2014). FOXP2 drives neuronal differentiation by interacting with retinoic acid signaling pathways. *Frontiers in Cellular Neuroscience*, *8*. https://doi.org/10.3389/fncel.2014.00305

Dolinoy, D. C., Weidman, J. R., & Jirtle, R. L. (2007). Epigenetic gene regulation: Linking early developmental environment to adult disease. *Reproductive Toxicology (Elmsford, N.Y.)*, *23*(3), 297–307. https://doi.org/10.1016/j.reprotox.2006.08.012

Dotti, C. G., Sullivan, C. A., & Banker, G. A. (1988). The establishment of polarity by hippocampal neurons in culture. *Journal of Neuroscience*, *8*(4), 1454–1468. https://doi.org/10.1523/JNEUROSCI.08-04-01454.1988

Duffney, L. J., Wei, J., Cheng, J., Liu, W., Smith, K. R., Kittler, J. T., & Yan, Z. (2013). Shank3 Deficiency Induces NMDA Receptor Hypofunction via an Actin-Dependent Mechanism. *Journal of Neuroscience*, *33*(40), 15767–15778. https://doi.org/10.1523/JNEUROSCI.1175-13.2013

Duffney, L. J., Zhong, P., Wei, J., Matas, E., Cheng, J., Qin, L., … Yan, Z. (2015). Autism-like Deficits in Shank3-Deficient Mice Are Rescued by Targeting Actin Regulators. *Cell Reports*, *11*(9), 1400–1413. https://doi.org/10.1016/j.celrep.2015.04.064

Duong, L., Klitten, L. L., Møller, R. S., Ingason, A., Jakobsen, K. D., Skjødt, C., … Tommerup, N. (2012). Mutations in NRXN1 in a family multiply affected with brain disorders: NRXN1 mutations and brain disorders. *American Journal of Medical Genetics. Part B, Neuropsychiatric Genetics: The Official Publication of the International Society of Psychiatric Genetics*, *159B*(3), 354–358. https://doi.org/10.1002/ajmg.b.32036

Durand, C. M., Perroy, J., Loll, F., Perrais, D., Fagni, L., Bourgeron, T., … Sans, N. (2012). SHANK3 mutations identified in autism lead to modification of dendritic spine morphology via an actin-dependent mechanism. *Molecular Psychiatry*, *17*(1), 71–84. https://doi.org/10.1038/mp.2011.57

Durand, Christelle M., Betancur, C., Boeckers, T. M., Bockmann, J., Chaste, P., Fauchereau, F., … Bourgeron, T. (2007). Mutations in the gene encoding the synaptic scaffolding protein SHANK3 are associated with autism spectrum disorders. *Nature Genetics*, *39*(1), 25–27. https://doi.org/10.1038/ng1933

Edelson, L. R., & Saudino, K. J. (2009). Genetic and Environmental Influences on Autistic-Like Behaviors in 2-Year-Old Twins. *Behavior Genetics*, *39*(3), 255–264. https://doi.org/10.1007/s10519-009-9270-3

Elsabbagh, M., Divan, G., Koh, Y.-J., Kim, Y. S., Kauchali, S., Marcín, C., … Fombonne, E. (2012). Global prevalence of autism and other pervasive developmental disorders. *Autism Research:*

Official Journal of the International Society for Autism Research, *5*(3), 160–179. https://doi.org/10.1002/aur.239

Etherton, M. R., Blaiss, C. A., Powell, C. M., & Südhof, T. C. (2009). Mouse neurexin-1α deletion causes correlated electrophysiological and behavioral changes consistent with cognitive impairments. *Proceedings of the National Academy of Sciences*, *106*(42), 17998–18003. https://doi.org/10.1073/pnas.0910297106

Fabrichny, I. P., Leone, P., Sulzenbacher, G., Comoletti, D., Miller, M. T., Taylor, P., … Marchot, P. (2007). Structural Analysis of the Synaptic Protein Neuroligin and Its β-Neurexin Complex: Determinants for Folding and Cell Adhesion. *Neuron*, *56*(6), 979–991. https://doi.org/10.1016/j.neuron.2007.11.013

Fasano, C. A., Chambers, S. M., Lee, G., Tomishima, M. J., & Studer, L. (2010). Efficient derivation of functional floor plate tissue from human embryonic stem cells. *Cell Stem Cell*, *6*(4), 336–347. https://doi.org/10.1016/j.stem.2010.03.001

Feng, J., Schroer, R., Yan, J., Song, W., Yang, C., Bockholt, A., … Sommer, S. S. (2006). High frequency of neurexin 1beta signal peptide structural variants in patients with autism. *Neuroscience Letters*, *409*(1), 10–13. https://doi.org/10.1016/j.neulet.2006.08.017

Flaherty, E., Zhu, S., Barretto, N., Cheng, E., Deans, P. J. M., Fernando, M. B., … Brennand, K. J. (2019). Neuronal impact of patient-specific aberrant NRXN1α splicing. *Nature Genetics*, *51*(12), 1679–1690. https://doi.org/10.1038/s41588-019-0539-z

Flavell, S. W., & Greenberg, M. E. (2008). Signaling Mechanisms Linking Neuronal Activity to Gene Expression and Plasticity of the Nervous System. *Annual Review of Neuroscience*, *31*(1), 563–590. https://doi.org/10.1146/annurev.neuro.31.060407.125631

Fregeac, J., Colleaux, L., & Nguyen, L. S. (2016). The emerging roles of MicroRNAs in autism spectrum disorders. *Neuroscience and Biobehavioral Reviews*, *71*, 729–738. https://doi.org/10.1016/j.neubiorev.2016.10.018

Gaspard, N., Bouschet, T., Hourez, R., Dimidschstein, J., Naeije, G., van den Ameele, J., … Vanderhaeghen, P. (2008). An intrinsic mechanism of corticogenesis from embryonic stem cells. *Nature*, *455*(7211), 351–357. https://doi.org/10.1038/nature07287

Gaugler, T., Klei, L., Sanders, S. J., Bodea, C. A., Goldberg, A. P., Lee, A. B., … Buxbaum, J. D. (2014). Most genetic risk for autism resides with common variation. *Nature Genetics*, *46*(8), 881–885. https://doi.org/10.1038/ng.3039

Gaur, R. K. (2006). RNA interference: A potential therapeutic tool for silencing splice isoforms linked to human diseases. *BioTechniques*, *40*(4S), S15–S22. https://doi.org/10.2144/000112165

Gauthier, J., Siddiqui, T. J., Huashan, P., Yokomaku, D., Hamdan, F. F., Champagne, N., … Rouleau, G. A. (2011). Truncating mutations in NRXN2 and NRXN1 in autism spectrum disorders and schizophrenia. *Human Genetics*, *130*(4), 563–573. https://doi.org/10.1007/s00439-011-0975-z

Gauthier, J., Spiegelman, D., Piton, A., Lafrenière, R. G., Laurent, S., St-Onge, J., … Rouleau, G. A. (2009). Novel de novo SHANK3 mutation in autistic patients. *American Journal of Medical Genetics. Part B, Neuropsychiatric Genetics: The Official Publication of the International Society of Psychiatric Genetics*, *150B*(3), 421–424. https://doi.org/10.1002/ajmg.b.30822

GeneCards—Human Genes | Gene Database | Gene Search. (n.d.). Retrieved 30 September 2020, from https://www.genecards.org/

Geschwind, D. H., & Levitt, P. (2007). Autism spectrum disorders: Developmental disconnection syndromes. *Current Opinion in Neurobiology*, *17*(1), 103–111. https://doi.org/10.1016/j.conb.2007.01.009

Gilbert, J., & Man, H.-Y. (2017). Fundamental Elements in Autism: From Neurogenesis and Neurite Growth to Synaptic Plasticity. *Frontiers in Cellular Neuroscience*, *11*, 359. https://doi.org/10.3389/fncel.2017.00359

Girirajan, S., Dennis, M. Y., Baker, C., Malig, M., Coe, B. P., Campbell, C. D., … Eichler, E. E. (2013). Refinement and Discovery of New Hotspots of Copy-Number Variation Associated with Autism Spectrum Disorder. *American Journal of Human Genetics*, *92*(2), 221–237. https://doi.org/10.1016/j.ajhg.2012.12.016

Glessner, J. T., Wang, K., Cai, G., Korvatska, O., Kim, C. E., Wood, S., … Hakonarson, H. (2009). Autism genome-wide copy number variation reveals ubiquitin and neuronal genes. *Nature*, *459*(7246), 569–573. https://doi.org/10.1038/nature07953

Graf, E. R., Zhang, X., Jin, S.-X., Linhoff, M. W., & Craig, A. M. (2004). Neurexins Induce Differentiation of GABA and Glutamate Postsynaptic Specializations via Neuroligins. *Cell*, *119*(7), 1013–1026. https://doi.org/10.1016/j.cell.2004.11.035

Grieshammer, U., & Shepard, K. A. (2014). Proceedings: Consideration of Genetics in the Design of Induced Pluripotent Stem Cell-Based Models of Complex Disease. *Stem Cells Translational Medicine*, *3*(11), 1253–1258. https://doi.org/10.5966/sctm.2014-0191

Guang, S., Pang, N., Deng, X., Yang, L., He, F., Wu, L., … Peng, J. (2018). Synaptopathology Involved in Autism Spectrum Disorder. *Frontiers in Cellular Neuroscience*, *12*. https://doi.org/10.3389/fncel.2018.00470

Guilmatre, A., Huguet, G., Delorme, R., & Bourgeron, T. (2014). The emerging role of SHANK genes in neuropsychiatric disorders. *Developmental Neurobiology*, *74*(2), 113–122. https://doi.org/10.1002/dneu.22128

Gupta, S., Kim, S. Y., Artis, S., Molfese, D. L., Schumacher, A., Sweatt, J. D., Paylor, R. E., & Lubin, F. D. (2010). Histone methylation regulates memory formation. *The Journal of Neuroscience: The Official Journal of the Society for Neuroscience*, *30*(10), 3589–3599. https://doi.org/10.1523/JNEUROSCI.3732-09.2010

Hackett, A., Tarpey, P. S., Licata, A., Cox, J., Whibley, A., Boyle, J., … Abidi, F. E. (2010). CASK mutations are frequent in males and cause X-linked nystagmus and variable XLMR phenotypes. *European Journal of Human Genetics*, *18*(5), 544–552. https://doi.org/10.1038/ejhg.2009.220

Hallmayer, J., Cleveland, S., Torres, A., Phillips, J., Cohen, B., Torigoe, T., … Risch, N. (2011). Genetic Heritability and Shared Environmental Factors Among Twin Pairs With Autism. *Archives of General Psychiatry*, *68*(11), 1095–1102. https://doi.org/10.1001/archgenpsychiatry.2011.76

Hannon, G. J. (2002). RNA interference. *Nature*, *418*(6894), 244–251. https://doi.org/10.1038/418244a

Harkin, L. F., Lindsay, S. J., Xu, Y., Alzu'bi, A., Ferrara, A., Gullon, E. A., James, O. G., & Clowry, G. J. (2017). Neurexins 1-3 Each Have a Distinct Pattern of Expression in the Early Developing Human Cerebral Cortex. *Cerebral Cortex (New York, N.Y.: 1991)*, *27*(1), 216–232. https://doi.org/10.1093/cercor/bhw394

Heise, C., Schroeder, J. C., Schoen, M., Halbedl, S., Reim, D., Woelfle, S., … Boeckers, T. M. (2016). Selective Localization of Shanks to VGLUT1-Positive Excitatory Synapses in the Mouse Hippocampus. *Frontiers in Cellular Neuroscience*, *10*. https://doi.org/10.3389/fncel.2016.00106

Heyes, S., Pratt, W. S., Rees, E., Dahimene, S., Ferron, L., Owen, M. J., & Dolphin, A. C. (2015). Genetic disruption of voltage-gated calcium channels in psychiatric and neurological disorders. *Progress in Neurobiology*, *134*, 36–54. https://doi.org/10.1016/j.pneurobio.2015.09.002

Ho, S.-M., Hartley, B. J., Tcw, J., Beaumont, M., Stafford, K., Slesinger, P. A., & Brennand, K. J. (2016). Rapid Ngn2-induction of excitatory neurons from hiPSC-derived neural progenitor cells. *Methods (San Diego, Calif.)*, *101*, 113–124. https://doi.org/10.1016/j.ymeth.2015.11.019

Hoekstra, R. A., Bartels, M., Verweij, C. J. H., & Boomsma, D. I. (2007). Heritability of autistic traits in the general population. *Archives of Pediatrics & Adolescent Medicine*, *161*(4), 372–377. https://doi.org/10.1001/archpedi.161.4.372

Hogart, A., Wu, D., LaSalle, J. M., & Schanen, N. C. (2010). The comorbidity of autism with the genomic disorders of chromosome 15q11.2-q13. *Neurobiology of Disease*, *38*(2), 181–191. https://doi.org/10.1016/j.nbd.2008.08.011

Hörmanseder, E., Simeone, A., Allen, G. E., Bradshaw, C. R., Figlmüller, M., Gurdon, J., & Jullien, J. (2017). H3K4 Methylation-Dependent Memory of Somatic Cell Identity Inhibits Reprogramming and Development of Nuclear Transfer Embryos. *Cell Stem Cell*, *21*(1), 135-143.e6. https://doi.org/10.1016/j.stem.2017.03.003

Huang, G., Chen, S., Chen, X., Zheng, J., Xu, Z., Doostparast Torshizi, A., … Shi, L. (2019). Uncovering the Functional Link Between SHANK3 Deletions and Deficiency in Neurodevelopment Using iPSC-Derived Human Neurons. *Frontiers in Neuroanatomy*, *13*. https://doi.org/10.3389/fnana.2019.00023

Huguet, G., Benabou, M., & Bourgeron, T. (2016). The Genetics of Autism Spectrum Disorders. In P. Sassone-Corsi & Y. Christen (Eds.), *A Time for Metabolism and Hormones*. Cham (CH): Springer. Retrieved from http://www.ncbi.nlm.nih.gov/books/NBK453174/

Hu, V. W., Sarachana, T., Sherrard, R. M., & Kocher, K. M. (2015). Investigation of sex differences in the expression of RORA and its transcriptional targets in the brain as a potential contributor to the sex bias in autism. *Molecular Autism*, *6*, 7. https://doi.org/10.1186/2040-2392-6-7

Huttenlocher, P. R., & Dabholkar, A. S. (1997). Regional differences in synaptogenesis in human cerebral cortex. *The Journal of Comparative Neurology*, *387*(2), 167–178. https://doi.org/10.1002/(sici)1096-9861(19971020)387:2<167::aid-cne1>3.0.co;2-z

Hyman, S. L., Levy, S. E., Myers, S. M., & Council on Children with Disabilities, S. on D. and B. P. (2020). Identification, Evaluation, and Management of Children With Autism Spectrum Disorder. *Pediatrics*, *145*(1). https://doi.org/10.1542/peds.2019-3447

ICD-10: International Statistical Classification of Diseases and Related Health Problems: Tenth Revision, 2nd ed.; World Health Organization: Geneva, Switzerland, 2004. World Health Organization.

Ichtchenko, K., Hata, Y., Nguyen, T., Ullrich, B., Missler, M., Moomaw, C., & Südhof, T. C. (1995). Neuroligin 1: A splice site-specific ligand for beta-neurexins. *Cell*, *81*(3), 435–443. https://doi.org/10.1016/0092-8674(95)90396-8

Ikeda, M., Aleksic, B., Kirov, G., Kinoshita, Y., Yamanouchi, Y., Kitajima, T., Kawashima, K., Okochi, T., Kishi, T., Zaharieva, I., Owen, M. J., O'Donovan, M. C., Ozaki, N., & Iwata, N. (2010). Copy number variation in schizophrenia in the Japanese population. *Biological Psychiatry*, *67*(3), 283–286. https://doi.org/10.1016/j.biopsych.2009.08.034

Imitola, J., Walleigh, D., Anderson, C. E., Jethva, R., Carvalho, K. S., Legido, A., & Khurana, D. S. (2014). Fraternal twins with autism, severe cognitive deficit, and epilepsy: Diagnostic role of chromosomal microarray analysis. *Seminars in Pediatric Neurology*, *21*(2), 167–171. https://doi.org/10.1016/j.spen.2014.04.027

Iossifov, I., Ronemus, M., Levy, D., Wang, Z., Hakker, I., Rosenbaum, J., … Wigler, M. (2012). De novo gene disruptions in children on the autistic spectrum. *Neuron*, *74*(2), 285–299. https://doi.org/10.1016/j.neuron.2012.04.009

Jacquemont, M.-L., Sanlaville, D., Redon, R., Raoul, O., Cormier-Daire, V., Lyonnet, S., … Philippe, A. (2006). Array-based comparative genomic hybridisation identifies high frequency of cryptic chromosomal rearrangements in patients with syndromic autism spectrum disorders. *Journal of Medical Genetics*, *43*(11), 843–849. https://doi.org/10.1136/jmg.2006.043166

Jamain, S., Quach, H., Betancur, C., Råstam, M., Colineaux, C., Gillberg, I. C., … Bourgeron, T. (2003). Mutations of the X-linked genes encoding neuroligins NLGN3 and NLGN4 are associated with autism. *Nature Genetics*, *34*(1), 27–29. https://doi.org/10.1038/ng1136

James, S. J., Cutler, P., Melnyk, S., Jernigan, S., Janak, L., Gaylor, D. W., & Neubrander, J. A. (2004). Metabolic biomarkers of increased oxidative stress and impaired methylation capacity in children with autism. *The American Journal of Clinical Nutrition*, *80*(6), 1611–1617. https://doi.org/10.1093/ajcn/80.6.1611

Jang, H. S., Shin, W. J., Lee, J. E., & Do, J. T. (2017). CpG and Non-CpG Methylation in Epigenetic Gene Regulation and Brain Function. *Genes*, *8*(6), 148. https://doi.org/10.3390/genes8060148

Jaramillo, T. C., Speed, H. E., Xuan, Z., Reimers, J. M., Liu, S., & Powell, C. M. (2016). Altered Striatal Synaptic Function and Abnormal Behaviour in Shank3 Exon4-9 Deletion Mouse Model of Autism. *Autism Research: Official Journal of the International Society for Autism Research*, *9*(3), 350–375. https://doi.org/10.1002/aur.1529

Jenkins, A. K., Paterson, C., Wang, Y., Hyde, T. M., Kleinman, J. E., & Law, A. J. (2016). Neurexin 1 (NRXN1) Splice Isoform Expression During Human Neocortical Development and Aging. *Molecular Psychiatry*, *21*(5), 701–706. https://doi.org/10.1038/mp.2015.107

Jenkins, A., Apud, J. A., Zhang, F., Decot, H., Weinberger, D. R., & Law, A. J. (2014). Identification of Candidate Single-Nucleotide Polymorphisms in NRXN1 Related to Antipsychotic Treatment Response in Patients with Schizophrenia. *Neuropsychopharmacology*, *39*(9), 2170–2178. https://doi.org/10.1038/npp.2014.65

Jiang, Y., & Ehlers, M. D. (2013). Modeling Autism by SHANK Gene Mutations in Mice. *Neuron*, *78*(1), 8–27. https://doi.org/10.1016/j.neuron.2013.03.016

Jiang, Y., Yuen, R. K. C., Jin, X., Wang, M., Chen, N., Wu, X., … Scherer, S. W. (2013). Detection of clinically relevant genetic variants in autism spectrum disorder by whole-genome sequencing. *American Journal of Human Genetics*, *93*(2), 249–263. https://doi.org/10.1016/j.ajhg.2013.06.012

Jirtle, R. L., & Skinner, M. K. (2007). Environmental epigenomics and disease susceptibility. *Nature Reviews. Genetics*, *8*(4), 253–262. https://doi.org/10.1038/nrg2045

Kanner, Leo. Autistic Disturbances of Affective Contact. Nervous Child: Journal of Psychopathology, Psychotherapy, Mental Hygiene, and Guidance of the Child 2 (1943): 217–50.

Karimi, P., Kamali, E., Mousavi, S. M., & Karahmadi, M. (2017). Environmental factors influencing the risk of autism. *Journal of Research in Medical Sciences: The Official Journal of Isfahan University of Medical Sciences*, *22*, 27. https://doi.org/10.4103/1735-1995.200272

Kathuria, A., Nowosiad, P., Jagasia, R., Aigner, S., Taylor, R. D., Andreae, L. C., … Price, J. (2018). Stem cell-derived neurons from autistic individuals with SHANK3 mutation show morphogenetic abnormalities during early development. *Molecular Psychiatry*, *23*(3), 735–746. https://doi.org/10.1038/mp.2017.185

Katz, L. C., & Shatz, C. J. (1996). Synaptic Activity and the Construction of Cortical Circuits. *Science*, *274*(5290), 1133–1138. https://doi.org/10.1126/science.274.5290.1133

Kim, H.-G., Kishikawa, S., Higgins, A. W., Seong, I.-S., Donovan, D. J., Shen, Y., … Gusella, J. F. (2008). Disruption of Neurexin 1 Associated with Autism Spectrum Disorder. *American Journal of Human Genetics*, *82*(1), 199. https://doi.org/10.1016/j.ajhg.2007.09.011

Kira, J.-I. (2017). Unexpected exacerbations following initiation of disease-modifying drugs in neuromyelitis optica spectrum disorder: Which factor is responsible, anti-aquaporin 4 antibodies, B cells, Th1 cells, Th2 cells, Th17 cells, or others? *Multiple Sclerosis (Houndmills, Basingstoke, England)*, *23*(9), 1300–1302. https://doi.org/10.1177/1352458517703803

Kirov, G., Gumus, D., Chen, W., Norton, N., Georgieva, L., Sari, M., … Ullmann, R. (2008). Comparative genome hybridization suggests a role for NRXN1 and APBA2 in schizophrenia. *Human Molecular Genetics*, *17*(3), 458–465. https://doi.org/10.1093/hmg/ddm323

Kirov, G., Rujescu, D., Ingason, A., Collier, D. A., O'Donovan, M. C., & Owen, M. J. (2009). Neurexin 1 (NRXN1) Deletions in Schizophrenia. *Schizophrenia Bulletin*, *35*(5), 851–854. https://doi.org/10.1093/schbul/sbp079

Kirwan, P., Turner-Bridger, B., Peter, M., Momoh, A., Arambepola, D., Robinson, H. P. C., & Livesey, F. J. (2015). Development and function of human cerebral cortex neural networks

from pluripotent stem cells in vitro. *Development*, *142*(18), 3178–3187. https://doi.org/10.1242/dev.123851

Kleijer, K. T. E., Schmeisser, M. J., Krueger, D. D., Boeckers, T. M., Scheiffele, P., Bourgeron, T., … Burbach, J. P. H. (2014). Neurobiology of autism gene products: Towards pathogenesis and drug targets. *Psychopharmacology*, *231*(6), 1037–1062. https://doi.org/10.1007/s00213-013-3403-3

Klusek, J., Martin, G. E., & Losh, M. (2014). Consistency between research and clinical diagnoses of autism among boys and girls with fragile X syndrome. *Journal of Intellectual Disability Research: JIDR*, *58*(10), 940–952. https://doi.org/10.1111/jir.12121

Kolevzon, A., Cai, G., Soorya, L., Takahashi, N., Grodberg, D., Kajiwara, Y., … Buxbaum, J. D. (2011). Analysis of a purported SHANK3 mutation in a boy with autism: Clinical impact of rare variant research in neurodevelopmental disabilities. *Brain Research*, *1380*, 98–105. https://doi.org/10.1016/j.brainres.2010.11.005

Kong, A., Frigge, M. L., Masson, G., Besenbacher, S., Sulem, P., Magnusson, G., … Stefansson, K. (2012). Rate of de novo mutations, father's age, and disease risk. *Nature*, *488*(7412), 471–475. https://doi.org/10.1038/nature11396

Koshimizu, E., Miyatake, S., Okamoto, N., Nakashima, M., Tsurusaki, Y., Miyake, N., … Matsumoto, N. (2013). Performance Comparison of Bench-Top Next Generation Sequencers Using Microdroplet PCR-Based Enrichment for Targeted Sequencing in Patients with Autism Spectrum Disorder. *PLOS ONE*, *8*(9), e74167. https://doi.org/10.1371/journal.pone.0074167

Kouser, M., Speed, H. E., Dewey, C. M., Reimers, J. M., Widman, A. J., Gupta, N., … Powell, C. M. (2013). Loss of predominant Shank3 isoforms results in hippocampus-dependent impairments in behavior and synaptic transmission. *The Journal of Neuroscience: The Official Journal of the Society for Neuroscience*, *33*(47), 18448–18468. https://doi.org/10.1523/JNEUROSCI.3017-13.2013

Kriks, S., Shim, J.-W., Piao, J., Ganat, Y. M., Wakeman, D. R., Xie, Z., … Studer, L. (2011). Dopamine neurons derived from human ES cells efficiently engraft in animal models of Parkinson's disease. *Nature*, *480*(7378), 547–551. https://doi.org/10.1038/nature10648

Krueger, D. D., Tuffy, L. P., Papadopoulos, T., & Brose, N. (2012). The role of neurexins and neuroligins in the formation, maturation, and function of vertebrate synapses. *Current Opinion in Neurobiology*, *22*(3), 412–422. https://doi.org/10.1016/j.conb.2012.02.012

Lai, M.-C., Lombardo, M. V., & Baron-Cohen, S. (2014). Autism. *The Lancet*, *383*(9920), 896–910. https://doi.org/10.1016/S0140-6736(13)61539-1

Lai, M.-C., Lombardo, M. V., Chakrabarti, B., & Baron-Cohen, S. (2013). Subgrouping the Autism "Spectrum": Reflections on DSM-5. *PLOS Biology*, *11*(4), e1001544. https://doi.org/10.1371/journal.pbio.1001544

Landa, R. J. (2008). Diagnosis of autism spectrum disorders in the first 3 years of life. *Nature Clinical Practice. Neurology*, *4*(3), 138–147. https://doi.org/10.1038/ncpneuro0731

LaSalle, J. M. (2013). Epigenomic strategies at the interface of genetic and environmental risk factors for autism. *Journal of Human Genetics*, *58*(7), 396–401. https://doi.org/10.1038/jhg.2013.49

LaSalle, J. M., Reiter, L. T., & Chamberlain, S. J. (2015). Epigenetic regulation of UBE3A and roles in human neurodevelopmental disorders. *Epigenomics*, *7*(7), 1213–1228. https://doi.org/10.2217/epi.15.70

Laumonnier, F., Bonnet-Brilhault, F., Gomot, M., Blanc, R., David, A., Moizard, M.-P., … Briault, S. (2004). X-Linked Mental Retardation and Autism Are Associated with a Mutation in the NLGN4 Gene, a Member of the Neuroligin Family. *American Journal of Human Genetics*, *74*(3), 552–557.

Leblond, C. S., Nava, C., Polge, A., Gauthier, J., Huguet, G., Lumbroso, S., … Bourgeron, T. (2014). Meta-analysis of SHANK Mutations in Autism Spectrum Disorders: A Gradient of Severity in Cognitive Impairments. *PLOS Genetics*, *10*(9), e1004580. https://doi.org/10.1371/journal.pgen.1004580

Lee, W.-C., Berry, R., Hohenstein, P., & Davies, J. (2008). SiRNA as a tool for investigating organogenesis. *Organogenesis*, *4*(3), 176–181. https://doi.org/10.4161/org.4.3.6642

Leenders, A. G. M., & Sheng, Z.-H. (2005). Modulation of neurotransmitter release by the second messenger-activated protein kinases: Implications for presynaptic plasticity. *Pharmacology & Therapeutics*, *105*(1), 69–84. https://doi.org/10.1016/j.pharmthera.2004.10.012

Li, J., Cai, T., Jiang, Y., Chen, H., He, X., Chen, C., … Wu, J. (2016). Genes with de novo mutations are shared by four neuropsychiatric disorders discovered from NPdenovo database. *Molecular Psychiatry*, *21*(2), 290–297. https://doi.org/10.1038/mp.2015.40

Lim, S., Naisbitt, S., Yoon, J., Hwang, J. I., Suh, P. G., Sheng, M., & Kim, E. (1999). Characterization of the Shank family of synaptic proteins. Multiple genes, alternative splicing, and differential expression in brain and development. *The Journal of Biological Chemistry*, *274*(41), 29510–29518. https://doi.org/10.1074/jbc.274.41.29510

Liu, Y., Hu, Z., Xun, G., Peng, Y., Lu, L., Xu, X., … Xia, K. (2012). Mutation analysis of the NRXN1 gene in a Chinese autism cohort. *Journal of Psychiatric Research*, *46*(5), 630–634. https://doi.org/10.1016/j.jpsychires.2011.10.015

Longair, M., Baker, Dean A., Armstrong, J. Douglas. (2011). Simple Neurite Tracer: open source software for reconstruction, visualization and analysis of neuronal processes, *Bioinformatics*, Volume 27, Issue 17, 1 September 2011, Pages 2453–2454, https://doi.org/10.1093/bioinformatics/btr390

Lotter, V. (1966). Epidemiology of autistic conditions in young children. *Social Psychiatry*, *1*(3), 124–135. https://doi.org/10.1007/BF00584048

Lu, Z., Liu, Z., Mao, W., Wang, X., Zheng, X., Chen, S., Cao, B., Huang, S., Zhang, X., Zhou, T., Zhang, Y., Huang, X., Sun, Q., & Li, J.-D. (2020). Locus-specific DNA methylation of Mecp2 promoter leads to autism-like phenotypes in mice. *Cell Death & Disease*, *11*(2), 1–11. https://doi.org/10.1038/s41419-020-2290-x

Ma, L., Hu, B., Liu, Y., Vermilyea, S. C., Liu, H., Gao, L., … Zhang, S.-C. (2012). Human embryonic stem cell-derived GABA neurons correct locomotion deficits in quinolinic acid-lesioned mice. *Cell Stem Cell*, *10*(4), 455–464. https://doi.org/10.1016/j.stem.2012.01.021

Maenner, M. J. (2020). Prevalence of Autism Spectrum Disorder Among Children Aged 8 Years—Autism and Developmental Disabilities Monitoring Network, 11 Sites, United States, 2016. *MMWR. Surveillance Summaries*, *69*. https://doi.org/10.15585/mmwr.ss6904a1

Maherali, N., Ahfeldt, T., Rigamonti, A., Utikal, J., Cowan, C., & Hochedlinger, K. (2008). A high efficiency system for the generation and study of human induced pluripotent stem cells. *Cell Stem Cell*, *3*(3), 340–345. https://doi.org/10.1016/j.stem.2008.08.003

Mäki, P., Veijola, J., Jones, P. B., Murray, G. K., Koponen, H., Tienari, P., … Isohanni, M. (2005). Predictors of schizophrenia—A review. *British Medical Bulletin*, *73–74*(1), 1–15. https://doi.org/10.1093/bmb/ldh046

Mameza, M. G., Dvoretskova, E., Bamann, M., Hönck, H.-H., Güler, T., Boeckers, T. M., … Kreienkamp, H.-J. (2013). SHANK3 Gene Mutations Associated with Autism Facilitate Ligand Binding to the Shank3 Ankyrin Repeat Region. *The Journal of Biological Chemistry*, *288*(37), 26697–26708. https://doi.org/10.1074/jbc.M112.424747

Marshall, C. R., Noor, A., Vincent, J. B., Lionel, A. C., Feuk, L., Skaug, J., … Scherer, S. W. (2008). Structural variation of chromosomes in autism spectrum disorder. *American Journal of Human Genetics*, *82*(2), 477–488. https://doi.org/10.1016/j.ajhg.2007.12.009

Martenson, J. S., & Tomita, S. (2015). Synaptic localization of neurotransmitter receptors: Comparing mechanisms for AMPA and GABAA receptors. *Current Opinion in Pharmacology*, *20*, 102–108. https://doi.org/10.1016/j.coph.2014.11.011

Maunakea, A. K., Nagarajan, R. P., Bilenky, M., Ballinger, T. J., D'Souza, C., Fouse, S. D., … Costello, J. F. (2010). Conserved role of intragenic DNA methylation in regulating alternative promoters. *Nature*, *466*(7303), 253–257. https://doi.org/10.1038/nature09165

McConkey, R. (2020). The rise in the numbers of pupils identified by schools with autism spectrum disorder (ASD): A comparison of the four countries in the United Kingdom. *Support for Learning*, *35*(2), 132–143. https://doi.org/10.1111/1467-9604.12296

Meyer, G., Schaaps, J. P., Moreau, L., & Goffinet, A. M. (2000). Embryonic and Early Fetal Development of the Human Neocortex. *Journal of Neuroscience*, *20*(5), 1858–1868. https://doi.org/10.1523/JNEUROSCI.20-05-01858.2000

Miles, J. H., Takahashi, T. N., Bagby, S., Sahota, P. K., Vaslow, D. F., Wang, C. H., … Farmer, J. E. (2005). Essential versus complex autism: Definition of fundamental prognostic subtypes. *American Journal of Medical Genetics. Part A*, *135*(2), 171–180. https://doi.org/10.1002/ajmg.a.30590

Miller, M. T., Mileni, M., Comoletti, D., Stevens, R. C., Harel, M., & Taylor, P. (2011). The crystal structure of the α-neurexin-1 extracellular region reveals a hinge point for mediating synaptic adhesion and function. *Structure(London, England:1993)*, *19*(6), 767–778. https://doi.org/10.1016/j.str.2011.03.011

Missler, M., Zhang, W., Rohlmann, A., Kattenstroth, G., Hammer, R. E., Gottmann, K., & Südhof, T. C. (2003). α-Neurexins couple Ca 2+ channels to synaptic vesicle exocytosis. *Nature*, *423*(6943), 939–948. https://doi.org/10.1038/nature01755

Missler, M., & Südhof, T. C. (1998). Neurexins: Three genes and 1001 products. *Trends in Genetics: TIG*, *14*(1), 20–26. https://doi.org/10.1016/S0168-9525(97)01324-3

Moessner, R., Marshall, C. R., Sutcliffe, J. S., Skaug, J., Pinto, D., Vincent, J., … Scherer, S. W. (2007). Contribution of SHANK3 Mutations to Autism Spectrum Disorder. *The American Journal of Human Genetics*, *81*(6), 1289–1297. https://doi.org/10.1086/522590

Møller, R. S., Weber, Y. G., Klitten, L. L., Trucks, H., Muhle, H., Kunz, W. S., Mefford, H. C., Franke, A., Kautza, M., Wolf, P., Dennig, D., Schreiber, S., Rückert, I.-M., Wichmann, H.-E., Ernst, J. P., Schurmann, C., Grabe, H. J., Tommerup, N., Stephani, U., … EPICURE Consortium. (2013). Exon-disrupting deletions of NRXN1 in idiopathic generalized epilepsy. *Epilepsia*, *54*(2), 256–264. https://doi.org/10.1111/epi.12078

Mondin, M., Labrousse, V., Hosy, E., Heine, M., Tessier, B., Levet, F., … Thoumine, O. (2011). Neurexin-Neuroligin Adhesions Capture Surface-Diffusing AMPA Receptors through PSD-95 Scaffolds. *Journal of Neuroscience*, *31*(38), 13500–13515. https://doi.org/10.1523/JNEUROSCI.6439-10.2011

Monteiro, P., & Feng, G. (2017). SHANK proteins: Roles at the synapse and in autism spectrum disorder. *Nature Reviews. Neuroscience*, *18*(3), 147–157. https://doi.org/10.1038/nrn.2016.183

Mor, M., Nardone, S., Sams, D. S., & Elliott, E. (2015). Hypomethylation of miR-142 promoter and upregulation of microRNAs that target the oxytocin receptor gene in the autism prefrontal cortex. *Molecular Autism*, *6*(1), 46. https://doi.org/10.1186/s13229-015-0040-1

Morrow, E. M., Yoo, S.-Y., Flavell, S. W., Kim, T.-K., Lin, Y., Hill, R. S., … Walsh, C. A. (2008). Identifying Autism Loci and Genes by Tracing Recent Shared Ancestry. *Science*, *321*(5886), 218–223. https://doi.org/10.1126/science.1157657

Mottron, L., Bouvet, L., Bonnel, A., Samson, F., Burack, J. A., Dawson, M., & Heaton, P. (2013). Veridical mapping in the development of exceptional autistic abilities. *Neuroscience and Biobehavioral Reviews*, *37*(2), 209–228. https://doi.org/10.1016/j.neubiorev.2012.11.016

Muhammad, K., Reddy-Alla, S., Driller, J. H., Schreiner, D., Rey, U., Böhme, M. A., Hollmann, C., Ramesh, N., Depner, H., Lützkendorf, J., Matkovic, T., Götz, T., Bergeron, D. D., Schmoranzer, J., Goettfert, F., Holt, M., Wahl, M. C., Hell, S. W., Scheiffele, P., … Sigrist, S. J. (2015). Presynaptic spinophilin tunes neurexin signalling to control active zone architecture and function. *Nature Communications*, *6*, 8362. https://doi.org/10.1038/ncomms9362

Myung, S. C., Lee, Y. E., Ji, Y. K., Chung, S., Yoon, H. C., Kim, D. S., … Kim, D. W. (2008). Highly efficient and large-scale generation of functional dopamine neurons from human embryonic stem cells. *Proceedings of the National Academy of Sciences of the United States of America*, *105*(9), 3392–3397. https://doi.org/10.1073/pnas.0712359105

Nagarajan, R. P., Hogart, A. R., Gwye, Y., Martin, M. R., & LaSalle, J. M. (2006). Reduced MeCP2 expression is frequent in autism frontal cortex and correlates with aberrant MECP2 promoter methylation. *Epigenetics*, *1*(4), e1-11. https://doi.org/10.4161/epi.1.4.3514

Naisbitt, S., Kim, E., Tu, J. C., Xiao, B., Sala, C., Valtschanoff, J., … Sheng, M. (1999). Shank, a Novel Family of Postsynaptic Density Proteins that Binds to the NMDA Receptor/PSD-95/GKAP Complex and Cortactin. *Neuron*, *23*(3), 569–582. https://doi.org/10.1016/S0896-6273(00)80809-0

Najm, J., Horn, D., Wimplinger, I., Golden, J. A., Chizhikov, V. V., Sudi, J., … Kutsche, K. (2008). Mutations of CASK cause an X-linked brain malformation phenotype with microcephaly and hypoplasia of the brainstem and cerebellum. *Nature Genetics*, *40*(9), 1065–1067. https://doi.org/10.1038/ng.194

Nam, C. I., & Chen, L. (2005). Postsynaptic assembly induced by neurexin-neuroligin interaction and neurotransmitter. *Proceedings of the National Academy of Sciences*, *102*(17), 6137–6142. https://doi.org/10.1073/pnas.0502038102

Negri, J., Menon, V., & Young-Pearse, T. L. (2020). Assessment of Spontaneous Neuronal Activity In Vitro Using Multi-Well Multi-Electrode Arrays: Implications for Assay Development. *ENeuro*, *7*(1). https://doi.org/10.1523/ENEURO.0080-19.2019

Nemirovsky, S. I., Córdoba, M., Zaiat, J. J., Completa, S. P., Vega, P. A., González-Morón, D., … Kauffman, M. A. (2015). Whole Genome Sequencing Reveals a De Novo SHANK3 Mutation in Familial Autism Spectrum Disorder. *PLoS ONE*, *10*(2). https://doi.org/10.1371/journal.pone.0116358

Nguyen, A., Rauch, T. A., Pfeifer, G. P., & Hu, V. W. (2010). Global methylation profiling of lymphoblastoid cell lines reveals epigenetic contributions to autism spectrum disorders and a novel autism candidate gene, RORA, whose protein product is reduced in autistic brain. *FASEB Journal: Official Publication of the Federation of American Societies for Experimental Biology*, *24*(8), 3036–3051. https://doi.org/10.1096/fj.10-154484

NHS Digital. https://digital.nhs.uk/data-and-information/publications/statistical/autism-statistics/q1-april-to-june-2020-21/data-quality-copy

Nia, F. H., & Kreienkamp, H.-J. (2018). Functional Relevance of Missense Mutations Affecting the N-Terminal Part of Shank3 Found in Autistic Patients. *Frontiers in Molecular Neuroscience*, *11*. https://doi.org/10.3389/fnmol.2018.00268

Onder, T. T., & Daley, G. Q. (2012). New lessons learned from disease modeling with induced pluripotent stem cells. *Current Opinion in Genetics & Development*, *22*(5), 500–508. https://doi.org/10.1016/j.gde.2012.05.005

Pak, C., Danko, T., Zhang, Y., Aoto, J., Anderson, G., Maxeiner, S., … Südhof, T. C. (2015). Human Neuropsychiatric Disease Modeling using Conditional Deletion Reveals Synaptic Transmission Defects Caused by Heterozygous Mutations in NRXN1. *Cell Stem Cell*, *17*(3), 316–328. https://doi.org/10.1016/j.stem.2015.07.017

Parikshak, N. N., Luo, R., Zhang, A., Won, H., Lowe, J. K., Chandran, V., … Geschwind, D. H. (2013). Integrative Functional Genomic Analyses Implicate Specific Molecular Pathways and Circuits in Autism. *Cell*, *155*(5), 1008–1021. https://doi.org/10.1016/j.cell.2013.10.031

Park, I.-H., Zhao, R., West, J. A., Yabuuchi, A., Huo, H., Ince, T. A., … Daley, G. Q. (2008). Reprogramming of human somatic cells to pluripotency with defined factors. *Nature*, *451*(7175), 141–146. https://doi.org/10.1038/nature06534

Paşca, S. P., Portmann, T., Voineagu, I., Yazawa, M., Shcheglovitov, A., Paşca, A. M., … Dolmetsch, R. E. (2011). Using iPSC-derived neurons to uncover cellular phenotypes associated with Timothy syndrome. *Nature Medicine*, *17*(12), 1657–1662. https://doi.org/10.1038/nm.2576

Pawlowski, M., Ortmann, D., Bertero, A., Tavares, J. M., Pedersen, R. A., Vallier, L., & Kotter, M. R. N. (2017). Inducible and Deterministic Forward Programming of Human Pluripotent Stem Cells into Neurons, Skeletal Myocytes, and Oligodendrocytes. *Stem Cell Reports*, *8*(4), 803–812. https://doi.org/10.1016/j.stemcr.2017.02.016

Peça, J., Feliciano, C., Ting, J. T., Wang, W., Wells, M. F., Venkatraman, T. N., … Feng, G. (2011). Shank3 mutant mice display autistic-like behaviours and striatal dysfunction. *Nature*, *472*(7344), 437–442. https://doi.org/10.1038/nature09965

Peters, S. U., Hundley, R. J., Wilson, A. K., Warren, Z., Vehorn, A., Carvalho, C., Lupski, J. R., & Ramocki, M. B. (2013). The behavioral phenotype in MECP2 duplication syndrome: A comparison to idiopathic autism. *Autism Research : Official Journal of the International Society for Autism Research*, *6*(1), 42–50. https://doi.org/10.1002/aur.1262

Pettersen, K. H., & Einevoll, G. T. (2008). Amplitude Variability and Extracellular Low-Pass Filtering of Neuronal Spikes. *Biophysical Journal*, *94*(3), 784–802. https://doi.org/10.1529/biophysj.107.111179

Phelan, K., & McDermid, H. E. (2012). The 22q13.3 Deletion Syndrome (Phelan-McDermid Syndrome). *Molecular Syndromology*, *2*(3–5), 186–201. https://doi.org/10.1159/000334260

Pinto, D., Pagnamenta, A. T., Klei, L., Anney, R., Merico, D., Regan, R., … Betancur, C. (2010). Functional impact of global rare copy number variation in autism spectrum disorders. *Nature*, *466*(7304), 368–372. https://doi.org/10.1038/nature09146

Popov, N. T., Stoyanova, V. K., Madzhirova, N. P., & Vachev, T. I. (2012). Epigenetic aspects in schizophrenia etiology and pathogenesis. *Folia Medica*, *54*(2), 12–16. https://doi.org/10.2478/v10153-011-0082-x

Prasad, A., Merico, D., Thiruvahindrapuram, B., Wei, J., Lionel, A. C., Sato, D., … Scherer, S. W. (2012). A discovery resource of rare copy number variations in individuals with autism spectrum disorder. *G3 (Bethesda, Md.)*, *2*(12), 1665–1685. https://doi.org/10.1534/g3.112.004689

Püschel, A. W., & Betz, H. (1995). Neurexins are differentially expressed in the embryonic nervous system of mice. *The Journal of Neuroscience: The Official Journal of the Society for Neuroscience*, *15*(4), 2849–2856.

Rabinowicz, T., de Courten-Myers, G. M., Petetot, J. M.-C., Xi, G., & de los Reyes, E. (1996). Human Cortex Development: Estimates of Neuronal Numbers Indicate Major Loss Late During Gestation. *Journal of Neuropathology & Experimental Neurology*, *55*(3), 320–328. https://doi.org/10.1097/00005072-199603000-00007

Rajamohan, D., Matsa, E., Kalra, S., Crutchley, J., Patel, A., George, V., & Denning, C. (2013). Current status of drug screening and disease modelling in human pluripotent stem cells. *BioEssays: News and Reviews in Molecular, Cellular and Developmental Biology*, *35*(3), 281–298. https://doi.org/10.1002/bies.201200053

Rao, D. D., Vorhies, J. S., Senzer, N., & Nemunaitis, J. (2009). siRNA vs. shRNA: Similarities and differences. *Advanced Drug Delivery Reviews*, *61*(9), 746–759. https://doi.org/10.1016/j.addr.2009.04.004

Reissner, C., Klose, M., Fairless, R., & Missler, M. (2008). Mutational analysis of the neurexin/neuroligin complex reveals essential and regulatory components. *Proceedings of the National Academy of Sciences*, *105*(39), 15124–15129. https://doi.org/10.1073/pnas.0801639105

Reissner, C., Runkel, F., & Missler, M. (2013). Neurexins. *Genome Biology*, *14*(9), 213. https://doi.org/10.1186/gb-2013-14-9-213

Richards, C., Jones, C., Groves, L., Moss, J., & Oliver, C. (2015). Prevalence of autism spectrum disorder phenomenology in genetic disorders: A systematic review and meta-analysis. *The Lancet. Psychiatry*, *2*(10), 909–916. https://doi.org/10.1016/S2215-0366(15)00376-4

Robinson, H. P., Kawahara, M., Jimbo, Y., Torimitsu, K., Kuroda, Y., & Kawana, A. (1993). Periodic synchronized bursting and intracellular calcium transients elicited by low magnesium in cultured cortical neurons. *Journal of Neurophysiology*, *70*(4), 1606–1616. https://doi.org/10.1152/jn.1993.70.4.1606

Rosa, F., Dhingra, A., Uysal, B., Mendis, G. D. C., Loeffler, H., Elsen, G., … Maljevic, S. (2020). In Vitro Differentiated Human Stem Cell-Derived Neurons Reproduce Synaptic Synchronicity Arising during Neurodevelopment. *Stem Cell Reports*, *15*(1), 22–37. https://doi.org/10.1016/j.stemcr.2020.05.015

Rowen, L., Young, J., Birditt, B., Kaur, A., Madan, A., Philipps, D. L., Qin, S., Minx, P., Wilson, R. K., Hood, L., & Graveley, B. R. (2002). Analysis of the human neurexin genes: Alternative splicing and the generation of protein diversity. *Genomics*, *79*(4), 587–597. https://doi.org/10.1006/geno.2002.6734

Rujescu, D., Ingason, A., Cichon, S., Pietiläinen, O. P. H., Barnes, M. R., Toulopoulou, T., … Collier, D. A. (2009). Disruption of the neurexin 1 gene is associated with schizophrenia. *Human Molecular Genetics*, *18*(5), 988–996. https://doi.org/10.1093/hmg/ddn351

Rusiecki, J. A., Baccarelli, A., Bollati, V., Tarantini, L., Moore, L. E., & Bonefeld-Jorgensen, E. C. (2008). Global DNA hypomethylation is associated with high serum-persistent organic pollutants in Greenlandic Inuit. *Environmental Health Perspectives*, *116*(11), 1547–1552. https://doi.org/10.1289/ehp.11338

Russo, F. B., Brito, A., de Freitas, A. M., Castanha, A., de Freitas, B. C., & Beltrão-Braga, P. C. B. (2019). The use of iPSC technology for modeling Autism Spectrum Disorders. *Neurobiology of Disease*, *130*, 104483. https://doi.org/10.1016/j.nbd.2019.104483

Sala, C., Piëch, V., Wilson, N. R., Passafaro, M., Liu, G., & Sheng, M. (2001). Regulation of dendritic spine morphology and synaptic function by Shank and Homer. *Neuron*, *31*(1), 115–130. https://doi.org/10.1016/s0896-6273(01)00339-7

Sanders, S. J., He, X., Willsey, A. J., Ercan-Sencicek, A. G., Samocha, K. E., Cicek, A. E., Murtha, M. T., Bal, V. H., Bishop, S. L., Dong, S., Goldberg, A. P., Jinlu, C., Keaney, J. F., Klei, L., Mandell, J. D., Moreno-De-Luca, D., Poultney, C. S., Robinson, E. B., Smith, L., … State, M. W. (2015). Insights into Autism Spectrum Disorder Genomic Architecture and Biology from 71 Risk Loci. *Neuron*, *87*(6), 1215–1233. https://doi.org/10.1016/j.neuron.2015.09.016

Sarachana, T., Xu, M., Wu, R.-C., & Hu, V. W. (2011). Sex Hormones in Autism: Androgens and Estrogens Differentially and Reciprocally Regulate RORA, a Novel Candidate Gene for Autism. *PLOS ONE*, *6*(2), e17116. https://doi.org/10.1371/journal.pone.0017116

Sarasua, S. M., Dwivedi, A., Boccuto, L., Chen, C.-F., Sharp, J. L., Rollins, J. D., … DuPont, B. R. (2014). 22q13.2q13.32 genomic regions associated with severity of speech delay, developmental delay, and physical features in Phelan-McDermid syndrome. *Genetics in Medicine: Official Journal of the American College of Medical Genetics*, *16*(4), 318–328. https://doi.org/10.1038/gim.2013.144

Schaaf, C. P., Boone, P. M., Sampath, S., Williams, C., Bader, P. I., Mueller, J. M., … Cheung, S. W. (2012). Phenotypic spectrum and genotype-phenotype correlations of NRXN1 exon deletions. *European Journal of Human Genetics: EJHG*, *20*(12), 1240–1247. https://doi.org/10.1038/ejhg.2012.95

Schaefer, G. B., Mendelsohn, N. J., & Professional Practice and Guidelines Committee. (2013). Clinical genetics evaluation in identifying the etiology of autism spectrum disorders: 2013 guideline revisions. *Genetics in Medicine: Official Journal of the American College of Medical Genetics*, *15*(5), 399–407. https://doi.org/10.1038/gim.2013.32

Schaefer, G. B., Starr, L., Pickering, D., Skar, G., Dehaai, K., & Sanger, W. G. (2010). Array comparative genomic hybridization findings in a cohort referred for an autism evaluation. *Journal of Child Neurology*, *25*(12), 1498–1503. https://doi.org/10.1177/0883073810370479

Schauer, C., & Leinders-Zufall, T. (2012). Imaging Calcium Responses in GFP-tagged Neurons of Hypothalamic Mouse Brain Slices. *Journal of Visualized Experiments : JoVE*, (66). https://doi.org/10.3791/4213

Schiele, M. A., & Domschke, K. (2018). Epigenetics at the crossroads between genes, environment and resilience in anxiety disorders. *Genes, Brain, and Behavior*, *17*(3), e12423. https://doi.org/10.1111/gbb.12423

Schmeisser, M. J., Ey, E., Wegener, S., Bockmann, J., Stempel, A. V., Kuebler, A., … Boeckers, T. M. (2012). Autistic-like behaviours and hyperactivity in mice lacking ProSAP1/Shank2. *Nature*, *486*(7402), 256–260. https://doi.org/10.1038/nature11015

Schroeter, M. S., Charlesworth, P., Kitzbichler, M. G., Paulsen, O., & Bullmore, E. T. (2015). Emergence of Rich-Club Topology and Coordinated Dynamics in Development of Hippocampal Functional Networks In Vitro. *Journal of Neuroscience*, *35*(14), 5459–5470. https://doi.org/10.1523/JNEUROSCI.4259-14.2015

Sebat, J., Lakshmi, B., Malhotra, D., Troge, J., Lese-Martin, C., Walsh, T., … Wigler, M. (2007). Strong association of de novo copy number mutations with autism. *Science (New York, N.Y.)*, *316*(5823), 445–449. https://doi.org/10.1126/science.1138659

Seno, M. M. G., Hu, P., Gwadry, F. G., Pinto, D., Marshall, C. R., Casallo, G., & Scherer, S. W. (2011). Gene and miRNA expression profiles in autism spectrum disorders. *Brain Research*, *1380*, 85–97. https://doi.org/10.1016/j.brainres.2010.09.046

Shcheglovitov, A., Shcheglovitova, O., Yazawa, M., Portmann, T., Shu, R., Sebastiano, V., … Dolmetsch, R. E. (2013). SHANK3 and IGF1 restore synaptic deficits in neurons from 22q13 deletion syndrome patients. *Nature*, *503*(7475), 267–271. https://doi.org/10.1038/nature12618

Shen, X., Yeung, H. T., & Lai, K.-O. (2019). Application of Human-Induced Pluripotent Stem Cells (hiPSCs) to Study Synaptopathy of Neurodevelopmental Disorders. *Developmental Neurobiology*, *79*(1), 20–35. https://doi.org/10.1002/dneu.22644

Shen, Y., Dies, K. A., Holm, I. A., Bridgemohan, C., Sobeih, M. M., Caronna, E. B., … Autism Consortium Clinical Genetics/DNA Diagnostics Collaboration. (2010). Clinical genetic testing for patients with autism spectrum disorders. *Pediatrics*, *125*(4), e727-735. https://doi.org/10.1542/peds.2009-1684

Sheng, M., & Kim, E. (2000). The Shank family of scaffold proteins. *Journal of Cell Science*, *113*(11), 1851–1856.

Shi, Y., Kirwan, P., & Livesey, F. J. (2012). Directed differentiation of human pluripotent stem cells to cerebral cortex neurons and neural networks. *Nature Protocols*, *7*(10), 1836–1846. https://doi.org/10.1038/nprot.2012.116

Shilatifard, A. (2008). Molecular implementation and physiological roles for histone H3 lysine 4 (H3K4) methylation. *Current Opinion in Cell Biology*, *20*(3), 341–348. https://doi.org/10.1016/j.ceb.2008.03.019

Shulha, H. P., Cheung, I., Whittle, C., Wang, J., Virgil, D., Lin, C. L., Guo, Y., Lessard, A., Akbarian, S., & Weng, Z. (2012). Epigenetic signatures of autism: Trimethylated H3K4 landscapes in prefrontal neurons. *Archives of General Psychiatry*, *69*(3), 314–324. https://doi.org/10.1001/archgenpsychiatry.2011.151

Song, J.-Y., Ichtchenko, K., Südhof, T. C., & Brose, N. (1999). Neuroligin 1 is a postsynaptic cell-adhesion molecule of excitatory synapses. *Proceedings of the National Academy of Sciences*, *96*(3), 1100–1105. https://doi.org/10.1073/pnas.96.3.1100

Soorya, L., Kolevzon, A., Zweifach, J., Lim, T., Dobry, Y., Schwartz, L., … Buxbaum, J. D. (2013). Prospective investigation of autism and genotype-phenotype correlations in 22q13 deletion syndrome and SHANK3 deficiency. *Molecular Autism*, *4*(1), 18. https://doi.org/10.1186/2040-2392-4-18

Srikanth, P., & Young-Pearse, T. L. (2014). Stem cells on the brain: Modeling neurodevelopmental and neurodegenerative diseases using human induced pluripotent stem cells. *Journal of Neurogenetics*, *28*(1–2), 5–29. https://doi.org/10.3109/01677063.2014.881358

Stelzer, G., Rosen, N., Plaschkes, I., Zimmerman, S., Twik, M., Fishilevich, S., … Lancet, D. (2016). The GeneCards Suite: From Gene Data Mining to Disease Genome Sequence Analyses. *Current Protocols in Bioinformatics*, *54*, 1.30.1-1.30.33. https://doi.org/10.1002/cpbi.5

Stessman, H. A. F., Xiong, B., Coe, B. P., Wang, T., Hoekzema, K., Fenckova, M., … Eichler, E. E. (2017). Targeted sequencing identifies 91 neurodevelopmental-disorder risk genes with autism and developmental-disability biases. *Nature Genetics*, *49*(4), 515–526. https://doi.org/10.1038/ng.3792

Stilp, R. L. H., Gernsbacher, M. A., Schweigert, E. K., Arneson, C. L., & Goldsmith, H. H. (2010). Genetic Variance for Autism Screening Items in an Unselected Sample of Toddler-Age Twins. *Journal of the American Academy of Child and Adolescent Psychiatry*, *49*(3), 267–276. https://doi.org/10.1016/j.jaac.2009.11.012

Südhof, T. C. (2008). Neuroligins and Neurexins Link Synaptic Function to Cognitive Disease. *Nature*, *455*(7215), 903–911. https://doi.org/10.1038/nature07456

Südhof, T. C. (2017). Synaptic Neurexin Complexes: A Molecular Code for the Logic of Neural Circuits. *Cell*, *171*(4), 745–769. https://doi.org/10.1016/j.cell.2017.10.024

Südhof, T. C. (2018). Towards an Understanding of Synapse Formation. *Neuron*, *100*(2), 276–293. https://doi.org/10.1016/j.neuron.2018.09.040

Swaminathan, S., Shen, L., Kim, S., Inlow, M., West, J. D., Faber, K. M., Foroud, T., Mayeux, R., Saykin, A. J., Alzheimer's Disease Neuroimaging Initiative, & NIA-LOAD/NCRAD Family Study Group. (2012). Analysis of copy number variation in Alzheimer's disease: The NIALOAD/ NCRAD Family Study. *Current Alzheimer Research*, *9*(7), 801–814. https://doi.org/10.2174/156720512802455331

Tabuchi, K., Blundell, J., Etherton, M. R., Hammer, R. E., Liu, X., Powell, C. M., & Südhof, T. C. (2007). A Neuroligin-3 Mutation Implicated in Autism Increases Inhibitory Synaptic Transmission in Mice. *Science (New York, N.Y.)*, *318*(5847), 71–76. https://doi.org/10.1126/science.1146221

Tabuchi, K., & Südhof, T. C. (2002). Structure and evolution of neurexin genes: Insight into the mechanism of alternative splicing. *Genomics*, *79*(6), 849–859. https://doi.org/10.1006/geno.2002.6780

Takahashi, K., Tanabe, K., Ohnuki, M., Narita, M., Ichisaka, T., Tomoda, K., & Yamanaka, S. (2007). Induction of Pluripotent Stem Cells from Adult Human Fibroblasts by Defined Factors. *Cell*, *131*(5), 861–872. https://doi.org/10.1016/j.cell.2007.11.019

Tall, A. R., Yvan-Charvet Laurent, & Wang Nan. (2007). The Failure of Torcetrapib. *Arteriosclerosis, Thrombosis, and Vascular Biology*, *27*(2), 257–260. https://doi.org/10.1161/01.ATV.0000256728.60226.77

Tatavarty, V., Torrado Pacheco, A., Groves Kuhnle, C., Lin, H., Koundinya, P., Miska, N. J., … Turrigiano, G. G. (2020). Autism-Associated Shank3 Is Essential for Homeostatic Compensation in Rodent V1. *Neuron*, *106*(5), 769-777.e4. https://doi.org/10.1016/j.neuron.2020.02.033

TCW, J., Wang, M., Pimenova, A. A., Bowles, K. R., Hartley, B. J., Lacin, E., … Brennand, K. J. (2017). An Efficient Platform for Astrocyte Differentiation from Human Induced Pluripotent Stem Cells. *Stem Cell Reports*, *9*(2), 600–614. https://doi.org/10.1016/j.stemcr.2017.06.018

Tong, X.-J., Hu, Z., Liu, Y., Anderson, D., & Kaplan, J. M. (2015). A network of autism linked genes stabilizes two pools of synaptic GABAA receptors. *ELife*, *4*, e09648. https://doi.org/10.7554/eLife.09648

Tong, X.-J., López-Soto, E. J., Li, L., Liu, H., Nedelcu, D., Lipscombe, D., … Kaplan, J. M. (2017). Retrograde Synaptic Inhibition Is Mediated by α-Neurexin Binding to the α2δ Subunits of N-

Type Calcium Channels. *Neuron*, *95*(2), 326-340.e5. https://doi.org/10.1016/j.neuron.2017.06.018

Tordjman, S., Cohen, D., Coulon, N., Anderson, G. M., Botbol, M., Canitano, R., & Roubertoux, P. L. (2017). Reframing autism as a behavioral syndrome and not a specific mental disorder: Implications of genetic and phenotypic heterogeneity. *Neuroscience and Biobehavioral Reviews*, *80*, 210. https://doi.org/10.1016/j.neubiorev.2017.01.030

Trounson, A., Shepard, K. A., & DeWitt, N. D. (2012). Human disease modeling with induced pluripotent stem cells. *Current Opinion in Genetics & Development*, *22*(5), 509–516. https://doi.org/10.1016/j.gde.2012.07.004

Tsui, D., Vessey, J. P., Tomita, H., Kaplan, D. R., & Miller, F. D. (2013). FoxP2 Regulates Neurogenesis during Embryonic Cortical Development. *Journal of Neuroscience*, *33*(1), 244–258. https://doi.org/10.1523/JNEUROSCI.1665-12.2013

Uchino, S., Wada, H., Honda, S., Nakamura, Y., Ondo, Y., Uchiyama, T., … Kohsaka, S. (2006). Direct interaction of post-synaptic density-95/Dlg/ZO-1 domain-containing synaptic molecule Shank3 with GluR1 alpha-amino-3-hydroxy-5-methyl-4-isoxazole propionic acid receptor. *Journal of Neurochemistry*, *97*(4), 1203–1214. https://doi.org/10.1111/j.1471-4159.2006.03831.x

Uchino, S., & Waga, C. (2013). SHANK3 as an autism spectrum disorder-associated gene. *Brain & Development*, *35*(2), 106–110. https://doi.org/10.1016/j.braindev.2012.05.013

Ullrich, B., Ushkaryov, Y. A., & Südhof, T. C. (1995). Cartography of neurexins: More than 1000 isoforms generated by alternative splicing and expressed in distinct subsets of neurons. *Neuron*, *14*(3), 497–507. https://doi.org/10.1016/0896-6273(95)90306-2

Ushkaryov, Y. A., Petrenko, A. G., Geppert, M., & Südhof, T. C. (1992). Neurexins: Synaptic cell surface proteins related to the alpha-latrotoxin receptor and laminin. *Science (New York, N.Y.)*, *257*(5066), 50–56. https://doi.org/10.1126/science.1621094

Vaags, A. K., Lionel, A. C., Sato, D., Goodenberger, M., Stein, Q. P., Curran, S., … Scherer, S. W. (2012). Rare deletions at the neurexin 3 locus in autism spectrum disorder. *American Journal of Human Genetics*, *90*(1), 133–141. https://doi.org/10.1016/j.ajhg.2011.11.025

Varoqueaux, F., Jamain, S., & Brose, N. (2004). Neuroligin 2 is exclusively localized to inhibitory synapses. *European Journal of Cell Biology*, *83*(9), 449–456. https://doi.org/10.1078/0171-9335-00410

Vasa, R. A., Mostofsky, S. H., & Ewen, J. B. (2016). The Disrupted Connectivity Hypothesis of Autism Spectrum Disorders: Time for the Next Phase in Research. *Biological Psychiatry:*

Cognitive Neuroscience and Neuroimaging, *1*(3), 245–252. https://doi.org/10.1016/j.bpsc.2016.02.003

Veenstra-Vanderweele, J., Christian, S. L., & Cook, E. H. (2004). Autism as a paradigmatic complex genetic disorder. *Annual Review of Genomics and Human Genetics*, *5*, 379–405. https://doi.org/10.1146/annurev.genom.5.061903.180050

Verpelli, C., Dvoretskova, E., Vicidomini, C., Rossi, F., Chiappalone, M., Schoen, M., … Sala, C. (2011). Importance of Shank3 protein in regulating metabotropic glutamate receptor 5 (mGluR5) expression and signaling at synapses. *The Journal of Biological Chemistry*, *286*(40), 34839–34850. https://doi.org/10.1074/jbc.M111.258384

Vicidomini, C., Ponzoni, L., Lim, D., Schmeisser, M. J., Reim, D., Morello, N., … Verpelli, C. (2017). Pharmacological enhancement of mGlu5 receptors rescues behavioral deficits in SHANK3 knock-out mice. *Molecular Psychiatry*, *22*(5), 689–702. https://doi.org/10.1038/mp.2016.30

Viñas-Jornet, M., Esteba-Castillo, S., Gabau, E., Ribas-Vidal, N., Baena, N., San, J., … Guitart, M. (2014). A common cognitive, psychiatric, and dysmorphic phenotype in carriers of NRXN1 deletion. *Molecular Genetics & Genomic Medicine*, *2*(6), 512–521. https://doi.org/10.1002/mgg3.105

Vitrac, A., & Cloëz-Tayarani, I. (2018). Induced pluripotent stem cells as a tool to study brain circuits in autism-related disorders. *Stem Cell Research & Therapy*, *9*(1), 226. https://doi.org/10.1186/s13287-018-0966-2

Voglis, G., & Tavernarakis, N. (2006). The role of synaptic ion channels in synaptic plasticity. *EMBO Reports*, *7*(11), 1104–1110. https://doi.org/10.1038/sj.embor.7400830

Voineagu, I., Wang, X., Johnston, P., Lowe, J. K., Tian, Y., Horvath, S., … Geschwind, D. H. (2011). Transcriptomic analysis of autistic brain reveals convergent molecular pathology. *Nature*, *474*(7351), 380–384. https://doi.org/10.1038/nature10110

Vorstman, J. a. S., Staal, W. G., van Daalen, E., van Engeland, H., Hochstenbach, P. F. R., & Franke, L. (2006). Identification of novel autism candidate regions through analysis of reported cytogenetic abnormalities associated with autism. *Molecular Psychiatry*, *11*(1), 1, 18–28. https://doi.org/10.1038/sj.mp.4001781

Waga, C., Okamoto, N., Ondo, Y., Fukumura-Kato, R., Goto, Y.-I., Kohsaka, S., & Uchino, S. (2011). Novel variants of the SHANK3 gene in Japanese autistic patients with severe delayed speech development. *Psychiatric Genetics*, *21*(4), 208–211. https://doi.org/10.1097/YPG.0b013e328341e069

Walker, S., & Scherer, S. W. (2013). Identification of candidate intergenic risk loci in autism spectrum disorder. *BMC Genomics*, *14*(1), 499. https://doi.org/10.1186/1471-2164-14-499

Walsh, T., McClellan, J. M., McCarthy, S. E., Addington, A. M., Pierce, S. B., Cooper, G. M., … Sebat, J. (2008). Rare structural variants disrupt multiple genes in neurodevelopmental pathways in schizophrenia. *Science (New York, N.Y.)*, *320*(5875), 539–543. https://doi.org/10.1126/science.1155174

Wang, K., Zhang, H., Ma, D., Bucan, M., Glessner, J. T., Abrahams, B. S., … Hakonarson, H. (2009). Common genetic variants on 5p14.1 associate with autism spectrum disorders. *Nature*, *459*(7246), 528–533. https://doi.org/10.1038/nature07999

Wang, T., Guo, H., Xiong, B., Stessman, H. A. F., Wu, H., Coe, B. P., … Eichler, E. E. (2016). De novo genic mutations among a Chinese autism spectrum disorder cohort. *Nature Communications*, *7*(1), 13316. https://doi.org/10.1038/ncomms13316

Wang, X., Bey, A. L., Chung, L., Krystal, A. D., & Jiang, Y.-H. (2014). Therapeutic approaches for shankopathies. *Developmental Neurobiology*, *74*(2), 123–135. https://doi.org/10.1002/dneu.22084

Wang, X., Bey, A. L., Katz, B. M., Badea, A., Kim, N., David, L. K., … Jiang, Y. (2016). Altered mGluR5-Homer scaffolds and corticostriatal connectivity in a Shank3 complete knockout model of autism. *Nature Communications*, *7*(1), 11459. https://doi.org/10.1038/ncomms11459

Wang, X., McCoy, P. A., Rodriguiz, R. M., Pan, Y., Je, H. S., Roberts, A. C., … Jiang, Y.-H. (2011). Synaptic dysfunction and abnormal behaviors in mice lacking major isoforms of Shank3. *Human Molecular Genetics*, *20*(15), 3093–3108. https://doi.org/10.1093/hmg/ddr212

Waye, M. M. Y., & Cheng, H. Y. (2018). Genetics and epigenetics of autism: A Review. *Psychiatry and Clinical Neurosciences*, *72*(4), 228–244. https://doi.org/10.1111/pcn.12606

Weick, J. P., Liu, Y., & Zhang, S.-C. (2011). Human embryonic stem cell-derived neurons adopt and regulate the activity of an established neural network. *Proceedings of the National Academy of Sciences*, *108*(50), 20189–20194. https://doi.org/10.1073/pnas.1108487108

Wenger, T. L., Kao, C., McDonald-McGinn, D. M., Zackai, E. H., Bailey, A., Schultz, R. T., … Hakonarson, H. (2016). The Role of mGluR Copy Number Variation in Genetic and Environmental Forms of Syndromic Autism Spectrum Disorder. *Scientific Reports*, *6*(1), 19372. https://doi.org/10.1038/srep19372

Williams, S. M., An, J. Y., Edson, J., Watts, M., Murigneux, V., Whitehouse, A. J. O., … Claudianos, C. (2019). An integrative analysis of non-coding regulatory DNA variations associated with autism spectrum disorder. *Molecular Psychiatry*, *24*(11), 1707–1719. https://doi.org/10.1038/s41380-018-0049-x

Wilson, H. L., Wong, A. C. C., Shaw, S. R., Tse, W.-Y., Stapleton, G. A., Phelan, M. C., … McDermid, H. E. (2003). Molecular characterisation of the 22q13 deletion syndrome supports the role of haploinsufficiency of SHANK3/PROSAP2 in the major neurological symptoms. *Journal of Medical Genetics*, *40*(8), 575–584. https://doi.org/10.1136/jmg.40.8.575

Wiśniowiecka-Kowalnik, B., Nesteruk, M., Peters, S. U., Xia, Z., Cooper, M. L., Savage, S., … Stankiewicz, P. (2010). Intragenic rearrangements in NRXN1 in three families with autism spectrum disorder, developmental delay, and speech delay. *American Journal of Medical Genetics Part B: Neuropsychiatric Genetics*, *153B*(5), 983–993. https://doi.org/10.1002/ajmg.b.31064

Wong, C. C. Y., Meaburn, E. L., Ronald, A., Price, T. S., Jeffries, A. R., Schalkwyk, L. C., Plomin, R., & Mill, J. (2014). Methylomic analysis of monozygotic twins discordant for autism spectrum disorder and related behavioural traits. *Molecular Psychiatry*, *19*(4), 495–503. https://doi.org/10.1038/mp.2013.41

Xu, J., Zwaigenbaum, L., Szatmari, P., & Scherer, S. (2004, May 1). Molecular Cytogenetics of Autism. Retrieved 27 September 2020, from Current Genomics website: https://www.eurekaselect.com/62724/article

Yan, Q., Weyn-Vanhentenryck, S. M., Wu, J., Sloan, S. A., Zhang, Y., Chen, K., Wu, J. Q., Barres, B. A., & Zhang, C. (2015). Systematic discovery of regulated and conserved alternative exons in the mammalian brain reveals NMD modulating chromatin regulators. *Proceedings of the National Academy of Sciences of the United States of America*, *112*(11), 3445–3450. https://doi.org/10.1073/pnas.1502849112

Yan, J., Noltner, K., Feng, J., Li, W., Schroer, R., Skinner, C., … Sommer, S. S. (2008). Neurexin 1alpha structural variants associated with autism. *Neuroscience Letters*, *438*(3), 368–370. https://doi.org/10.1016/j.neulet.2008.04.074

Yang, M., Bozdagi, O., Scattoni, M. L., Wöhr, M., Roullet, F. I., Katz, A. M., … Crawley, J. N. (2012). Reduced Excitatory Neurotransmission and Mild Autism-Relevant Phenotypes in Adolescent Shank3 Null Mutant Mice. *Journal of Neuroscience*, *32*(19), 6525–6541. https://doi.org/10.1523/JNEUROSCI.6107-11.2012

Yangngam, S., Plong-On, O., Sripo, T., Roongpraiwan, R., Hansakunachai, T., Wirojanan, J., … Limprasert, P. (2014). Mutation Screening of the Neurexin 1 Gene in Thai Patients with Intellectual Disability and Autism Spectrum Disorder. *Genetic Testing and Molecular Biomarkers*, *18*(7), 510–515. https://doi.org/10.1089/gtmb.2014.0003

Yi, F., Danko, T., Botelho, S. C., Patzke, C., Pak, C., Wernig, M., & Südhof, T. C. (2016). Autism-associated SHANK3 haploinsufficiency causes Ih channelopathy in human neurons. *Science*, *352*(6286). https://doi.org/10.1126/science.aaf2669

Yoon, S. H., Choi, J., Lee, W. J., & Do, J. T. (2020). Genetic and Epigenetic Etiology Underlying Autism Spectrum Disorder. *Journal of Clinical Medicine*, *9*(4), 966. https://doi.org/10.3390/jcm9040966

Yu, J., Vodyanik, M. A., Smuga-Otto, K., Antosiewicz-Bourget, J., Frane, J. L., Tian, S., … Thomson, J. A. (2007). Induced Pluripotent Stem Cell Lines Derived from Human Somatic Cells. *Science*, *318*(5858), 1917–1920. https://doi.org/10.1126/science.1151526

Yuan, H., Wang, Q., Liu, Y., Yang, W., He, Y., Gusella, J. F., … Shen, Y. (2018). A rare exonic NRXN3 deletion segregating with neurodevelopmental and neuropsychiatric conditions in a three-generation Chinese family. *American Journal of Medical Genetics. Part B, Neuropsychiatric Genetics : The Official Publication of the International Society of Psychiatric Genetics*, *177*(6), 589–595. https://doi.org/10.1002/ajmg.b.32673

Zalcman, G., Federman, N., & Romano, A. (2018). CaMKII Isoforms in Learning and Memory: Localization and Function. *Frontiers in Molecular Neuroscience*, *11*. https://doi.org/10.3389/fnmol.2018.00445

Zeng, L., Zhang, P., Shi, L., Yamamoto, V., Lu, W., & Wang, K. (2013). Functional impacts of NRXN1 knockdown on neurodevelopment in stem cell models. *PloS One*, *8*(3), e59685. https://doi.org/10.1371/journal.pone.0059685

Zhang, B., Seigneur, E., Wei, P., Gokce, O., Morgan, J., & Südhof, T. C. (2017). Developmental plasticity shapes synaptic phenotypes of autism-associated neuroligin-3 mutations in the calyx of Held. *Molecular Psychiatry*, *22*(10), 1483–1491. https://doi.org/10.1038/mp.2016.157

Zhang, P., Lu, H., Peixoto, R. T., Pines, M. K., Ge, Y., Oku, S., Siddiqui, T. J., Xie, Y., Wu, W., Archer-Hartmann, S., Yoshida, K., Tanaka, K. F., Aricescu, A. R., Azadi, P., Gordon, M. D., Sabatini, B. L., Wong, R. O. L., & Craig, A. M. (2018). Heparan Sulfate Organizes Neuronal Synapses through Neurexin Partnerships. *Cell*, *174*(6), 1450-1464.e23. https://doi.org/10.1016/j.cell.2018.07.002

Zhang, L. I., & Poo, M. M. (2001). Electrical activity and development of neural circuits. *Nature Neuroscience*, *4 Suppl*, 1207–1214. https://doi.org/10.1038/nn753

Zhang, W., Rohlmann, A., Sargsyan, V., Aramuni, G., Hammer, R. E., Südhof, T. C., & Missler, M. (2005). Extracellular Domains of α-Neurexins Participate in Regulating Synaptic Transmission by Selectively Affecting N- and P/Q-Type Ca2+ Channels. *Journal of Neuroscience*, *25*(17), 4330–4342. https://doi.org/10.1523/JNEUROSCI.0497-05.2005

Zhang, Y., Pak, C., Han, Y., Ahlenius, H., Zhang, Z., Chanda, S., … Südhof, T. C. (2013). Rapid Single-Step Induction of Functional Neurons from Human Pluripotent Stem Cells. *Neuron*, *78*(5), 785–798. https://doi.org/10.1016/j.neuron.2013.05.029

Zoghbi, H. Y. (2003). Postnatal Neurodevelopmental Disorders: Meeting at the Synapse? *Science*, *302*(5646), 826–830. https://doi.org/10.1126/science.1089071

S1. List of antibodies

Gene	Species	Clonality	Company	Order number	Dilution
MAP2	Chicken	Polyclonal	Abcam	ab5392	1:500
TUBB3	Mouse	Monoclonal	Millipore	MAB1637	1:1000
OCT4	Rabbit	Polyclonal	Abcam	Ab3209	1:500
SYN1	Rabbit	Polyclonal	Abcxam	Ab64581	1:200
HOMER1	Rabbit	Polyclonal	Synaptic Systems	160 103	1:500
SHANK3	Rabbit	Polyclonal	Atlas	HPA003446	1:200
GLUA2	Mouse	Monoclonal	Synaptic Systems	182 211	1:200
GAPDH	Mouse	Monoclonal	Abcam	Ab8245	1:1000
SYP	Mouse	Monoclonal	abcam	ab8049	1:250
TBR1	Rabbit	Polyclonal	abcam	ab31940	1:500
BRN2	Mouse	Monoclonal	Santa cruz	sc393324	1:500

S2. List of primers for qRT-PCR

Gene	**Direction**	**Sequence**
PBGD	F	ATTACCCCGGGAGACTGAAC
	R	GGCTGTTGCTTGGACTTCTC
SHANK1	F	AGTTCCGATACAAGACCCGAG
	R	CCGAGCTGCACATACTCCA
SHANK2	F	TGAAGGAGTCTCAACAGGGAC
	R	CCTGGTGACCGTAGGGAAG
SHANK3	F	GTCCTGCTCTTCCGTGGAG
	R	TGGGTCTTGATAACCTCTGCAA
SYN1	F	CCCCAATCACAAAGAAATGCTC
	R	ATGTCCTGGAAGTCATGCTG
VGLUT1	F	TCAATAACAGCACGACCCAC
	R	TCCTGGAATCTGAGTGACAATG
PSD95	F	TCACAACCTCTTATTCCCAGCA
	R	CATGGCTGTGGGGTAGTCG
TBR1	F	GCCTTTCTCCTTCTATCATGCTC
	R	GTCAGTGGTCGAGATAATGGGA
BRN2	F	ACCCGCTTTATCGAAGGCAA
	R	CCTCCATAACCTCCCCCAGA
NGN2	F	TGTTCGTCAAATCCGAGACCT
	R	CGATCCGAGCAGCACTAACA
GAPDH	F	AGGGCTGCTTTTAACTCTGGT
	R	CCCCACTTGATTTTGGAGGGA